

**STUDIES IN CARBON-CARBON COUPLING  
REACTIONS USING PALLADIUM  
COMPLEXES**

**A THESIS  
SUBMITTED TO  
THE UNIVERSITY OF PUNE  
FOR THE DEGREE OF  
DOCTOR OF PHILOSOPHY**

**IN  
CHEMISTRY**

**BY**

**ABHISHEK SUD**

**UNDER THE GUIDANCE OF  
Dr. RAGHUNATH V. CHAUDHARI**

**AT  
HOMOGENEOUS CATALYSIS DIVISION  
NATIONAL CHEMICAL LABORATORY**

**PUNE-411 008**

**INDIA**

**May 2007**



राष्ट्रीय रासायनिक प्रयोगशाला  
(वैज्ञानिक तथा औद्योगिक अनुसंधान परिषद)  
डॉ. होमी भाभा मार्ग पुणे - 411 008, भारत  
**NATIONAL CHEMICAL LABORATORY**  
(Council of Scientific & Industrial Research)  
Dr. Homi Bhabha Road, Pune - 411 008, India.



## CERTIFICATE

This is to certify that the work incorporated in the thesis, “**Studies in Carbon-Carbon Coupling Reactions using Palladium Complexes**” submitted by **Mr. Abhishek Sud**, for the Degree of **Doctor of Philosophy**, was carried out by the candidate under my supervision in the Homogeneous Catalysis Division, National Chemical Laboratory, Pune – 411 008, India. Such material as has been obtained from other sources has been duly acknowledged in the thesis.

Dr. R. V. Chaudhari  
(Research Supervisor)

## **DECLARATION**

I hereby declare that the thesis “**Studies in Carbon-Carbon Coupling Reactions using Palladium Complexes**” submitted for the degree of Doctor of Philosophy to the University of Pune has not been submitted by me for a degree to any other University.

**Date:**

**Abhishek Sud**

**Place:**

---

*Dedicated to*

*My Beloved Family*

*- One for All. All for One*

---

## **ACKNOWLEDGEMENT**

*I wish to express my sincere gratitude to Dr. R. V. Chaudhari, my research supervisor, for his constant support and encouragement during the course of this work. His enthusiasm, optimism, and positive energy have always been a great motivator.*

*I would like to express my sincere gratitude to Dr. R. M. Deshpande for being a friend, mentor, and a guiding light when I needed it the most. His ideas, thoughts, and philosophy have indeed enriched my life.*

*I am grateful to Council of Scientific and Industrial Research (CSIR), India for the research fellowship. I am thankful to Director, NCL for allowing me to carry out the research work and providing all the possible infrastructural facilities.*

*I sincerely acknowledge Dr. A. A. Kelkar, Dr. S. P. Gupte, Dr. R. Jagannathan, Dr. V. V. Ranade, Dr. V. H. Rane, Mr. O. S. Ozarde, Mr. S. S. Joshi, and Mr. H. M. Raheja for their valuable help and co-operation during my stay in NCL. I would like to thank all other members of homogeneous catalysis division, for a healthy working atmosphere.*

*I also wish to thank my seniors and friends Dr Yogi, Dr. Tonde, and Mr. Makki who have contributed significantly towards fulfillment of this work. I would like to express my gratitude to my other seniors, friends, and colleagues Amit, Anand, Bibhas, Charu, Debu, Deepak, Kapil, Kausik, Lalita, Mahesh, Manisha & Manisha, Nandu, Nitin, PP, Rajesh, Rashmi, Sangeeta, Savita, Shashi, Shinde, and Shrikant for their friendship and helping hands. I would like to acknowledge my friends from NCL golden Jubilee Hostel for making my hostel stay enjoyable.*

*No thanks can be enough to acknowledge the love and encouragement of my parents, grandparents, buas, buaijis, chachas, chachi, brother, bhabhi, and Shweta. They have been my constant source of strength. But for them I might not have embarked on this journey of Life and Science.*

*I also express my deep sense of gratitude and indebtedness to Bhagwan Sri Sathya Sai Baba for reasons beyond words.*

**May 2007**  
**Pune**

**Abhishek Sud**

## List of Contents

Description	Page No.
<b>Abstract</b>	vi
<b>Chapter1: Introduction and Literature Survey</b>	
1.1. General background	2
1.2. Literature survey on Heck reaction	3
1.2.1. Homogeneous palladium catalyst systems	4
1.2.1.1. Phosphine ligands in palladium catalyzed Heck reaction	4
1.2.1.2. Palladacycle catalysts in Heck reaction	8
1.2.1.3. Phosphine free catalysts for Heck reaction	10
1.2.2. Heterogeneous catalysis	29
1.2.2.1. Liquid- Liquid system (Biphasic catalysis)	30
1.2.2.2. Solid- Liquid systems	31
1.2.2.2.1. Palladium nano particles as catalysts	31
1.2.2.2.2. Palladium complexes bound to polymeric supports as catalysts	32
1.2.2.2.3. Palladium complexes bound to inorganic supports as catalysts	34
1.2.2.2.4. Supported palladium metal catalysts	38
1.2.3. Promoters in Heck chemistry	46
1.2.4. Mechanism of Heck reaction	48
1.2.5. Kinetic studies on Heck reaction	52
1.3. Summary of the literature surveyed	56
1.4. Scope and objective	57
1.5. References	59
<b>Chapter 2: Preliminary Investigations on Heck Reactions Using Palladium Complex Catalysts Containing N- and P- Ligands</b>	
2.1. Introduction	67
2.2. Experimental	67
2.2.1. Materials	67
2.2.2. Analytical techniques	68

2.2.3. Synthesis of palladium complexes	70
2.2.4. General procedure for Heck reactions	82
2.3. Results and discussion	82
2.3.1. Screening of palladium complex catalyst precursor for the Heck reaction	82
2.3.1.1. Palladium-phosphine catalyst systems	83
2.3.1.2. Palladium-amine catalyst systems	84
2.3.1.3. Palladium-N-N bidentate amine catalyst systems	85
2.3.2. Effect of solvent on the reaction rate	87
2.3.3. Screening of aryl halides for the Heck reaction	88
2.3.4. Screening of the olefins for the Heck reaction	92
2.3.5. Screening of the bases for the Heck reaction	105
2.3.6. Effect of quaternary ammonium salts on the Heck reaction	107
2.4. Conclusions	109
2.5. References	110

### **Chapter 3: Kinetics of Heck Vinylation of 4'-Bromoacetophenone with n-Butyl acrylate Using P-C Palladacycle Catalyst**

3.1. Introduction	113
3.2. Experimental section	113
3.2.1. Chemicals and apparatus	113
3.2.2. General procedure for Heck reaction	114
3.3. Effect of reaction parameter variation on the rate of reaction	115
3.3.1. Effect of catalyst concentration on the rate of reaction	117
3.3.2. Effect of 4'-bromo acetophenone concentration on the rate of reaction	123
3.3.3. Effect of n-butyl acrylate concentration on the rate of reaction	127
3.3.4. Effect of NaOAc concentration on the rate of reaction	131
3.3.5. Effect of TBAB concentration on the rate of reaction	135
3.4. Kinetic analysis	139
3.4.1. Empirical rate models and model discrimination	139
3.4.2. Mechanistic rate models and model discrimination	146
3.4.2.1. Oxidative addition of aryl halide to Pd as the rate determining step	147

3.4.2.2. Olefin insertion in the Pd-C bond as the rate determining step	150
3.4.2.3. $\beta$ -Hydride elimination as the rate determining step	152
3.4.2.4. Comparison of different mechanistic models	154
3.5. Conclusions	156
3.6. References	157

#### **Chapter 4: Studies on Lewis Acid Promoted Heck Reactions**

4.1. Introduction	159
4.2. Experimental	161
4.3. Effect of different Lewis acids on the rate of reaction	162
4.3.1. Effect of LiCl addition on the rate of reaction	163
4.3.2. Effect of TiCl <sub>4</sub> addition on the rate of reaction	163
4.3.3. Effect of ZnCl <sub>2</sub> addition on the rate of reaction	164
4.3.4. Effect of SnCl <sub>2</sub> addition on the rate of reaction	165
4.3.5. Effect of SnCl <sub>4</sub> addition on the rate of reaction	166
4.3.6. Effect of FeCl <sub>3</sub> addition on the rate of reaction	167
4.3.7. Effect of AlCl <sub>3</sub> addition on the rate of reaction	168
4.3.8. Comparison of the effect of different Lewis acids on the reaction rate	169
4.4. Influence of FeCl <sub>3</sub> on the rate of reaction	174
4.4.1. Effect of FeCl <sub>3</sub> on the rate of reaction with different palladium catalyst precursors	174
4.4.2. Effect of FeCl <sub>3</sub> on the rate of reaction at different temperatures	176
4.4.3. Effect of FeCl <sub>3</sub> on the rate of reaction with different bases	178
4.4.4. Effect of FeCl <sub>3</sub> on the rate of reaction with different olefins	181
4.4.5. Effect of FeCl <sub>3</sub> on the rate of reaction with different aryl halides	182
4.5. Comparison of the promoting effect of FeCl <sub>3</sub> with tetrabutylammonium bromide	184
4.6. Understanding the mode of action of Lewis acid promoters	185
4.7. Conclusions	191
4.8. References	192



## **Chapter 5: Synthesis and Characterization of Ossified Palladium Complexes and their Application to Heck Reactions**

5.1. Introduction	194
5.2. Experimental	195
5.2.1. Materials	195
5.2.2. Synthesis of triphenylphosphine trisulphonate, sodium salt (TPPTS-Na)	196
5.2.3. Syntheses of palladium complexes	197
5.2.3.1. Pd(pyca)(PPh <sub>3</sub> )(OTs) complex	197
5.2.3.2. Pd(acpy)(PPh <sub>3</sub> )(OTs) complex	197
5.2.3.3. Pd(pycald)(PPh <sub>3</sub> )(OTs) complex	197
5.2.3.4. Pd(bipy)(PPh <sub>3</sub> )(OTs) complex	198
5.2.4. Synthesis of aqueous-soluble complexes	198
5.2.5. Ossification of palladium complexes	199
5.2.6. General procedure for recycling the catalyst for Heck reaction	200
5.2.7. General procedure for screening of substrates and bases for Heck reaction	201
5.3. Results and discussion	201
5.3.1. Characterization of the catalysts	201
5.3.1.1. <sup>31</sup> P Cross-Polarized Magic Angle Spinning NMR Spectroscopy	201
5.3.1.2. Powder X-Ray Diffraction	204
5.3.1.3. X-Ray Photoelectron Spectroscopy	207
5.3.1.4. Scanning Electron Microscopy	211
5.3.1.5. Surface Area Measurements	213
5.3.1.6. Palladium Content Analysis	214
5.3.2. Heck reactions using ossified palladium complexes:	215
5.3.2.1. Recycle studies with different ossified complexes	215
5.3.2.2. Comparison of different ossified complexes	219
5.3.2.3. Screening of bases for the Heck reaction	220
5.3.2.4. Screening of aryl halides for the Heck reaction	221
5.3.2.5. Screening of olefins for the Heck reaction	223
5.4. Conclusions	224

5.5. References	224
-----------------	-----

**Chapter 6: Kinetics of Heck Vinylation of Iodobenzene with n-Butyl acrylate Using Ossified Pd(Pyca)(TPPTS) Catalyst**

6.1. Introduction	227
6.2. Experimental	227
6.3. Preliminary experiments	228
6.3.1. Effect of catalyst concentration on the rate of reaction	230
6.3.2. Effect of iodobenzene concentration on the rate of reaction	233
6.3.3. Effect of n-butyl acrylate concentration on the rate of reaction	235
6.3.4. Effect of NaOAc concentration on the Reaction Rates	237
6.4. Kinetic analysis	240
6.4.1. Empirical rate models and model discrimination	240
6.4.2. Mechanistic rate models and model discrimination	247
6.4.2.1. Oxidative addition of aryl halide to Pd as the rate determining step	248
6.4.2.2. Olefin insertion in the Pd-C bond as the rate determining step	251
6.4.2.3. $\beta$ -Hydride elimination as the rate determining step	253
6.4.2.4. Comparison of different mechanistic models	254
6.5. Conclusions	257
6.6. References	257

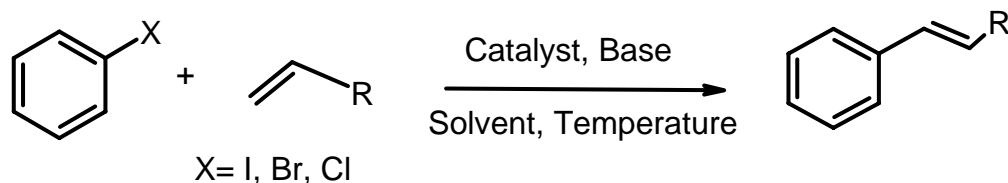
<b>Appendix</b>	258
-----------------	-----

<b>Publications and Symposia</b>	273
----------------------------------	-----

## Abstract of the Thesis

### General Background

Catalysis has revolutionized the chemical industry by cutting down the need for stoichiometric reagents and reducing the side/unwanted reactions. Catalysis has been an integral part of petrochemical and petroleum refining industry. In recent times, catalysts have found increasing demand in the synthesis of fine chemicals, pharmaceuticals, and specialty chemicals, which were conventionally manufactured using stoichiometric organic synthesis having the drawback of using corrosive and toxic reagents, and formation of stoichiometric amounts of by products and waste products consisting of inorganic salts. With increasing environmental awareness and global competition, it is imperative to design alternate processes that are clean, atom efficient, and use non-toxic and non-hazardous raw materials. In this respect, homogeneous and heterogeneous catalysts have played a vital role towards the development of environmentally benign and industrially lucrative processes. Hydrogenation, hydroformylation, carbonylation, C-C coupling, polymerization, and amination reactions are some of the industrially important reactions carried out with the help of catalysts. These reactions either give important products in a single step synthesis from the starting materials, or are part of the multi-step synthesis. C-C bond formation reactions like Mizoroki-Heck, Suzuki, Sonogashira, and Stille coupling reactions are especially useful organic synthesis tools. Among these Mizoroki-Heck reaction catalyzed by palladium metal complexes has perhaps become the most important tool in synthetic chemistry for C-C bond formation while retaining the olefinic structure. These reactions were reported separately by Mizoroki and Heck in early 1970s and then developed by Heck in a series of reports (Scheme 1).



**Scheme 1**

This reaction has also gained importance due to its inertness to a variety of functional groups, thus avoiding the need for protection and deprotection of functional

groups during synthesis. The use of Heck reactions in the multistep synthesis of complex molecules like estrone, morphine, vernolepin, prepinnaterpene, capnellene, abietic acid, retinoids, etc. has been reported, thus showing the wide applicability and usefulness of these reactions.

Both, homogeneous as well as heterogeneous catalysts have been reported for Heck reactions. In spite of three and a half decades of Heck chemistry, its use in the industry remains limited due to the use of palladium as catalyst, often with costly non-recoverable ligands, deactivation of the palladium catalysts, use of costly promoters in large amount, and limited studies on high performance recyclable catalysts. Over that, very few reports on the kinetic behavior of these reactions are available. The kinetic studies help in the optimization of the reaction conditions, understanding of the reaction mechanism, and in designing of the reactors.

Considering the above facts, the present study was focused on the Heck reaction of haloarenes with acrylates to give cinnamic acid derivatives as the model reaction. The cinnamate products obtained are used as UV absorbers, antioxidants, and as intermediates in perfumery, pharmaceutical, and dye industry. The main objective of this study was to develop improved homogeneous as well as heterogeneous catalyst systems with respect to activity and selectivity and to study the kinetics of this system. With these objectives in mind, the following specific problems were chosen for the present work:

- ❖ Synthesis, characterization, and catalytic properties of different palladium complexes for the Heck reactions and optimization of the reaction conditions in order to study the kinetics of these reactions.
- ❖ Kinetic studies on the vinylation of 4'-bromo acetophenone with n-butyl acrylate to give (E)-Butyl-3-(4-acetylphenyl)acrylate using P-C palladacycle catalyst.
- ❖ Investigations into a novel class of promoters to enhance the activity of the palladium complexes for the Heck reaction of haloarenes with different olefins.
- ❖ Synthesis, characterization, and catalytic properties of ossified palladium complexes and their use in the Heck coupling of acrylates with halo arenes.
- ❖ Kinetic studies using ossified palladium complex  $\{Pd(Pyca)(TPPTS)\}$  [ $Pyca = 2$ -pyridine carboxylic acid and  $TPPTS-Ba = P(C_6H_4SO_3)_3-Ba_{3/2}\}$ ] for the vinylation of iodobenzene with n-butyl acrylate.

The research work carried out for this thesis has been presented in six chapters, the brief outline of which is given below.

## **Chapter 1: Introduction and Literature Survey**

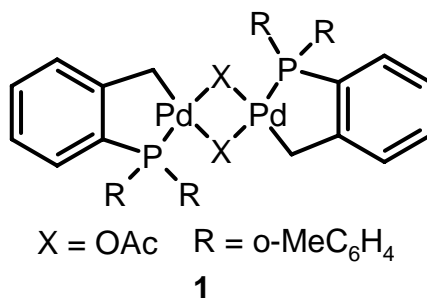
This chapter presents a detailed survey of the literature on the homogeneous and heterogeneous catalyst systems used for the Heck reactions. Use of highly active palladium complexes and the techniques to immobilize these complexes on various supports has been reviewed critically. Finally, the mechanism and the kinetic studies on Heck reactions have been discussed. The following observations emerged from the literature review:

- Though palladium, platinum, nickel, cobalt, rhodium, iridium, and ruthenium complexes have been shown to be active catalysts for Heck reactions, most of the research focuses on palladium catalysts. Palladium in almost every form has been tried and tested for these reactions and has been found to be active to varying degrees.
- Presently research on Heck reactions is devoted towards minimization of the catalyst cost and reduction in catalyst deactivation. One approach for reducing the catalyst cost and deactivation is to design catalysts that have higher activity and stability and thus can give very high TON. Research in this direction has led to the development of palladacycle catalysts, which have turned out to be one of the most active catalysts employed for Heck reactions of bromo and chloro arenes in terms of TON and TOF.
- Another approach to reduce the catalyst cost is the design and utilization of heterogeneous catalysts that can be re-used and thus can give very high cumulative TON. Heterogeneous catalysts, like palladium bipyridyl complex anchored on MCM 41, that can give high TON (> million) have been reported for the reaction of iodobenzene and 4'-bromoacetophenone with n-butyl acrylate.
- Some Heck reactions have been reported to occur at room temperatures with either the use of promoters like quarternary ammonium salts or in the ionic liquids as solvent. Heck reactions have been studied in biphasic and also in supercritical media.

- The doubts regarding the active catalytic species involved in the reaction still remain and different reports claim different active species.
- There are very few kinetic studies with homogeneous catalyst complexes and no such study with heterogeneous catalyst system for the Heck reaction.
- Significant challenges like increasing the reactivity of chloro arenes, reducing the waste generated due to the use of stoichiometric amount of base, and establishing the identity of the true catalytic species involved remain to be solved.

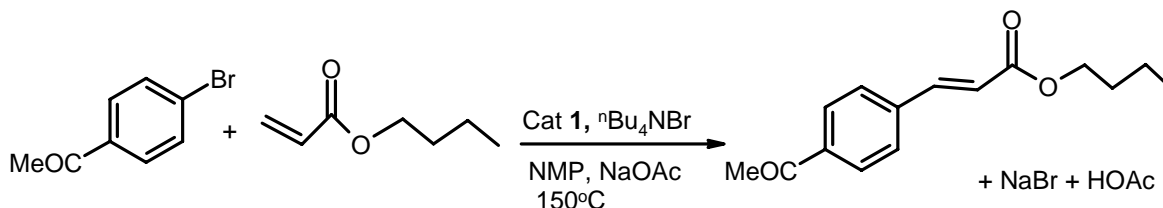
## **Chapter 2: Preliminary Investigations on Heck Reactions Using Palladium Complex Catalysts Containing N- and P- Ligands**

The second chapter presents the experimental results on the vinylation of halo arenes using palladium complex catalysts. Palladium complexes containing phosphorus and nitrogen ligands were synthesized by the procedures reported in the literature. The aim behind synthesis of these complexes for Heck reaction was that they contained cheaply available or easy to synthesize ligands and thus could help in reducing the reaction cost. These complexes were tested for Heck reaction of 4'-bromoacetophenone with n-butyl acrylate. The reactions were carried out in a 50 ml two necked stirred glass reactor, equipped with a condenser, under nitrogen atmosphere. The glass reactor was immersed in an oil bath equipped with a mechanical stirrer and maintained at the required temperature. The reaction was then started by switching the stirrer on. Samples were withdrawn at regular intervals and analyzed by GC. At the end of the reaction, the products were isolated by column chromatography and analyzed by IR spectroscopy, microanalysis technique, and GC-mass spectroscopy. The comparison of these results showed palladacycle catalyst precursor **1** (Scheme 2) to be the catalyst with best activity and stability. This catalyst was tested under different reaction conditions in order to standardize the reaction system for further studies. Screening of solvents, bases, promoters, olefins, and halo arenes for Heck reaction using palladium catalyst precursor **1** was carried out. The reaction rates were faster in polar solvents than in non-polar solvents. Both organic and inorganic bases were active for these reactions and gave >95% yield.



**Scheme 2**

The rate of the reaction decreased with variation of acrylates in the following order; methyl acrylate > ethyl acrylate > butyl acrylate. Iodobenzene was found to be more reactive than bromobenzene. Chlorobenzene did not react under the reaction conditions. It was observed that halo arenes with electron withdrawing functional groups gave higher rates than those having electron donating groups as substituents. In case of promoters like quaternary ammonium salts (R<sub>4</sub>NX, where X is the anion) the activity decreased with the variation of anion in the following order: Cl<sup>-</sup> > Br<sup>-</sup> > I<sup>-</sup>. When the alkyl group (R) was varied, the rates initially increased with the increase in the chain length and then the rates dropped as the length of the alkyl chain increased. After these preliminary experiments, the following reaction system (Scheme 3) was taken as the standard reaction system for the kinetic study.



**Scheme 3**

### Chapter 3: Kinetics of Heck Vinylation of 4'-Bromoacetophenone with n-Butyl acrylate Using P-C Palladacycle Catalyst

This chapter discusses the kinetics of 4'-bromoacetophenone with n-butyl acrylate using catalyst precursor **1** in the concentration ranges of 0.1 to 0.75 kmol.m<sup>-3</sup>, 0.25 to 1.1 kmol.m<sup>-3</sup>, and 4.26 x 10<sup>-5</sup> to 2.55 x 10<sup>-4</sup> kmol.m<sup>-3</sup>, respectively. The reaction was carried out in presence of sodium acetate as a base and tetrabutylammonium bromide as a promoter in the concentration ranges of 0.1 to 1.1 kmol m<sup>-3</sup> and 0.03 to 0.2 kmol m<sup>-3</sup>, respectively. This

kinetic study was undertaken in order to develop a deeper understanding into the Heck reactions and to optimize the reaction conditions. The experiments were carried out in a 50 ml two necked stirred glass reactor equipped with a condenser elaborated in the earlier chapter. The concentration of the catalyst precursor **1**, 4'-bromoacetophenone, n-butyl acrylate, sodium acetate, and tetrabutylammonium bromide was varied one at a time and the initial rates were observed at four different temperatures (403 to 433 K). The rate was found to be first order with respect to 4'-BAP, half order with the catalyst, and first order tending to zero order with NaOAc concentration. The rates passed through a maximum with variation of TBAB and n-butyl acrylate concentrations. Various empirical and mechanistic rate models were considered to explain the trends observed. The following empirical model was found to best fit the data at all the temperatures studied.

$$R = \frac{k[A][B][C][D][Q]^{0.5}}{(1 + K_B[B]^2)(1 + K_C[C])(1 + K_D[D]^2)} \quad \text{Model I}$$

Where R is the rate of reaction, expressed in kmol/m<sup>3</sup>/s, [A] is the concentration of p-bromo acetophenone (kmol/m<sup>3</sup>), [B] is the concentration of n-butyl acrylate (kmol/m<sup>3</sup>), [C] is the concentration of NaOAc (kmol/m<sup>3</sup>), [D] is the concentration of TBAB (kmol/m<sup>3</sup>), and [Q] is the concentration of the palladacycle catalyst **1** (kmol/m<sup>3</sup>). k is the rate constant [(m<sup>3</sup>/kmol)<sup>4.5</sup>], and K<sub>B</sub> [(m<sup>3</sup>/kmol)<sup>2</sup>], K<sub>C</sub> [(m<sup>3</sup>/kmol)] and K<sub>D</sub> [(m<sup>3</sup>/kmol)<sup>2</sup>] are equilibrium constants.

A comparison of the experimental rates with the rates predicted using this model indicates a good agreement between experimental and predicted rates. The average percent error between the experimental and predicted data was 1.12%. The activation energy for this model was calculated to be 114.49 kJ/mol.

#### **Chapter 4: Studies on Lewis Acid Promoted Heck Reactions**

This chapter presents the results on the investigation into a new class of promoters. Quarternary ammonium and phosphonium salts have been reported to act as promoter in the Heck reaction. These promoters are used in large amounts, usually 20 mol% of the haloarenes. These promoters are costly and contribute to increasing the cost of the Heck reactions. Since, Heck reaction involves the cleavage of carbon-halogen bond during the oxidative addition step, it was expected that the addition of Lewis acids to the reaction



mixture could have a beneficial effect on the reaction rate in a manner similar to the Friedel Crafts alkylation reactions. The effect of addition of catalytic amount of Lewis acids to the reaction system was studied. The Lewis acids LiCl, SnCl<sub>4</sub>, SnCl<sub>2</sub>, ZnCl<sub>2</sub>, TiCl<sub>4</sub>, FeCl<sub>3</sub>, and AlCl<sub>3</sub> were screened. Apart from AlCl<sub>3</sub>, all the Lewis acids gave significant enhancement in the rate as compared to the standard reaction. FeCl<sub>3</sub> was the best additive in terms of the magnitude of enhancement of the reaction rates. The optimum concentration of FeCl<sub>3</sub>, where maximum enhancement was observed, was 70% of the palladium. It was found that for all the Lewis acids, the maximum enhancement in the rate was obtained at particular concentration which varied from Lewis acid to Lewis acid. The rate enhancement was observed with Lewis acids for various catalysts and at different temperatures. The effect of Lewis acids was further substantiated for different bases, olefins, and halo arenes. It was observed that when the base or the substrate contained a nitrogen atom with free lone pair of electrons, there was no enhancement in the rate of reaction on addition of Lewis acid. The effect of Lewis acid addition on the rate was more pronounced when the aromatic ring had an electron donating substituent like OMe. It was also observed that presence of small amount of moisture in the reaction mixture was necessary for the rate enhancement.

## **Chapter 5: Synthesis and Characterization of Ossified Palladium Complexes and their Application to Heck Reactions**

This chapter discusses the synthesis, characterization, and catalytic properties of ossified catalysts for Heck reactions. The aim of this study was to provide an efficient and recyclable catalyst system for the Heck reaction. The literature on Heck reactions contains very few reports on highly recyclable immobilized catalysts capable of giving high TONs and TOFs. Since, the immobilization of metal complexes by the ossification technique was recently developed; we decided to investigate the catalytic properties of these catalysts for Heck reactions. Pd(Pyca)(PPh<sub>3</sub>)(OTs) [Pyca= 2-pyridine carboxylic acid] was converted to its water soluble analogue by exchanging the PPh<sub>3</sub> ligand with a water soluble ligand TPPTS [P(C<sub>6</sub>H<sub>4</sub>SO<sub>3</sub>Na)<sub>3</sub>]. Aqueous solution of this complex was subjected to treatment with heavier group IIA cations resulting in precipitation of insoluble solid palladium complex catalyst. These complexes were characterized by powder XRD, <sup>31</sup>P CP-MAS NMR, and SEM. These complexes were intrinsically insoluble due to the formation of

barium-sulphonate ion pair- which is well known. These complexes were then compared for their activity and stability in the Heck reaction of iodo benzene with n-butyl acrylate. Recycle studies were carried out in N, N- dimethyl formamide solvent and it was observed that there was less than 1 % palladium leaching in the reaction medium. All the catalysts were recycled without any significant loss in activity. TON of up to  $9.7 \times 10^5$  were achieved by the use of these catalysts for the vinylation of iodobenzene with n-butyl acrylate. Ossified Pd(Pyca)(TPPTS) catalyst turned out to be the best catalyst in terms of activity. A further study with this catalyst involving the screening of bases, olefins, and halo arenes was carried out. This catalyst was active in presence of both organic and inorganic bases. The catalyst was active for iodo and bromo arenes but not for chloro arenes under the reaction conditions.

### **Chapter 6: Kinetics of Heck Vinylation of Iodobenzene with n-Butyl acrylate Using Ossified Pd(Pyca)(TPPTS) Catalyst**

In this chapter a detailed kinetic analysis for the vinylation reaction of iodobenzene with n-butyl acrylate using ossified Pd(Pyca)(TPPTS) catalyst has been presented. The ossified catalysts are a new class of heterogeneous catalysts employed for Heck reactions. Hence, it becomes important to carry out a detailed kinetic investigation so as to understand their mode of action and the effect they have on the reaction rates under different reaction parameters. The concentration of catalyst, base, olefin, and iodobenzene was systematically varied and its effect on the reaction rate was observed at different temperatures. The rates were found to be first order with respect to catalyst and iodobenzene concentrations. The rates showed a first order tending to zero order dependence with n-butyl acrylate and sodium acetate concentrations. These results were then compared with the results obtained with the reaction of Pd(Pyca)(PPh<sub>3</sub>)(OTs) catalyst under homogeneous reaction conditions. Various empirical and mechanistic rate models were considered to explain the trends observed. Following empirical model was found to best fit the data at all temperatures

$$R = \frac{k[A][B][C][Q]}{(1 + K_B[B]) (1 + K_C[C])} \quad \text{Model II}$$

Where R is the rate of reaction, expressed in kmol/m<sup>3</sup>/s, [A] is the concentration of iodobenzene (kmol/m<sup>3</sup>), [B] is the concentration of n-butyl acrylate (kmol/m<sup>3</sup>), [C] is the

concentration of NaOAc ( $\text{kmol/m}^3$ ), and  $[Q]$  is the ossified catalyst loading ( $\text{kg/m}^3$ ).  $k$  is the rate constant ( $\text{m}^{12}/\text{kg kmol}^3$ ), and  $K_B$  ( $\text{m}^3/\text{kmol}$ ) and  $K_C$  ( $\text{m}^3/\text{kmol}$ ) are equilibrium constants.

The recommended rate model predicted the trends observed showing a good agreement between the experimental and predicted values. The activation energy was found to be 110.81 kJ/mol.

### Key References:

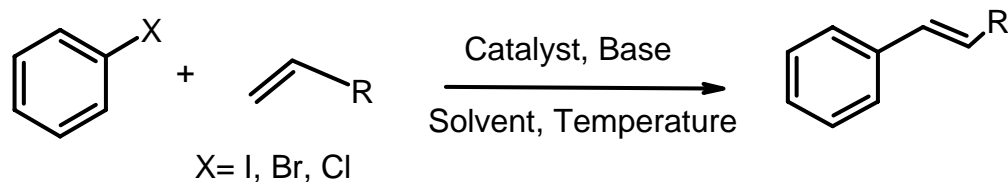
1. a) Mizoroki, T.; Mori, K.; Ozaki, A. *Bull. Chem. Soc. Jpn.* **1971**, 44, 581 b) Heck, R. F.; Nolley, J. P. *J. Org. Chem.* **1972**, 37, 2320 c) Mori, K.; Mizoroki, T.; Ozaki, A. *Bull. Chem. Soc. Jpn.* **1973**, 46, 1505 d) Dieck, H. A.; Heck, R. F. *J. Am. Chem. Soc.* **1974**, 96, 1133
2. Dounay, A. B.; Overman, L. E. *Chem. Rev.* **2003**, 103, 2945
3. a) Herrmann, W. A.; Brossmer, C.; Ofele, K.; Reisinger, C. P.; Priermeier, T.; Beller, M.; Fischer, H. *Angew. Chem. Int. Ed. Engl.* **1995**, 34, 1844 b) Takenaka, K.; Uozumi, Y. *Adv. Synth. Catal.* **2004**, 346, 1693
4. Tsai, F. Y.; Wu, C. L.; Mou, C. Y.; Chao, M. C.; Lin, H. P.; Liu, S. T. *Tetrahedron Lett.* **2004**, 45, 7503
5. a) Shaw, B. L. *New J. Chem.* **1998**, 77 b) Amatore, C.; Jutand, A. *Acc. Chem. res.* **2000**, 33, 314
6. a) Consorti, C. S.; Flores, F. R.; Dupont, J. *J. Am. Chem. Soc.* **2005**, 127, 12054 b) Zhao, F. G.; Bhanage, B. M.; Shirai, M.; Arai, M. *Stud. Surf. Sci. Catal.* **1999**, 122, 427
7. a) Beletskaya, I. P.; Cheprakov, A. V. *Chem. Rev.* **2000**, 100, 3009 b) Phan, N. T. S.; Sluys, M. V. D.; Jones, C. W. *Adv. Synth. Catal.* **2006**, 348, 609 c) Parshall, G.; Ittel, S. D. *Homogeneous Catalysis: The Applications and Chemistry of Soluble Transition-Metal Complexes*; 2<sup>nd</sup> ed. John Wiley & Sons, New York, **1992** d) *Handbook of Heterogeneous Catalysis*, Ed. Ertl, G.; Knözinger, H. J. eitkamp, Wiley-VCH, Weinheim, **1997**

*Chapter 1:*

*Introduction and  
Literature Survey*

## 1.1. General Background

Catalysis has revolutionized the chemical industry by cutting down the need for stoichiometric reagents and reducing the side/unwanted reactions. Catalysis has been an integral part of petrochemical and petroleum refining industry<sup>1a-d</sup>. In recent times, catalysts have found increasing demand in the synthesis of fine chemicals, pharmaceuticals, and specialty chemicals, which were conventionally manufactured using stoichiometric organic synthesis. These conventional synthesis have the drawback of using corrosive and toxic reagents, and formation of stoichiometric amount of by- products and waste products consisting of inorganic salts<sup>2a-e</sup>. With increasing environmental awareness and global competition, it is imperative to design alternate processes that are clean, atom efficient, and use non-toxic and non-hazardous raw materials. In this respect, homogeneous and heterogeneous catalysts have played a vital role towards the development of environmentally benign and industrially lucrative processes. Hydrogenation, hydroformylation, carbonylation, C-C coupling, polymerization, and amination reactions are some of the industrially important reactions carried out with the help of catalysts<sup>3a-m</sup>. These reactions either give important products in a single step synthesis from the starting materials, or are part of the multi-step synthesis. C-C bond formation reactions like Mizoroki-Heck<sup>4a-c</sup>, Suzuki<sup>5</sup>, Sonogashira<sup>6</sup>, and Stille<sup>7</sup> coupling reactions are especially useful organic synthesis tools. Among these, Mizoroki-Heck reaction catalyzed by palladium metal complexes has perhaps become the most important tool in synthetic chemistry for C-C bond formation, while retaining the olefinic structure. These reactions were reported separately by Mizoroki and Heck in early 1970s and then developed by Heck in a series of reports<sup>8a-h</sup> (Scheme 1.1). This reaction has also gained importance due to its inertness to a variety of functional groups, thus avoiding the need for protection and deprotection of functional groups during synthesis. The use of Heck reactions in the multistep synthesis of complex molecules like estrone, morphine, vernolepin, prepinaterpene, capnellene, abietic acid, retinoids, etc. have been reported, thus showing the wide applicability and usefulness of these reactions<sup>9</sup>.



Scheme 1.1

Both, homogeneous as well as heterogeneous catalysts have been reported for Heck reaction. In spite of three and a half decades of Heck chemistry, its use in the industry remains limited due to the use of palladium as catalyst, often with costly non-recoverable ligands, deactivation of the palladium catalysts, use of costly promoters in large amount, and limited studies on high performance recyclable catalysts<sup>10a-b</sup>. In addition, very few reports on the kinetic behavior of these reactions are available<sup>11a-f</sup>. The kinetic studies help in the optimization of the reaction conditions, understanding of the reaction mechanism, and in designing of the reactors.

Considering the above facts, the present study was focused on the development of improved homogeneous as well as heterogeneous catalyst systems with respect to activity and selectivity for the Heck reaction and to study the kinetics of these reactions. With these objectives in mind, a detailed survey of the literature on the homogeneous and heterogeneous catalyst systems used for the Heck coupling reaction has been carried out in order to gain insight into the prior art on Heck reaction. Use of highly active palladium complexes and the techniques to immobilize these complexes on various supports has been reviewed critically. Finally, the mechanism and the kinetic studies on Heck reaction have been discussed.

## 1.2. Literature Survey on Heck Reaction

Synthesis of arylated and vinyolated olefins is of great importance in organic chemistry. The palladium catalyzed Heck coupling reaction between an olefin and an aryl halide provide an efficient way for the synthesis of these products. The Heck or Mizoroki-Heck<sup>4a-c</sup> reaction, discovered independently by Heck and Mizoroki and improved upon by Heck<sup>8a-h</sup> into a general synthetic methodology, is associated with the catalytic arylation and alkenylation of olefins. A variety of substituent groups, both on olefin and the aryl

halide, are tolerated in Heck chemistry, thereby making these reactions still more relevant. This does away with the need for protection and deprotection in the case of organic synthesis, thus reducing the number of reaction steps and the cost involved in a particular process and also widens the scope of the substrates that can be used for Heck coupling reaction. Palladium, copper, nickel, platinum, cobalt, rhodium, iridium, and ruthenium complexes have been used as catalysts in Heck chemistry with varying degrees of success<sup>12a-f</sup>. Palladium has been the catalyst of choice for these reactions due to its high activity. Palladium catalyzed Heck reaction, with and without ligands, in presence and absence of promoters, and under homogeneous, biphasic, and heterogeneous conditions has been reported and found to give good results.

### 1.2.1. Homogeneous palladium catalyst systems

The initial reactions reported by Heck and Mizoroki were carried out with Pd black or PdCl<sub>2</sub> as the catalyst in the absence of any ligand. The vinylation of iodobenzene with styrene under these ligand free conditions gave Turn Over Numbers (TONs, defined as moles of product formed per unit moles of catalyst) of up to 100 in methanol solvent [Table 1.1 (homogeneous catalysts for vinylation of iodoarenes), entries 1 and 2]<sup>4a,c</sup>. The obvious reason for low TONs was the instability of the catalyst in absence of any ligand. Later, the beneficial effects of phosphine ligands were also reported by Heck and co-workers<sup>8a-h</sup>.

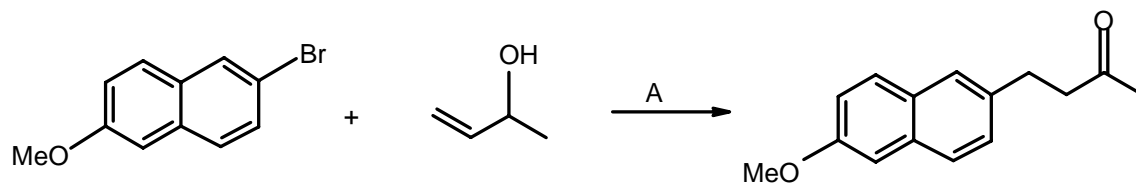
#### 1.2.1.1. Phosphine ligands in palladium catalyzed Heck reaction.

Tri-phenylphosphine was the first ligand reported for the Heck reaction<sup>8a</sup>. The aim of Heck and co workers in these reports was to show the versatility of these reactions and expand their applicability<sup>8a-h</sup>. Therefore, though they reported the use of other phosphine catalysts<sup>8d</sup> for these reactions, no attempt was made to showcase the high activity associated with these catalysts. The best TON reported was a modest 1480 for the reaction of allyl alcohol with bromobenzene in presence of tri-ethylamine base using Pd(OAc)<sub>2</sub>/PPh<sub>3</sub> catalyst system [Table 1.2 (homogeneous catalysts for vinylation of bromoarenes), entry 2]<sup>8c</sup>.

The electronic environment around palladium becomes very important in determining the ability of the catalyst to promote Heck reaction, especially in the case of

less reactive substrates. Since the oxidative addition of aryl halide to Pd complex is generally expected to be the rate determining step, the presence of electron withdrawing groups on the ligand can prove to be detrimental, as has been shown in the case of a study carried out with phosphine ligands bearing one, two, or three 2-pyrimidyl residues  $\text{Ph}_2\text{P}(2\text{-C}_4\text{H}_3\text{N}_3)$ ,  $\text{PhP}(2\text{-C}_4\text{H}_3\text{N}_3)_2$ , and  $\text{P}(2\text{-C}_4\text{H}_3\text{N}_3)_3$ . The yields in the first case were similar to that obtained with  $\text{PPh}_3$  for the reaction of bromobenzene with styrene<sup>13</sup>. The yield drops with the bis-pyrimidyl ligand and goes to a negligible 3% for the tris-pyrimidyl ligand. Thus, it is evident that as the electron withdrawing character of the ligand increases, the rate of the Heck reaction decreases.

Since the cleavage of C-Cl, and C-Br bond requires high energy, it is expected that the oxidative addition of these halides to the palladium will be the rate determining step. For this to occur, presence of highly electron donating ligands is a prerequisite for these reactions<sup>14</sup>. But the problem arises as electron donating ligands may not be beneficial in the further steps of Heck catalytic cycle. Over that, such ligands are air and moisture sensitive, which makes their use, especially in the industrial processes, difficult. Instead of designing new phosphine ligands to overcome this problem, a report on the use of cheap and more stable phosphites as ligands is worth looking at. The application of phosphites as ligands was described for the first time in 1983<sup>15</sup>. Though the results were good, due to weak binding of the ligand to the metal, the precipitation of the palladium occurred. To overcome this problem a large excess of these phosphites needs to be employed. Activated chloroarenes (having electron withdrawing groups on the ring) react in presence of trialkyl phosphites to give moderate to good yields, when the phosphites are taken in 10 to 100 fold excess with respect to palladium. This method has been applied for a single step synthesis of a nonsteroid anti-inflammatory drug nabumethone (Scheme 1.2)<sup>16</sup>.

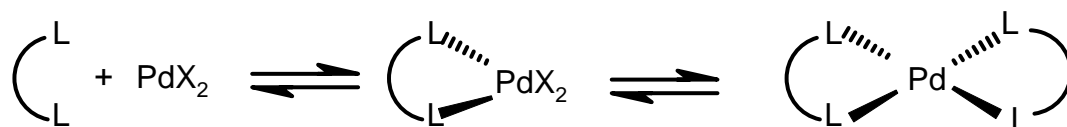


A;  $\text{Pd}(\text{OAc})_2$ , 10 Eq.  $\text{P}(\text{OC}_6\text{H}_3\text{Bu}_2^{t-2,4})_3$ ,  $\text{Na}_2\text{CO}_3$ , DMA, 160 °C

**Scheme 1.2**



The precipitation of palladium is an inherent problem associated with the use of these ligands, when used in low ligand to palladium ratios (3:1). If the ratio is increased, the reaction rates tend to decrease because of the non-availability of the free palladium for binding with the substrates. In order to increase the life time of the catalysts and reduce the precipitation of the palladium, the use of chelating ligands has been proposed<sup>17a-f</sup>. From the earlier stages itself, chelating phosphines were considered to be inferior ligands for Heck reaction of aryl halides. In the earlier stages of Heck chemistry, the thrust was towards (i) the use of halide quenchers and (ii) the use of triflates in place of halides. Both these strategies made the choice of chelating ligands a bad proposition. But chelating ligands can actually be very useful as they can serve the following purposes: (i) reduce the need for addition of excess ligands as 1:1 ratio of ligand to metal is sufficient for catalytic activity (ii) more stable complexes mean a longer life for the catalyst and (iii) higher stability of the catalysts makes it easier for the design of recyclable catalysts. In the later stages of Heck chemistry it has been demonstrated that preformed complexes of palladium with chelating phosphines as well as diisopropylphosphinoferrrocene (dppf) are efficient catalysts for the Heck reaction of aryl halides with styrene in DMF and tributylammonium base<sup>17b-c</sup>. The earlier reports pertaining to poor performance of chelating phosphines have been attributed to the easy and quantitative formation of very stable bis-diphosphine complexes, which can not form any catalytically active species. This complex is easy to form as very high *trans* effect of phosphine ligands helps in easy exchange of halide ligand with another phosphine (Scheme 1.3)<sup>14</sup>.

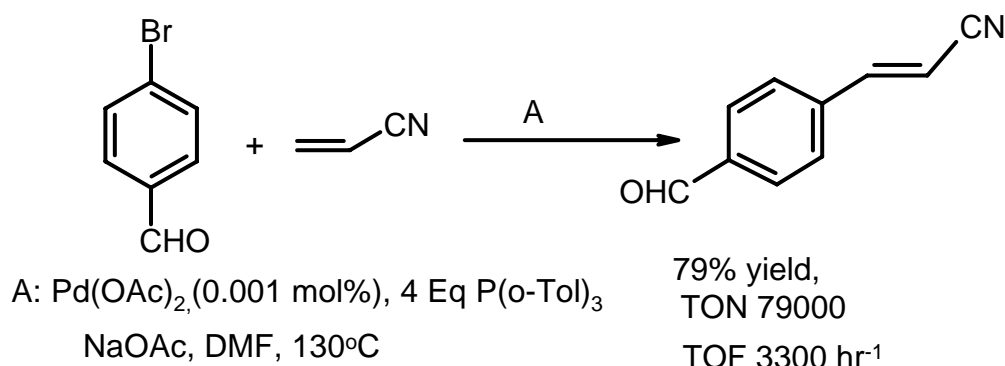


Scheme 1.3

Tris(*t*-butyl)phosphine has been shown to be a good ligand for the activation of not only activated chloroarenes but also for chlorobenzene itself and for deactivated *p*-methoxychlorobenzene and *o*-chlorotoluene<sup>18</sup>. Under these conditions, all other phosphines (PPh<sub>3</sub>, P(*o*-Tol)<sub>3</sub>, BINAP, dppf, and P(*n*-Bu)<sub>3</sub>) failed to catalyze the reaction to any

measurable extent, revealing that the donor character or the cone angle is not a good predictor in the search of a better ligand<sup>14</sup>. A summary of the phosphine catalysts used for Heck reaction is presented in Tables 1.2 to 1.3.

The first significant effort to boost the activity and productivity over the Pd/PPh<sub>3</sub> catalyst in the Heck reaction was made by Spencer in early 1980s<sup>15</sup>. He carried out the arylation of olefins in polar aprotic solvents in presence of tri-orthotolylphosphine ligands to obtain high TON (Scheme 1.4).

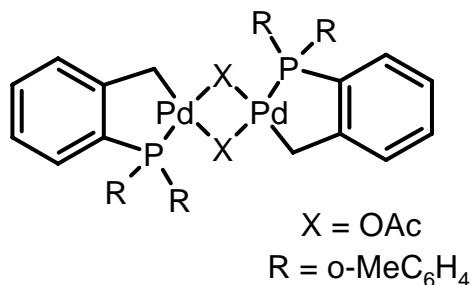


**Scheme 1.4**

The reactions thus carried out by Spencer with P(o-Tol)<sub>3</sub> ligand provided a benchmark for further reactions. After this study, the aim of all further developments in phosphine assisted catalysts for these type of reactions was to obtain highly active catalysts, which could give improved TONs and Turn Over Frequencies (TOFs, defined as moles of product formed per unit moles of catalyst per unit time) at low catalyst concentrations and also activate aryl chlorides to undergo Heck reaction. Since tri-orthotolylphosphine turned out to be a good ligand for Heck reaction, it was imperative that the use of preformed complex of palladium with this ligand be tested for Heck reaction. The use of such a complex was reported by Herrmann and Beller<sup>19a-b</sup> for the first time and this set a precedent for a new class of catalysts christened- palladacycles- to be synthesized and utilized for Heck reaction.

### 1.2.1.2. Palladacycle catalysts in Heck reaction

The discovery, or rather a rediscovery, of a well known palladium dimeric complex  $\text{Pd}_2(\text{P}(\text{o-Tol})_3)_2(\mu\text{-OAc})_2$  (Scheme 1.5) by Herrmann and Beller<sup>19a-b</sup> has set a milestone in palladium catalyzed Heck reaction. For the first time, TON of a million was achieved for the Heck reaction of 4'-bromoacetophenone with n-butyl acrylate using this palladacycle complex. The complexes of this type (Scheme 1.5) are stable to air and moisture and are easy to synthesize in good yields. These are one of the most easy to handle catalysts and hence can be said to be most convenient forms of palladium complexes to be used in homogeneous Heck chemistry. This catalyst is more reactive towards chloro and bromoarenes than for iodoarenes. This was the reason why this catalyst had earlier been discarded as useless for the Heck reaction by Heck himself<sup>8</sup>, who was working mainly on iodoarenes.

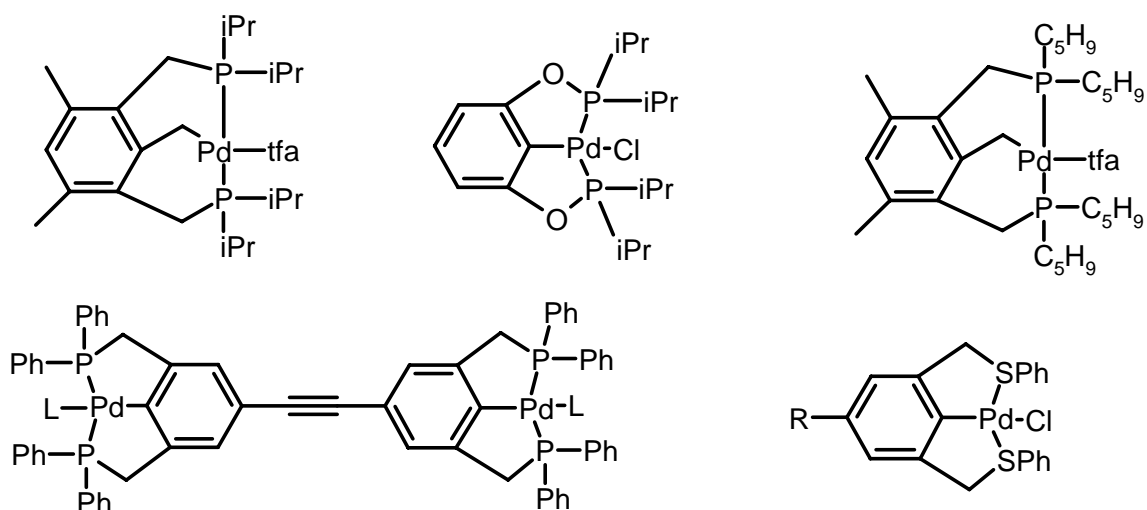


**Scheme 1.5**

Another advantageous aspect of this catalyst is its ability to generate an underligated single phosphine catalyst under the reaction conditions. Such single phosphine catalysts are not only highly reactive due to an almost free coordination shell but are much more stable than the phosphine free systems due to the presence of a ligand. Thus, while phosphine free systems are capable of high activity for the activated haloarenes, but are not stable enough to survive longer reaction times with less reactive substrates, palladacycles are capable of not only high activity but also high stability. The extraordinary activity of the palladacycles is attributed to their high thermal stability, which allows for the reaction to be carried out at higher temperature and also for longer duration. The palladacycle

catalyst (Scheme 1.5) discovered by Herrmann remains the most studied catalyst of this type.

To keep palladium from precipitating from the reaction medium, it is important that the ligands hold the palladium in a stable state. Palladacycles do this by binding to palladium through phosphorus and carbon atoms. An extension of this is the development of another type of very active Heck palladacycle catalysts in subsequent years (Scheme 1.6)<sup>20a-d</sup>. These catalysts are known as pincer complexes and have the advantage of palladium being bound to ligand through three atoms. This ensures that at least one of the bond is retained during the catalytic cycle, where dissociation of the ligand is required to create vacant sites for the substrates to bind to palladium.

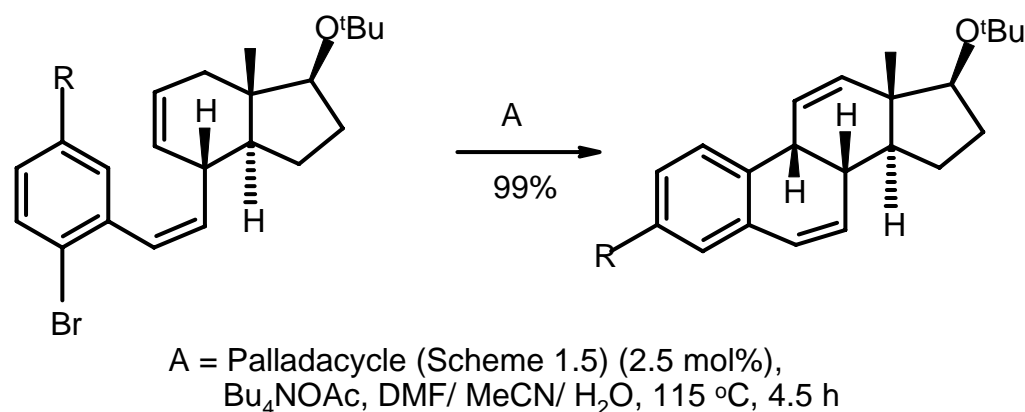


**Scheme 1.6**

These catalysts were shown to be stable to air and moisture and did not deactivate on prolonged heating at 140°C under the Heck reaction conditions. Apart from some model reactions being tried with newly synthesized palladacycle complexes, the use of palladacycle catalysts for the synthetic purposes has been limited to the use of palladacycle complex (shown in Scheme 1.5) reported by Herrmann and Beller<sup>19a-b</sup>. This palladacycle has been successfully applied in the synthesis of several complex molecules<sup>21a-b</sup>, like the enantioselective synthesis of estrone by intramolecular cyclization. The reaction in aqueous solvent with the catalyst was very fast and gave a quantitative yield of the desired estrone

precursor. In presence of other catalysts such as  $\text{Pd}(\text{OAc})_2/\text{PPh}_3$  yields in the range of 63 – 85% were obtained, with a fifteen time longer reaction period (Scheme 1.7)<sup>22</sup>. A summary of palladacycle catalysts used for Heck reaction is included in Tables 1.1 to 1.3.

In addition to phosphine modified complexes, a number of phosphine free ligands have been used for developing novel active and stable complexes for Heck reaction. The next section deals with a few such catalysts.

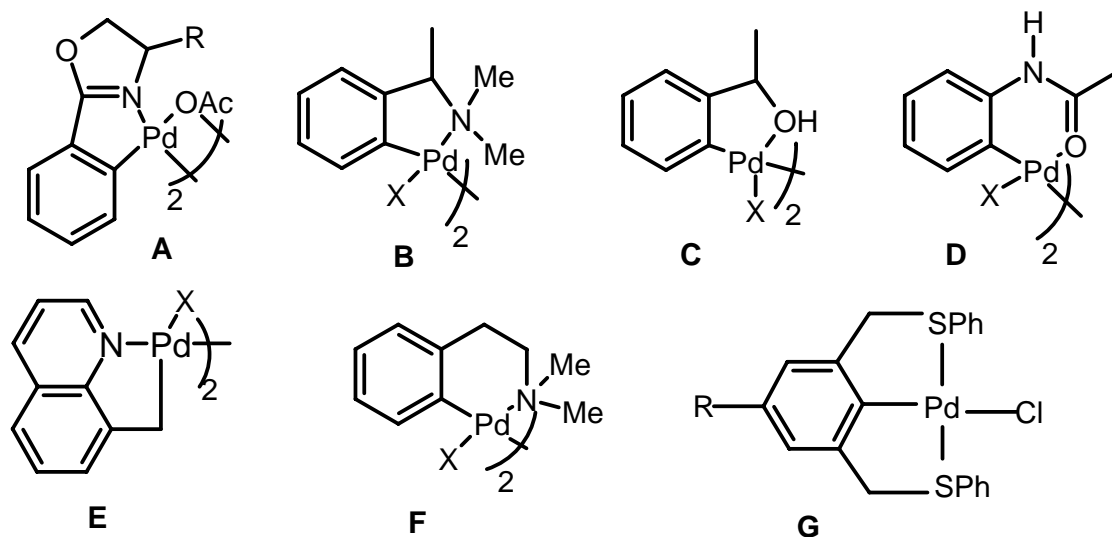


**Scheme 1.7**

### 1.2.1.3 .Phosphine free catalysts for Heck reaction

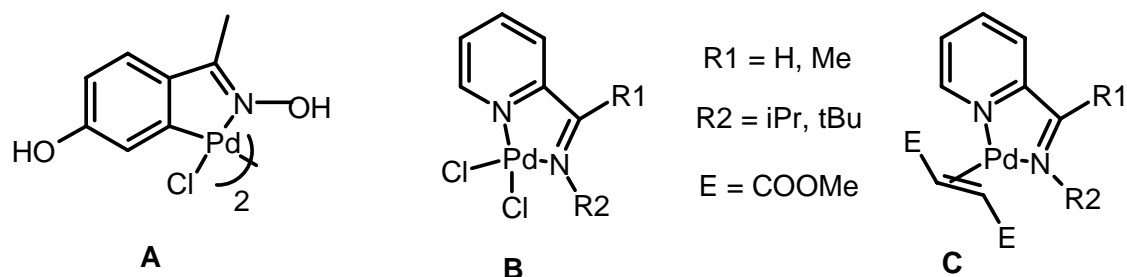
It is beneficial to have ligands that can easily dissociate from palladium to provide vacant binding sites for the substrates. This activation step preceded the actual catalytic cycle. As soon as the activation step comes into picture, i.e where the dissociation of the ligand from the palladium takes place to give active catalytic species, expensive phosphine ligands can be done away with, and instead, cheaper ligands that can easily dissociate from palladium can be employed. Nitrogen-, oxygen-, and sulphur- containing palladacycles have been shown as excellent pre catalysts for the Heck reaction. Milstein et al<sup>23a</sup> prepared a number of oxazoline based palladacycles and showed that such complexes can be used in the arylation of olefins with iodoarenes to give very high TONs. For the reaction of iodobenzene with ethyl acrylate, a TON of  $4 \times 10^6$  was achieved after 24 h of reaction (Table 1.1, entries 27 and 29)<sup>23a-b</sup>. C-N and C-O type palladacycles (Scheme 1.8, **A-F**) formed from very cheap starting materials have also been synthesized and shown to be

highly active catalysts for the Heck reaction of bromobenzene with styrene (TONs of up to  $7.4 \times 10^5$ , Table 1.1, entries 12,28 and Table 1.2, entry 15)<sup>23c-d</sup>.

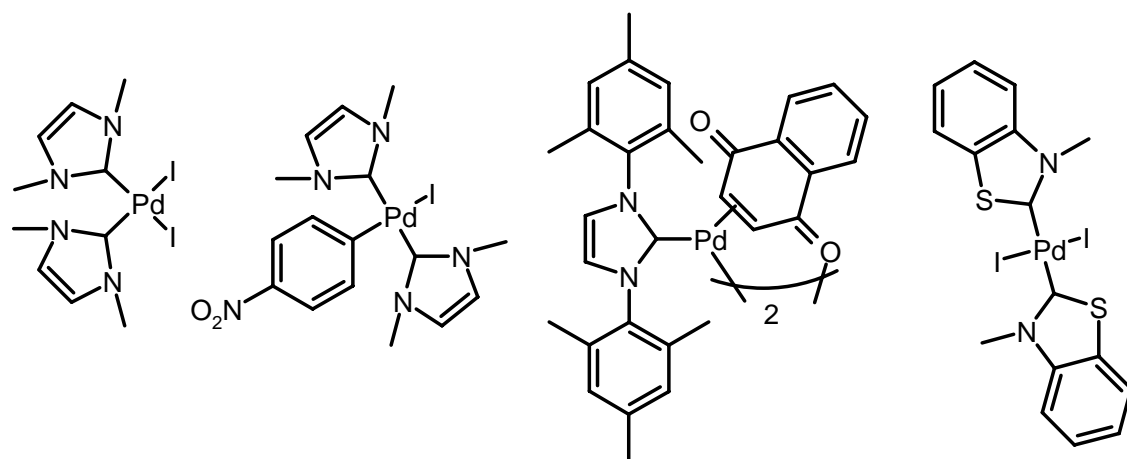


**Scheme 1.8**

Sulphur containing palladacycles (Scheme 1.8, **G**) have also been synthesized and have proved to be good catalysts for the Heck vinylation with iodoarenes (Table 1.1, entry, 34)<sup>24</sup>. Recently, oxime based palladacycles (Scheme 1.9, **A**) have been shown to be active catalysts for the Heck reaction of iodoarenes with t-butyl acrylate in water as solvent and different organic bases, with (dicyclohexyl)methyl amine being the base of choice, giving TONs of 7000 within 10 min of reaction under microwave irradiation (Table 1.1, entry 16, 17)<sup>25</sup>. The high activity is attributed to the use of microwave as the energy source. Pd(0) and Pd(II) complexes containing pyridyl-alimine or pyridyl-ketimine ligands (Scheme 1.9, **B**, **C**) have been reported for the Heck reaction of iodobenzene and methyl acrylate. Pd(II) complexes showed higher activity than the Pd(0) complexes tested. Overall modest TONs (up to 1000) were achieved (Table 1.1, entry 12)<sup>26</sup>.

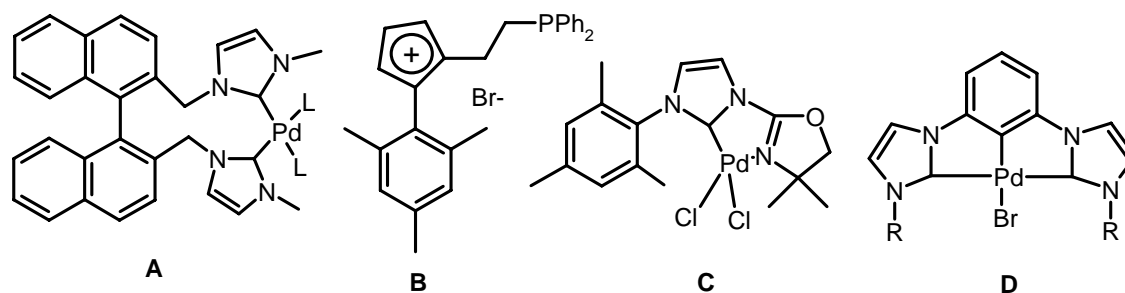


Carbene palladium complexes constitute another class of stable and active catalysts. Herrmann et al<sup>27a-f</sup> have shown that N-heterocyclic carbenes derived from imidazole and pyrazole can lead to TONs nearing a million for both iodo-, and bromoarenes. (Table 1.1, entry 43, Table, 1.2, entries 37,38) (Scheme 1.10).



Different types of chelating carbene ligands have been reported for Heck coupling reaction, but in most cases without any significant improvement in the catalyst performance. A chelating biscarbene ligand with a binaphthyl core (Scheme 1.11, **A**) has been described for the olefination of phenyl iodide and bromide<sup>28</sup>. The mixed carbene-phosphine ligand precursor (Scheme 1.11, **B**) has been used for the coupling of number of bromoarenes (Table 1.2, entry 12)<sup>29</sup> with TOFs of 800 h<sup>-1</sup> and TONs of 200. The oxazoline-carbene complex (Scheme 1.11, **C**) catalyse the formation of stilbenes from aryl bromides

and activated aryl chlorides achieving a TON of up to 500 after 16 h of reaction time<sup>30</sup>. Even tridentate pincer biscarbene complexes (Scheme 1.11, **D**) can be used for the coupling of aryl iodides, bromides, and activated chlorides<sup>31a-b</sup>. These ligands (of the type **D** shown in Scheme 1.11) are one of the best known so far for the olefination of chloroarenes, giving TONs in the region of 75000 for p-chlorobenzaldehyde with styrene [Table 1.3 (homogeneous catalysts for vinylation of chloroarenes), entry 9].



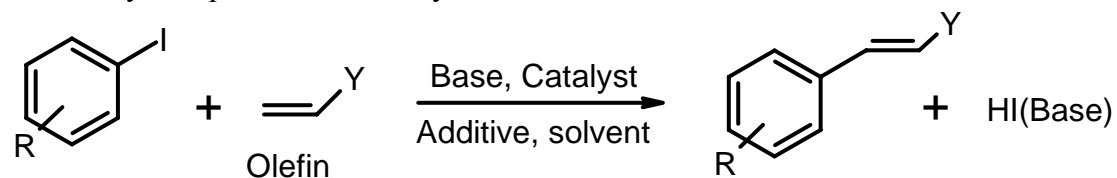
**Scheme 1.11**

The instability of carbene complexes in stoichiometric tests coupled with the need for high reaction temperatures brings these systems very close to P-C palladacycle catalysts<sup>14</sup>. Thus, it is very much possible that the catalysis may proceed through a primary decomposition of carbene complex to liberate an under-ligated palladium which can then catalyze the reaction.

TONs greater than million are repeatedly obtained with phosphine assisted as well as phosphine free catalysts in Heck reaction<sup>19,32a-d</sup>. Till date the highest TONs obtained for the Heck reaction have been reported by Takenaka et al<sup>33</sup>. They have used a N-C-N pincer palladacycle complex for the reaction of iodobenzene with methyl acrylate in presence of sodium bicarbonate base to achieve the TONs of  $5.2 \times 10^8$  at 140°C. The TOF for this reaction was  $2 \times 10^6 \text{ h}^{-1}$  (Table 1.1, entry 11).

A summary of the various categories of homogeneous catalysts employed for Heck reaction is presented in Tables 1.1 to 1.3.



**Table 1.1:** Key homogeneous catalysts reported for the vinylation of iodoarenes

No	Cat, (Mol%)	R	Olefin, Equiv	Base, Equiv	Solvent	Additive, Mol%	Ti, h	Tm, °C	Yield, %	TON	TOF, h <sup>-1</sup>	Ref
1	<b>1</b> (1)	H	Sty, 2	KOAc, 1.2	MeOH		2	120	100	100	50	4a
2	<b>2</b> (3)	H	C <sub>2</sub> H <sub>4</sub>	KOAc, 1.2	MeOH		3	120	90	30	10	4c
3	<b>3</b> (1)	H	MA, 1.5	NaHCO <sub>3</sub> , 2.5	DMF	TBAC, 100	24	30	94	94	4	34
4	<b>4</b> (5)	H	MA, 1.5	NaHCO <sub>3</sub> , 2.5	DMF	TBAC, 100 + M S	2	50	99	20	10	35
5	<b>4</b> (5)	H	MA, 1.5	K <sub>2</sub> CO <sub>3</sub> , 2.5	H <sub>2</sub> O	TBAB, 20	2	50	95	19	9	36
6	<b>10</b> (1.25 x 10 <sup>-5</sup> )	H	BA, 1.5	TEA, 1	Dioxane		338	100	92	7.36 x 10 <sup>6</sup>	2.17 x 10 <sup>4</sup>	37
7	<b>13</b> (6.6 x 10 <sup>-4</sup> )	H	MA, 1.5	TBA, 1.2	DMF		216	95	92	1.39 x 10 <sup>5</sup>	643	17c
8	<b>14</b> (3.6 x 10 <sup>-4</sup> )	H	Sty, 1.5	TBA, 1.2	DMF		72	125	62	1.70 x 10 <sup>5</sup>	2.36 x 10 <sup>3</sup>	17c
9	<b>15</b> (0.2)	H	MA, 1.5	TEA, 2	NMP		16	116	100	500	31	38
10	<b>8</b> (2 x 10 <sup>-4</sup> )	H	BA, 1.2	NaOAc, 1.4	DMA	TBAB, 20	50	120	100	5.02 x 10 <sup>5</sup>	1.00 x 10 <sup>4</sup>	39
11	<b>20</b> (1 x 10 <sup>-7</sup> )	H	MA, 1.2	NaHCO <sub>3</sub> , 1.1	NMP		22	140	52	5.20 x 10 <sup>8</sup>	2.30 x 10 <sup>6</sup>	33
12	<b>22</b> (5 x 10 <sup>-4</sup> )	H	EA, 2	K <sub>2</sub> CO <sub>3</sub> , 1.1	NMP		7	140	96	1.45 x 10 <sup>5</sup>	2.07 x 10 <sup>4</sup>	40
13	<b>23</b> (0.1)	H	MA, 1.1	TEA, 1	DMF		¾	80	94	940	1.25 x 10 <sup>3</sup>	26

**Table 1.1 (Continued):** Key homogeneous catalysts reported for the vinylation of iodoarenes

No	Cat, (Mol%)	R	Olefin, Equiv	Base, Equiv	Solvent	Additive, Mol%	Ti, h	Tm, °C	Yield, %	TON	TOF, h <sup>-1</sup>	Ref
14	<b>25</b> (1.6 x 10 <sup>-4</sup> )	4-NO <sub>2</sub>	EA, 1	TEA, 2	NMP		12	140	99	5.90 x 10 <sup>5</sup>	4.95 x 10 <sup>4</sup>	41
15	<b>24</b> (0.1)	H	BA <sup>t</sup> , 1.2	TEA, 2	DMF		2	110	98	980	490	42
16	<b>26</b> (0.001)	4-Cl	BA <sup>t</sup> , 1.5	Cy <sub>2</sub> NMe, 1.5	H <sub>2</sub> O		24	120	59	5.90 x 10 <sup>4</sup>	2.45 x 10 <sup>3</sup>	25
17	<b>26</b> (0.013)	4-Cl	BA <sup>t</sup> , 1.5	Cy <sub>2</sub> NMe, 1.5	H <sub>2</sub> O		1/6	hv, 120	91	7.00 x 10 <sup>3</sup>	4.20 x 10 <sup>4</sup>	25
18	<b>27</b> (0.002)	4-Me	Sty, 1.4	NaOAc, 1.1	DMA	TBAB, 20	20	150	91	4.55 x 10 <sup>4</sup>	2.27 x 10 <sup>3</sup>	31b
19	<b>28/29</b> (2 x 10 <sup>-5</sup> )	H	MA, 1.2	TEA, 1.4	DMA		38	140	37	1.85 x 10 <sup>6</sup>	4.86 x 10 <sup>4</sup>	43
20	<b>31/32</b> (1 x 10 <sup>-4</sup> )	H	BA, 1.2	NaOAc, 1.4	DMA	TBAB, 20	24	150	100	1.00 x 10 <sup>6</sup>	4.16 x 10 <sup>4</sup>	44
21	<b>37</b> (0.001)	H	BA, 1.5	TBA, 1.4	DMF		4	140	99	9.90 x 10 <sup>4</sup>	2.50 x 10 <sup>4</sup>	32b
22	<b>38</b> (7.1 x 10 <sup>-5</sup> )	H	MA, 1.2	TEA, 2	DMF		14	140	100	1.40 x 10 <sup>6</sup>	1.00 x 10 <sup>5</sup>	32b
23	<b>41</b> (1 x 10 <sup>-4</sup> )	H	BA, 1.2	NaOAc, 1.4	DMA	TBAB, 20	24	150	100	1.00 x 10 <sup>6</sup>	4.16 x 10 <sup>4</sup>	45
24	<b>42/43</b> (0.001)	4-OMe	EA, 2	NaOAc, 2	NMP			150	65	6.25 x 10 <sup>4</sup>		46
25	<b>44/45</b> (5 x 10 <sup>-5</sup> )	H	BA, 2	NaOAc, 2	DMF		48	100	100	2.00 x 10 <sup>6</sup>	4.16 x 10 <sup>4</sup>	47
26	<b>46/47/48</b> (7 x 10 <sup>-5</sup> )	H	MA, 1.5	TEA, 1	NMP		168	130	80	1.14 x 10 <sup>6</sup>	6.80 x 10 <sup>3</sup>	48

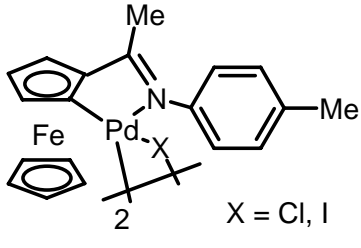
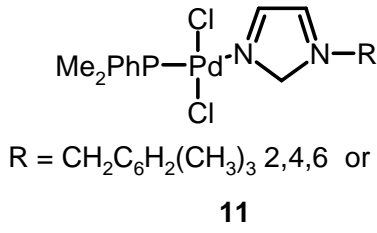
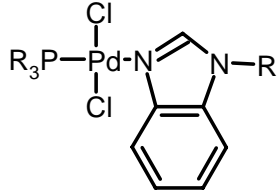
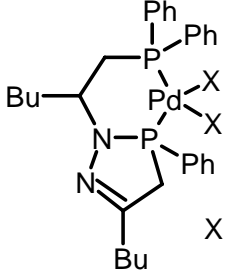
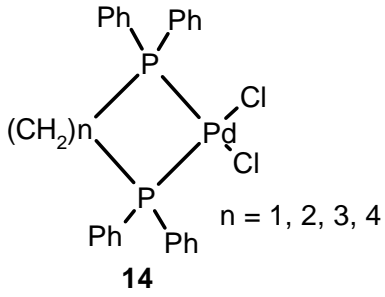
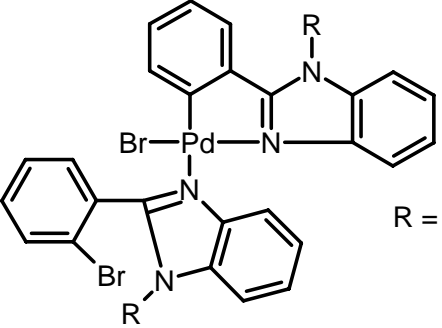
**Table 1.1 (Continued):** Key homogeneous catalysts reported for the vinylation of iodoarenes

No	Cat, (Mol%)	R	Olefin, Equiv	Base, Equiv	Solvent	Additive, Mol%	Ti, h	Tm, °C	Yield, %	TON	TOF, h <sup>-1</sup>	Ref
27	<b>49</b> (1 x 10 <sup>-5</sup> )	H	EA, 1.2	TBA, 1	DMA		24	140	41	4.00 x 10 <sup>6</sup>	1.70 x 10 <sup>5</sup>	23b
28	<b>50/51</b> (1 x 10 <sup>-4</sup> )	H	BA, 1.8	Na <sub>2</sub> CO <sub>3</sub>	NMP		8	160	72	7.20 x 10 <sup>5</sup>	9.00 x 10 <sup>4</sup>	49
29	<b>52</b> (7 x 10 <sup>-5</sup> )	H	MA, 1.2	TEA, 1.4	NMP		18	140	100	1.40 x 10 <sup>6</sup>	7.70 x 10 <sup>4</sup>	23a
30	<b>53</b> (1.8 x 10 <sup>-4</sup> )	H	MA, 1.2	Na <sub>2</sub> CO <sub>3</sub> , 1	NMP		40	140	100	5.28 x 10 <sup>5</sup>	1.32 x 10 <sup>4</sup>	20a
31	<b>55</b> (1 x 10 <sup>-5</sup> )	H	BA, 1.2	Na <sub>a</sub> CO <sub>3</sub> , 1	NMP	Hydroquinone, 10	22	180	89	8.90 x 10 <sup>6</sup>	4.00 x 10 <sup>5</sup>	32a
32	<b>56</b> (1 x 10 <sup>-5</sup> )	4-Me	MA	TEA	DMF		12	110	43	4.30 x 10 <sup>6</sup>	3.58 x 10 <sup>5</sup>	32b
33	<b>57</b> (2 x 10 <sup>-6</sup> )	H	Sty	Cy <sub>2</sub> NMe	NMP		39	160	91	4.50 x 10 <sup>7</sup>	1.17 x 10 <sup>6</sup>	51
34	<b>58</b> (0.1)	H	MA, 1.5	TEA, 1.5	DMF		5	110	92	920	184	24
35	<b>59</b> (5 x 10 <sup>-5</sup> )	H	MA	TBA	DMF		312	95	56	1.12 x 10 <sup>6</sup>	3.60 x 10 <sup>3</sup>	52
36	<b>60</b> (0.125)	H	BA, 1.1	TEA, 1.1	NMP		1/10	80	100	800	8.00 x 10 <sup>3</sup>	11c
37	<b>60</b> (2 x 10 <sup>-4</sup> )	H	BA, 1.1	TEA, 1.1	NMP			80	100	5 x 10 <sup>5</sup>		11c
38	<b>61</b> (1 x 10 <sup>-5</sup> )	H	EA, 1.2	TBA, 1	DMA		24	140	41	4.10 x 10 <sup>6</sup>	1.71 x 10 <sup>5</sup>	23b
39	<b>64</b> (5 x 10 <sup>-5</sup> )	H	MA	TBA	NMP		100	120	98	1.18 x 10 <sup>6</sup>	1.17 x 10 <sup>4</sup>	53

**Table 1.1 (Continued):** Key homogeneous catalysts reported for the vinylation of iodoarenes

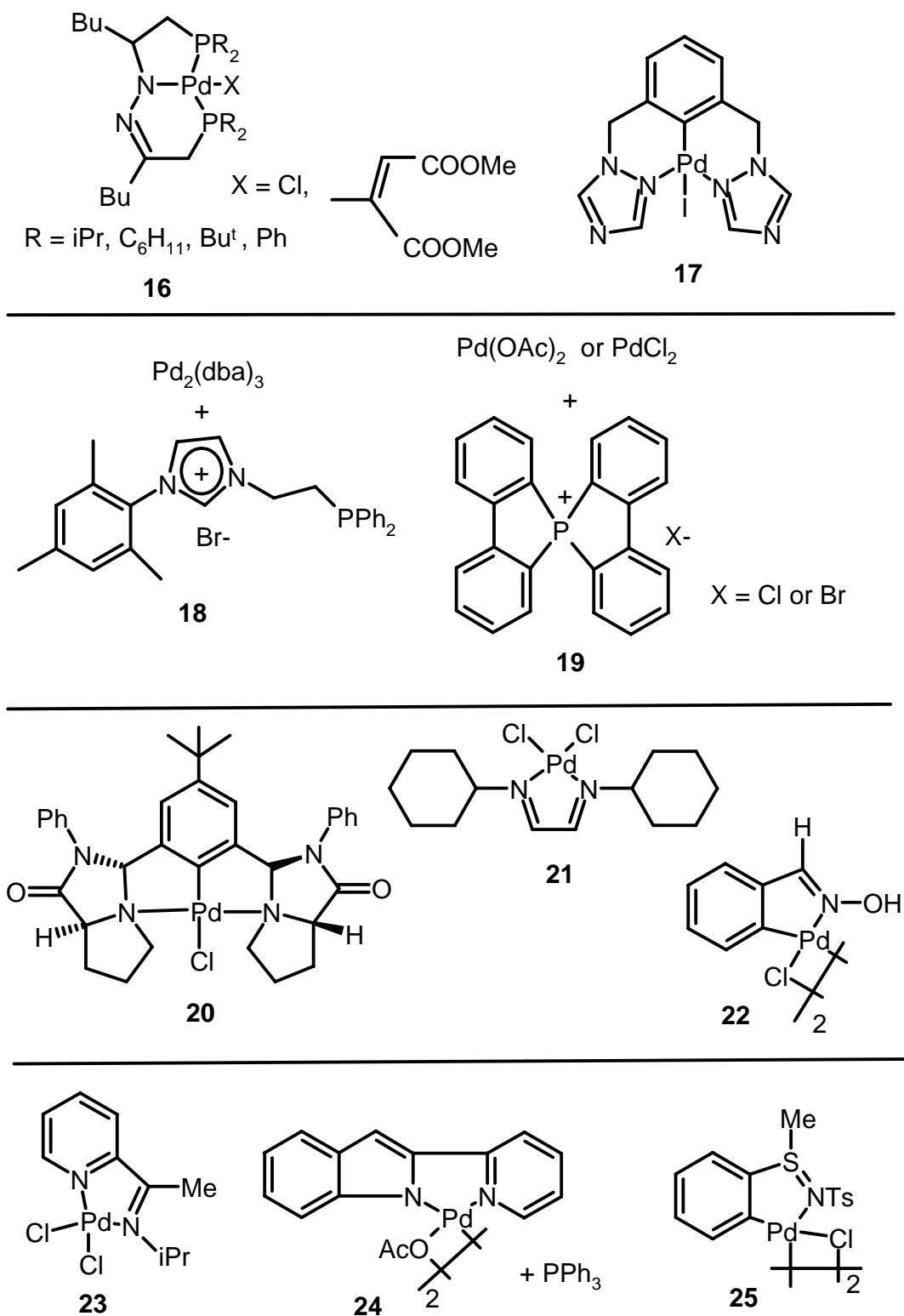
No	Cat, (Mol%)	R	Olefin, Equiv	Base, Equiv	Solvent	Additive, Mol%	Ti, h	Tm, °C	Yield, %	TON	TOF, h <sup>-1</sup>	Ref
40	<b>65</b> (0.001)	H	BA <sup>t</sup> , 1.2	TEA, 1.2			17	100	72	7.19 x 10 <sup>4</sup>	4.22 x 10 <sup>3</sup>	54
41	<b>71</b> (1 x 10 <sup>-4</sup> )	H	BA, 2	K <sub>2</sub> CO <sub>3</sub>	Xylene		48	130	100	1.00 x 10 <sup>6</sup>	2.08 x 10 <sup>4</sup>	55
42	<b>73</b> (3.5 x 10 <sup>-5</sup> )	H	MA, 1.2	TEA, 1.4	NMP		38	140	100	2.86 x 10 <sup>6</sup>	7.52 x 10 <sup>4</sup>	56
43	<b>76</b> (1 x 10 <sup>-4</sup> )	H	BA, 1.5	NaOAc, 2	DMA		39	130	90	9.00 x 10 <sup>5</sup>	2.30 x 10 <sup>4</sup>	57
44	<b>70</b> (1 x 10 <sup>-6</sup> )	H	BA, 2	K <sub>2</sub> CO <sub>3</sub> , 2	DMF		20	130	99	1.00 x 10 <sup>8</sup>	4.95 x 10 <sup>6</sup>	58

Table 1.1 (Continued):

$\text{PdCl}_2$ <b>1</b>	Pd black <b>2</b>	$\text{Pd}(\text{OAc})_2$ <b>3</b>	$\text{Pd}(\text{OAc})_2/\text{PPh}_3$ <b>4</b>	$\text{Pd}(\text{OAc})_2/\text{P}(\text{o-Tol})_3$ <b>5</b>
$\text{Pd}_2(\text{dba})_3/\text{P}(\text{o-Tol})_3$ <b>6</b>		Pd solution stabilized with 20 % HCl <b>7</b>		$\text{PdCl}_2(\text{SEt}_2)_2$ <b>8</b>
$\text{Pd}_2(\text{dba})_3/\text{P}(\text{Bu}^t)_3$ <b>9</b>	 <b>10</b>		 <b>11</b>	
 R = $\text{CH}_2\text{C}_6\text{H}_2(\text{CH}_3)_3$ 2,4,6 or $(\text{CH}_2)_2\text{OMe}$ PR <sub>3</sub> = PPhMe <sub>2</sub> , PPh <sub>3</sub> , PPh <sub>2</sub> Me <b>12</b>		 X = Cl, Br, I <b>13</b>		
 n = 1, 2, 3, 4 <b>14</b>		 R = n-Butyl or benzyl <b>15</b>		

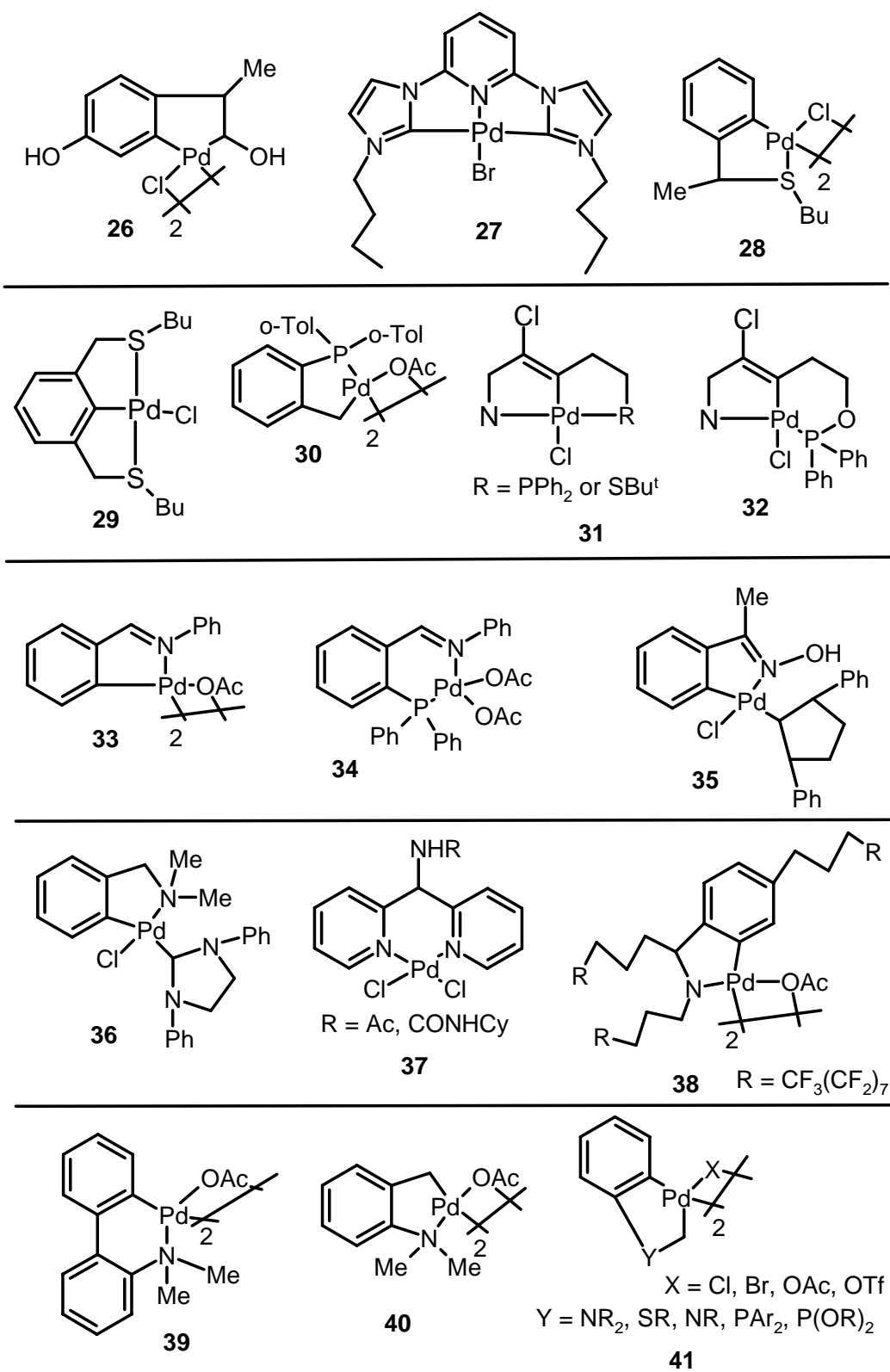
Homogeneous catalyst systems employed for the Heck reaction

Table 1.1 (Continued):



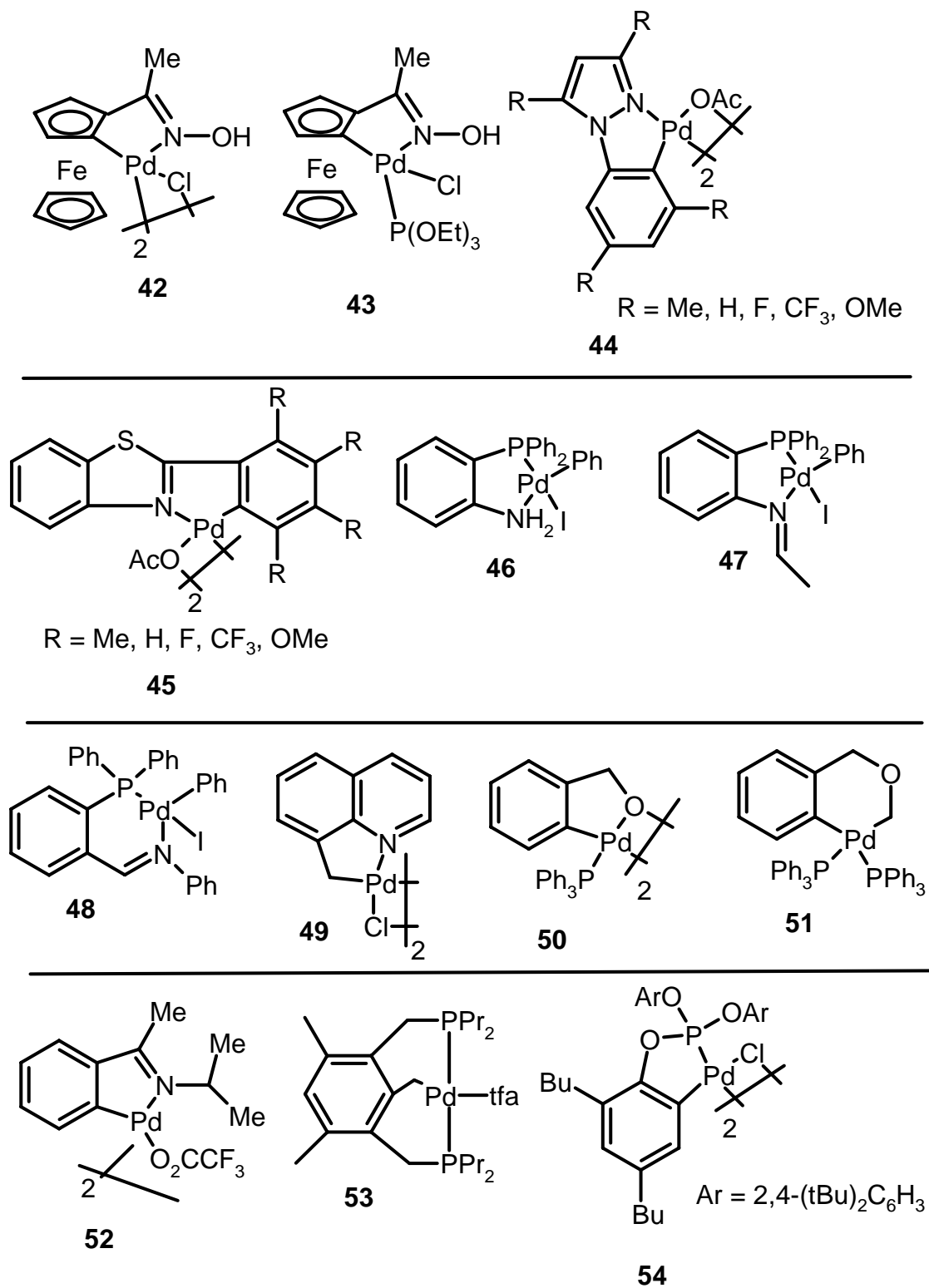
Homogeneous catalyst systems employed for the Heck reaction

Table 1.1 (Continued):



Homogeneous catalyst systems employed for the Heck reaction

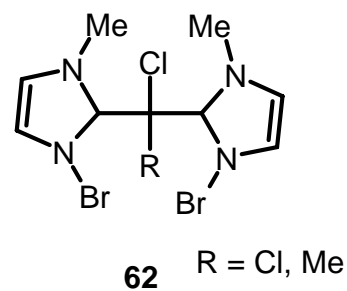
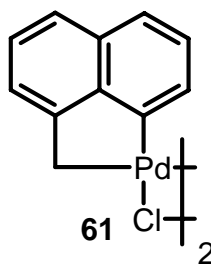
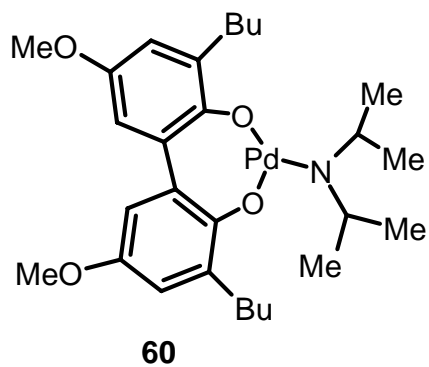
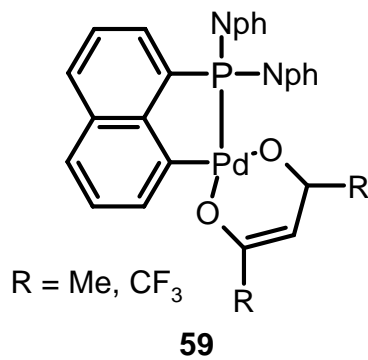
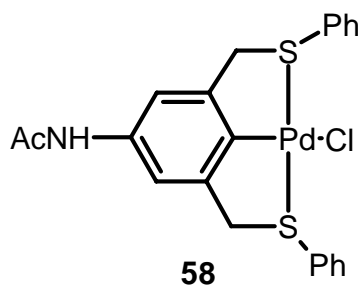
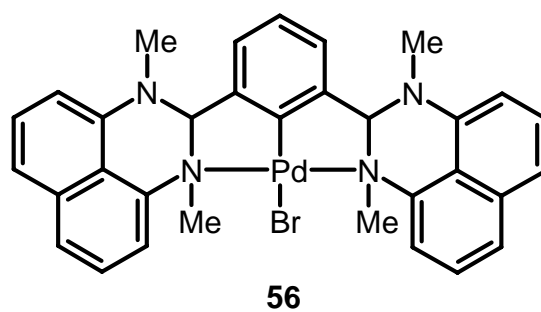
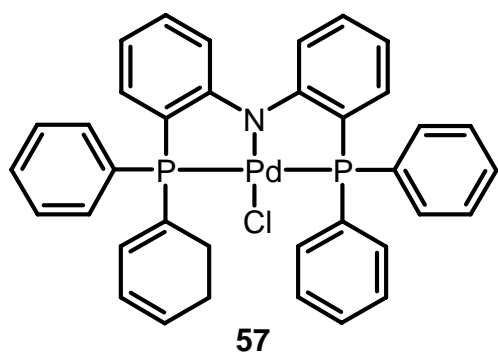
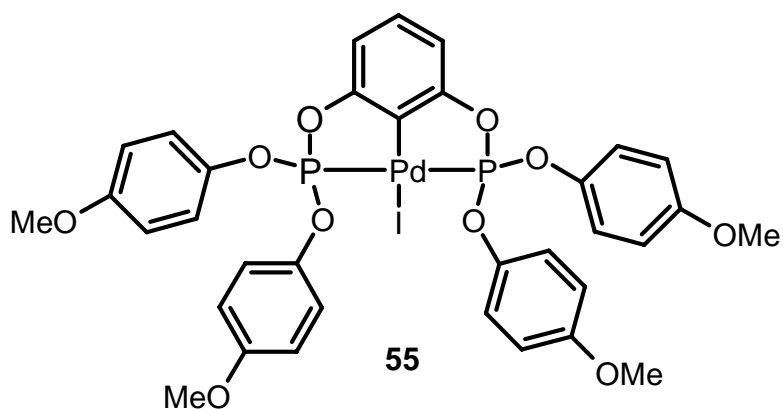
Table 1.1 (Continued):



Homogeneous catalyst systems employed for the Heck reaction

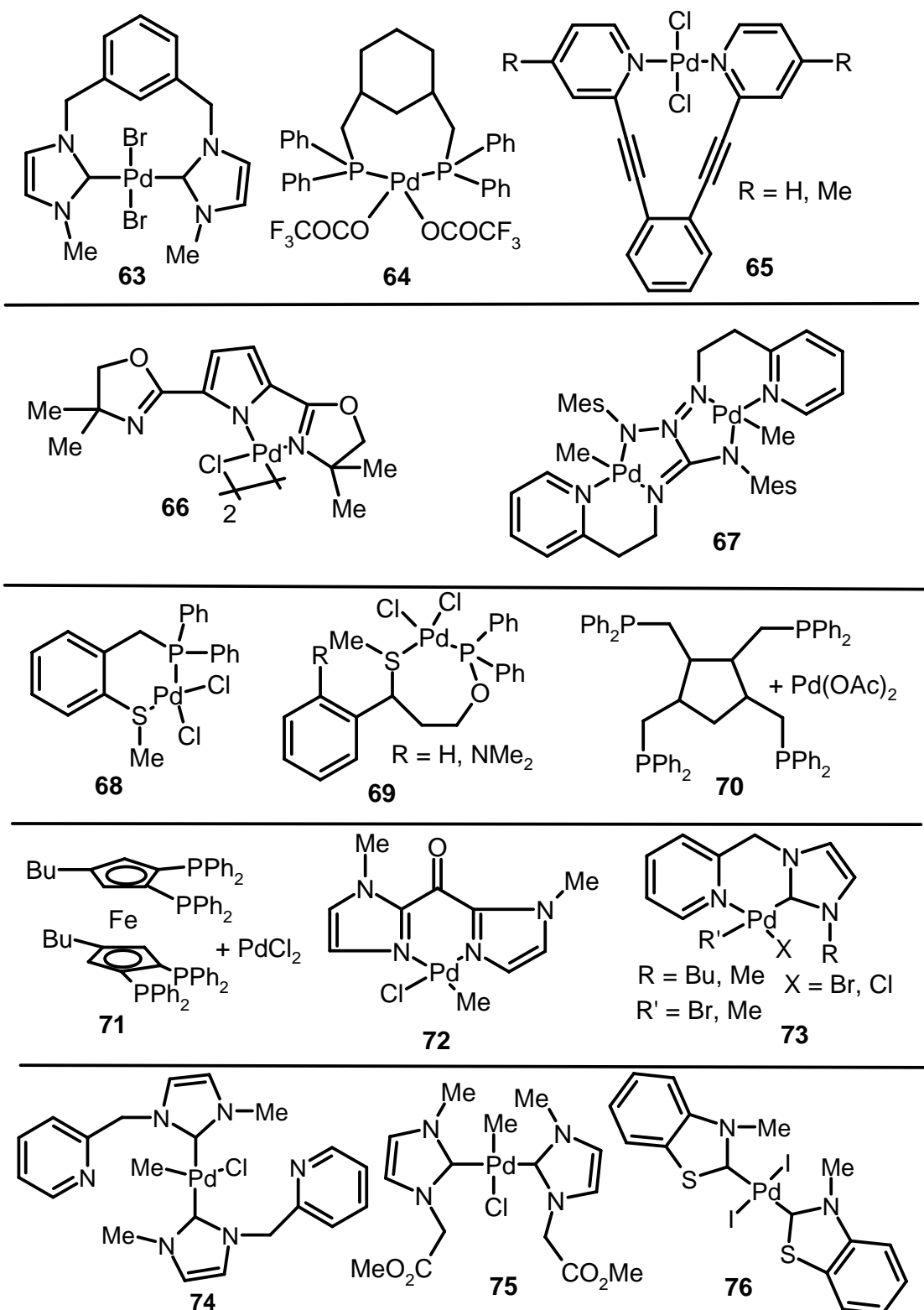


Table 1.1 (Continued):

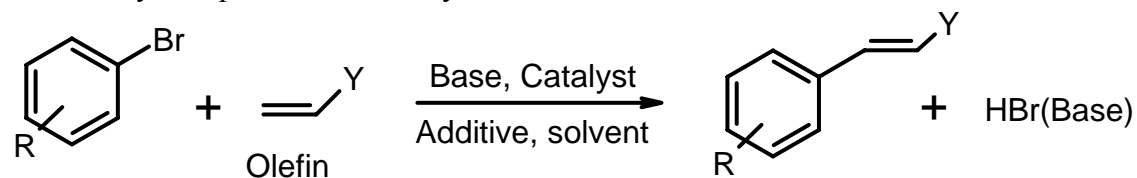


Homogeneous catalyst systems employed for the Heck reaction

Table 1.1 (Continued):



Homogeneous catalyst systems employed for the Heck reaction

**Table 1.2:** Key homogeneous catalysts reported for the vinylation of bromoarenes

No	Cat, (Mol%)	R	Olefin, Equiv	Base, Equiv	Solvent	Additive, Mol%	Ti, h	Tm, °C	Yield, %	TON	TOF, h <sup>-1</sup>	Ref
1	<b>4</b> (1)	4-NO <sub>2</sub>	MA	TBA			7	100	73	73	10	8a
2	<b>4</b> (0.05)	H	AA	TEA, 1.25			2	150	74	1.48 x 10 <sup>3</sup>	740	8c
3	<b>5</b> (1)	4-OH	MA	TEA			22	75	98	98	4	8d
4	<b>3</b> (0.0024)	H	Sty, 2	K <sub>3</sub> PO <sub>4</sub> , 1.4	DMA		44	140	95	3.85 x 10 <sup>4</sup>	875	59
5	<b>10</b> (2.73 x 10 <sup>-5</sup> )	4-NO <sub>2</sub>	EA, 1.5	TEA, 1	DMA	TBAB, 100	55	140	64	2.34 x 10 <sup>6</sup>	4.26 x 10 <sup>4</sup>	37
6	<b>11</b> (1.5)	4-CHO	Sty, 1.5	Cs <sub>2</sub> CO <sub>3</sub> , 1.5	Dioxane		2.5	80	90	60	25	60
7	<b>15</b> (1)	H	MA, 1.5	TEA, 2	NMP		21	116	45	45	2	38
8	<b>16</b> (1.12 x 10 <sup>-4</sup> )	4-CN	Sty, 1.2	TEA, 1.5	DMA		88	150	77	6.82 x 10 <sup>5</sup>	7.71 x 10 <sup>3</sup>	61
9	<b>7</b> (9 x 10 <sup>-4</sup> )	4-OMe	Sty, 2	K <sub>2</sub> CO <sub>3</sub> , 3.7	H <sub>2</sub> O		1/3	hv, 170	90	8.89 x 10 <sup>4</sup>	5.3 x 10 <sup>5</sup>	62
10	<b>8</b> (0.002)	4-COMe	Sty, 1.2	NaOAc, 1.4	DMA	TBAB, 20	13	120	100	5.00 x 10 <sup>4</sup>	3.12 x 10 <sup>3</sup>	39
11	<b>17</b> (0.0011)	4-CHO	BA	NaOAc	DMA	TBAB, 100	6	125	95	8.60 x 10 <sup>4</sup>	1.38 x 10 <sup>4</sup>	63
12	<b>18</b> (0.5)	4-CHO	BA, 1.4	Cs <sub>2</sub> CO <sub>3</sub> , 2	DMA		¼	120	100	200	800	29
13	<b>5</b> (5 x 10 <sup>4</sup> )	4-NO <sub>2</sub>	AA, 1.1	NaOAc, 1.1	DMF		6	130	67	1.30 x 10 <sup>5</sup>	2.23 x 10 <sup>4</sup>	8c

For the structures of the catalyst complexes refer to Table 1.1

**Table 1.2 (Continued):** Key homogeneous catalysts reported for the vinylation of bromoarenes:

No	Cat, (Mol%)	R	Olefin, Equiv	Base, Equiv	Solvent	Additive, Mol%	Ti, h	Tm, °C	Yield, %	TON	TOF, h <sup>-1</sup>	Ref
14	<b>21</b> (4 x 10 <sup>-4</sup> )	H	Sty, 1	K <sub>2</sub> CO <sub>3</sub> , 1.1	NMP		48	140	15	3.76 x 10 <sup>4</sup>	783	40
15	<b>22</b> (5 x 10 <sup>-4</sup> )	H	Sty, 1.2	K <sub>2</sub> CO <sub>3</sub> , 1.1	NMP		48	140	52	7.80 x 10 <sup>4</sup>	1.62 x 10 <sup>3</sup>	40
16	<b>30</b> (1 x 10 <sup>-4</sup> )	4-COMe	BA, 1.4	NaOAc, 1.1	DMA	TBAB, 20	24	130	99	1.00 x 10 <sup>6</sup>	4.17 x 10 <sup>4</sup>	19b
17	<b>31/32</b> (1 x 10 <sup>-4</sup> )	4-CN	BA, 1.2	NaOAc, 1.4	DMA	TBAB, 20	24	150	63	6.30 x 10 <sup>5</sup>	2.62 x 10 <sup>4</sup>	44
18	<b>33/34</b> (0.01)	H	Sty, 1.5	NaOAc, 1.5	DMA		24	140	97	9.70 x 10 <sup>3</sup>	404	64
19	<b>35</b> (1.6 x 10 <sup>-3</sup> )	H	Sty, 1.2	NaOAc, 1.2	NMP		24	150	80	5.00 x 10 <sup>4</sup>	2.08 x 10 <sup>3</sup>	65
20	<b>37</b> (0.01)	H	BA <sup>t</sup> , 1.5	Pr <sub>2</sub> NH, 1.4	NMP	TBAB, 50	92	140	93	9.30 x 10 <sup>3</sup>	101	66
21	<b>38</b> (7.1 x 10 <sup>-5</sup> )	4-Ac	MA, 1.25	TEA, 2	DMF		48	140	49	2.60 x 10 <sup>5</sup>	5.41 x 10 <sup>3</sup>	32d
22	<b>41</b> (0.001)	4-CN	BA, 1.2	NaOAc, 1.4	DMA	TBAB, 20	24	150	100	1.00 x 10 <sup>5</sup>	4.16 x 10 <sup>3</sup>	45
23	<b>42/43</b> (0.005)	H	EA, 2	NaOAc, 2	NMP			150	79	1.52 x 10 <sup>4</sup>		46
24	<b>46/47/48</b> (3.5 x 10 <sup>-4</sup> )	4-COMe	MA, 1.5	TEA, 1	NMP	NaI	70	140	35	1.00 x 10 <sup>5</sup>	1.42 x 10 <sup>3</sup>	48

For the structures of the catalyst complexes refer to Table 1.1

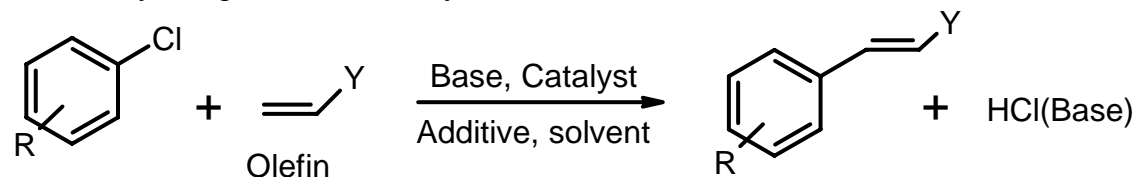
**Table 1.2 (Continued):** Key homogeneous catalysts reported for the vinylation of bromoarenes

No	Cat, (Mol%)	R	Olefin, Equiv	Base, Equiv	Solvent	Additive, Mol%	Ti, h	Tm, °C	Yield, %	TON	TOF, h <sup>-1</sup>	Ref
25	<b>54</b> (1 x 10 <sup>-5</sup> )	4-COMe	Sty, 1.4	NaOAc, 1.1	DMA		69	180	57	5.75 x 10 <sup>6</sup>	8.33 x 10 <sup>4</sup>	32c
26	<b>56</b> (1 x 10 <sup>-3</sup> )	4-NO <sub>2</sub>	MA	TEA	DMF		12	110	67	6.70 x 10 <sup>4</sup>	5.58 x 10 <sup>3</sup>	32b
27	<b>57</b> (0.002)	4-COMe	Sty	Cy <sub>2</sub> NMe	NMP		110	160	67	3.36 x 10 <sup>4</sup>	305	51
28	<b>62</b> (0.001)	4-COMe	BA, 1.4	NaOAc, 1.1	DMA		24	120	18	1.80 x 10 <sup>4</sup>	750	67
29	<b>63</b> (1 x 10 <sup>-4</sup> )	4-COMe	BA, 1.4	NaOAc, 1.1	DMA	TPAB, 20	93	120	97	9.70 x 10 <sup>5</sup>	1.04 x 10 <sup>4</sup>	67
30	<b>64</b> (2.6 x 10 <sup>-4</sup> )	H	MA	TBA	NMP		79	140	94	2.35 x 10 <sup>5</sup>	2.97 x 10 <sup>3</sup>	53
31	<b>66</b> (0.005)	H	Sty	K <sub>3</sub> PO <sub>4</sub>	NMP		120	110	4704	9.48 x 10 <sup>3</sup>	79	68
32	<b>67</b> (2 x 10 <sup>-4</sup> )	4-COMe	BA, 1.08	NaOAc, 1.1	DMA		15	120	87	4.35 x 10 <sup>5</sup>	2.9 x 10 <sup>4</sup>	69
33	<b>68</b> (8 x 10 <sup>-5</sup> )	H	Sty, 1.2	Na <sub>2</sub> CO <sub>3</sub>	DMF		72	120	99	1.25 x 10 <sup>6</sup>	1.73 x 10 <sup>4</sup>	70
34	<b>69</b> (0.001)	4-NO <sub>2</sub>	Sty, 1.5	NaOAc, 2	DMF		24	130	100	1.00 x 10 <sup>5</sup>	4.16 x 10 <sup>3</sup>	71
35	<b>70</b> (0.001)	C <sub>2</sub> H <sub>4</sub>	BA, 2	K <sub>2</sub> CO <sub>3</sub> , 2	DMF		24	130	66	6.60 x 10 <sup>4</sup>	3.30 x 10 <sup>3</sup>	72
36	<b>72</b> (0.001)	4-COMe	BA	NaOAc	DMA		24	120	100	1.00 x 10 <sup>5</sup>	4.16 x 10 <sup>3</sup>	73

For the structures of the catalyst complexes refer to Table 1.1

**Table 1.2 (Continued):** Key homogeneous catalysts reported for the vinylation of bromoarenes:

No	Cat, (Mol%)	R	Olefin, Equiv	Base, Equiv	Solvent	Additive, Mol%	Ti, h	Tm, °C	Yield, %	TON	TOF, h <sup>-1</sup>	Ref
37	<b>74</b> (0.03)	4-COMe	BA, 1.1	NaOAc, 1.1	DMA		4.5	140	98	3.27 x 10 <sup>3</sup>	726	74
38	<b>75</b> (1 x 10 <sup>-4</sup> )	4-COMe	BA, 1.1	NaOAc, 1.1	DMA		140	140	70	7.00 x 10 <sup>5</sup>	5.00 x 10 <sup>3</sup>	74
39	<b>70</b> (1 x 10 <sup>-7</sup> )	3,5-diCF <sub>3</sub>	BA, 2	K <sub>2</sub> CO <sub>3</sub> , 2	DMF		72	130	21	1.00 x 10 <sup>9</sup>	3.8 x 10 <sup>6</sup>	58

**Table 1.3:** Key homogeneous catalysts reported for the vinylation of chloroarenes

No	Cat, (Mol%)	R	Olefin, Equiv	Base, Equiv	Solvent	Additive, Mol%	Ti, h	Tm, °C	Yield, %	TON	TOF, h <sup>-1</sup>	Ref
1	<b>6</b> (0.5)	4-CN	EA, 1.1	TEA, 1.1	DMF	NaI 100 + NiBr <sub>r</sub> 20	18	140	85	170	10	75
2	<b>10</b> (0.02)	4-NO <sub>2</sub>	EA, 1.5	TEA, 1	DMA	TBAB, 100	10	140	73	3.65 x 10 <sup>3</sup>	365	37

For the structures of the catalyst complexes refer to Table 1.1

**Table 1.3 (Continued):** Key homogeneous catalysts reported for the vinylation of chloroarenes:

No	Cat, (Mol%)	R	Olefin, Equiv	Base, Equiv	Solvent	Additive, Mol%	Ti, h	Tm, °C	Yield, %	TON	TOF, h <sup>-1</sup>	Ref
3	<b>12</b> (1.5)	4-OMe	Sty, 1.5	Cs <sub>2</sub> CO <sub>3</sub> , 1.5	Dioxane		4	80	90	60	15	60
4	<b>16</b> (0.13)	4-CN	Sty, 1.2	TEA, 1.5	DMA		61	150	99	729	12	61
5	<b>17</b> (0.5)	4-NO <sub>2</sub>	BA	NaOAc	DMA	TBAB, 100	2	140	73	146	73	63
6	<b>9</b> (1.5)	4-COMe	MA	Cs <sub>2</sub> CO <sub>3</sub> , 1.1	Dioxane		21	120	84	56	2.5	18
7	<b>19</b> (2)	H	Sty	NaOAc	NMP	DMG, 12	12	150	96	48	4	76
8	<b>22</b> (0.2)	4-NO <sub>2</sub>	Sty, 1.2	K <sub>2</sub> CO <sub>3</sub> , 1.1	NMP		40	140	69	350	8	40
9	<b>27</b> (0.0002)	4-CHO	Sty, 1.4	NaOAc, 1.1	DMA	TBAB, 20	22	200	15	7.50 10 <sup>4</sup> x	3.41 10 <sup>3</sup> x	31b
10	<b>28/29</b> (0.002)	4-NO <sub>2</sub>	BA, 1.2	NaOAc, 1.4	DMA	TBAB, 20	2	170	10	5.00 10 <sup>3</sup> x	2.50 10 <sup>3</sup> x	43
11	<b>30</b> (1 x 10 <sup>-3</sup> )	4-COMe	BA, 1.4	NaOAc, 1.1	DMA	TBAB, 20	72	130	40	4.00 10 <sup>4</sup> x	555	19b
12	<b>36</b> (0.018)	4-CN	Sty, 1.2	NaOAc, 1.2	NMP		24	150	73	4.11 10 <sup>3</sup> x	171	65
13	<b>39/40</b> (0.5)	4-OMe	BA	Na <sub>2</sub> CO <sub>3</sub>	DMA		20	140	71	150	7.5	77
14	<b>41</b> (0.1)	4-NO <sub>2</sub>	BA, 1.2	NaOAc, 1.4	DMA	TBAB, 20	24	150	100	1.00 10 <sup>3</sup> x	41	45

For the structures of the catalyst complexes refer to Table 1.1

For the Heck reaction, maximum attention has been focussed on palladium complex catalysts. After the initial studies with phosphine ligands, the discovery of palladacycle catalysts for these reactions provided a fresh thrust for the innovations in catalyst design to achieve very high TONs. The present highest TON attained under homogeneous reaction conditions is more than half a billion for the reaction of iodobenzene with methyl acrylate<sup>33</sup>. In spite of such high TONs achieved under homogeneous Heck reaction conditions, the basic problem of catalyst-product separation persists. The traditional techniques like distillation of the reaction mixture and solvent extraction not only add to the cost of catalyst recovery but also lead to the decomposition of the catalyst. Instead of using these techniques, the use of heterogeneous catalysts, where the catalyst and the products are in separate phase, can provide an easier and cheaper route for catalyst-product separation.

### **1.2.2. Heterogeneous Catalysis**

Although development of highly active catalysts can enhance the productivity, another approach to do so is the design of a catalyst system in which the catalyst can be easily separated from the products and recycled. Thus a higher cumulative productivity (TON) is achievable. It is therefore preferable that catalyst be reused several times before being regenerated in this strategy<sup>78</sup>.

Heck reaction presents a tough challenge for the design of recyclable catalysts. This is due to various factors. The reaction itself requires at least four reagents (electrophile, unsaturated substrate, base, and a solvent) besides promoters and catalyst. Apart from the product, there is the formation of a conjugate acid of the base and the leaving group, which yields a salt. From the point of view of process development, the heterogenisation of the catalyst seems a possible strategy to achieve an efficient and very stable catalyst. A number of attempts to design such catalysts have been made and various methods have been reported towards achieving this goal. These efforts on designing a recyclable catalyst for the Heck reaction can broadly be divided into two categories: liquid-liquid systems and solid-liquid systems.



### 1.2.2.1. Liquid- Liquid system (Biphasic catalysis)

In the biphasic liquid-liquid system, the reagents and products are held in one phase (organic) while the catalyst is held in a second non-miscible phase like water or other hydroxylic solvents of which ethylene glycol is the most common<sup>79a-b</sup>. A biphasic toluene-ethylene glycol system has been reported for the Pd catalyzed Heck reaction of iodobenzene with acrylates and styrene using a TPPTS ligand. When two equivalents of the TPPTS ligand are added to the reaction mixture, the palladium catalyst decomposes to Pd metal. It has been reported that this system requires four equivalents of TPPTS to prevent the palladium from leaching into the organic phase and achieve stable catalysis<sup>80a-b</sup>.

Controlled phase separation can also be achieved by selecting solvents with temperature dependent miscibility and by designing ligands with temperature dependent solubility<sup>81</sup>. Carbohydrates are hydrophilic at ambient temperature but lose their water of hydration and become hydrophobic on heating. This property of carbohydrates has been successfully applied to design ligands which have been used for Heck reaction. The use of triphenylphosphine attached to the residues of natural carbohydrates (D-glucose, D-galactose, D-N-acetylglucosamine) were tested as ligands for Pd catalyzed Heck reaction and found to be more active than TPPTS ligands under the same conditions. This is because at higher temperature, due to the presence of the carbohydrate based ligands, the catalyst migrates to the organic phase where the reaction takes place. On cooling, the entire catalyst returns to the polar phase and is easily separated<sup>82</sup>.

Another way of increasing the productivity of the biphasic catalytic systems is to increase the area of contact between two phases. This can be done by distributing one of the phases over a solid support with a high surface area. This type of system is called Supported Liquid Phase Catalysis (SLPC) or more specifically Supported Glycol Phase Catalysis (SGPC)<sup>83a-c</sup>. The catalyst is dissolved in the supported liquid phase. Usually mesoporous silica with a narrow pore size distribution is used as a support. The support is impregnated with a solution of Pd(OAc)<sub>2</sub> or PdCl<sub>2</sub> and TPPTS or TPPMS ligands in ethylene glycol. The resulting catalyst had a modest activity for the reaction of iodoarenes with methyl acrylate giving TONs of up to 100. The catalyst showed less than 1 ppm palladium leaching into the reaction mixture.

### 1.2.2.2. Solid- Liquid systems

In solid-liquid phase catalysis, the catalyst is bound to solid supports. The difference between the liquid-liquid and solid-liquid phase catalysis is the degree of mobility of the catalyst. In liquid- liquid systems, the catalyst is in liquid phase and hence retains diffusional mobility within the phase. In solid- liquid systems, the catalyst is bound to a solid support and hence has no mobility of its own. Thus, the solid- liquid systems are more persistent and allow for better and more recycles. The disadvantage is that the limited mobility imposes severe mass transfer limitations on the rate of catalytic process<sup>14</sup>.

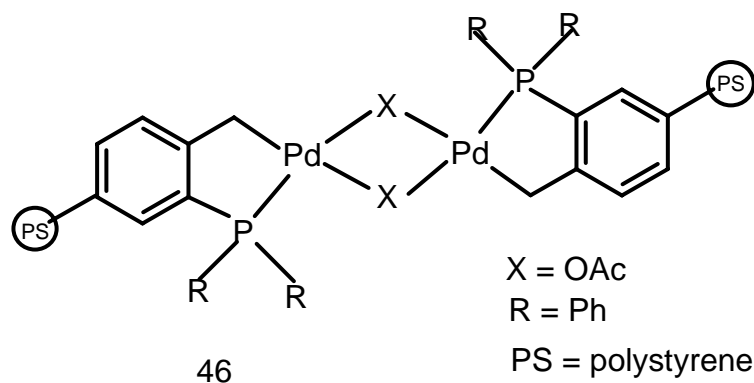
#### 1.2.2.2.1. Palladium nano particles as catalysts

In phosphine free and under-ligated systems, the degradation of palladium complex occurs by formation of particles of palladium metal<sup>84</sup>. Several recent reports describe the catalytic activity of palladium nano particles obtained by different methods in Heck reaction<sup>85a-g</sup>. Palladium does not readily afford stable reproducible sols in the absence of stabilizing agents. Therefore in the reaction mixture the formation of metallic particles, if started, swiftly goes to full sedimentation of palladium metal sediments of unknown morphology. The growth of particles can not be stopped at monodispersed sols<sup>14</sup>.

Several methods of palladium sol stabilization have been published. In most of the methods palladium salts are reduced in the presence of either surfactants or polymers, the molecules of which form a protective layer around the palladium particles, thus preventing their further growth. Surfactants are absorbed at the surface of palladium particle by the interaction of the head groups with the metal. Thus the nano particles are exposed to the solvent by hydrocarbon tails, making these particles dispersible in the organic solvents but not in water<sup>85a-d</sup>. The sols are obtained under oxygen free conditions and consist of large clusters of palladium with highly reactive palladium atoms on the surface. Such colloids are good catalysts for Heck reaction, even catalyzing the reaction of aryl chlorides giving 55% conversion (TON: 16) for the reaction of chlorobenzene with styrene at 155°C, thus corroborating the conclusion that palladium metal is enough to catalyze the Heck reaction<sup>85c</sup>. The TONs of 10<sup>5</sup> have been reported with palladium nano particles for the reaction of 4'-bromobenzaldehyde with n-butyl acrylate at 140°C<sup>85f</sup>.

### 1.2.2.2.2. Palladium complexes bound to polymeric supports as catalysts

Palladium catalyst based on triphenylphosphine bonded polystyrene resin has been reported for the arylation of olefins by iodoarenes. The catalyst showed better activity than its soluble counterpart when compared at a 50% conversion level of iodobenzene<sup>86</sup>. No attempt to optimize the reaction conditions was made and the reactions were carried out at 1 mol% of Pd loading. In a similar development, palladacycle catalyst bound to polystyrene (Scheme 1.12) was shown to be an active catalyst for the arylation of acrylates with bromo and iodo arenes. The TON of 50000 was reported for the reaction of 2'-bromobenzaldehyde with methyl acrylate after 10 h of reaction at 100°C (Table 1.4 (heterogeneous catalysts for vinylation of haloarenes), entry 15). The catalyst was recycled seven times with triethylamine as a base without any loss in activity<sup>87</sup>.



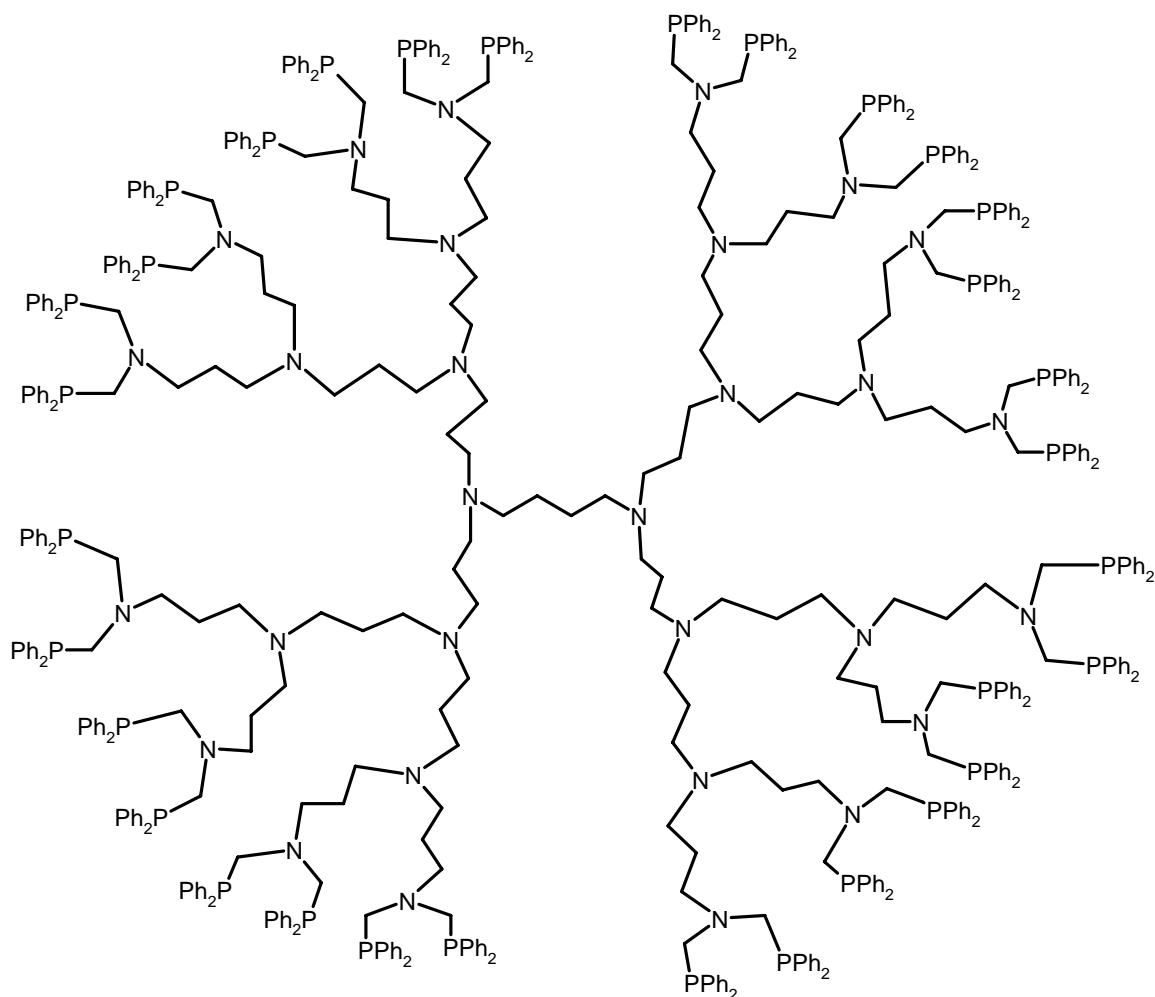
**Scheme 1.12**

Another study on polymer supported 1,2-bis(diisopropylphosphino)benzene as a ligand has been reported for preparing a palladium catalyst for the reaction of iodobenzene with methyl acrylate. This catalyst showed higher TON values (780) than the soluble palladium complex with the corresponding ligand (TON: 50) under the similar reaction conditions. This is because the catalyst is more stable towards the formation of palladium black and hence has a longer life time<sup>88</sup>.

Another set of supports reported for Heck vinylation reaction are the dendrimers. Dendrimers can be better supports than linear or irregularly branched macromolecules because they are individual well characterized compounds and hence the catalysts formed from such ligands have definite structures. Another advantage of dendrimer bound metals is that the catalytic centre is fully exposed to the reaction environment. Commercially

available dendrimer based on 1,4-diaminobutane bearing peripheral amino groups was derivatized with diphenylphosphine residues to give a macromolecule with 16 chelating diphosphine units (Scheme 1.13) which can bind with transition metals to form complexes<sup>89</sup>. These types of catalysts can be precipitated from the reaction mixture by addition of weakly interacting solvents. A simple addition of ether can lead to the precipitation of these catalysts which can then be recycled.

A comparison between homogeneous and polymer bound dichloropalladiumdi-(pyrid-2-yl)amide complexes has been reported. Where homogeneous catalysts showed the formation of palladium black, no such observation was made for the polymer bound species. This was explained on the basis of surplus ligand available in the case of polymer supported catalyst. This surplus ligand could bind to the palladium after it had leached into the solution, thus facilitating the recovery of the catalyst precursor. Reproducible kinetics was observed on recycling. These results point to a truly recoverable catalyst<sup>90</sup>. TON of  $2.06 \times 10^5$  was obtained for the reaction of iodobenzene with styrene and TON of  $1.57 \times 10^5$  was observed for the reaction of cyanobromobenzene with styrene. No reaction occurred when chloroarenes were used as the substrates (Table 1.4, entry 40, 41).



Scheme 1.13

### 1.2.2.2.3. Palladium complexes bound to inorganic supports as catalysts

Pd(II) species immobilized on various amine functionalized silicas have been reported as active catalysts for the Heck reaction of aryl iodides with up to 10 recycles in some cases. Silica is generally functionalized with poly(benzimidazole), N-methylaniline, 2 and 3- methylpyridine moieties<sup>91</sup>. Silica or other supports can also be used for derivatization with phosphine ligands. This approach also suffers from the same drawbacks as in the case of polymer supported catalysts. There is irreversible loss of the catalyst due to degradation of the phosphine and the problem of leaching.

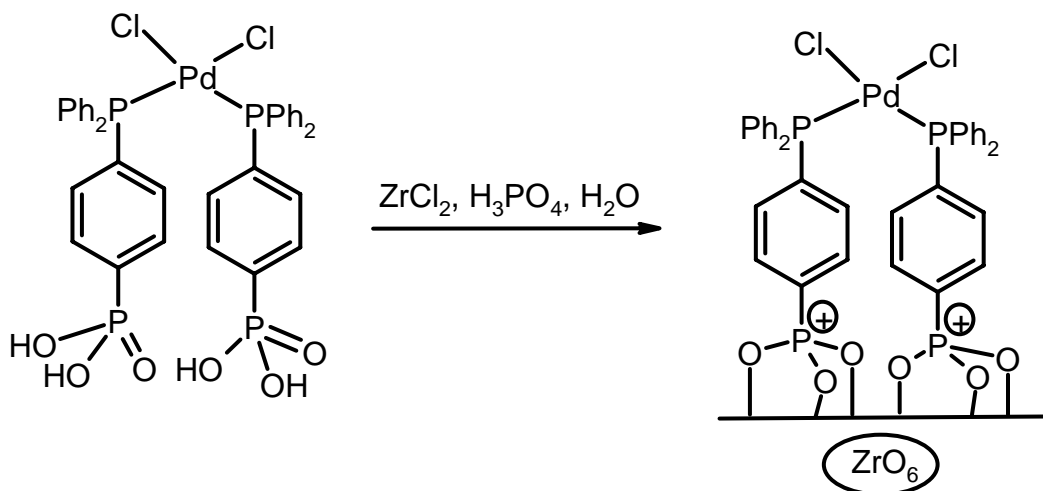
Palladium complexes entrapped in zeolite NaY have been tested as catalysts for the Heck reaction. These zeolite pores are rather narrow (7.4 Å), which sets the limits on the

dimensions of the species involved in catalytic reaction. Of the four complexes of palladium studied,  $\text{Pd}(\text{NH}_3)_4\text{Cl}_2$ , the smallest, gave the most active supported catalyst<sup>92</sup>.  $\text{Pd}(\text{OAc})_2$  and  $[\text{Pd}(\text{C}_3\text{H}_5)\text{Cl}]_2$  were moderately active, while the palladacycle catalysts reported by Herrmann and Beller (Scheme 1.5) apparently choked the zeolite pores to show only marginal activity. Thus, these supports can be used only in the case of phosphine free catalysts. The zeolite supported  $\text{Pd}(\text{NH}_3)_4\text{Cl}_2$  complex showed considerable activity for the reaction of bromoarenes with styrene and methyl acrylate comparable to that of the same catalyst in the homogeneous phase. The catalyst was recycled 3 times and > 93% yields of the product were obtained which corresponds to TON of 930 after 20 h of reaction. The data showed that the entrapped catalyst behaved in the same way as the homogeneous catalyst but was more stable. The narrow zeolite pores impose limitations for the mobility of the species, which may have a strong positive effect by avoiding interactions between the catalytically active species, thus preventing the formation of clusters.

Mesoporous materials can be another type of support for the catalysts<sup>93</sup>. These materials have larger pore size (20- 100 Å) and enormous surface area (up to 1200 m<sup>2</sup>/ gm) which allow the larger molecules to pass through. The binding of the complex to such supports can not be based on physical phenomenon as this would lead to leaching. Therefore, the complexes have to be chemically bound to such materials. These materials grafted with palladium have been reported as catalysts for the Heck reaction of bromo and chloroarenes with butyl acrylate<sup>94a-b</sup>. In this report palladium was uniformly dispersed over the pores of MCM 41 support (26 Å diameter). This catalyst showed high activity for bromoarenes and was also active for chlorobenzene. The highest TONs obtained with this catalyst were 5000 for the Heck reaction of 4'-bromoacetophenone with n-butyl acrylate (Table 1.4, entry 6). The catalyst was recycled for three times only. Further recycles were not conducted as the support structure is fragile.

Another type of mesoporous material reported for supporting the Pd catalyst is based on zirconia. Zirconia based ligands have been used for the synthesis of Pd catalysts for the Heck reaction. The zirconium hydroxide structure can be doped with phosphites, phosphates, or organic phosphonates. The functionalized support facilitates the attachment of the ligands to the pores of the material (Scheme 1.14)<sup>95</sup>. This catalyst was tested for the reaction of iodoarenes with methyl acrylate. This catalyst fully retains its activity over four

recycles, provided all reactions are carried out under inert atmosphere as this catalyst is sensitive to oxidation. No effort to optimize the reaction conditions was made and a TON of 160 was reported for the reaction of iodobenzene with methyl acrylate after 24 h of reaction.

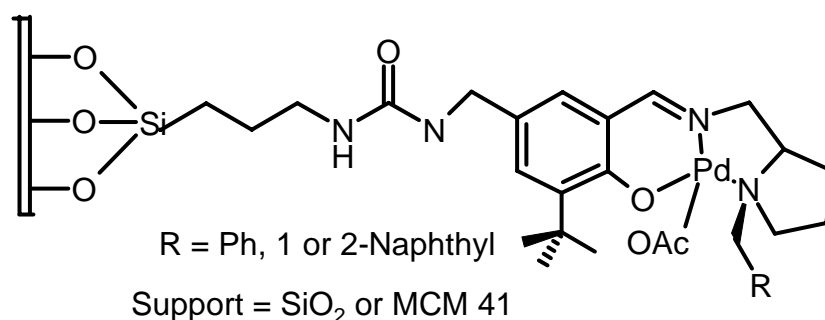


**Scheme 1.14**

Bidentate iminopyridine ligands grafted onto mesoporous silica gel were used as ligands for Pd(II) complex catalysed Heck reaction. An induction period of one hour was observed for the reaction of iodobenzene with methyl acrylate after which the reaction occurred at a very slow rate (4% conversion h<sup>-1</sup>). Further recycles showed no induction period thus indicating that during the first run active catalytic species is formed and is retained during recycles. 5 recycles were carried out and palladium leaching of 1 ppm was observed. Hot filtration test showed marginal activity for the solution phase. Cumulative TONs of 2000 were reported after 5 recycles<sup>96</sup>. In another report PdCl<sub>2</sub> was functionalized by the same ligands and used for the Heck reaction of iodo and bromoarenes. Addition of tetrabutylammonium bromide induced the palladium to leach from the solid support (based on the filtration test results). It is known that TBAB can stabilize the small amount of leached palladium, thus increasing the lifetime of the leached species. This makes it possible for detecting the leached palladium. In the case where no additive is present to stabilize the leached palladium, the palladium can redeposit on the support, thus leading to the conclusion that the entire reaction occurs due to heterogenized palladium species. For

the Heck coupling of 4'-iodoanisole with methyl acrylate using this catalyst, TONs of 10000 after 3 h of reaction were reported (Table 1.4, entry 42)<sup>97</sup>.

In another study tridentate N-N-O Pd(II) complexes (Scheme 1.15) were immobilized on MCM 41. In this catalyst too it was noticed that the solid catalysts had longer lifetime than their homogeneous counterparts. The yields in the second recycle were more than that of the first run. But in subsequent runs the yields decreased slowly. The catalyst was recycled 6 times. The reaction did not occur with less than 2 mol% Pd. Even after 24 h of reaction, the maximum conversions of aryl halide observed were 74%. Elemental analysis of the solid after the reaction showed minimal palladium loss and no activity was observed for the solution after hot filtration<sup>98</sup>.



**Scheme 1.15**

In a report by Davis and co workers<sup>99</sup>, thiol functionalized silica was complexed with Pd(OAc)<sub>2</sub> and used for the reaction of iodobenzene with methyl acrylate in presence of triethylamine as a base. The entire activity was attributed to the leached palladium. The authors made an observation that oxidative addition of iodobenzene led to the leaching of palladium in Pd(0) state whereas, the addition of base led to the leaching of palladium in Pd(II) state.

Use of palladium bipyridyl complex anchored on amine functionalized MCM-41 for the reaction of iodobenzene with n-butyl acrylate in presence of tributylamine base has been reported to give TONs of  $1.05 \times 10^6$  at 100°C (Table 1.4, entry 27). This catalyst was also used for the Heck reaction of 4'-bromoacetophenone with n-butyl acrylate. Similar TONs were observed but at higher temperatures (170°C). The catalyst was active for 5



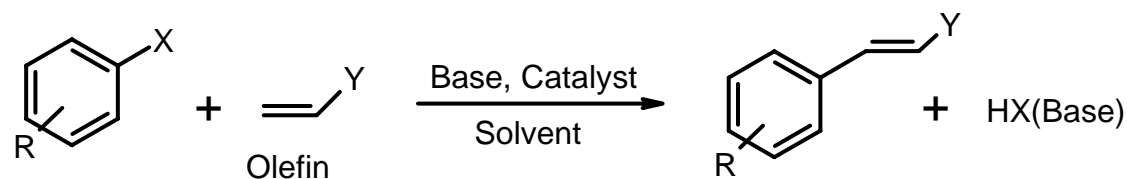
recycles and no leaching was observed. These are the highest TONs reported with heterogeneous catalysts<sup>100</sup>.

#### 1.2.2.2.4. Supported palladium metal catalysts

The use of Pd/C, Pd/Al<sub>2</sub>O<sub>3</sub>, Pd/SiO<sub>2</sub> etc. has been described for the Heck reaction<sup>101a-b</sup>. It has been shown that Pd/C catalyst is active for the arylation of styrene by chloroarenes. The reaction is carried out at 150°C. Low TONs are obtained and addition of PPh<sub>3</sub> leads to the suppression of the reaction. After the publication of these results, Pd/C has been occasionally used for the Heck reaction, but has shown no outstanding results<sup>102</sup>. It has been shown that the entire activity of Pd/C catalyst is due to the palladium leached into the solution. The excellent recovery and recyclability of this catalyst can be attributed to the fast redeposition of the leached palladium on the surface<sup>103a-c</sup>. Controlled experiments where the palladium concentration during the reaction was tracked and correlated to the reaction rates showed that all the activity for the Heck reaction with Pd/C was due to the leached Pd<sup>59a-b</sup>.

The true nature of the active species involved in the case of heterogeneous catalyst is still arguable. For Sonogashira and Suzuki coupling reaction, it was reported that the reactions could be carried out without the addition of palladium. But the authors later found out that the trace amount of palladium present in the commercial Na<sub>2</sub>CO<sub>3</sub> as actually catalyzing the reaction<sup>104a-d</sup>. Another group made the observation that even the trace amount of palladium deposited on the walls of the apparatus from the previous reactions could catalyze the reactions<sup>104e</sup>. These reports go on to show that very small amount of palladium (in some cases even in the range of ppt levels) could catalyze the reaction. This leads to the conclusion that very small amount of leaching from the heterogeneous catalyst can lead to complete conversions in some cases. Thus it is very much possible that the heterogeneous catalysts are just a source of soluble palladium species that in turn acts as the true catalyst

A summary of key heterogeneous catalysts reported for Heck reaction is presented in Table 1.4.

**Table 1.4:** Key heterogeneous catalysts reported for the vinylation of haloarenes:

No	Cat mol%	X	R	Olefin, equiv	Base, equiv	Solvent	Ti, h	Tm, °C	Leaching	Yield, %	Recycle no	TON	TOF, h <sup>-1</sup>	Ref
1	1 (1)	Br	2-CN	AA	NaHCO <sub>3</sub>	NMP		100	-	90	No	90		101a
2	2 (0.003)	Cl	H	Sty	Na <sub>2</sub> CO <sub>3</sub>		5	150	-	32	No	1.07 x 10 <sup>4</sup>	2.13 x 10 <sup>3</sup>	105
3	3 (0.1)	Br	H	Sty, 1.5	NaOAc, 1.2	DMA	20	140	-	33	No	330	16.5	106
4	4 (0.1)	Br	H	Sty, 1.5	NaOAc, 1.2	DMA	20	140	-	49	No	490	24.5	106
5	5 (0.1)	Br	H	Sty, 1.5	NaOAc, 1.2	DMA	20	140	-	8	No	80	4	106
6	6 (0.02)	Br	4-COMe	BA, 1.2	TEA, 1.1	DMA	1	120	-	100	No	5.00 x 10 <sup>3</sup>	5.00 x 10 <sup>3</sup>	94b
7	6 (0.1)	Br	4-NO <sub>2</sub>	Ba, 1.2	TEA, 1.1	DMA	1/4	170	-	99	No	990	3.96 x 10 <sup>3</sup>	107
8	7 (0.2)	Br	4-NO <sub>2</sub>	Sty, 1.5	NaOAc, 1.5	DMA	20	140	-	96	No	480	24	107
9	8 (0.2)	Br	4-F	Sty, 1.5	NaOAc, 1.5	DMA	20	140	-	93	No	465	23.2	107

**Table 1.4 (Continued):** Key heterogeneous catalysts reported for the vinylation of haloarenes

No	Cat mol%	X	R	Olefin, equiv	Base, equiv	Solvent	Ti, h	Tm, °C	Leaching	Yield, %	Recycle no	TON	TOF, h <sup>-1</sup>	Ref
10	9 (0.045)	Br	4-NO <sub>2</sub>	MA, 1.5	TBA, 1.1	DMA	24	120	-	96	1	2.13 x 10 <sup>3</sup>	89	108
11	10 (3)	I	H	BA, 3	TEA, 3	DMA		90	No	70	4	23		109
12	11 (0.1)	I	H	BA, 1.2	Pr <sub>2</sub> Net, 1.2	BMIPF <sub>6</sub>	14	100	-	86	No	860	61	110
13	12 (3)	I	H	MA	TEA	DMF	2	120	-	100	4	33	16	111
14	13 (0.5)	Br	4-COMe	Sty, 1.5	NaOAc, 2	DMF	15	120	0.23ppm	99	2	198	13	112
15	14 (0.002)	Br	4-CHO	MA, 1.5	TEA, 1.5	DMA	10	100	-	100	7	5.00 x 10 <sup>4</sup>	5.00 x 10 <sup>3</sup>	87
16	15 (0.2)	I	H	AA	TEA	HEP/DMA	24	100	No	99	3	495	20	113
17	16 (3)	Cl	H	Sty, 1.2	TBA, 1.2	TBAB	0.5	Hv 130	No	95	-	32	64	114
18	16 (3)	Cl	H	Sty, 1.2	TBA, 1.2	TBAB	30	130	No	98	-	33	1	114
19	16 (3)	Cl	4-OMe	Sty, 1.2	TBA, 1.2	TBAB	1	Hv 130	No	80	5	26	26	114
20	16 (3)	Cl	4-OMe	Sty, 1.2	TBA, 1.2	TBAB	40	130	No	75	5	25	0.75	114
21	17 (0.12)	I	H	BA, 2	TEA, 1.1	DMF	1.5	120	-	99	3	764	509	140a

**Table 1.4 (Continued):** Key heterogeneous catalysts reported for the vinylation of haloarenes

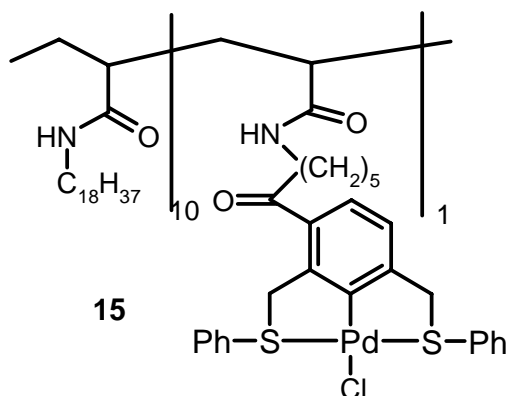
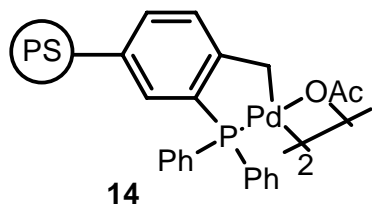
No	Cat mol%	X	R	Olefin, equiv	Base, equiv	Solvent	Ti, h	Tm, °C	Leaching	Yield, %	Recycle no	TON	TOF, h <sup>-1</sup>	Ref
22	18 (5)	I	H	BA	KOAc, 1.1	EG/Tol	24	140	No	70	6	14	0.5	98
23	19 (0.3)	I	H	EA, 1.2	TBA, 1.1	Toluene	2	120	-	100	13	300	150	115
24	20 (0.2)	I	H	AA, 1.1	TBA, 2	DMF	3	90	40%	99	3	495	165	116
25	21 (0.1)	Br	4-F	Sty	NaOAc	DMA	20	140	-	93	2	930	46	92
26	23 (0.1)	Br	4-F	Sty	NaOAc	DMA	20	140	-	3	0	30	1.5	92
27	24 (9.3 x 10 <sup>-5</sup> )	I	H	BA	TBA	NMP	96	100	No	98	5	1.05 x 10 <sup>6</sup>	1.09 x 10 <sup>4</sup>	100
28	24 (9.3 x 10 <sup>-5</sup> )	Br	4-COMe	BA	TBA	NMP	16	170	No	98	-	1.05 x 10 <sup>6</sup>	6.56 x 10 <sup>4</sup>	100
29	25 (0.08)	I	H	BA, 1	TEA, 2	Dioxane	42	100	-	82	-	1.32 x 10 <sup>3</sup>	31	117
30	26 (1)	I	H	BA	TBA	DMA	3	120	-	95	-	95	32	118
31	27 (0.32)	I	H	Sty, 1.1	TBA, 1.1	None	4	100	Yes	90	2	281	140	119
32	27 (0.32)	I	H	Sty, 1.1	NaOAc, 1.1	DMF/H <sub>2</sub> O	4	130	-	89	5	278	69	120
33	27 (0.32)	Br	H	Sty, 1.1	NaOAc, 1.1	DMF/H <sub>2</sub> O	5	130	No reaction on recycle	80	2	250	50	119

**Table 1.4 (Continued):** Key heterogeneous catalysts reported for the vinylation of haloarenes

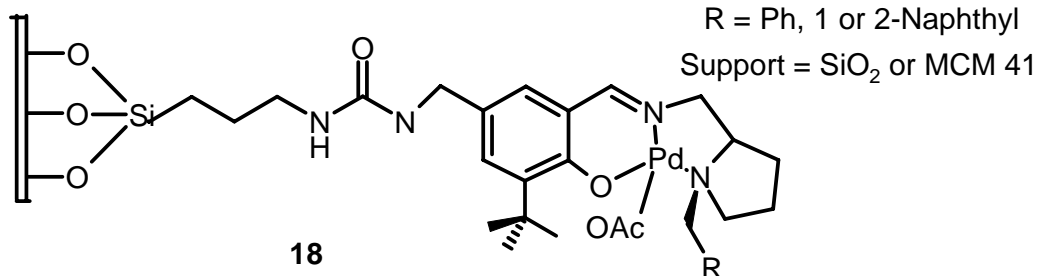
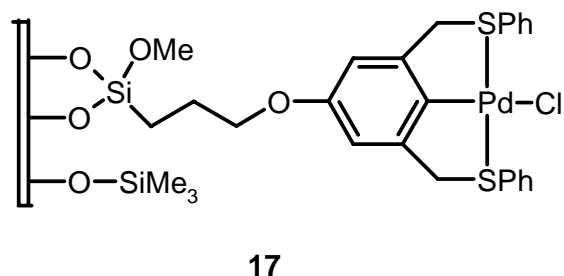
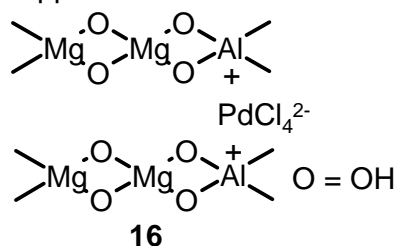
No	Cat mol%	X	R	Olefin, equiv	Base, equiv	Solvent	Ti, h	Tm, °C	Leaching	Yield, %	Recycle no	TON	TOF, h <sup>-1</sup>	Ref
34	29 (1)	I	H	Sty, 1.1	TBA, 1.1	DMF	6	130	-	50	3	50	8	121
35	28 (0.005)	I	H	Sty, 1.1	TBA, 1.1	DMF	3	130	No	80	11	1.68 x 10 <sup>4</sup>	5.59 x 10 <sup>3</sup>	121
36	30 (0.086)	Br	4-COMe	Sty, 1.3	TEA, 1.4	DMF	2	80	No	96	2	1.12 x 10 <sup>3</sup>	558	122
37	31 (0.1)	I	H	MA	TEA	Benzene	1	100	-	99	-	990	990	123
38	32	Br	4-COMe	Sty	NaOAc, 1	Dioxane	24	70	-	91	-			124
39	33 (0.94)	I	H	MA, 1	TEA, 1	MeCN	8	82	-	96	-	102	13	125
40	34 (3.8 x 10 <sup>-4</sup> )	I	H	Sty 1.1	TBA	DMF	90	140	-	78.3	3	2.06 x 10 <sup>5</sup>	2.29 x 10 <sup>3</sup>	92
41	34 (3.8 x 10 <sup>-4</sup> )	Br	4-CN	Sty 1.1	TBA	DMF	90	140	-	83	-	1.57 x 10 <sup>5</sup>	1.74 x 10 <sup>3</sup>	92
42	19 (0.01)	I	4-OMe	MA, 1	TEA, 1	NMP	3	130	No	99	7	1.00 x 10 <sup>4</sup>	3.33 x 10 <sup>3</sup>	97

Table 1.4 (Continued):

Pd/C 1	Pd/MgO 2	Pd/ZnO 3	Pd/ZrO <sub>2</sub> 4	Pd/SiO <sub>2</sub> 5	Pd/Nb-MCM 41 6
Pd/Na-Mordenite 7		Pd/HY Si:Al = 10-50 8		Pd-nano particles on silica 9	
Pd nano particles encapsulated in poly(propyleneimine) dendrimers 10				Pd nano particles dispersed in 1-Butyl-3-methylimidazolium hexafluorophosphate (BMIPF <sub>6</sub> ) 11	
Silicoaluminiumphosphate 31 with Pd (Pd-SAPO31) 12			Pd on sulfur activated silica (Pd-SiO <sub>2</sub> -SH) 13		

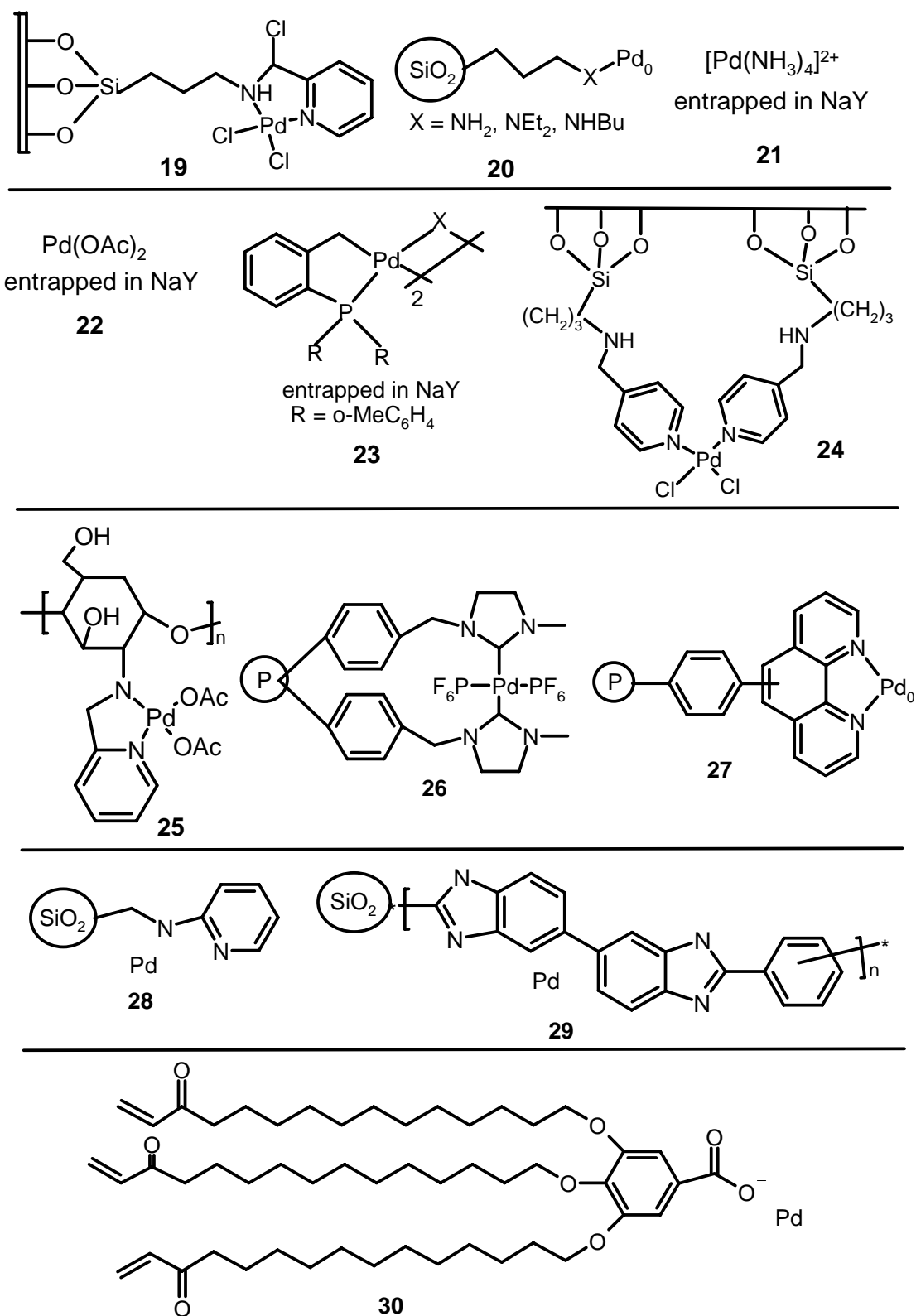


Layered double hydroxide  
supported nano Pd



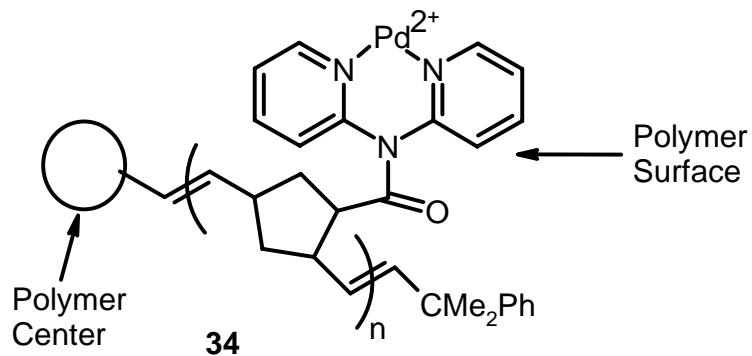
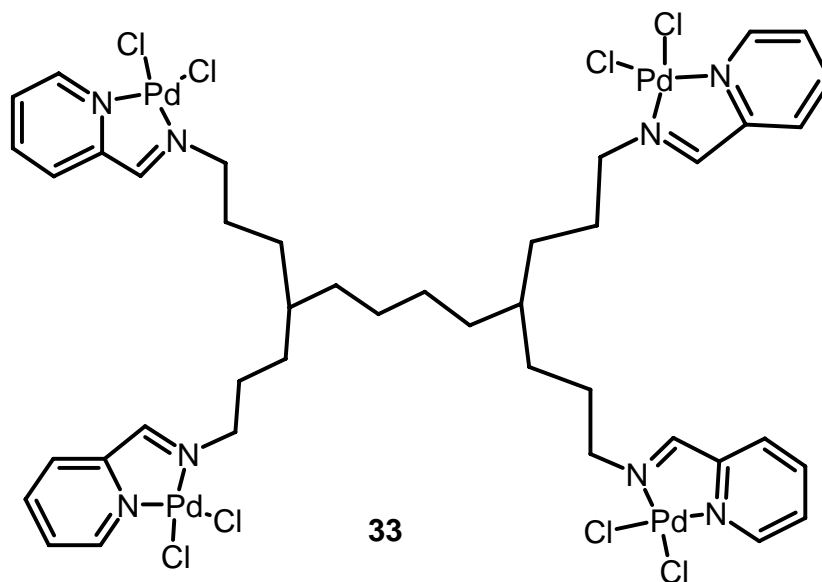
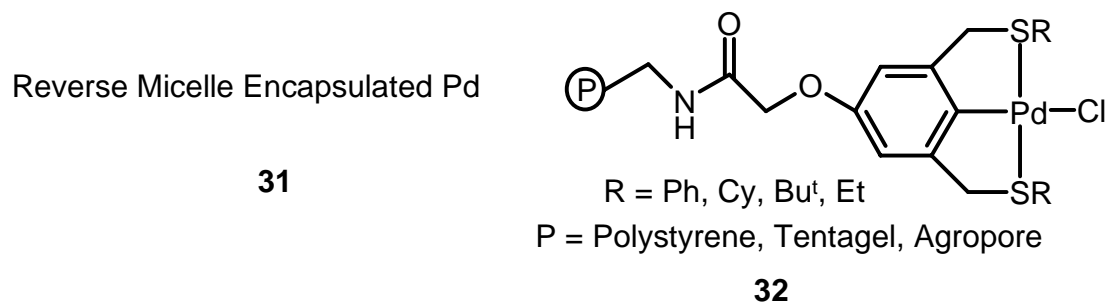
Heterogeneous catalyst systems employed for the Heck reaction

Table 1.4 (Continued):



Heterogeneous catalyst systems employed for the Heck reaction

Table 1.4 (Continued):



Heterogeneous catalyst systems employed for the Heck reaction



### 1.2.3. Promoters in Heck chemistry

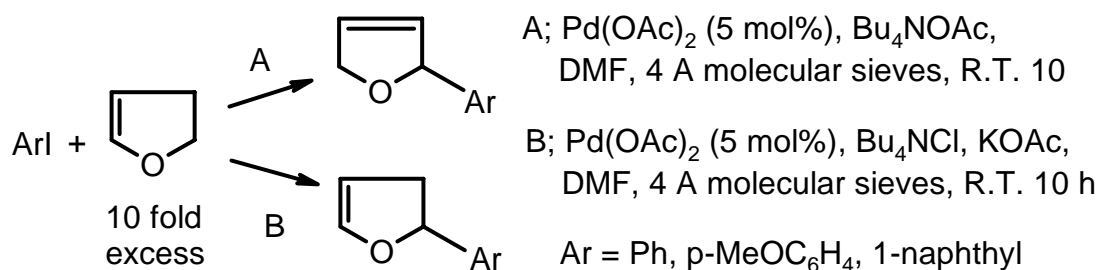
The beneficial effect of quaternary ammonium salts on the Heck reaction was first discovered and elaborated by Jeffery<sup>126a-b</sup>. This model of carrying out Heck reaction gained popularity after Larock et al<sup>127</sup> advanced it from simple model reactions to intramolecular cyclization and hence revealed the potential of this system for complex organic synthesis.

The effect of quaternary ammonium salts on the Heck reaction cannot be limited to one reason but is to be seen as a combination of various influences. These salts can act as solid-liquid phase transfer agents in the Heck reaction involving inorganic bases such as sodium or potassium acetates, carbonates, and bicarbonates etc., which are practically insoluble in organic solvents. They can also act as liquid-liquid phase transfer agents in aqueous solvents where the base is soluble but the substrates are not. The anionic moiety can serve as a promoter by increasing the rate of specific reaction steps by enhancing the electron density on palladium<sup>14</sup>. This effect has been reported by Amatore and Jutand<sup>128</sup>. These quaternary ammonium salts can also act as stabilizers to increase the lifetime of underligated Pd(0) species to match slower oxidative addition rates with less reactive substrates. This effect is exerted by bromide or chloride ions which can enter the coordination sphere of palladium. The stabilization of catalytic systems by halide salts has been demonstrated by extending the lifetime of the Herrmann's palladacycle catalyst<sup>19</sup>. In most cases the exact nature of the influence of quaternary salts on the rate and selectivity of a given reaction can not be tracked down to a single effect and it is rather a superposition of several such effects.

Detailed studies by Jeffery describe the influence of tetrabutylammonium salts on the model reaction of methyl acrylate with iodobenzene both in anhydrous and aqueous media and in presence as well as absence of phosphine ligands<sup>129</sup>. The salts with three different ions, Cl, Br, and HSO<sub>4</sub> showed similar behaviour with some minor variations, depending on the nature of the base, solvent, and catalyst. Under the phosphine free conditions n-Bu<sub>4</sub>NCl was found to give the best activity.

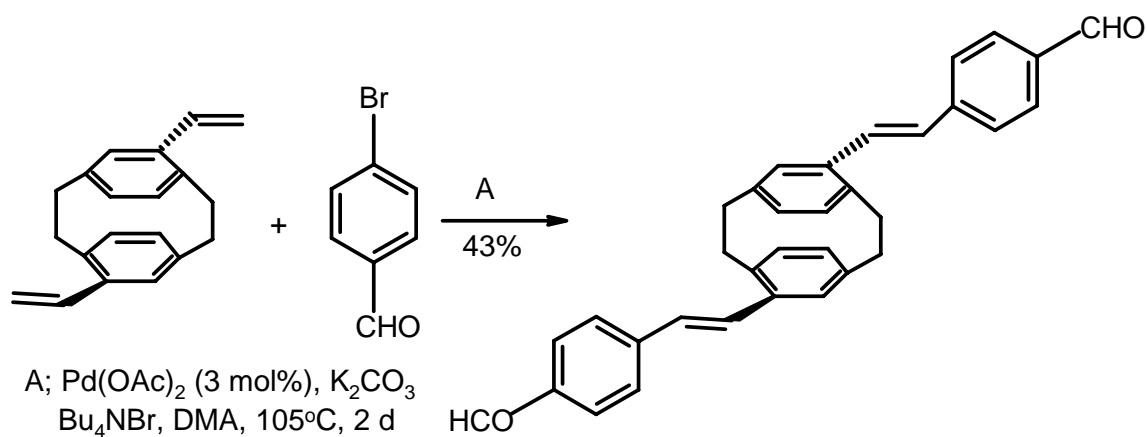
Another positive influence of the Jeffery reaction conditions is that it allows for the reactions to be conducted under mild reaction conditions (temperatures below 100°C) at least for the reactions of the iodides, which could be run even at room temperature for select cases<sup>34,35,36,126a-b</sup>. A small difference in the basicity can have dramatic effect on the

reaction. This has been demonstrated for the reaction of aryl iodides with dihydrofuran without phosphine ligands and in presence of ammonium salts<sup>130</sup>. The primary product of Heck arylation is formed in the presence of *n*-Bu<sub>4</sub>NOAc, while the product of double bond migration is formed in the presence of separately added base and the ammonium salt (Scheme 1.16). The soluble salt *n*-Bu<sub>4</sub>NOAc can furnish higher basicity to immediately trap palladium hydride. Whereas, the combination of KOAc and *n*-Bu<sub>4</sub>NCl leaves palladium hydride free at room temperature to accomplish near to quantitative transformation of primary product to thermodynamically more stable 2,3 dihydrofuran. The same system at higher temperature has higher basicity that results in formation of mixture of primary and rearranged product.



Scheme 1.16

Heck reaction with Quaternary ammonium salts using Pd(OAc)<sub>2</sub> as catalyst have been applied to the construction of large highly conjugated molecules like benzocyclobutenoacenaphthylene (Scheme 1.17)<sup>131</sup>.



Scheme 1.17

Promoting effect can also be exhibited by the use of bimetallic catalysts, in which the co-catalyst helps in bypassing the slow oxidative addition step for the palladium catalytic cycle when chloroarenes are the reactants. The use of nickel salts as co-catalysts in presence of sodium iodide is shown to be beneficial in palladium catalyzed reactions<sup>75</sup>. In reality the chloro derivatives are first converted to iodo derivatives which then undergo the oxidative addition. This method is quite efficient though it requires 80 fold excess of the phosphine to fill the coordination spheres of both the metals.

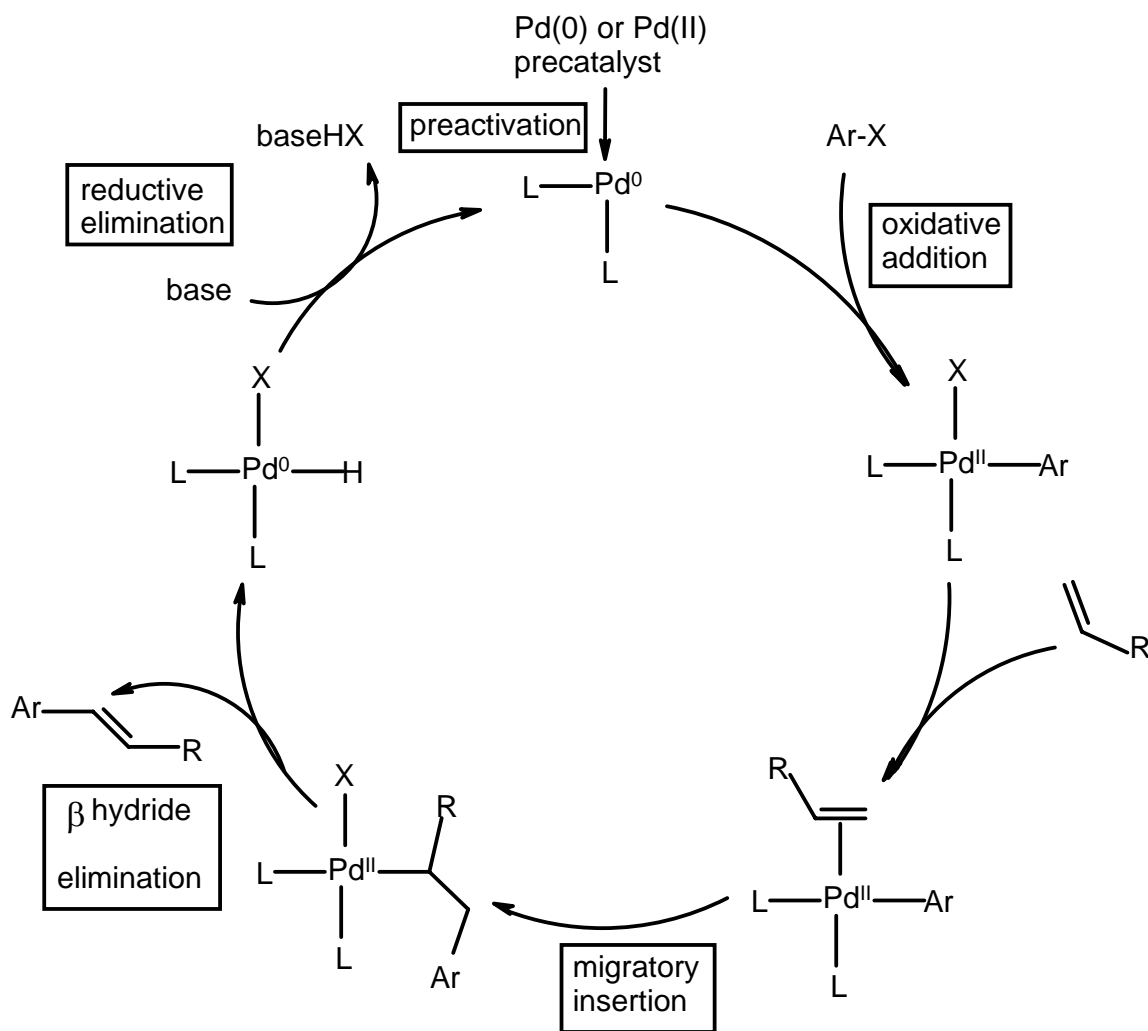
Though, quarternary ammonium salts are reported to promote Heck reaction, their use in large quantities and significant cost associated with them makes them an unattractive option for large scale use. Discovery of novel promoters for Heck reaction can lead to the better activation of chloroarenes and can also reduce the amount of palladium required to catalyze the Heck reaction,

#### 1.2.4. Mechanism of Heck reaction

The basic steps of the Heck reaction mechanism are shown in Scheme 1.18<sup>14</sup>. The catalyst precursor added to the reaction mixture first undergoes an activation step whereby, it is converted to the active catalytic species. This species is, under most circumstances, a Pd(0) species. The proof of the activation step is revealed by the induction period involved. The activation step has been the subject of investigation, under phosphine assisted conditions, by Amatore and Jutand<sup>128,132</sup>. The reduction of Pd(II) to Pd(0) is assisted by nucleophiles, of which most common are, hydroxide and alkoxide ions<sup>133a-c</sup>, water<sup>134</sup>, and acetate ions<sup>135</sup>.

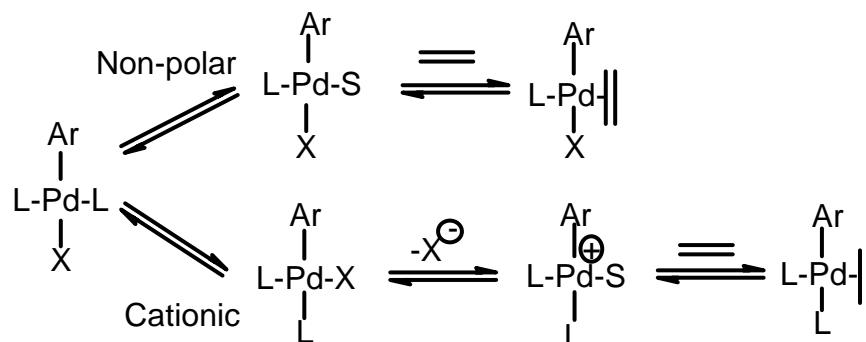
To enter the catalytic cycle through the oxidative addition step, Pd(0) species should not have more than two strongly binding ligands. The oxidative addition step is one of the basic processes of organometallic chemistry. In case of Heck reaction, oxidative addition of C-X bond occurs to generate a Pd(II) species. The oxidative addition proceeds as a concerted process in which C-X bond breaking is more or less perfectly synchronized with the formation of M-C and M-X bonds. The order of reactivity is  $I \gg OTf > Br \gg Cl$ <sup>136</sup>. Except for the complexes with chelating ligands, the product of the oxidative addition possesses *trans* geometry<sup>14</sup>, though it is obvious that *cis* isomer must be formed

first. Over that it is the *cis* complex that enters the next stage of the catalytic cycle. Recent studies have revealed both the formation of *cis* adduct and *cis-trans* isomerization<sup>137</sup>.



The migratory insertion step is the one where product formation of the Heck reaction takes place. In this step a new C-C bond is formed. For this step to occur, palladium needs to dissociate one of its ligands to make space for alkene addition. This can occur by two routes. If a neutral ligand is dissociated from the palladium coordination sphere, then the reaction occurs via a non-polar route. Whereas, if an anionic ligand dissociates then the reaction proceeds via cationic route (Scheme 1.19)<sup>138a-c</sup>. For monodentate phosphine complexes, both routes are possible. In case of bidentate phosphine

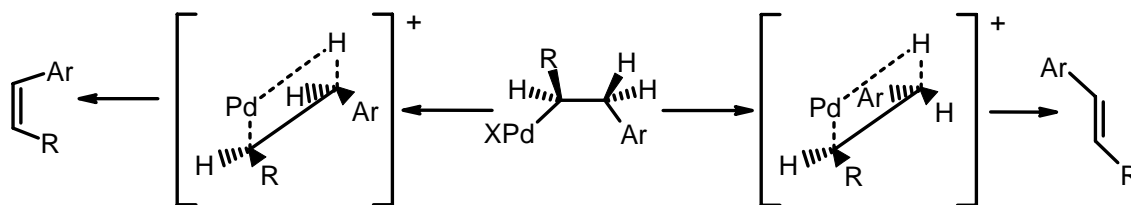
complexes, non-polar route appears doubtful, but can not be altogether ruled out especially in case of large bite angle diphosphines.



**Scheme 1.19**

After the migratory insertion step,  $Pd(0)$  is released and this then launches the next catalytic cycle. This happens by the Heck product being released from the catalytic cycle and palladium hydride being formed. The base added to the reaction then scavenges  $HX$  and releases the active  $Pd(0)$  species for a fresh cycle.

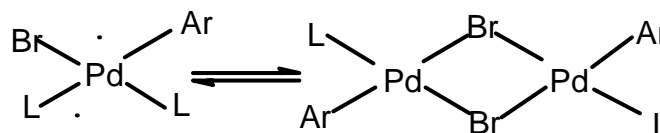
The selectivity data of the Heck reaction can be explained on the basis of syn elimination of  $PdH$ . This defines the stereoselectivity of the Heck reaction. The ratio of *E* and *Z* isomers reflects the relative energy of the respective transition states. Unless  $R$  is very small (like  $CN$ ) *E* isomer is predominant and the reaction is highly stereospecific as shown in Scheme 1.20<sup>14</sup>.



**Scheme 1.20**

*Mechanism with palladacycle complexes*

It has been proposed that palladacycles act as a reservoir of Pd(0) species<sup>11d</sup>. During the reaction these palladacycles decompose slowly to liberate Pd(0) species which is the true catalytic species for the Heck reaction. After the oxidative addition to the Pd(0) species, a halide bridged dimer is formed and exists in equilibrium with the monomeric Pd(0) species. The formation of the dimer is also reported for the case of ligand free Pd(OAc)<sub>2</sub> catalyzed reactions when used in very low concentrations. This dimer is of the form [Pd<sub>2</sub>I<sub>6</sub>]<sup>2-</sup>. An intermediate species [Pd<sub>2</sub>I<sub>6</sub>][DMFH]<sub>2</sub> has been isolated at the end of the reaction between iodobenzene and methyl acrylate in DMF solvent using palladium pyridyl-imine complexes<sup>26</sup>. It has also been shown that Pd(OAc)<sub>2</sub> and palladacycle catalyst shown in Scheme 1.5 kinetically behave identically, indicating that same catalytic species may be involved (Scheme 1.21)<sup>11d,139a-c</sup>.

**Scheme 1.21**

Further evidence for the palladacycles giving Pd(0) species as an active catalyst during the reaction was shown for the case of P-C-P and S-C-S pincer complexes by using poisoning techniques and metal leaching studies<sup>140a-d</sup>. In another study, chiral non-racemic S-C palladacycles were evaluated for the Heck reaction and shown to give a racemic mixture of products. This gives further evidence that during the reaction, a catalyst without any chiral centre is formed, which catalyzes the reaction<sup>141</sup>.

The questions regarding the catalytic cycle involved in the Heck reaction mechanism still exist. The mechanistic cycles involving Pd(0)/Pd(II) and Pd(II)/Pd(IV) species have been reported. It has also been suggested that the mechanism of the reaction varies with the substrates, promoters, catalyst, and even with the solvent. In general, the mechanistic cycle involving Pd(0)/Pd(II) species is well accepted.

### 1.2.5. Kinetic studies on Heck reaction

In spite of the volume of work done in the field of Heck chemistry, the kinetics of these reactions remains relatively untouched. Very few studies are reported on the kinetics of Heck reaction using homogeneous catalysts (Table 1.5) and no such study is reported with heterogeneous catalysts. A kinetic study is important in order to optimise the reaction conditions and reaction parameters. It is useful in understanding the mechanism of the reaction, and also helps in the designing of the reactors to carry out the reaction.

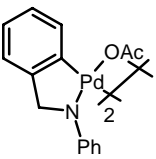
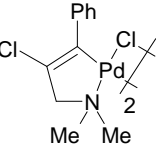
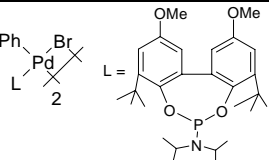
The initial studies carried out on the Heck reaction used Pd(OAc)<sub>2</sub> as the catalyst and PPh<sub>3</sub> as the ligand<sup>11a</sup>. The arylation of methyl acrylate with iodobenzene in presence of triethylamine as base was chosen as the reaction system. The rates were first order with respect to iodobenzene concentration and first order tending to zero order with methyl acrylate concentration. The rates passed through a maximum on varying the base concentration. The rates showed a partial dependence on the concentration of Pd(OAc)<sub>2</sub>. Increasing the PPh<sub>3</sub> concentration initially led to a decrease in the rates, after which it had no effect. The following rate equation was found to best fit the data obtained<sup>11a</sup>:

$$\text{Rate} = \frac{k A B^2 C D}{(1 + K_B B^2) (1 + K_C C^4) (1 + K_D D)^3 (1 + K_E E)} \quad \text{Eq 1.1}$$

Where,  $k$  = rate constant [ $\text{m}^{12} \text{kmol}^{-4} \text{s}^{-1}$ ];  $A$  = concentration of iodobenzene [ $\text{kmol m}^{-3}$ ];  $B$  = concentration of methyl acrylate [ $\text{kmol m}^{-3}$ ];  $C$  = concentration of triethylamine [ $\text{kmol m}^{-3}$ ];  $D$  = concentration of catalyst precursor [ $\text{kmol m}^{-3}$ ];  $E$  = concentration of PPh<sub>3</sub> [ $\text{kmol m}^{-3}$ ];  $K_B$ ,  $K_C$ ,  $K_D$ , and  $K_E$  are the respective constants. The activation energy was found to be 23 kcal/mol.

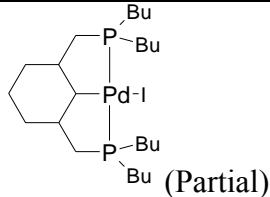
Further studies by the authors on the PPh<sub>3</sub>: Pd concentration showed that the ratio of 2 gave the best results when the reaction was carried out in non-polar solvents. Above this ratio the rates dropped. In case of polar solvents like, N,N-dimethylacetamide and N-methyl pyrrolidinone, the rates were highest for the reaction without any PPh<sub>3</sub> ligand. The rates decreased as the concentration of PPh<sub>3</sub> increased<sup>11b</sup>.

**Table 1.5:** Different kinetic studies reported on Heck coupling reaction

No	Halide (Order)	Olefin (Order)	Base (Order)	Catalyst (Order)	Solvent	Model, Rate =	Ref
1	IB (1 <sup>st</sup> )	MA (1 <sup>st</sup> to zero)	TEA (Pass through a maximum)	Pd(OAc) <sub>2</sub> /TPP (Partial)	NMP	$\frac{k [\text{IB}][\text{MA}]^2 [\text{TEA}][\text{Pd}]}{(1 + K_B[\text{MA}]^2)(1 + K_C[\text{TEA}]^4)(1 + K_D[\text{Pd}])^3(1 + K_E E)}$	11a
2	BBz (1 <sup>st</sup> to Zero)	BA (1 <sup>st</sup> )	KOAc (Zero)	 (Partial)	DMA	$\left( \frac{k}{[\text{BA}]_0 - [\text{BBz}]_0} \right) [\text{BBz}][\text{BA}][\text{Pd}]$	11d
3	IB (1 <sup>st</sup> to zero)	BA (1 <sup>st</sup> to zero)	NaOAc (Zero)	 (1 <sup>st</sup> )	DMA	$\frac{k [\text{IB}][\text{BA}][\text{Pd}]}{K_B[\text{BA}] + K_C[\text{IB}][\text{BA}] + K_D[\text{IB}]}$	11e
4	IB	Sty (1 <sup>st</sup> )		 (Partial)	MeCN	$k[\text{Sty}][\text{Pd}]^{0.5}$	11c



**Table 1.5 (Continued):** Different kinetic studies reported on Heck coupling reaction

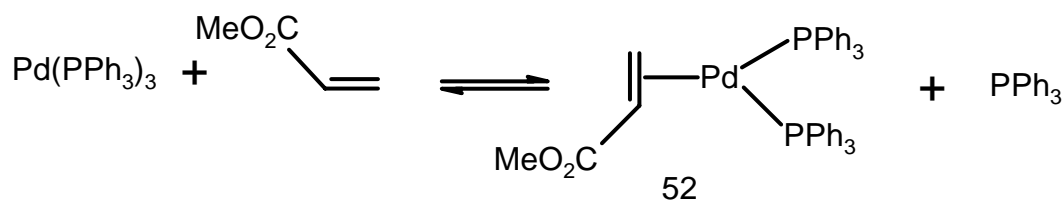
No	Halide (Order)	Olefin (Order)	Base (Order)	Catalyst (Order)	Solvent	Model, Rate =	Ref
5	IB	MA (Partial)	NaOAc (Partial)	PdCl <sub>2</sub>	DMF		142
6	IAN (1 <sup>st</sup> )	Sty (1 <sup>st</sup> to zero)	TEA	 (Partial)		$\frac{k [\text{IAN}][\text{Sty}][\text{Pd}]}{1 + K[\text{Sty}]}$	143

IB: Iodobenzene, BBz: 4'-bromobenzaldehyde, IAN: 4'-Iodoanisole, MA: Methyl acrylate, BA: Butyl acrylate, Sty: Styrene, TEA: Triethylamine

The partial order dependence of the reaction rates on the catalyst concentration was also observed and explained by Blackmond et al<sup>11d</sup> on the basis of formation of a halide bridged dimeric species (Scheme 1.21). It was argued that this species exists in equilibrium with the monomeric species. The dimer species acts like the storehouse of the catalyst and releases the active catalytic species during the reaction. In this study the rates were found to depend linearly on the concentration of the olefin but were found to be independent of the halide concentration. The presence of water in the reaction mixture increased the rates of the reaction.

A recent study on the reaction of iodobenzene with butyl acrylate and NaOAc base in presence of TBAB promoter found the rates to be first order with the palladacycle catalyst concentration. The rates showed zero order dependence on the concentration of NaOAc and TBAB. Saturation kinetics was observed for the iodobenzene and butyl acrylate substrates. It was suggested that the mechanism involves an activation step wherein the conversion of the palladacycle into the catalytically active Pd(0) species takes place. The oxidative addition is proposed to be the slowest step of the catalytic cycle<sup>11e</sup>.

A study carried out by Amatore et al<sup>144</sup> using Pd(OAc)<sub>2</sub>/PPh<sub>3</sub> catalyst system showed that the rate of oxidative addition of iodobenzene to the palladium decreased in the presence of olefin. This was attributed to the decrease in active palladium concentration on account of the olefin coordination. The olefin coordination forms an unreactive complex as shown in Scheme 1.22.



**Scheme 1.22**

### 1.3. Summary of the literature surveyed

The following observations emerged from the literature review:

- Though palladium, platinum, nickel, cobalt, rhodium, iridium, and ruthenium complexes have been shown to be active catalysts for Heck reaction, most of the research focuses on palladium catalysts. Palladium in almost every form has been tried and tested for these reactions and has been found to be active to varying degrees.
- Presently research on Heck reaction is devoted to design catalysts that have higher activity and stability and thus can give very high TON. Research in this direction has led to the development of palladacycle catalysts, which have turned out to be one of the most active catalysts employed for Heck reaction of bromo and chloro arenes in terms of TON and TOF.
- Another approach to have efficient catalysts for Heck reaction is the design and utilization of heterogeneous catalysts that can be re-used and thus can give very high cumulative TON. Heterogeneous catalysts, like palladium bipyridyl complex anchored on MCM 41, that can give high TON (> million) have been reported for the reaction of iodobenzene and 4'-bromoacetophenone with n-butyl acrylate.
- Heck reaction has also been reported to occur at room temperatures with either the use of promoters like quaternary ammonium salts or in ionic liquids as solvent. Heck reaction has also been studied in biphasic and also in supercritical media.
- The doubts regarding the active catalytic species involved in the reaction still remain and different reports claim different active species.
- There are very few kinetic studies with homogeneous catalyst complexes and no such study with heterogeneous catalyst system for the Heck reaction.
- Significant challenges like increasing the reactivity of chloro arenes, reducing the waste generated due to the use of stoichiometric amount of base, and establishing the identity of the true catalytic species involved remain to be solved.

#### 1.4. Scope and objective

Considering the above facts, the present study was focused on the Heck reaction of haloarenes with acrylates to give cinnamic acid derivatives as the model reaction. The cinnamate products obtained are used as UV absorbers, antioxidants, and as intermediates in perfumery, pharmaceutical, and dye industry. The main objective of this study was to develop improved homogeneous as well as heterogeneous catalyst systems with respect to activity and selectivity and to study the kinetics of this system. With these objectives in mind, the following specific problems were chosen for the present work:

- ❖ Synthesis, characterization, and catalytic properties of different palladium complexes for the Heck reaction and optimization of the reaction conditions in order to study the kinetics of these reaction.
- ❖ Kinetic studies on the vinylation of 4'-bromo acetophenone with n-butyl acrylate to give butyl(4'-acyl)cinnamate using P-C palladacycle catalyst.
- ❖ Investigations into a novel class of promoters to enhance the activity of the palladium complexes for the Heck reaction of haloarenes with different olefins.
- ❖ Synthesis, characterization, and catalytic properties of ossified palladium complexes and their use in the Heck coupling of acrylates with halo arenes.
- ❖ Kinetic studies using ossified palladium complex  $\{Pd(Pyca)(TPPTS) [Pyca = 2\text{-pyridine carboxylic acid and TPPTS-Ba} = P(C_6H_4SO_3)Ba_{3/2})_3]\}$  for the vinylation of iodobenzene with n-butyl acrylate.

**Glossary of terms used**

Cat:	Catalyst
Equiv:	Equivalents
TON:	Turn Over Number
TOF:	Turn Over Frequency
Ti:	Time
Tm:	Temperature
Ref:	Reference
MA:	Methyl acrylate
EA:	Ethyl acrylate
BA:	n-Butyl acrylate
BA <sup>t</sup> :	<sup>t</sup> Butyl acrylate
Sty:	Styrene
AA:	Acrylic acid
TEA:	Triethylamine
TBA:	Tributylamine
DMF:	N,N-Dimethylformamide
Tol:	Toluene
EG:	Ethylene glycol
Hep:	Heptane
DMA:	N,N-Dimethylacetamide
NMP:	N-Methyl-2-pyrrolidone
TBAB:	Tetrabutylammonium bromide
TBAC:	Tetrabutylammonium chloride
TPAB:	Tetrapropylammonium bromide
Ac:	Acetyl
h $\nu$ :	Microwave irradiation
Cy:	Cyclohexyl
MS:	Molecular Sieves
Pr:	Propyl
DMG:	Dimethyl glycine

## 1.5. References

- 
- 1 a) Parshall, G.; Ittel, S. D. *Homogeneous Catalysis: The Applications and Chemistry of Soluble Transition-Metal Complexes*, 2nd ed. John Wiley & Sons, New York, **1992** b) *Handbook of Heterogeneous Catalysis*, Ed. Ertl, G.; Knözinger, H. J. Eitkamp, Wiley-VCH, Weinheim, **1997** c) Thomas, J. M. *Principles and Practice of Heterogeneous Catalysis*, VCH, Weinheim, **1997** d) Gates, B. C. *Catalytic Chemistry*, John Wiley & Sons, New York, **1992**, 310
- 2 a) *Applied Homogeneous Catalysis with Organometallic Compounds*, Ed. Cornils, B.; Herrmann, W. A. Wiley-VCH Verlag, Weinheim, **2002** b) Weissermel, K.; Arpe, H. J. *Industrial Organic Chemistry*, 2<sup>nd</sup> Ed, Verlag Chemie, Weinheim **1993** c) Masters, C.; *Homogeneous Transition-Metal Catalysis*, Chapman & Hall, London, **1981** d) *Aqueous-Phase Organometallic Catalysis*, Ed. Cornils, B.; Herrman, W. A. VCH, Weinheim, **1998** e) *Transition Metals for Organic Synthesis: building blocks and fine chemicals*, Beller, M.; Bolm, C. VCH, Weinheim, **1998**
- 3 a) BASF AG, *Hydrocarbon Process* **1977**, 11, 135 b) BASF AG, *Hydrocarbon Process* **1977**, 11, 172 c) Jira, R. *Ethylene and Its Industrial Derivatives*, Miller, S. A. (Ed.) Ernest Benn Ltd. **1969**, 650 d) Hohenshutz, H.; Kutepow, N.; Himmele, W. *Hydrocarbon Process* **1966**, 45,141 e) Falbe, J. *J. Organomet. Chem.* **1975**, 94, 213 f) Roth, J.; Craddock, J.; Hershmann, A.; Paulik, F. *Chemtech.* **1971**, 600 g) Roth, J. F. *Platinum Met. Rev* **1975**, 19, 12 h) Paulik, F. E.; Roth, J. F. *Chem. Commun.* **1968**, 1578 i) Dekleva, T.; Forster, D. *Adv. Catal.* **1986**, 34, 81 j) Adamson, G. W.; Daly, J. J.; Forster, D. *J. Organomet. Chem.* **1974**, 71, C17 k) Garland, C. S.; Giles, M. F.; Sunley, J. G. *Eur. Pat.* 643034, **1995** l) Garland, C. S.; Giles, M. F.; Poole, A. D.; Sunley, J. G. *Eur. Pat.* 728726, **1994** m) Zeigler, K. *Brit. Pat.* 799392, **1958**
- 4 a) Mizoroki, T.; Mori, K.; Ozaki, A. *Bull. Chem. Soc. Jpn.* **1971**, 44, 581, b) Heck, R. F.; Nolley, J. P. *J. Org. Chem.* **1972**, 37, 2320 c) Mori, K.; Mizoroki, T.; Ozaki, A. *Bull. Chem. Soc. Jpn.* **1973**, 46, 1505
- 5 a) Miyaura, N.; Yamada, K.; Suzuki, A. *Tetrahedron Lett.* **1979**, 3437 b) Miyaura, N.; Suzuki, A. *Chem. Rev.* **1995**, 95, 2457
- 6 Sonogashira, K.; Tohda, Y.; Hagihara, N. *Tetrahedron Lett.* **1975**, 4467
- 7 Stille, J. K. *Angew. Chem. Int. Ed.* **1986**, 25, 508
- 8 a) Dieck, H. A.; Heck, R. F. *J. Am. Chem. Soc.* **1974**, 96, 1133, b) Melpolder, J. B.; Heck, R. F. *J. Org. Chem.* **1976**, 41, 265, c) Patel, B. A.; Ziegler, C. B.; Cortese, N. A.; Plevyak, J. E.; Zebovitz, T. C.; Terpkow, M.; Heck, R. F. *J. Org. Chem.* **1977**, 42, 3903, d) Ziegler, C. B.; Heck, R. F. *J. Org. Chem.* **1978**, 43, 2941, e) Plevyak, J. E.; Heck, R. F. *J. Org. Chem.* **1978**, 43, 2454, f) Heck, R. F. *Accs. Chem. Res.* **1979**, 12, 146, g) Plevyak, J. E.; Dickerson, J. E.; Heck, R. F. *J. Org. Chem.* **1979**, 44, 4078, h) Mitsudo, T.; Fischetti, W.; Heck, R. F. *J. Org. Chem.* **1984**, 49, 1640
- 9 Dounay, A. B.; Overman, L. E. *Chem. Rev.* **2003**, 103, 2945
- 10 a) Smith, G. S.; Mapolie, S. F. *J. Mol. Catal. A: Chem.* **2004**, 213, 187 b) Nowotny, M.; Hanefeld, U.; Koningsveld, H.; Maschmeyer, T. *Chem. Commun.* **2000**, 1877
- 11 a) Zhao, F. G.; Bhanage, B. M.; Shirai, M.; Arai, M. *Reaction Kinetics Development Catal. Procedures* . **1999**, 427, b) Zhao, F.; Bhanage, B. M.; Shirai, M.; Arai, M. *J. Mol. Catal. A: Chem.* **1999**, 142, 383 c) Van Strijdonck, G. P. F.; Boele, M. D. K.; Kamer, P. C. J.; de Vries, J. G.; van Leeuwen, P. W. N. M. *Eur. J. Inorg. Chem.* **1999**,

- 1073 d) Rosner T.; Bars J. L.; Pfaltz A.; Blackmond D. G. *J. Am. Chem. Soc.* **2001**, 123, 1848 e) Consorti, C. S.; Flores, F. R.; Dupont, J. *J. Am. Chem. Soc.* **2005**, 127, 12054 f) Zhao F. G.; Bhanage B. M.; Shirai M.; Arai M. *Stud. Surf. Sci. Catal.* **1999**, 122, 427
- 12 a) Iyer, S.; Ramesh, C.; Sarkar, A.; Wadgaonkar, P. P. *Tetrahedron Lett.* **1997**, 38, 8113 b) Boldrini, G. P.; Savoia, D.; Tagliavini, E.; Trombini, C.; Ronchi, A. U. *J. Organomet. Chem.* **1986**, 301, C62. c) Lebedev, S. A.; Lopatina V. S.; Petrov, E. S.; Beletskaya, I. P. *J. Organomet. Chem.* **1988**, 344, 253 d) Kelkar, A. A. *Tetrahedron Lett.* **1996**, 37, 8917 e) Iyer, S. *J. Organomet. Chem.* **1995**, 490, C27 f) Mitsudo, T. A.; Takagi, M.; Zhang, S. W.; Watanabe, Y. *J. Organomet. Chem.* **1992**, 423, 405
- 13 Reetz, M. T.; Demuth, R.; Goddard, R. *Tetrahedron Lett.* **1998**, 39, 7089
- 14 Beletskaya, I. P.; Cheprakov, A. V. *Chem. Rev.* **2000**, 100, 3009
- 15 Spencer, A. *J. Organomet. Chem.* **1983**, 258, 101
- 16 Beller, M.; Zapf, A. *Synlett* **1998**, 7, 792
- 17 a) Shibasaki, M.; Vogl, E. M. *J. Organomet. Chem.* **1999**, 576, 1 b) Boyes, A. L.; Butler, J. R.; Quayle, S. C. *Tetrahedron Lett.* **1998**, 39, 7763 c) Shaw, B. L.; Perera, S. D. *Chem. Commun.* **1998**, 1863 d) Protonoy, M.; Ben-David, Y.; Milstein, D. *Organometallics* **1993**, 12, 4734 e) Ben-David, Y.; Protonoy, M.; Cozin, M.; Milstein, D. *Organometallics* **1992**, 11, 1995 f) Protonoy, M.; Ben-David, Y.; Rousso, I.; Milstein, D. *Organometallics* **1994**, 13, 3465
- 18 Littke, A. F.; Fu, G. C. *J. Org. Chem.* **1999**, 64, 10
- 19 a) Herrmann, W. A.; Brossmer, C.; Ofele, K.; Reisinger, C. P.; Priermeier, T.; Beller, M.; Fischer, H. *Angew. Chem. Int. Ed. Engl.* **1995**, 34, 1844 b) Herrmann, W. A.; Brossmer, C.; Reisinger, C. P.; Riermeier, T. H.; Ofele, K.; Beller, M. *Chem. Eur. J.* **1997**, 3, 8, 1357
- 20 a) Ohff, M.; Ohff, A.; Boom, M. E.; Milstein, D. *J. Am. Chem. Soc.* **1997**, 119, 11687 b) Morales, D.; Redon, R.; Yung, C.; Jensen, C. M. *Chem. Commun.* **2000**, 1619 c) Morales, D.; Grause, C.; Kasaoka, K.; Redon, R.; Crammer, R. E.; Jensen, C. M. *Inorg. Chim. Acta.* **2000**, 300-302, 958 d) Beletskaya, I. P.; Chuchurjukin, A. V.; Dijkstra, H. P.; van Klink, G. P. M.; van Koten, G. *Tetrahedron Lett.* **2000**, 41, 1075
- 21 a) Tietze, L. F.; Schirok, H. *Angew. Chem. Int. Ed. Engl.* **1997**, 36, 1124 b) Tietze, L. F.; Schirok, H. *J. Am. Chem. Soc.* **1999**, 121, 10264
- 22 Tietze, L. F.; Noebel, T.; Spescha, M. *J. Am. Chem. Soc.* **1998**, 120, 8971
- 23 a) Ohff, M.; Ohff, D.; Milstein, D. *J. Chem. Soc., Chem. Commun.* **1999**, 357 b) Beletskaya, I. P.; Kashin, A. N.; Karstedt, N. B.; Mitin, A. V.; Cheprakov, A. V.; Kazankov, G. M. *J. Organomet. Chem.* **2001**, 622, 89 c) Iyer, S.; Kulkarni, G. M.; Ramesh, C. *Tetrahedron*, **2004**, 60, 2163 d) Munoz, M. P.; Matute, B. M.; Rivas, C. F.; Cardenas, D. J.; Echavarren, A. M. *Adv. Synth. Catal.* **2001**, 343, 4, 338
- 24 Bergbreiter, D. E.; Osburn, P. L.; Liu, Y. S. *J. Am. Chem. Soc.* **1999**, 121, 9531
- 25 Botella, L.; Najera, C. *Tetrahedron Lett.* **2004**, 45, 1833
- 26 Pelagatti, P.; Carcelli, M.; Costa, M.; Ianelli, S.; Pelizzi, C.; Rogolino, D. *J. Mol. Catal. A: Chem.* **2005**, 226, 107
- 27 a) Herrmann, W. A.; Elison, M.; Fischer, J.; Kocher, C.; Artus, G. R. *J. Angew. Chem. Int. Ed. Engl.* **1995**, 34, 2371 b) Herrmann, W. A.; Reisinger, C. P.; Spiegler, M. *J. Organomet. Chem.* **1998**, 557, 93 c) Herrmann, W. A.; Schwarz, J.; Gardiner, M. G.;

- Spiegler, M. J. *Organomet. Chem.* **1999**, 575, 80 d) Herrmann, W. A.; Fischer, J.; Oefele, K.; Artus, G. R. J. *J. Organomet. Chem.* **1997**, 530, 259 e) Herrmann, W. A.; Elison, M.; Fischer, J.; Koecher, C.; Artus, G. R. J. *Angew. Chem.* **1995**, 107, 2602 f) Enders, D.; Gielen, H.; Raabe, G.; Runsink, J.; Teles, J. H. *Chem. Ber.* **1996**, 129, 1483
- 28 Clyne, D. S.; Jin, J.; Genest, E.; Gallucci, J. C.; Rajanbabu, T. V. *Org. Lett.* **2000**, 2, 1125
- 29 Yang, C.; Lee, H. M.; Nolan, S. P. *Org. Lett.* **2001**, 3, 1511
- 30 Cesar, V.; Bellemin-Laponnaz, S.; Gade, L. H. *Organometallics* **2002**, 21, 5204
- 31 a) Peris, E.; Loch, J. A.; Mata, J.; Crabtree, R. H. *Chem. Commun.* **2001**, 201. b) Loch, A.; Albrecht, M.; Peris, E.; Mata, J.; Faller, J. W.; Crabtree, R. H. *Organometallics* **2002**, 21, 700
- 32 a) Miyazaki, F.; Yamaguchi, K.; Shibasaki, M. *Tetrahedron Lett.* **1999**, 40, 7379 b) Jung, I. G.; Son, S. U.; Park, K. H.; Chung, K. C.; Lee, J. W.; Chung, Y. K. *Organometallics* **2003**, 22, 4715 c) Albisson, D. A.; Bedford, R. B.; Scully, P. N. *Tetrahedron Lett.* **1998**, 39, 9793 d) Rocaboy, C.; Gladysz, J. A. *Org. Lett.* **2002**, 4, 1993
- 33 Takenaka, K.; Uozumi, Y. *Adv. Synth. Catal.* **2004**, 346, 1693
- 34 Jeffery, T. *J. Chem. Soc., Chem. Commun.* **1984**, 19, 1287
- 35 Jeffery, T.; Galland, J. C. *Tetrahedron Lett.* **1994**, 35, 4103
- 36 Jeffery, T. *Tetrahedron Lett.* **1994**, 35, 3051
- 37 Wu, Y.; Hou, J.; Yun, H.; Cui, X.; Yuan, R. *J. Organomet. Chem.* **2001**, 637, 793
- 38 Reddy, K. R.; Krishna, G. G. *Tetrahedron. Lett.* **2005**, 46, 661
- 39 Gruber, A. S.; Pozebon, D.; Monteiro, A. L.; Dupont, J. *Tetrahedron, Lett.* **2001**, 42, 7345
- 40 Iyer, S.; Kulkarni, G. M.; Ramesh, C. *Tetrahedron*, **2004**, 60, 2163
- 41 Thakur, V. V.; Ramesh, N. S. C.; Sudalai, A. *Tetrahedron Lett.* **2004**, 45, 2915
- 42 Cravotto, G.; Demartin, F.; Palmisano, G.; Penoni, A.; Radice, T.; Tollari, S. *J. Organomet. Chem.* **2005**, 690, 2017
- 43 Gruber, A. S.; Zim, D.; Ebeling, G.; Monteiro, A. L.; Dupont, J. *Org. Lett.* **2000**, 2, 1287
- 44 Consorti, C. S.; Ebeling, G.; Flores, F. R.; Rominger, F.; Dupont, J. *Adv. Synth. Catal.* **2004**, 346, 617
- 45 Consorti, C. S.; Zanini, M. L.; Leal, S.; Ebeling, G.; Dupont, J. *Org. Lett.* **2003**, 5, 983
- 46 Iyer, S.; Jayanthi, A. *Tetrahedron Lett.* **2001**, 42, 7877
- 47 Gai, X.; Grigg, R.; Ramzan, M. I.; Sridharan, V.; Collard, S.; Muir, J. E. *Chem. Commun.* **2000**, 2053
- 48 Reddy, K. R.; Surekha, K.; Lee, G. H.; Peng, S. M.; Liu, S. T. *Organometallics* **2000**, 19, 2637
- 49 Munoz, M. P.; Matute, B. M.; Rivas, C. F.; Cardenas, D. J.; Echavarren, A. M. *Adv. Synth. Catal.* **2001**, 343, 4, 338
- 50 Bedford, R. B. *Chem. Commun.* **2003**, 1787
- 51 Huang, M. H.; Liang, L. C. *Organometallics*, **2004**, 23, 2813
- 52 Shaw, B. L.; Perera, S. D.; Staley, E. A. *Chem. Commun.* **1998**, 1361
- 53 a) Sjoevall, S.; Johansson, M. H.; Andersson, C.; *Eur. J. Inorg. Chem.* **2001**, 2907, b) Sjoevall, S.; Wendt, O. F.; Andersson, C. *J. Chem. Soc., Dalton Trans.* **2002**, 1396



- 54 Kawano, T.; Shinomaru, T.; Ueda, J. *Org. Lett.* **2002**, 4, 2545
- 55 Hierso, J. C.; Fihri, A.; Amardeil, R.; Meunier, P. *Organometallics* **2003**, 22, 4490
- 56 Tulloch, A. A. D.; Danopoulos, A. A.; Cafferkey, S. M.; Kleinhenz, S.; Hursthouse, M. B.; Tooze, R. P. *Chem. Commun.* **2000**, 1247
- 57 Calo, V.; Del Sol R.; Nacci, A.; Schingaro, F.; Scordari, F. *Eur. J. Org. Chem.* **2000**, 869
- 58 Feuerstein, M.; Doucet, H.; Santelli, M. *J. Org. Chem.* **2001**, 66, 5923
- 59 a) Heidenreich, R. G.; Krauter, J. G. E.; Pietsch, J.; Kohler, K. *J. mol. Catal. A: Chem.* **2002**, 182, 499 b) Kohler, K.; Heidenreich, R. G.; Krauter, J. G. E.; Pietsch, M. *Chem. Eur. J.* **2002**, 8, 622
- 60 Ozdemir, I.; Cetinkaya, B.; Demir, S. *J. Mol. Catal. A: Chem.* **2004**, 208, 109
- 61 Veelak, J.; Storch, J.; Czakoova, M.; Cermak, J. *J. Mol. Catal. A: Chem.* **2004**, 222, 121
- 62 Arvela, R. K.; Leadbeater, N. E. *J. Org. Chem.* **2005**, 70, 1786
- 63 Barra, E. D.; Guerra, J.; Hornillos, V.; Merino, S.; Tajeda, J. *Organometallics* **2003**, 22, 4610
- 64 Schultz, T.; Schmees, N.; Pfaltz, A. *Appl. Organomet. Chem.* **2004**, 18, 595
- 65 Iyer, S.; Jayanthi, A. *Synlett* **2003**, 8, 1125
- 66 Najera, C.; Gil Molto, G. J.; Karlstrom, S.; Palvello, L. R.; *Org. Lett.* **2003**, 5, 1451
- 67 Magill, A. M.; McGuinness, D. S.; Cavell, K. J.; Britovsek, G. J. P.; Gibson, V. S.; White, A. J. P.; Williams, D. J.; White, A. H.; Skelton, B. W.; *J. Organomet. Chem.* **2001**, 617, 546
- 68 a) Mazet, C.; Gade, L. H. *Organometallics* **2001**, 20, 4144, b) Mazet, C.; Gade, L. H. *Eur. J. Inorg. Chem.* **2003**, 1161
- 69 Lamm, K.; Stollenz, M.; Meier, M.; Goerls, H.; Walther, D. *J. Organomet. Chem.* **2003**, 681, 24
- 70 Morales, D. M.; Redon, R.; Zheng, Y.; Dilworth, J. R. *Inorg. Chim. Acta.* **2002**, 328, 39
- 71 Kostas, I. D.; Steele, B. R.; Terzis, A.; Amosova, S. V. *Tetrahedron* **2003**, 59, 3467
- 72 Berthiol, F.; Doucet, H.; Santelli, M. *Synlett.* **2003**, 841
- 73 Done, M. C.; Ruether, T.; Cavell, K. J.; Kilner, M.; Peacock, E. J.; Braussaud, N.; Skelton, B. W.; White, A. *J. Organomet. Chem.* **2000**, 607, 78
- 74 McGuinness, D. S.; Cavell, K. J.; *Organometallics* **2000**, 19, 741
- 75 Bozell, J. J.; Voght, C. E. *J. Am. Chem. Soc.* **1988**, 110, 2655
- 76 Reetz, M. T.; Lohmer, G.; Schwickardi, R. *Angew. Chem. Int. Ed. Engl.* **1998**, 37, 4, 481
- 77 Schnyder, A.; Indolese, A. F.; Studer, M.; Blaser, H. U. *Angew. Chem. Int. Ed. Engl.* **2002**, 41, 19, 3668
- 78 Herrmann, W. A.; Cornils, B. *Angew. Chem. Int. Ed. Engl.* **1997**, 36, 1049
- 79 a) Cornils, B. *J. Mol. Catal. A: Chem.* **1999**, 143, 1 b) Kuntz, E. C. *CHEMTECH* **1987**, 17, 570
- 80 a) Bhanage, B. M.; Zhao, F. G.; Shirai, M.; Arai, M. *Tetrahedron Lett.* **1998**, 39, 9509  
b) Bhanage, B. M.; Ikushima, Y.; Shirai, M.; Arai, M. *Tetrahedron Lett.* **1999**, 40, 6427
- 81 Bergbreiter, D. E.; Liu, Y. S.; Osburn, P. L. *J. Am. Chem. Soc.* **1998**, 120, 4250
- 82 Beller, M.; Krauter, J. G. E.; Zapf, A. *Angew. Chem. Int. Ed. Engl.* **1997**, 36, 772
- 83 a) Davis, M. E. *CHEMTECH* **1992**, 498 b) Tonks, L.; Anson, M. S.; Hellgardt, K.; Mirza, A. R.; Thompson, D. F.; Williams, J. M. J. *Tetrahedron Lett.* **1997**, 38, 4319 c)

- Anson, M. S.; Mirza, A. R.; Tonks, L.; Williams, J. M. J. *Tetrahedron Lett.* **1999**, 40, 7147
- 84 Schmid, G. *Clusters and Colloids*; VCH; Weinheim. **1994**
- 85 a) Klingelhofer, S.; Heitz, W.; Greiner, A.; Oestreich, S.; Forster, S.; Antonietti, M. *J. Am. Chem. Soc.* **1997**, 119, 10116 b) Reetz, M. T.; Breinbauer, R.; Wanninger, K. *Tetrahedron Lett.* **1996**, 37, 4499 c) Reetz, M. T.; Lohmer, G. *J. Chem. Soc., Chem. Commun.* **1996**, 16, 1921 d) Beller, M.; Fischer, H.; Kuehlein, K.; Reisinger, C. P.; Herrmann, W. A. *J. Organomet. Chem.* **1996**, 520, 257 e) Fowley, L.A.; Michos, D.; Luo, X. I.; Crabtree, R. H. *Tetrahedron Lett.* **1993**, 34, 3075 f) Le Bars, J.; Sprecht, U.; Bradley, J. S.; Blackmond, D. G. *Langmuir* **1999**, 15, 7621 g) Reetz, M. T.; Westermann, E. *Angew. Chem. Int. Ed. Engl.* **2000**, 39, 165
- 86 Andersson, C. M.; Karabelas, K.; Hallberg, A.; Andersson, C. *J. Org. Chem.* **1985**, 50, 3891
- 87 Lin, C. A.; Luo, F. T. *Tetrahedron Lett.* **2003**, 44, 7565
- 88 Wang, P. W.; Fox, M. A. *J. Org. Chem.* **1994**, 59, 5358
- 89 Reetz, M. T.; Lohmer, G.; Schwickardi, R. *Angew. Chem. Int. Ed. Engl.* **1997**, 36, 1526
- 90 Buchmeiser, M. R.; Wurst, K. *J. Am. Chem. Soc.* **1999**, 121, 11101
- 91 Pan, Y.; Zhang, Z. Y.; Hu, H. W. *J. Mol. Catal.* **1990**, 62, 297
- 92 Djakovitch, L.; Heise, H.; Kohler, K. *J. Organomet. Chem.* **1999**, 584, 16
- 93 Corma, A. *Chem. Rev.* **1997**, 97, 2373
- 94 a) Mehnert, C. P.; Ying, J. Y. *J. Chem. Soc., Chem. Commun.* **1997**, 22, 2215 b) Mehnert, C. P.; Weaver, D. W.; Ying, J. Y. *J. Am. Chem. Soc.* **1998**, 120, 12289
- 95 Villemin, D.; Jaffres, P. A.; Nechab, B.; Courivaud, F. *Tetrahedron Lett.* **1997**, 38, 6581
- 96 Clark, J. H.; Macquarrie, D. J.; Mubofu, E. B. *Green Chem.* **2000**, 2, 53
- 97 Horniakova, J.; Raja, T.; Kubola, Y.; Sugi, Y. *J. Mol. Catal. A: Chem.* **2004**, 217, 73
- 98 Arellana, C. G.; Corma, A.; Iglesias, M.; Sanchez, F. *Adv. Synth. Catal.* **2004**, 346, 1758
- 99 Ji, Y. Y.; Jain, S. I.; Davis, R. J. *J. Phys. Chem. B.* **2005**, 109, 17232
- 100 Tsai, F. Y.; Wu, C. L.; Mou, C. Y.; Chao, M. C.; Lin, H. P.; Liu, S. T.; *Tetrahedron Lett.* **2004**, 45, 7503
- 101 a) Wall, V. M.; Eisenstadt, A.; Ager, D. J.; Laneman, S. A. *Platinum Met. Rev.* **1999**, 43, 138 b) Julia, M.; Duteil, M.; Grard, C.; Kuntz, E. *Bull. Chem. Soc. Chim. Fr.* 1973, 2791
- 102 Andersson, C. M.; Hallberg, A. *J. Org. Chem.* **1988**, 53, 235
- 103 a) Zhao, F. Y.; Bhanage, B. M.; Shirai, M.; Arai, M. *Chem. Eur. J.* **2000**, 6, 843 b) Zhao, F. Y.; Murakami, K.; Shirai, M.; Arai, M. *J. Catal.* **2000**, 194, 479 c) Zhao, F. Y.; Shirai, M.; Arai, M. *J. Mol. Catal. A: Chem.* **2000**, 154, 39
- 104 a) Leadbeater, N. E.; Marco, M. *J. Org. Chem.* **2003**, 68, 5660 b) Leadbeater, N. E.; Marco, M. *Angew. Chem. Int. Ed. Engl.* **2003**, 42, 1407 c) Leadbeater, N. E.; Marco, M.; Tominack, B. *J. Org. Lett.* **2003**, 5, 3919 d) Arvela, R. K.; Leadbeater, N. E.; Sangi, M. S.; Williams, V. A.; Granados, P.; Singer, R. D. *J. Org. Chem.* **2005**, 70, 161 e) Biffis, A.; Zecca, M.; Basato, M. *J. Mol. Catal. A: Chem.* **2001**, 173, 249
- 105 Kaneda, K.; Miguchi, M.; Imanaka, J. *J. Mol. Catal. A: Chem.* **1990**, 63, L33
- 106 Wagner, M.; Kohler, K.; Djakovitch, L.; Weinkauff, S.; Hagen, V.; Muhler, M. *Top. Catal.* **2000**, 13, 319
- 107 Djakovitch, L.; Kohler, K. *J. Mol. Catal. A: Chem.* **1999**, 142, 275

- 
- 108 Galow, T. H.; Drechsler, U.; Hanson, J. A.; Rotello, V. M. *Chem. Commun.* **2002**, 1076
- 109 Yeung, L. K.; Crooks, R. M. *Nano Lett.* **2001**, 1, 1, 14
- 110 Cassol, C. C.; Umpierre, A. P.; Machado, G.; Wolke, S. I.; Dupont, J. *J. Am. Chem. Soc.* **2005**, 127, 3298
- 111 Srivastava, R.; Venkatathri, N.; Srinivas, D.; Ratnasamy, P. *Tetrahedron Lett.* **2003**, 44, 3649
- 112 Crudden C. M.; Sateesh, M.; Lewis, R. *J. Am. Chem. Soc.* **2005**, 127, 10045
- 113 Bergbreiter, D. E.; Osburn, P. L.; Frels, J. D. *J. Am. Chem. Soc.* **2001**, 123, 11105
- 114 Choudary, B. M.; Madhi, S.; Chowdari, N. S.; Kantam, M. L.; Sreedhar, B. *J. Am. Chem. Soc.* **2002**, 124, 14127
- 115 Lagasi, M.; Moggi, P. *J. Mol. Catal. A: Chem.* **2002**, 182, 61
- 116 Zhao, S. F.; Zhou, R. X.; Zheng, X. M. *J. Mol. Catal. A: Chem.* **2004**, 211, 139
- 117 Hardy, J. J. E.; Hubert, S.; Macquarrie, D. J.; Wilson, A. J. *Green Chem.* **2004**, 6, 53
- 118 Shokouhimehr, M.; Kim, J. H.; Lee, Y. S. *Synlett.* **2006**, 4, 618
- 119 Zhuangyu, Z.; Hongwen, H.; Yu, K. T. *React. Polym.* **1988**, 9, 249
- 120 Zhuangyu, Z.; Hongwen, H.; Yu, K. T. *React. Polym.* **1990**, 12, 229
- 121 Yi, P.; Zhuangyu, Z.; Hongwen, H. *J. Mol. Catal.* **1990**, 62, 297
- 122 Ding, J. H.; Gin, D. L.; *Chem. Mater.* **2000**, 12, 22
- 123 Price, K. E.; Mcquade, D. T. *Chem. Commun.* **2005**, 1714
- 124 McNamara, C. A.; King, F.; Bradley, M. *Tetrahedron Lett.* **2004**, 45, 8239
- 125 Smith, G. S.; Mapolie, S. P. *J. Mol. Catal. A: Chem.* **2004**, 213, 187
- 126 a) Jeffery, T. *Tetrahedron Lett.* **1985**, 26, 2667 b) Jeffery, T. *Synthesis* **1987**, 1, 70
- 127 Larock, R.; Babu, S. *Tetrahedron Lett.* **1987**, 28, 5291
- 128 Amatore, C.; Jutand, A. *J. Organomet. Chem.* **1999**, 576, 254
- 129 Jeffery, T. *Tetrahedron* **1996**, 52, 10113
- 130 Jeffery, T.; David, M. *Tetrahedron Lett.* **1998**, 39, 5751
- 131 Buchacher, P.; Helgeson, R.; Wudl, F. *J. Org. Chem.* **1998**, 63, 9698
- 132 Amatore, C.; Jutand, A. *Acc. Chem. res.* **2000**, 33, 314
- 133 a) Grushin, V. V.; Alper, H. *Organometallics* **1993**, 12, 1890 b) Grushin, V. V. *J. Am. Chem. Soc.* **1999**, 121, 5831 c) Roffia, P.; Gregorio, G.; Conti, F.; Pregaglia, G. F. *J. Mol. Catal.* **1977**, 2, 191
- 134 Amatore, C.; Jutand, A.; Medeiros, M. J. *New J. Chem.* **1996**, 20, 1143
- 135 Ozawa, F.; Kubo, A.; Hayashi, T. *Chem. Lett.* **1992**, 11, 2177
- 136 Jutand, A.; Mosleh, A. *Organometallics* **1995**, 14, 1810
- 137 Casado, A. L.; Espinet, P. *Organometallics* **1998**, 17, 954
- 138 a) Ozawa, F.; Kubo, A.; Hayashi, T. *J. Am. Chem. Soc.* **1991**, 113, 1417 b) Cabri, W.; Candiani, I.; DeBernardinis, S.; Francalanci, F.; Penco, S.; Santi, R. *J. Org. Chem.* **1991**, 56, 5796 c) Sato, Y.; Sodeoka, M.; Shibasaki, M. *Chem. Lett.* **1990**, 10, 1953
- 139 a) Fiddy, S. G.; Evans, J.; Newton, M. A.; Neisius, T.; Tooze, R. P.; Oldman, R. *Chem. Commun.* **2003**, 2682 b) Evans, J.; O'Neill, L.; Kambhampati, V. L.; Rayner, G.; Turin, S.; Genge, A.; Dent, A. J.; Neisius, T. *J. Chem. Soc., Dalton Trans* **2002**, 2307 c) de Vries, A. H. M.; Mulders, J. M. C. A.; Mommers, J. H. M.; Henderickx, H. J. W.; de Vries, J. G. *Org. Lett.* **2003**, 5, 3285

- 
- 140 a) Yu, K.; Sommer, W.; Weck, M.; Jones, C. W. *J. Catal.* **2004**, 226, 101 b)  
Bergbreiter, D. E.; Osburn, P. L.; Frels, J. D. *Adv. Synth. Catal.* **2005**, 347, 172 c)  
Bergbreiter, D. E.; Osburn, P. L.; Wilson, A.; Sink, E. M. *J. Am. Chem. Soc.* **2000**, 122,  
9058 d) Eberhard, M. *Org. Lett.* **2004**, 6, 2125
- 141 Dupont, J.; Gruber, A. S.; Fonseca, G. S.; Monteiro, A. L.; Ebeling, G.; Burrow, R. A.  
*Organometallics*, **2001**, 20, 171
- 142 Shmidt, A. F.; Smirnov, V. V. *Kins and Catal.* **2001**, 42, 6, 876
- 143 Nilsson, P.; Wendt, O. F. *J. Organomet. Chem.* **2005**, 690, 4197
- 144 Amatore, C.; Carre, E.; Jutand, A.; Medjour, Y. *Organometallics*. **2002**, 21, 4540

*Chapter 2:*

*Preliminary Investigations on Heck  
Reactions Using Palladium Complex  
Catalysts Containing N- and P-  
Ligands*

## 2.1. Introduction

The use of Heck reaction in industrial synthesis has largely remained limited due to the high cost of catalyst precursors, promoters, phosphine ligands and stability of catalysts under practically useful conditions<sup>1</sup>. Also, the cheaply available chloro arenes do not undergo Heck reaction easily and therefore most of the literature deals with the reaction of the costlier iodo- and bromo arenes<sup>2</sup>. The emphasis of the research in Heck chemistry is towards the development of catalysts that are either able to activate the chloroarenes or are capable of giving enormously high turnover numbers (TON) with iodo and bromoarenes<sup>3</sup>, as has been discussed in Chapter 1. Since the coordination sphere of palladium determines the activity of the palladium complex for a particular reaction, it was decided to screen few known Pd complexes having phosphorus or nitrogen ligands in order to investigate their activity and efficiency for Heck reactions. The purpose of this was to ascertain the utility of cheaper phosphine free ligands for Heck reaction and to optimize the reaction conditions in order to study the kinetics of Heck reactions.

This chapter presents the experimental results on the vinylation of halo arenes with palladium complex catalysts. The results on the factors influencing the reaction efficiency and the role of substituents on the substrates have been discussed. A study on the role of quaternary ammonium salts as promoters in Heck reaction has also been presented.

## 2.2. Experimental

### 2.2.1. Materials

Pd(OAc)<sub>2</sub>, PdCl<sub>2</sub>, triphenylphosphine, aryl halides, styrene, and quaternary ammonium salts were purchased from Aldrich Chemical Co. USA, and used as received without any further purification. The inorganic and organic salts, solvents, and amine ligands were procured from the commercial sources (s-d Fine and Loba chemicals India) and used as received. The reactions were carried out in a 50 ml 2-necked stirred glass reactor fitted with a condenser, immersed in an oil bath held at a desired temperature. The stirring was by means of a magnetic stirrer.

### 2.2.2. Analytical Techniques

The analysis of the contents of the reaction mixture was done using Agilent 6850 series II gas chromatograph, on HP-I capillary column of 30 m length, 320 $\mu$ m diameter, and 0.25 $\mu$ m stationary phase film thickness (methyl siloxane as stationary phase, helium gas as the mobile phase) and a Flame Ionization Detector. The GC was equipped with an auto sampler. The quantitative analysis was done using a calibration curve prepared using synthetic standards in the range of concentration studied. Complete mass balance was obtained from the quantitative GC analysis. Conditions for GC analysis are given in Table 2.1. A typical GC chart for the Heck coupling of 4'-bromoacetophenone with n-butyl acrylate is given in Figure 2.1.

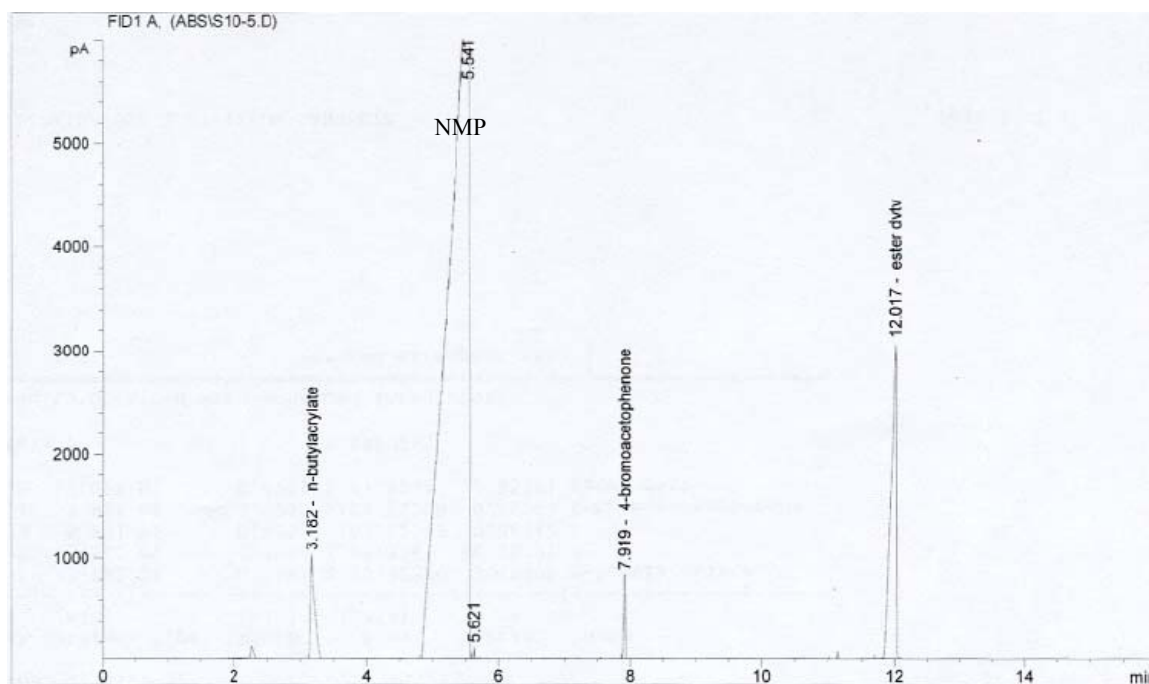


**Figure 2.1:** A typical GC chart for the Heck reaction of 4'-bromoacetophenone with n-butyl acrylate

**Table 2.1:** Conditions used for GC analysis

Injector Temperature	523 K		
Flame Ionization Detector Temp	573 K		
Inlet Flow Total (He)	81 ml/min		
Split Ratio for Injector	50 : 1		
Oven Temperature	Rate (K/min)	Temp (K)	Hold Time (min)
		253	4
	30	523	3
Column Pressure	10 Psi		

Based on the GC analysis, the conversion of aryl halide (ArX), selectivity to Heck vinylation product, TON, and Turnover Frequency (TOF) were calculated according to equations 2.1 to 2.4.

$$\% \text{Conversion} = \frac{100 \times [(\text{Initial Mol}_{\text{ArX}}) - (\text{Final Mol}_{\text{ArX}})]}{(\text{Initial Mol}_{\text{ArX}})} \quad \text{Eq 2.1}$$

$$\% \text{Selectivity}_{\text{Prod}} = \frac{100 \times (\text{Final Mol}_{\text{Prod}})}{[(\text{Initial Mol}_{\text{ArX}}) - (\text{Final Mol}_{\text{ArX}})]} \quad \text{Eq 2.2}$$

$$\text{TON} = \frac{\text{Moles of Heck vinylation product formed}}{\text{Moles of palladium charged}} \quad \text{Eq 2.3}$$

$$\text{TOF} = \frac{\text{Moles of Heck vinylation product formed}}{\text{Moles of palladium charged per unit time}} \quad \text{Eq 2.4}$$

The products obtained for the Heck reaction were separated from the reaction mixture by column chromatography. A glass column of length 70 cm and internal diameter 2 cm was used for the separation using silica gel 100-200 mesh as the stationary phase.

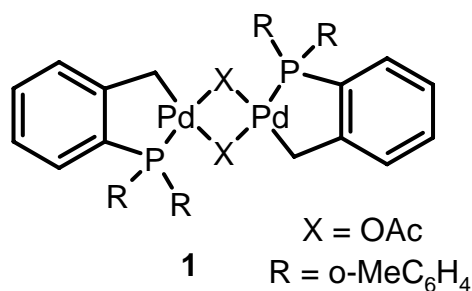


Petroleum ether and ethyl acetate mixed in various proportions constituted the mobile phase. The identification and characterization of the products was done using IR and elemental analysis. IR analysis was obtained on Bio Rad FTS 175C spectrophotometer. Elemental analysis of the complexes was carried out on a CHNS-O EA1108, Elemental analyzer of Carlo Erba Instruments. GC-MS analysis was carried out on Agilent 6890 N GC with 5973 N Mass selective detector.

### 2.2.3. Synthesis of palladium complexes

Palladium complexes containing phosphorus and nitrogen ligands were synthesized by the procedures given below.

#### 2.2.3.1. Synthesis of *trans*-di( $\mu$ -acetato)-bis[*o*-(*di*-*o*-tolylphosphino)benzyl]dipalladium(II) (Catalyst 1):



The procedure reported in the literature<sup>4</sup> was followed for the synthesis of the catalyst precursor **1**. Pd(OAc)<sub>2</sub> (224mg, 1 mmol) was dissolved in 25 ml toluene. A red-brown solution was obtained. To this solution P(*o*-tolyl)<sub>3</sub> (400mg, 1.1 mmol) was added. The bright orange mixture was heated in a water bath at 50°C for 3 minutes and then cooled to room temperature. The solvent was reduced to a quarter of its volume under vacuum. To this, hexane (25 ml) was added in order to precipitate the complex. After filtration and drying under vacuum, 0.42 g of the yellow solid was obtained, which corresponds to 90% yield with respect to Pd(OAc)<sub>2</sub> added. This complex was characterized by IR and microanalysis techniques. The IR spectrum (Figure 2.2, Table 2.2) matched the reported

values and the major frequencies of absorption were at  $\nu = 1578 \text{ cm}^{-1}$  (C=O), and  $1416 \text{ cm}^{-1}$  (C-O). The elemental analysis also matched the calculated values for C and H.

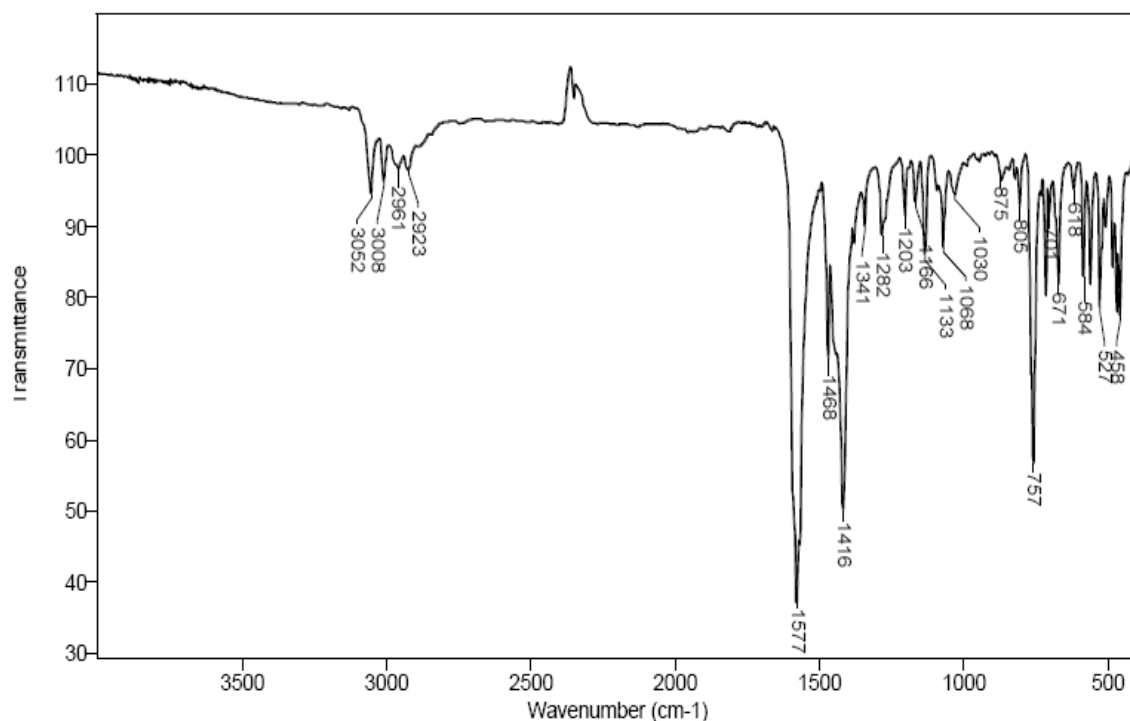
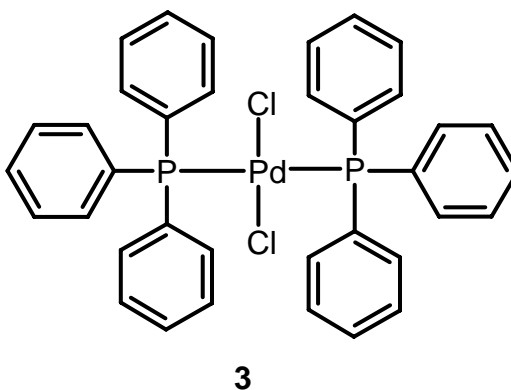


**Figure 2.2:** IR spectra of the palladium complex **1**

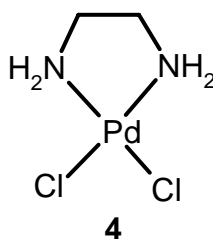
### 2.2.3.2. Synthesis of dichloro(bistriphenylphosphine)palladium(II) (Catalyst **3**):



Dichloro(bistriphenylphosphine)palladium(II) was synthesized by the following procedure. A solution of  $\text{PdCl}_2$  (1 mmol) in 25 ml of dilute aqueous hydrochloric acid (20% v/v) was slowly added to a warm solution of  $\text{PPh}_3$  (2.1 mmol) in ethanol (20 ml) and was stirred at 333 K for 2 h. The bright yellow complex precipitated, and was filtered, washed

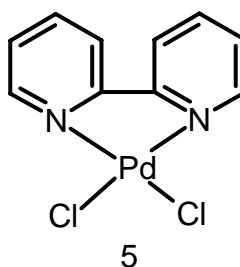
with hot ethanol, and dried in vacuum. The complex was re-crystallized from chloroform to obtain a 95% yield of  $\text{PdCl}_2(\text{PPh}_3)_2$  based on  $\text{PdCl}_2$ . This complex was characterized by IR and elemental analysis techniques (Table 2.2). The elemental analysis matched the values calculated for C and H. The major IR frequencies were at  $\nu = 1434 \text{ cm}^{-1}$  and  $1481 \text{ cm}^{-1}$  corresponding to the presence of aromatic ring.

2.2.3.3. *Synthesis of dichloro(ethylenediamine)palladium(II) (Catalyst 4):*



The dichloro(ethylenediamine)palladium(II) complex was prepared by the following procedure. In a 50 ml round bottom flask containing 10 ml methanol, 0.372g (2.1 mmol)  $\text{PdCl}_2$  was added followed by 0.127 (2.1 mmol) ethylenediamine. The mixture was stirred at room temperature for 6 h. A yellow orange solid had precipitated by this time. The reaction mixture was then filtered and the yellow orange solid obtained was washed with methanol, and dried under vacuum. Yield of the complex was 0.40g (84%). This complex was also characterized by IR and elemental analysis techniques (Table 2.2). The elemental analysis matched the values calculated for C, H, and N. The major IR frequencies were at  $\nu = 1596 \text{ cm}^{-1}$  (N-H) and  $1056 \text{ cm}^{-1}$  (C-N).

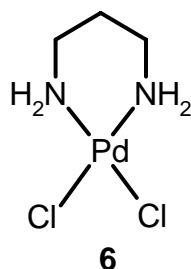
2.2.3.4. *Synthesis of dichloro(2,2'-bipyridine)palladium(II) (Catalyst 5):*



In a 50 ml round bottom flask containing 10 ml methanol, 0.266g (1.3 mmol)  $\text{PdCl}_2$  was added followed by 0.234g (1.3 mmol) 2,2'-bipyridine. The mixture was stirred at room

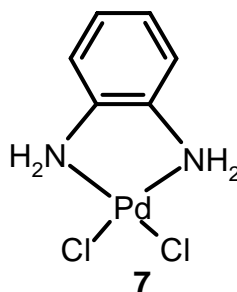
temperature for 6 h. An orange solid had precipitated after this time. The reaction mixture was filtered and the orange solid washed with methanol and dried under vacuum. Yield of the complex was 0.440g (88%). This complex was characterized by IR and elemental analysis techniques (Table 2.2). The elemental analysis matched the values calculated for C, H, and N. The major IR frequencies were at  $\nu = 1596 \text{ cm}^{-1}$  (N-H) and  $1132 \text{ cm}^{-1}$  (C-N).

2.2.3.5. *Synthesis of dichloro(propylenediamine)palladium(II) (Catalyst 6):*



The dichloro(propylenediamine)palladium(II) complex was prepared by the procedure given for the preparation of dichloro(ethylenediamine)palladium(II) complex. The charge taken for the metal complex preparation was 0.355g (2.0 mmol)  $\text{PdCl}_2$ , 0.149g (2.0 mmol) 1,3-diaminopropane, and 10 ml methanol. Yield of the complex was 0.40g (80%). This complex was characterized by IR and elemental analysis techniques (Table 2.2). The elemental analysis matched the values calculated for C, H, and N. The major IR frequencies were at  $\nu = 1594 \text{ cm}^{-1}$  (N-H) and  $1064 \text{ cm}^{-1}$  (C-N).

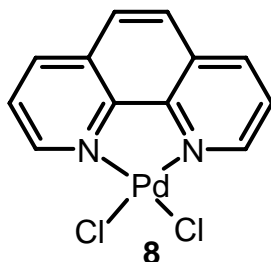
2.2.3.6. *Synthesis of dichloro(1,2-phenylenediamine)palladium(II) (Catalyst 7):*



The dichloro(1,2-phenylenediamine)palladium(II) complex was synthesized as per the procedure given for the preparation of dichloro(ethylenediamine)palladium(II) complex. The charge taken for the Pd complex preparation was 0.355g (2.0 mmol)  $\text{PdCl}_2$ ,

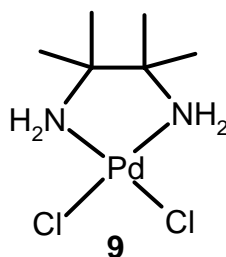
0.216g (2.0 mmol) 1,2-phenylenediamine, and 10 ml methanol. Yield of the complex was 0.485g (85%). This complex was characterized by IR and elemental analysis techniques (Table 2.2). The elemental analysis matched the values calculated for C, H, and N. The major IR frequencies were at  $\nu = 1523 \text{ cm}^{-1}$  (N-H) and  $1276 \text{ cm}^{-1}$  (C-N).

2.2.3.7. *Synthesis of dichloro(1,10-phenanthroline)palladium(II) (Catalyst 8):*



The  $\text{PdCl}_2(\text{bis}1,10\text{-phenanthroline})$  complex was synthesized by the procedure given for the preparation of dichloro(ethylenediamine)palladium(II) complex. The charge taken for the metal complex preparation was 0.236g (1.3 mmol)  $\text{PdCl}_2$ , 0.264g (1.3 mmol) 1,10-Phenanthroline, and 10 ml methanol. Yield of the complex was 0.450g (90%). This complex was characterized by IR and elemental analysis techniques (Table 2.2). The elemental analysis matched the values calculated for C, H, and N. The major IR frequencies were at  $\nu = 1596 \text{ cm}^{-1}$  (N-H) and  $1132 \text{ cm}^{-1}$  (C-N).

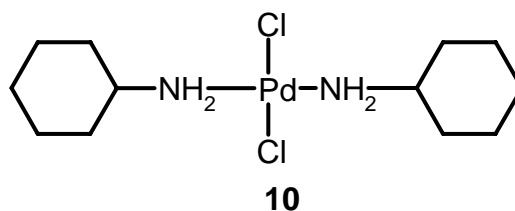
2.2.3.8. *Synthesis of dichloro(2,3-diamino-2,3-dimethylbutane)palladium(II) (Catalyst 9):*



The dichloro(2,3-diamino-2,3-dimethylbutane)palladium(II) complex was synthesized by a procedure given for the preparation of dichloro(ethylenediamine)palladium(II) complex. The charge taken for the metal complex preparation was 0.301g (1.7 mmol)  $\text{PdCl}_2$ , 0.198g (1.7 mmol) 2,3-diamino-2,3-dimethylbutane, and 10 ml methanol. Yield of the complex was 0.40g (80%). This complex

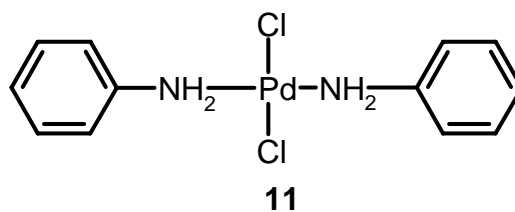
was characterized by IR and elemental analysis techniques (Table 2.2). The elemental analysis matched the values calculated for C, H, and N. The major IR frequencies were at  $\nu = 1631 \text{ cm}^{-1}$  (N-H) and  $1125 \text{ cm}^{-1}$  (C-N).

2.2.3.9. *Synthesis of dichloro(biscyclohexylamine)palladium(II) (Catalyst 10):*



The dichloro(biscyclohexylamine)palladium(II) complex was synthesized as per the procedure given for the preparation of dichloro(ethylenediamine)palladium(II) complex. The charge taken for the metal complex preparation was 0.236g (1.3 mol)  $\text{PdCl}_2$ , 0.265g (2.7 mmol) cyclohexylamine, and 10 ml methanol. Yield of the complex was 0.30g (80%). This complex was characterized by IR and elemental analysis techniques (Table 2.2). The elemental analysis matched the values calculated for C, H, and N. The major IR frequencies were at  $\nu = 1573 \text{ cm}^{-1}$  (N-H) and  $1146 \text{ cm}^{-1}$  (C-N).

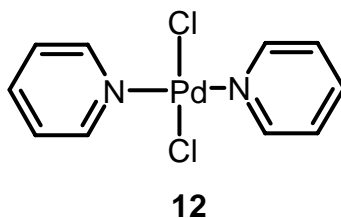
2.2.3.10. *Synthesis of dichloro(bisaniline)palladium(II) (Catalyst 11):*



The dichloro(bisaniline)palladium(II) complex was synthesized by a procedure similar to that for the preparation of dichloro(ethylenediamine)palladium(II) complex. The charge taken for the metal complex preparation was 0.243g (1.4 mmol)  $\text{PdCl}_2$ , 0.256g (2.7 mmol) aniline, and 10 ml methanol. Yield of the complex was 0.40g (80%). This complex was characterized by IR and elemental analysis techniques (Table 2.2). The elemental

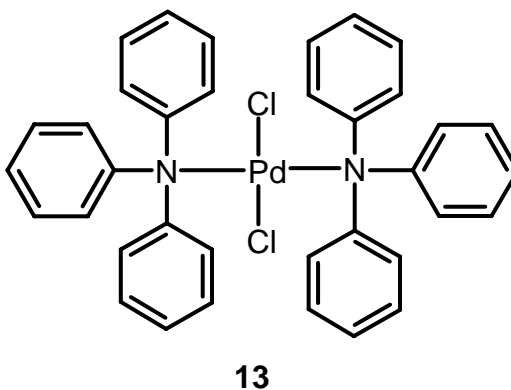
analysis matched the values calculated for C, H, and N. The major IR frequencies were at  $\nu = 1570 \text{ cm}^{-1}$  (N-H) and  $1217 \text{ cm}^{-1}$  (C-N).

2.2.3.11. *Synthesis of dichloro(bispyridine)palladium(II) (Catalyst 12):*



The dichloro(bispyridine)palladium(II) complex was synthesized according to the procedure given for the preparation of dichloro(ethylenediamine)palladium(II) complex. The charge taken for the metal complex preparation was 0.264g (1.5 mmol)  $\text{PdCl}_2$ , 0.238g (3.0 mmol) pyridine, and 10 ml methanol. Yield of the complex was 0.43g (86%). This complex was characterized by IR and elemental analysis techniques (Table 2.2). The elemental analysis matched the values calculated for C, H, and N. The major IR frequencies were at  $\nu = 1596 \text{ cm}^{-1}$  (N-H) and  $1132 \text{ cm}^{-1}$  (C-N).

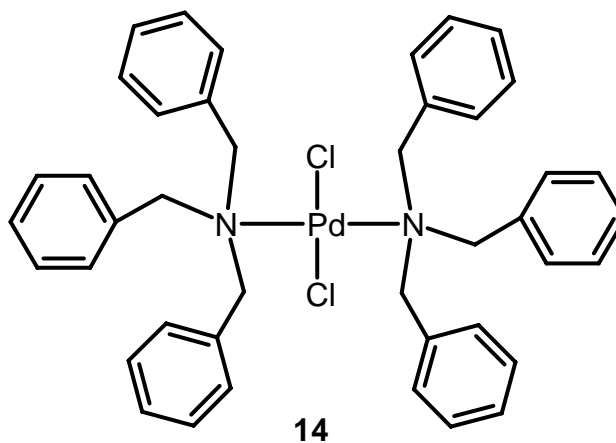
2.2.3.12. *Synthesis of dichloro(bistriphenylamine)palladium(II) (Catalyst 13):*



The dichloro(bistriphenylamine)palladium(II) complex was synthesized according to the procedure described for the preparation of dichloro(ethylenediamine)palladium(II) complex. The charge taken for the metal complex preparation was 0.133g (0.7 mmol)  $\text{PdCl}_2$ , 0.368g (1.5 mmol) triphenylamine, and 10 ml methanol. Yield of the complex was 0.35g (70%). This complex was characterized by IR and elemental analysis techniques

(Table 2.2). The elemental analysis matched the values calculated for C, H, and N. The major IR frequencies were at  $\nu = 1277 \text{ cm}^{-1}$  (C-N).

2.2.3.13. *Synthesis of dichloro(bis(tribenzylamine)palladium(II) (Catalyst 14):*



The dichloro(bis(tribenzylamine)palladium(II) complex was synthesized as per the procedure given for the preparation of dichloro(ethylenediamine)palladium(II) complex. The charge taken for the metal complex preparation was 0.118g (0.7 mmol)  $\text{PdCl}_2$ , 0.382g (1.3 mmol) tribenzylamine, and 10 ml methanol. Yield of the complex was 0.35g (70%). This complex was characterized by IR and elemental analysis techniques (Table 2.2). The elemental analysis matched the values calculated for C, H, and N. The major IR frequencies were at  $\nu = 1262 \text{ cm}^{-1}$  (C-N).



**Table 2.2:** IR and elemental analysis data for the synthesized palladium complexes

Complex	Yield %	IR Peaks wavenumber $\text{cm}^{-1}$ (intensity)	Theoretical, %			Analyzed, %		
			C	H	N	C	H	N
1	90	470(s), 527(s), 560(m), 584(m), 671(m), 717(m), 757(s), 805(w), 1030(w), 1068(m), 1133(m), 1203(w), 1282(w), 1341(w), 1416(vs), 1468(s), 1577(vs), 2923(m), 2957(w), 3008(m), 3052(m)	58.93	4.95	–	58.61	4.89	–
3	95	436(m), 455(m), 499(vs), 508(vs), 520(vs), 692(vs), 707(s), 745(vs), 921(w), 999(m), 1027(m), 1071(w), 1099(vs), 1186(m), 1309(w), 1434(vs), 1481(s), 1573(m), 1587(m), 3049(m), 3074(m)	61.60	4.31	–	61.78	4.27	–
4	84	458(s), 514(s), 577(s), 794(m), 895(m), 1056(vs), 1132(vs), 1273(s), 1292(m), 1317(s), 1366(s), 1390(w), 1453(vs), 1596(vs), 3073(vs br), 3198(vs br)	10.12	3.40	11.80	9.97	3.34	11.77
5	88	412(m), 474(w), 562(s), 617(s), 675(w), 721(s), 766(vs), 972(w), 1042(s), 1054(s), 1075(m), 1119(vs), 1253(w), 1320(w), 1382(w), 1450(s), 1471(s), 1500(m), 1565(w), 1604(s), 3057(s br), 3111(s br), 3411(s br)	36.02	2.42	8.40	36.31	2.33	8.27

**Table 2.2 (Continued):** IR and elemental analysis data for the synthesized palladium complexes

Complex	Yield %	IR Peaks wavenumber $\text{cm}^{-1}$ (intensity)	Theoretical, %			Analyzed, %		
			C	H	N	C	H	N
6	80	474(w), 584(w), 907(w), 942(w), 1031(vs), 1064(m), 1211(s), 1325(m), 1409(m), 1421(w), 1462(w), 1594(s), 3073(vs), 3198(vs), 3241(s)	14.33	4.01	11.14	14.12	3.89	11.02
7	85	475(m), 542(m), 664(w), 649 (s), 754(vs), 933(w), 1034(w), 1151(vs), 1215(m), 1275 (vs), 1329(m), 1383(m), 1434(s), 1459(s), 1483(s), 1523(vs), 1604(vs), 2918(w), 3025 (s), 3078(s), 3370(m), 3460(s)	25.25	2.83	9.81	25.46	2.74	9.65
8	90	476(w), 500(w), 650(w), 710(vs), 723(m), 786(w), 842(vs), 872(w), 1114(m), 1153(s), 1220(m), 1350(w), 1409(w), 1425(vs), 1515(s), 1581(m), 1593(m), 3057(m), 3082(m)	40.32	2.26	7.84	40.19	2.07	7.70
9	80	486(m), 512(m), 772(s), 807(vs), 954(s), 1008(vs), 1048(s), 1064(m), 1104(m), 1125(s), 1280(s), 1401(w), 1449(m), 1457(vs), 1631 (m), 2839(w), 2914(m), 2986(m), 3024(m)	24.55	5.49	9.64	24.68	5.37	9.72

**Table 2.2 (Continued):** IR and elemental analysis data for the synthesized palladium complexes

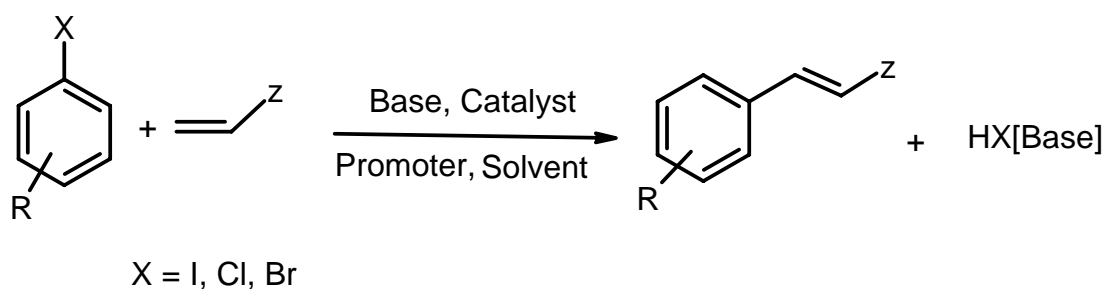
Complex	Yield %	IR Peaks wavenumber $\text{cm}^{-1}$ (intensity)	Theoretical, %			Analyzed, %		
			C	H	N	C	H	N
10	80	474(m), 580(w), 601(m), 799(m), 853(m), 894(s), 967(m), 1039(s), 1057(vs), 1076(s), 1146(vs), 1226(s), 1251(m), 1349(m), 1387(m), 1444(vs), 1573(vs), 2842(vs), 2902(m), 2934(vs), 3120(vs), 3201(vs), 3281(vs)	38.37	6.90	7.46	38.29	6.88	7.48
11	80	449(s), 551(s), 582(s), 619(m), 689(vs), 756(vs), 764(vs), 805(m), 904(m), 1027(m), 1067(s), 1116(vs), 1145(s), 1217(s), 1467(s), 1493(vs), 1570(vs), 1599(vs), 1856(m), 3045(m), 3121(vs), 3186(s), 3204(vs), 3287(vs)	39.64	3.88	7.71	39.45	3.74	7.65
12	86	471(m), 655(m), 695(vs), 769(vs), 828(m), 1018(m), 1069(vs), 1148(s), 1204(s), 1248(s), 1448(vs), 1475(m), 1604(s), 2912(m), 3029(m), 3216(m)	36.80	3.00	8.35	36.99	3.10	8.49

**Table 2.2 (Continued):** IR and elemental analysis data for the synthesized palladium complexes

Complex	Yield %	IR Peaks wavenumber $\text{cm}^{-1}$ (intensity)	Theoretical, %			Analyzed, %		
			C	H	N	C	H	N
13	70	503(vs), 622(vs), 696(vs), 749(vs), 894(m), 1028(m), 1075(s), 1173(s), 1277(vs), 1313(m), 1329(vs), 1491(vs), 1585(vs), 1939(m), 3040(m br), 3070(m br)	64.73	4.63	4.19	64.59	4.58	4.22
14	70	441(w), 501(m), 622(w), 699(vs), 749(vs), 854(w), 915(w), 1027(m), 1041(w), 1204(w), 1262(s), 1452(s), 1495(m), 1561(w), 1577(m), 2361(w), 2470(w), 2866(w), 3004(w), 3032(m), 3061(m)	67.07	5.63	3.72	67.00	5.55	3.78

### 2.2.4. General Procedure for Heck reactions (Scheme 2.1)

In a typical experiment, 10 mmol of 4'-bromoacetophenone, 15 mmol n-butyl acrylate, 15 mmol sodium acetate, 2 mmol tetrabutylammonium bromide, and 2  $\mu$ mol palladium complex catalyst precursor were taken in N-methyl 2-pyrrolidinone solvent in a 50 ml 2-necked stirred glass reactor, under nitrogen atmosphere. This was then immersed in an oil bath pre-heated to a required temperature. The reaction was then started by switching on the stirrer. Samples were withdrawn at regular intervals, filtered and analyzed by GC for conversion of aryl halide and the coupling product formed. After the reaction, the reaction mixture was washed with 5% HCl (3 washes with 25 ml each) and extracted with  $\text{CH}_2\text{Cl}_2$  (50 ml) and dried over  $\text{MgSO}_4$ . The solvent was removed under vacuum and then the mixture was separated by column chromatography to isolate the products.



**Scheme 2.1**

## 2.3. Results and Discussion

### 2.3.1. Screening of palladium complex catalyst precursor for the Heck reaction

The different catalyst precursors synthesized were screened for the Heck reaction of 4'-bromoacetophenone with n-butyl acrylate in presence of sodium acetate as the base and tetrabutylammonium bromide promoter. The results are discussed in this section.

### 2.3.1.1. Palladium-phosphine catalyst systems

The palladacycle catalyst precursor **1**, Pd(OAc)<sub>2</sub>/2PPh<sub>3</sub> **2**, and PdCl<sub>2</sub>(PPh<sub>3</sub>)<sub>2</sub> **3** were screened for their activity for Heck reaction. Complete conversions of 4'-bromoacetophenone were obtained for all three catalyst precursors within 30 minutes of the reaction. A typical concentration vs time profile for the reaction is presented in Figure 2.3 for the Heck vinylation of 4'-bromoacetophenone (4'-BAP) with n-butyl acrylate (n-BA) using palladium complex **1** as catalyst. The selectivity towards the Heck vinylation product was in excess of 95%.

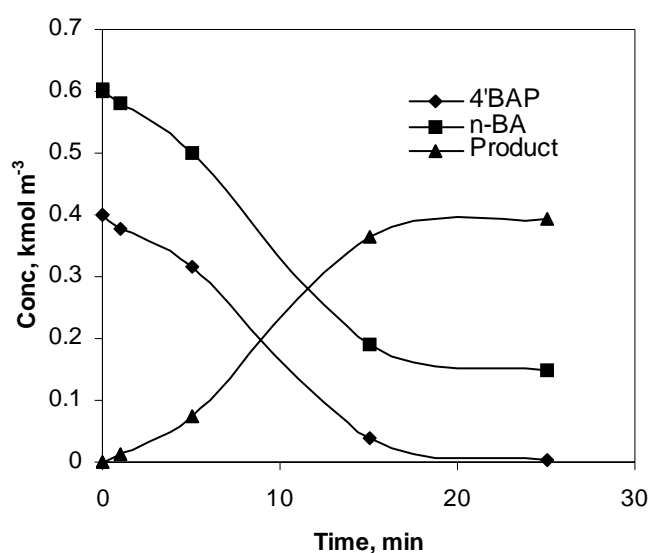


**Figure 2.3:** A typical Concentration- Time profile for the vinylation of 4'-BAP with n-BA at 423 K using catalyst **1**

**Reaction conditions:** 4'-BAP: 0.399 kmol/m<sup>3</sup>, n-BA: 0.602 kmol/m<sup>3</sup>, NaOAc: 0.6 kmol/m<sup>3</sup>, TBAB: 0.074 kmol/m<sup>3</sup>, Catalyst **1**: 8.51 x 10<sup>-5</sup> kmol/m<sup>3</sup>, Solvent: NMP, Total Volume: 2.5 x 10<sup>-5</sup> m<sup>3</sup>, Temp: 423 K.

All the three catalyst systems screened turned out to be highly active for the Heck reactions. The activity of these catalyst precursors was compared based on their initial turnover frequencies calculated for the first 10 min of the reaction, presented in Figure 2.4.

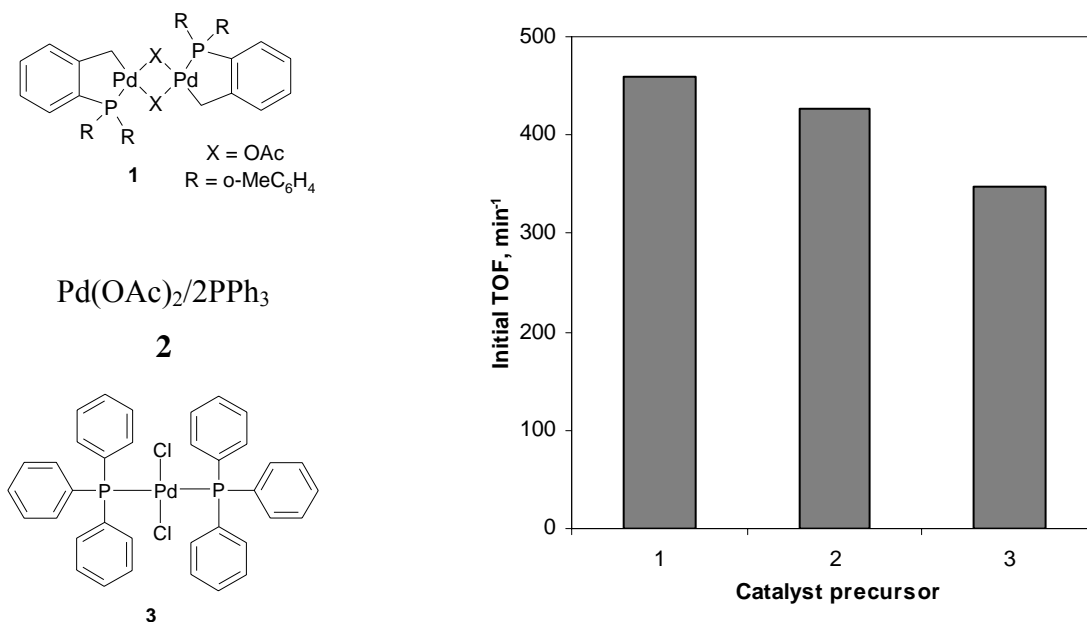


**Figure 2.4:** Comparison of palladium-phosphine catalyst systems for Heck reaction

**Reaction conditions:** 4'-BAP: 0.399 kmol/m<sup>3</sup>, n-BA: 0.602 kmol/m<sup>3</sup>, NaOAc: 0.6 kmol/m<sup>3</sup>, TBAB: 0.74 kmol/m<sup>3</sup>, Catalyst: 8.51 x 10<sup>-5</sup> kmol/m<sup>3</sup>, solvent: NMP, Total Volume: 2.5 x 10<sup>-5</sup> m<sup>3</sup>, Temp: 423K.

Palladacycle catalyst **1** gave the highest rate of reaction. The rate of reaction with the catalyst system **3** was lower than that obtained with catalyst systems **1** and **2**. This can be attributed to the comparative ease of dissociation of acetate ligand as compared to that of the chloride to give the active catalytic species L<sub>2</sub>Pd(0).

### 2.3.1.2. Palladium-amine catalyst systems

The catalyst precursors **10** to **14** containing monodentate amine ligands were compared for their activity for the Heck reactions. All these catalyst precursors led to complete conversion of 4'-bromoacetophenone within 40 minutes of the reaction. These catalyst precursors were compared based on their Initial TOFs calculated for the first 15 min of the reaction. The results are presented in Figure 2.5.

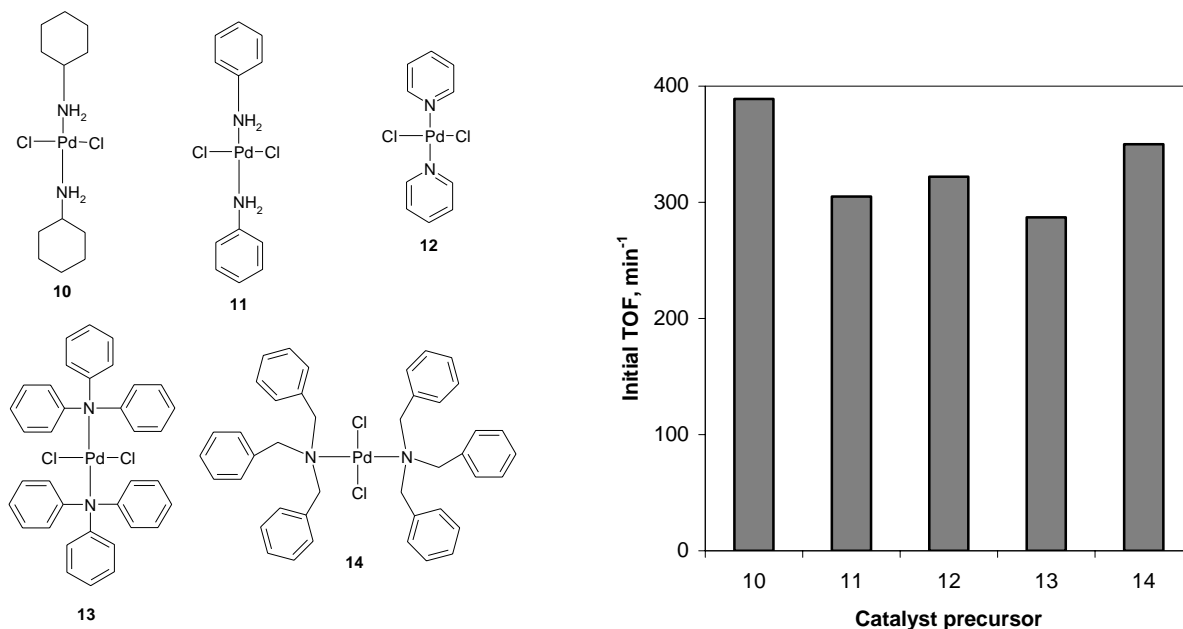


**Figure 2.5:** Comparison of palladium-amine monodentate catalyst systems for Heck reaction

**Reaction conditions:** 4'-BAP:  $0.399 \text{ kmol/m}^3$ , n-BA:  $0.602 \text{ kmol/m}^3$ , NaOAc:  $0.6 \text{ kmol/m}^3$ , TBAB:  $0.74 \text{ kmol/m}^3$ , Catalyst:  $8.51 \times 10^{-5} \text{ kmol/m}^3$ , solvent: NMP, Total Volume:  $2.5 \times 10^{-5} \text{ m}^3$ , Temp: 423K.

The highest rates were achieved with palladium complex having cyclohexylamine ligand. The order of reactivity of these complexes was dependent on the electron density on the Pd. The catalyst precursors with a higher electron density on the palladium reacted faster than those having lower electron density. The higher electron density on palladium increases the rate of the oxidative addition step which in turn leads to higher rate of reaction<sup>5</sup>.

### 2.3.1.3. Palladium-N-N bidentate amine catalyst systems

For this study, the activity of various palladium complexes having N-N bidentate ligands (complexes 4 to 9) was investigated for the Heck vinylation reaction of 4'-bromoacetophenone with n-butyl acrylate. The rates obtained with these catalysts were in general lower than those obtained for the monodentate systems. These catalysts led to



complete conversions of 4'-bromoacetophenone but after a longer reaction period. The reaction with the catalyst complex **8** took 2 hours for complete conversions of 4'-bromoacetophenone. The comparison of the TOFs obtained for the first 20 minutes of the reaction is given in Figure 2.6.

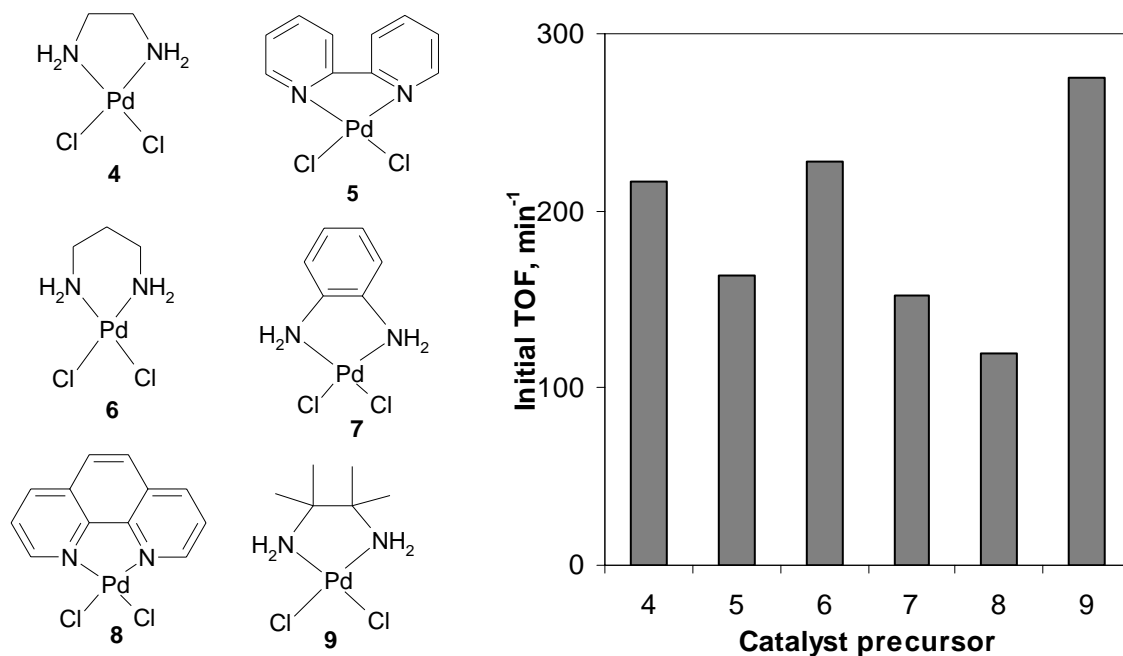


**Figure 2.6:** Comparison of palladium-amine bidentate catalyst systems for Heck reaction  
**Reaction conditions:** 4'-BAP: 0.399 kmol/m<sup>3</sup>, n-BA: 0.602 kmol/m<sup>3</sup>, NaOAc: 0.6 kmol/m<sup>3</sup>, TBAB: 0.74 kmol/m<sup>3</sup>, Catalyst: 8.51 x 10<sup>-5</sup> kmol/m<sup>3</sup>, solvent: NMP, Total Volume: 2.5 x 10<sup>-5</sup> m<sup>3</sup>, Temp: 423K

Here too it was observed that the higher electron density on Pd translated into higher reaction rate. The highest rates were obtained with the complex **9** which had the highest electron density on Pd amongst the bidentate complexes screened. The rates obtained with rigid bidentate complexes like **8** were very low.

Overall it was observed that the phosphine ligands gave better rate of reaction than the nitrogen containing ligands. Amongst the nitrogen containing ligands, the rates were higher for Pd complexes with monodentate ligands than with bidentate ligands.

### 2.3.2. Effect of Solvent on the Reaction Rate

In order to ascertain the best and the most convenient solvent to work with, different solvents were screened and their influence on the activity and selectivity of Heck vinylation reaction of 4'-bromoacetophenone with n-butyl acrylate using catalyst **1** in presence of NaOAc as base and tetrabutylammonium bromide as a promoter was observed. N-methylpyrrolidinone (NMP), N,N-dimethylformamide (DMF), ethyleneglycol, diethyleneglycoldibutylether, quinoline, and n-decane were chosen as the solvents to be screened. This was done with the view of testing both polar and non-polar solvents. The results of this study are presented in Figure 2.7.

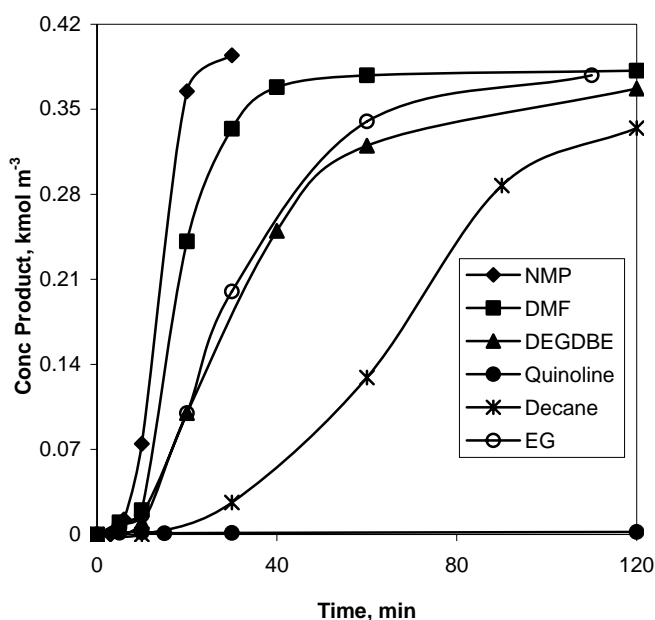


**Figure 2.7:** Plot of product formation as a function of time for various solvents

**Reaction conditions:** 4'-BAP:  $0.399 \text{ kmol/m}^3$ , n-BA:  $0.602 \text{ kmol/m}^3$ , NaOAc:  $0.6 \text{ kmol/m}^3$ , TBAB:  $0.74 \text{ kmol/m}^3$ , Catalyst precursor **1**:  $8.51 \times 10^{-5} \text{ kmol/m}^3$ , solvent, Total Volume:  $2.5 \times 10^{-5} \text{ m}^3$ , Temp: 423 K..

NMP: N-methylpyrrolidinone, DMF: N,N-dimethylformamide, DEGDBE: diethyleneglycoldibutylether, EG: ethyleneglycol

In case of ethyleneglycol, the substrates and product were partially soluble in the solvent. Hence, each sample was extracted with toluene and then analyzed by GC. There was an induction period observed with all the solvents screened. This induction period can

be attributed to time required for the formation of active catalytic species from the palladacycle catalyst precursor **1**. The dimeric palladacycle forms a monomeric species in the reaction mixture which is the active species involved in the catalytic cycle<sup>6</sup>.

No product formation was observed when quinoline was used as a solvent. Quinoline can act as a ligand by donation of the free lone pair of electrons to palladium. The Pd is thus unavailable for taking part in the catalytic cycle. With ethyleneglycol (EG) and diethyleneglycoldibutylether (DEGDBE), the concentration time profile for the product formation was very similar in the initial stages (~ 40 min). But for extended reaction periods, EG gave higher yields of Butyl-3-(4-acetylphenyl)acrylate as shown in Figure 2.7. In DEGDBE the reactants and products (apart from sodium acetate) were completely soluble. Whereas, in ethyleneglycol the halide, olefin and the product dissolved partially thus allowing for the easy separation of the products from the reaction mixture. Thus, overall, ethyleneglycol turned out to be a better solvent than DEGDBE.

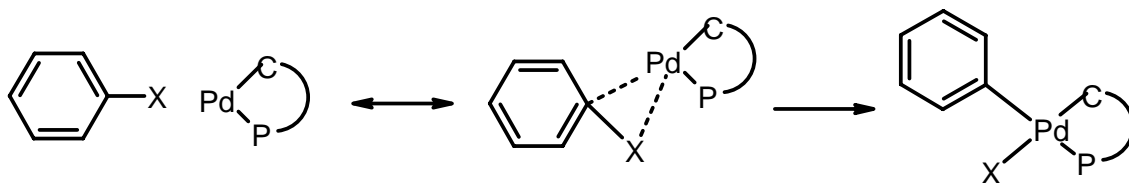
The rate of reaction was faster in polar solvents than in non-polar solvents. In case of NMP, the reaction was complete in 20 minutes. With DMF, it took 30 minutes to achieve maximum conversion. Whereas with non-polar decane, the reaction rate was very slow and the reaction was not complete even after 2 hours of reaction time. These results are in conformity with the earlier reports on Heck reactions, which state that the reaction proceeds faster in polar solvents than in non-polar solvents<sup>7</sup>. One more factor responsible for enhanced rates in polar solvents is the solubility of the base in the reaction medium. The solubility of sodium acetate is higher in polar solvents than in non-polar solvents, thus in polar solvents the base can more easily remove HX from the catalytic cycle and convert the palladium to Pd(0) species for the next cycle, thereby giving higher rates as compared to the non-polar solvents.

Out of all the solvents screened, NMP turned out to be the best solvent in terms of the rate of reaction. NMP being polar was also efficient in solubilizing the base. Hence, for the further screening studies on Heck reactions, NMP was used as the solvent.

### 2.3.3. Screening of aryl halides for the Heck reaction

Initially the effect of halogen on the reaction was investigated. Reactions were carried out for the Heck vinylation of iodobenzene, bromobenzene, and chlorobenzene with

n-butyl acrylate. Under the reaction conditions employed, chlorobenzene did not undergo any reaction, while the reaction of iodobenzene was faster than that of bromobenzene. The oxidative addition of the arylhalide to the Pd(0) species is the first step in the mechanism for the Heck reaction. In this step, the catalytically active 14 electron  $L_2Pd(0)$  species oxidatively adds to the aryl halide (Scheme 2.2). The chelating coordination of the ligands to palladium leads to the formation of the complex that has the halide and the aryl group in a mutual cis orientation<sup>8</sup>. Thus a three member cyclic intermediate is formed between Pd and Ar-X, after which the cleavage of C-X bond of the aryl halide occurs leading to the completion of oxidative addition step. The ease of C-X bond cleavage will depend on the strength of C-X bond (X being the halide), which will determine the rate of reaction. The strength of this bond decreases in the order C-Cl > C-Br > C-I, hence, their reactivity for the Heck reaction will increase as we go from chloride to iodide.



**Scheme 2.2**

After investigating the effect of different halides on the activity of the palladacycle catalyst for the Heck reaction, a study was conducted to understand the effect of various substituents on the activity of Heck vinylation of bromobenzenes. The results obtained for the reaction of bromoarenes having electron donating groups at *para*- position are presented in Figure 2.8.

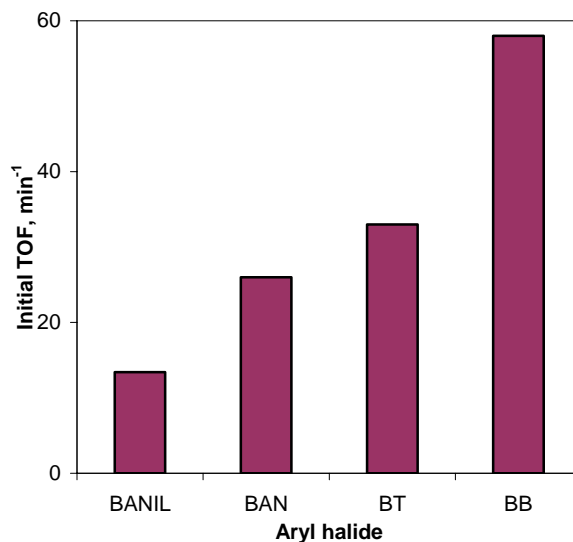


**Figure 2.8:** Effect of different aryl halides on the rate of Heck reaction

**Reaction conditions:** Aryl halide:  $0.399 \text{ kmol/m}^3$ , *n*-BA:  $0.602 \text{ kmol/m}^3$ , NaOAc:  $0.6 \text{ kmol/m}^3$ , TBAB:  $0.74 \text{ kmol/m}^3$ , Catalyst precursor 1:  $8.51 \times 10^{-5} \text{ kmol/m}^3$ , Solvent NMP, Total Volume:  $2.5 \times 10^{-5} \text{ m}^3$ , Temp: 423K.

BANIL: 4'-bromoaniline, BAN: 4'-bromoanisole, BT: 4'-bromotoluene, BB: bromobenzene.

It was observed that the rates decreased as the electron donating ability of the substituent, as quantified by Hammett<sup>9</sup>, increased. As the Hammett constant for a substituent increased, an increase in the reaction rate for that particular substrate was observed. All the bromoarenes having electron donating substituents in *para* position gave lower reaction rates than those obtained with unsubstituted bromobenzene. This can be explained based on the oxidative addition of aryl halides to the palladium. Electron donating substituents like -Me, -NH<sub>2</sub>, and -OMe present on the ring increase the electron density on the ring. These groups thus supply the C-X bond with more electrons and hence strengthen it. This makes it difficult for palladium to oxidatively add such aryl halides by cleaving the C-X bond, which in turn leads to the lower rates for Heck reactions. -NH<sub>2</sub> increases the electron density on the aromatic ring to a maximum and hence gives the lowest reaction rates.

The activities observed in the case of bromoarenes having electron withdrawing groups as substituents (Figure 2.9) were also as per the Hammett correlation. The nitro group, which has the highest electron withdrawing ability, gave the highest reaction rates for the Heck reaction. All the bromoarenes having electron withdrawing substituents gave the reaction rates higher than that of unsubstituted bromobenzene. These observations were similar to those reported in the literature<sup>10</sup>. This too can be explained by taking into account the ease of oxidative addition of aryl halide to the palladium as described in the earlier section.

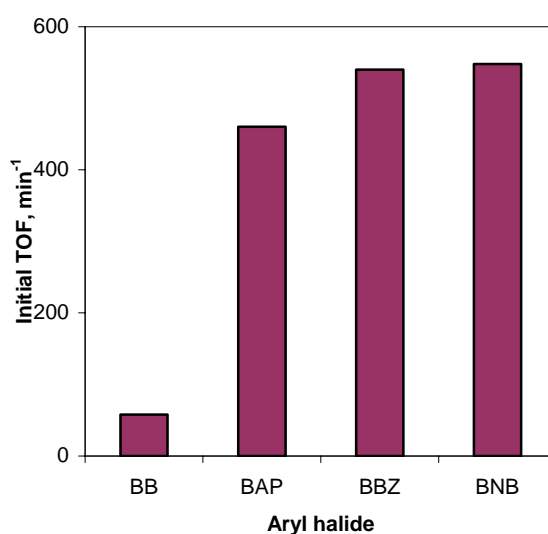


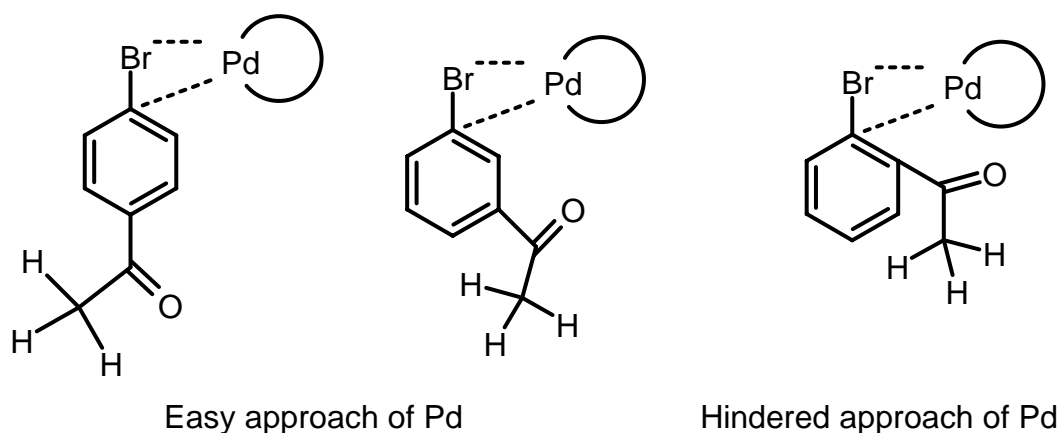
**Figure 2.9:** Effect of different aryl halides on the rate of Heck reaction

**Reaction conditions:** Aryl halide:  $0.399 \text{ kmol/m}^3$ , *n*-BA:  $0.602 \text{ kmol/m}^3$ , NaOAc:  $0.6 \text{ kmol/m}^3$ , TBAB:  $0.74 \text{ kmol/m}^3$ , Catalyst precursor **1**:  $8.51 \times 10^{-5} \text{ kmol/m}^3$ , Solvent NMP, Total Volume:  $2.5 \times 10^{-5} \text{ m}^3$ , Temp: 423K.

BB: bromobenzene, BAP: 4'-bromoacetophenone, BBZ: 4'-bromobenzaldehyde, BNB: 4'-bromonitrobenzene

Heck vinylation of *ortho*-, *meta*-, and *para*- bromoacetophenone was carried out to study the effect of bromoarene substituted at different positions. It was found that the *para*-bromoacetophenone gave the highest reaction rates followed by *meta*-bromoacetophenone. The reaction rate observed with *ortho*-bromoacetophenone was very low. The reaction was

not complete even after 6 hours of reaction time and the TOF obtained was only 15 per minute as compared to 460 per minute for the *para*-bromoacetophenone. Though, in general the electronic effects are observed in the order *para* > *ortho* > *meta*, here the order of reaction observed was *para* > *meta* > *ortho*. In case of *ortho*-bromoacetophenone the steric effects become more pronounced. The substituent at *ortho* position will hinder the approach of palladium catalyst as shown in Scheme 2.3, and will thus, reduce the rate of oxidative addition.



Scheme 2.3

#### 2.3.4. Screening of the olefins for the Heck reaction

The effect of different olefins on the rate of Heck reaction was studied for the reaction of 4'-bromoacetophenone in presence of sodium acetate base, palladacycle **1** as the catalyst precursor, and TBAB as promoter in NMP solvent. The results obtained are presented in Figure 2.10.

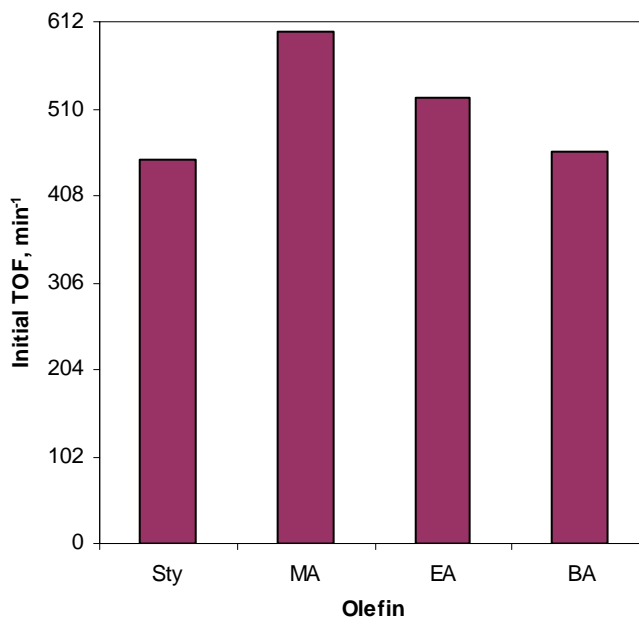


**Figure 2.10:** Activity of palladium complex 1 for the Heck vinylation of 4'-bromoacetophenone with olefins

**Reaction conditions:** 4'-bromoacetophenone:  $0.399 \text{ kmol/m}^3$ , olefin:  $0.602 \text{ kmol/m}^3$ , NaOAc:  $0.6 \text{ kmol/m}^3$ , TBAB:  $0.74 \text{ kmol/m}^3$ , Catalyst precursor 1:  $8.51 \times 10^{-5} \text{ kmol/m}^3$ , Solvent NMP, Total Volume:  $2.5 \times 10^{-5} \text{ m}^3$ , Temp: 423 K.

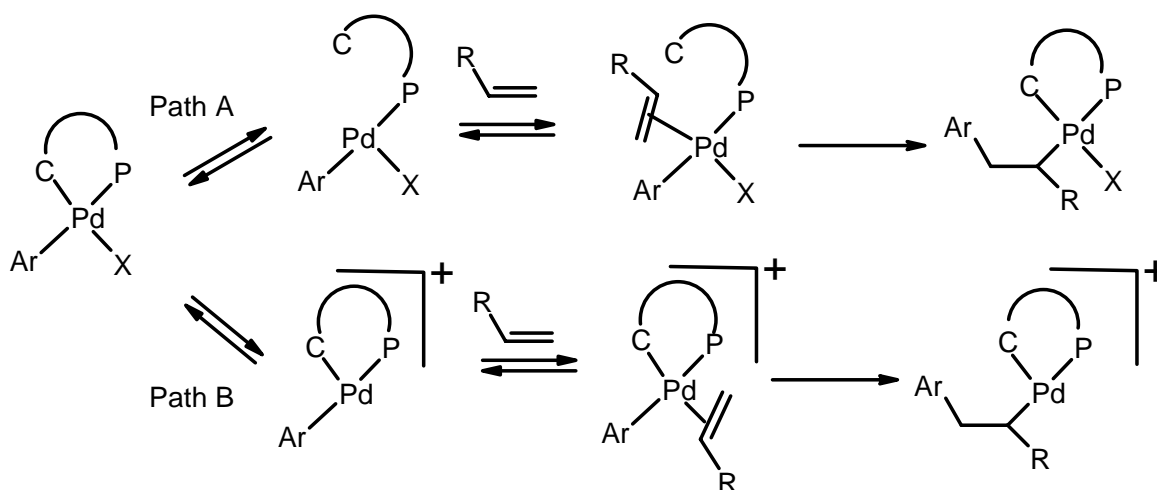
Sty: Styrene, MA: Methyl acrylate, EA: Ethyl acrylate, BA: n-Butyl acrylate.

With all the four olefins tested, 100% conversions were achieved at different reaction times. The reaction with styrene was the slowest. The rates obtained with n-butyl acrylate were comparable to the rates for the reaction of styrene. It was observed that among the acrylates, methyl acrylate reacted faster than ethyl acrylate, which in turn reacted faster than n-butyl acrylate. So, as the electron density on the olefin increased, the rate of the reaction decreased.

The olefin insertion is the second step in the mechanism of the Heck reaction. The olefin first coordinates to the metal center via the  $\pi$  electrons and then the insertion of the olefin between the palladium-carbon bond takes place. For this to occur, a coplanar assembly of the metal, olefin, and the hydride is required. Therefore the insertion process is stereoselective and occurs in a syn manner. The orbital studies carried out also show that the energy barrier for the generation of reactive configuration in a tetracoordinated complex



is lower than the pentacoordinated one<sup>11</sup>. Therefore, for the olefin insertion to take place it is necessary that dissociation of an already present ligand should take place from the palladium metal. For the olefin insertion step in the mechanism, two pathways are possible as shown in Scheme 2.4.



**Scheme 2.4**

Pathway A involves coordination of olefin via dissociation of a neutral ligand, whereas, pathway B involves the coordination of the olefin via dissociation of the anionic ligand. When the X is a halide, the bond between halide and Pd is strong. Therefore, the coordination of the olefin takes place via dissociation of one of the neutral ligands, which results in the formation of a neutral palladium complex. This is illustrated in pathway A in the Scheme 2.3. The olefin insertion thus depends on the charge density on the olefin. In case of pathway A, the olefin with lower electron density (good  $\pi$  acceptor and poor  $\sigma$  donor) will undergo the reaction faster than the olefin with higher electron density. This has been reported earlier based on the competitive experiments with different olefins<sup>12</sup>.

The products obtained for the reaction of different aryl halides with different olefins were isolated by column chromatography and characterized by IR spectroscopy, microanalysis technique, and GC-Mass spectroscopy. The results of these analysis are presented in Figure 2.11-2.12, Table 2.3, 2.4, and 2.5.

**Table 2.3:** Products obtained with different aryl halides on vinylation with n-butyl acrylate and their microanalysis results

*Reaction conditions:* Aryl halide:  $0.399 \text{ kmol/m}^3$ , n-BA:  $0.602 \text{ kmol/m}^3$ , NaOAc:  $0.6 \text{ kmol/m}^3$ , TBAB:  $0.74 \text{ kmol/m}^3$ , Catalyst precursor 1:  $8.51 \times 10^{-5} \text{ kmol/m}^3$ , Solvent NMP, Total Volume:  $2.5 \times 10^{-5} \text{ m}^3$ , Temp: 423 K

S. No.	Aryl halide	Product obtained	Time, h	Yield (GC), %	Theoretical, %			Analyzed, %		
					C	H	N	C	H	N
1	Chlorobenzene	–	6	0	76.5	7.8	–	75.9	7.3	–
2	4'-Chloroacetophenone	(E)-Butyl-3-(4-acetylphenyl)acrylate	6	19	73.2	7.3	–	72.9	7.0	–
3	Bromobenzene	n-Butyl cinnamate	2	99	76.5	7.8	–	75.9	7.3	–
4	Iodobenzene	n-Butyl cinnamate	1	100	76.5	7.8	–	75.9	7.3	–
5	4'-Bromoaniline	(E)-Butyl-3-(4-aminophenyl)acrylate	6	75	71.6	7.8	6.4	71.8	8.1	7.6
6	4'-Bromoanisole	(E)-Butyl-3-(4-methoxyphenyl)acrylate	6	79	71.8	7.7	–	71.1	7.2	–
7	4'-Bromotoluene	(E)-Butyl-3-p-tolylacrylate	6	92	77.1	8.3	–	77.5	8.1	–
8	4'-Bromoacetophenone	(E)-Butyl-3-(4-acetylphenyl)acrylate	0.5	99	73.2	7.3	–	72.9	7.0	–

**Table 2.3 (Continued):** Products obtained with different aryl halides on vinylation with n-butyl acrylate and their microanalysis results

**Reaction conditions:** Aryl halide:  $0.399 \text{ kmol/m}^3$ , n-BA:  $0.602 \text{ kmol/m}^3$ , NaOAc:  $0.6 \text{ kmol/m}^3$ , TBAB:  $0.74 \text{ kmol/m}^3$ , Catalyst precursor **I**:  $8.51 \times 10^{-5} \text{ kmol/m}^3$ , Solvent NMP, Total Volume:  $2.5 \times 10^{-5} \text{ m}^3$ , Temp: 423 K

S. No.	Aryl halide	Product obtained	Time, h	Yield (GC), %	Theoretical, %			Analyzed, %		
					C	H	N	C	H	N
9	4'-Bromobenzaldehyde	(E)-Butyl-3-(4-formylphenyl)acrylate	0.5	98	72.4	6.9	–	72.8	7.2	–
10	4'-Bromonitrobenzene	(E)-Butyl-3-(4-nitrophenyl)acrylate	0.5	99	62.6	6.0	5.6	62.3	5.8	5.8
11	3'-Bromoacetophenone	(E)-Butyl-3-(3-acetylphenyl)acrylate	0.5	96	73.2	7.3	–	72.8	7.6	–
12	2'-Bromoacetophenone	(E)-Butyl-3-(2-acetylphenyl)acrylate	6	88	73.2	7.3	–	73.1	7.1	–

**Table 2.4:** Products obtained with different olefins on Heck reaction with 4'-bromoacetophenone and their microanalysis results

**Reaction conditions:** 4'-Bromoacetophenone:  $0.399 \text{ kmol/m}^3$ , Olefin:  $0.602 \text{ kmol/m}^3$ , NaOAc:  $0.6 \text{ kmol/m}^3$ , TBAB:  $0.74 \text{ kmol/m}^3$ , Catalyst precursor 1:  $8.51 \times 10^{-5} \text{ kmol/m}^3$ , Solvent NMP, Total Volume:  $2.5 \times 10^{-5} \text{ m}^3$ , Temp: 423 K.

S. No.	Olefin	Product obtained	Time, min	Yield (GC), %	Theoretical, %			Analyzed, %		
					C	H	N	C	H	N
1	Methyl acrylate	(E)-Methyl-3-(4-acetylphenyl)acrylate	25	100	70.5	5.8	–	70.8	5.9	–
2	Ethyl acrylate	(E)-Ethyl-3-(4-acetylphenyl)acrylate	25	98	71.5	6.4	–	71.4	6.2	–
3	n-Butyl acrylate	(E)-Butyl-3-(4-acetylphenyl)acrylate	30	99	73.2	7.3	–	72.9	7.0	–
4	Styrene	(Z)-1-(4-styrylphenyl)ethanone	35	13	86.5	6.4	–	86.8	6.2	–
		(E)-1-(4-styrylphenyl)ethanone		85	86.5	6.4	–	86.9	6.1	–

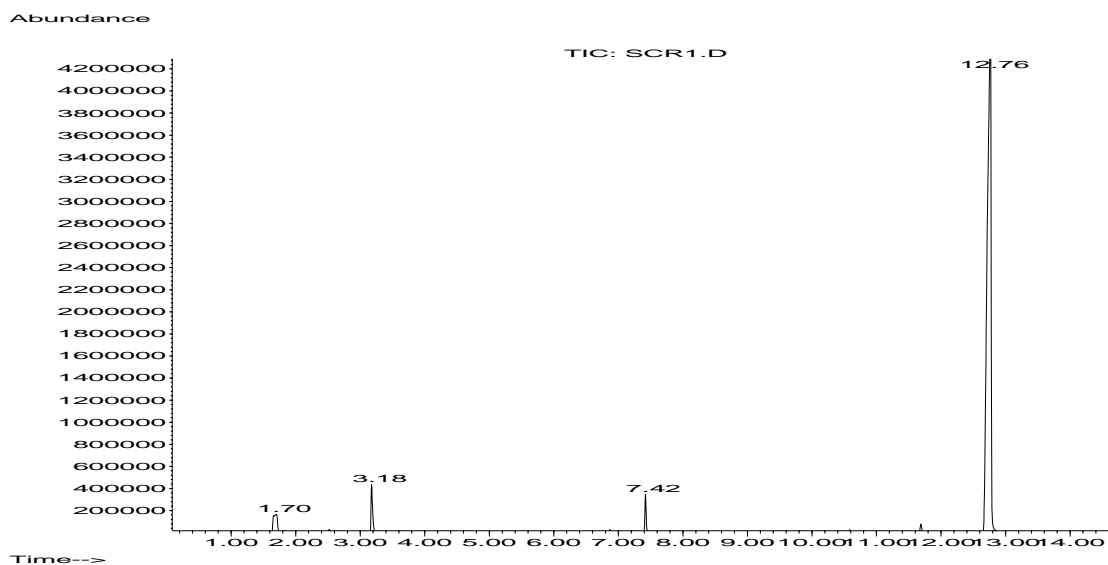


**Figure 2.11a:** GC-MS analysis for the reaction of 4'-bromoacetophenone with n-butyl acrylate [GC Chart for the reaction of p-bromoacetophenone with n-butyl acrylate  
Peaks; 1.78: Butanol, 3.18: n-Butyl acrylate, 7.12: 4'-Bromoacetophenone, 12.747: New peak (product)]

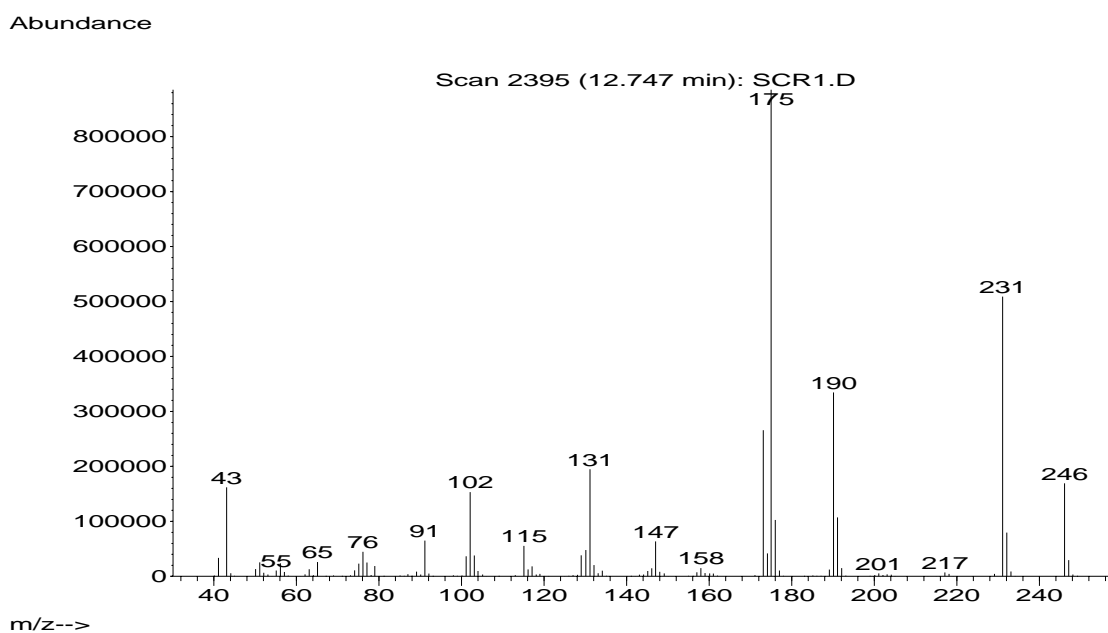


**Figure 2.11b:** GC-MS spectra for the reaction of 4'-bromoacetophenone with n-butyl acrylate [MS for the product peak {(E)-Butyl-3-(4-acetylphenyl)acrylate} at 12.747 min]

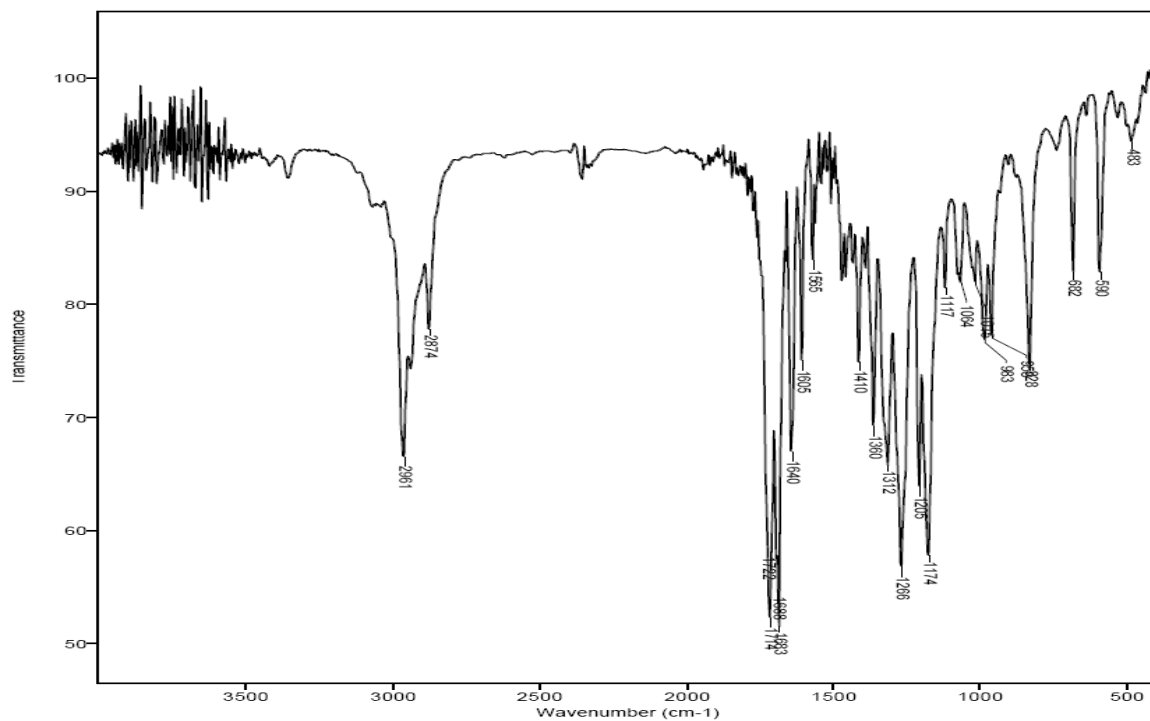


**Figure 2.12:** IR analysis for the product {(E)-Butyl-3-(4-acetylphenyl)acrylate} obtained from the reaction of 4'-bromoacetophenone with n-butyl acrylate

**Table 2.5:** MS and IR analysis of the products obtained for the Heck reaction between different aryl halides and different olefins

No.	Product	MS Peaks M/z (relative intensity %)	IR Peaks wavenumber $\text{cm}^{-1}$ (intensity)
1	(Z)-1-(4-styrylphenyl)ethanone	222(64), 207(100), 178(65), 152(12), 103(7), 89(16), 76(11), 43(9)	498(m), 522(m), 582(w), 594(s), 613(m), 651(w), 572(w), 701(vs), 721(w), 757(s), 802(vs), 821(vs), 860(s), 925(m), 984(s), 1016(vs), 1075(vs), 1079(vs), 1181(s), 1288(vs), 1302(s), 1359(s), 1405(m), 1443(m), 1494(m), 1603(vs), 1682(vs), 1738(w), 2965(w), 3036(w)
2	(E)-1-(4-styrylphenyl)ethanone	222(57), 207(100), 178(53), 152(9), 103(5), 89(11), 76(7), 43(5)	498(w), 522(m), 572(w), 583(s), 612(m), 690(vs), 723(m), 754(s), 821(vs), 852(m), 858(m), 965(vs), 1074(m), 1174(m), 1180(m), 1240(w), 1266(s), 1334(w), 1359(m), 1410(m), 1450(m), 1533(m), 1601(s), 1678(vs), 3024(w), 3052(w), 3098(w)
3	(E)-Methyl-3-(4-acetylphenyl)acrylate	204(32), 189(100), 173(9), 161(12), 131(9), 118(6), 102(12), 76(6), 65(5), 51(6), 43(14)	466(m), 485(m), 512(m), 592(m), 596(m), 684(s), 740(m), 828(s), 849(s), 935(m), 956(m), 1007(s), 1176(vs), 1201(vs), 1256(vs), 1330(vs), 1353(m), 1411(m), 1438(m), 1603(m), 1635(vs), 1674(vs), 1411(m), 1438(m), 1603(m), 1635(vs), 1674(vs), 1714(vs), 2402(w), 2418(w), 2953(m), 3074(w)

**Table 2.5 (Continued):** MS and IR analysis of the products obtained for the Heck reaction between different aryl halides and different olefins

No.	Product	MS Peaks M/z (relative intensity %)	IR Peaks wavenumber cm <sup>-1</sup> (intensity)
4	(E)-Ethyl-3-(4-acetylphenyl)acrylate	218(40), 203(100), 175(24), 147(11), 131(15), 115(5), 102(16), 91(8), 76(7), 65(5), 43(16)	481(m), 518(m), 578(m), 594(s), 683(s), 741(w), 832(vs), 868(w), 879(w), 960(s), 995(s), 1038(s), 1072(m), 1119(m), 1181(vs), 1209(vs), 1258(vs), 1329(s), 1367(s), 1412(s), 1479(m), 1554(s), 1603(s), 1641(vs), 1677(vs), 1714(vs), 2409(w), 2418(w), 2892(w), 2906(w), 2982(w)
5	(E)-Butyl-3-(4-acetylphenyl)acrylate	246(22), 231(61), 190(39), 175(100), 147(9), 131(23), 115(9), 102(20), 91(8), 43(20)	483(w), 590(m), 682(m), 828(m), 968(m), 983(m), 1084(w), 1117(w), 1174(vs), 1205(s), 1256(vs), 1312(s), 1316(s), 1410(m), 1465(w), 1565(w), 1605(m), 1640(s), 1683(vs), 1688(vs), 1714(vs), 1722(vs), 2400(w), 2420(w), 2874(m), 2950(m), 2961(s), 3102(w)
6	n-Butyl cinnamate	204(25), 148(67), 131(100), 103(40), 77(22), 51(6)	485(w), 684(s), 711(s), 788(vs), 865(w), 980(s), 1025(w), 1066(w), 1172(vs), 1205(vs), 1256(s), 1281(s), 1311(vs), 1326(s), 1386(w), 1450(m), 1497(w), 1579(w), 1639(vs), 1714(vs), 2410(w), 2421(w), 2874(m), 2960(m), 2961(s), 3060(w), 3070(w)



**Table 2.5 (Continued):** MS and IR analysis of the products obtained for the Heck reaction between different aryl halides and different olefins

No.	Product	MS Peaks (relative intensity %)	M/z	IR Peaks wavenumber $\text{cm}^{-1}$ (intensity)
7	(E)-Butyl-3-(4-aminophenyl)acrylate	219(68), 146(100), 106(11), 81(17), 65(8), 41(5)	163(60), 119(53)	503(w), 815(m), 1032(w), 1072(m), 1125(w), 1179(vs), 1250(m), 1320(m), 1402(w), 1421(w), 1498(w), 1504(vs), 1597(vs), 1702(vs), 2410(w), 2421(w), 2874(m), 2933(m), 2960(vs), 2980(w), 3401(m)
8	(E)-Butyl-3-(4-methoxyphenyl)acrylate	234(44), 161(100), 121(16), 89(8), 77(8)	178(94), 134(35)	499(w), 520(w), 829(s), 838(w), 983(m), 1031(s), 1062(w), 1148(w), 1171(vs), 1204(m), 1253(vs), 1283(s), 1302(m), 1389(w), 1423(m), 1454(m), 1513(vs), 1576(m), 1605(vs), 1635(s), 1712(vs), 2410(w), 2421(w), 2840(w), 2892(w), 2939(m), 2960(s)
9	(E)-Butyl-3-p-tolylacrylate	218(34), 145(100), 115(38), 91(17), 65(6), 41(4)	162(92), 131(5), 105(6)	496(m), 813(s), 983(m), 1011(w), 1024(w), 1048(w), 1169(vs), 1205(s), 1257(s), 1276(s), 1311(s), 1402(w), 1465(w), 1515(m), 1609(m), 1639(s), 1714(vs), 2410(w), 2421(w), 2876(m), 2934(m), 2960(s), 3041(w)

**Table 2.5 (Continued):** MS and IR analysis of the products obtained for the Heck reaction between different aryl halides and different olefins

No.	Product	MS Peaks (relative intensity %)	M/z	IR Peaks wavenumber $\text{cm}^{-1}$ (intensity)
10	(E)-Butyl-3-(4-nitrophenyl)acrylate	249(15), 176(100), 130(31), 102(31), 76(11), 56(29), 41(9)	194(58), 146(11), 118(9), 90(11)	421(w), 490(m), 538(m), 574(m), 717(m), 738(m), 759(m), 845(vs), 933(m), 963(m), 982(s), 994(m), 1028(w), 1109(m), 1177(vs), 1188(vs), 1195(s), 1281(s), 1308(vs), 1344(vs), 1414(m), 1496(w), 1514(m), 1519(vs), 1602(s), 1643(s), 1709(vs), 2409(w), 2424(w), 2496(w), 2874(w), 2938(m), 2959(m), 3058(w), 3109(m)
11	(E)-Butyl-3-(3-acetylphenyl)acrylate	246(13), 190(50), 155(60), 115(9), 91(11), 76(10), 43(27)	231(40), 175(100), 131(15), 102(15)	498(w), 524(w), 587(m), 894(w), 683(m), 724(w), 801(m), 865(m), 981(m), 1024(m), 1054(m), 1162(w), 1176(vs), 1253(s), 1259(s), 1318(s), 1309(vs), 1361(s), 1387(w), 1429(s), 1487(w), 1579(m), 1598(m), 1641(vs), 1688(vs), 1694(vs), 1714(vs), 2402(w), 2418(w), 2874(m), 2954(s), 2961(vs), 3042(w)

**Table 2.5 (Continued):** MS and IR analysis of the products obtained for the Heck reaction between different aryl halides and different olefins

No.	Product	MS Peaks (relative intensity %)	M/z	IR Peaks wavenumber $\text{cm}^{-1}$ (intensity)
12	(E)-Butyl-3-(2-acetylphenyl)acrylate	246(47), 171(14), 131(58), 103(24), 77(18), 57(11), 41(13)	190(40), 145(100), 115(29), 91(10)	512(w), 648(w), 586(w), 607(m), 728(w), 768(m), 848(w), 965(m), 975(m), 1021(w), 1061(w), 1119(w), 1176(vs), 1195(w), 1253(vs), 1279(vs), 1315(s), 1359(m), 1470(m), 1475(m), 1594(w), 1606(w), 1634(m), 1683(vs), 1714(vs), 2406(w), 2419(w), 2875(m), 2942(m), 2961(s), 3021(w)
13	(E)-Butyl-3-(4-formylphenyl)acrylate	232(21), 159(49), 131(31), 77(18), 56(7), 41(5)	176(100), 147(11), 103(34)	499(w), 820(w), 825(m), 983(m), 1082(w), 1142(w), 1175(vs), 1204(vs), 1262(m), 1281(s), 1312(s), 1385(m), 1390(w), 1428(w), 1570(w), 1605(m), 1639(m), 1704(vs), 2410(w), 2421(w), 2875(w), 2961(m)

### 2.3.5. Screening of the bases for the Heck reaction

Various organic and inorganic bases were screened in NMP solvent for their activity and selectivity for the Heck reaction of 4'-BAP and n-BA to give (E)-Butyl-3-(4-acetylphenyl)acrylate. The role of the base is to remove the halogen from the palladium and thus make palladium available for the next catalytic cycle. For this purpose, sodium acetate, sodium hydroxide, sodium carbonate, sodium bicarbonate, potassium acetate, potassium hydroxide, potassium carbonate, and n-tributyl amine were screened. The results are shown in Table 2.6.

**Table 2.6:** Effect of different bases on the rate of Heck reaction

S.No	Base	Time, min	Conversion (4'-BAP) %	Selectivity %
1	NaOAc	20	98.9	99.8
2	KOAc	20	99.5	99.1
3	KOH	200	75.4	2.5
4	NaOH	180	81.0	0.4
5	K <sub>2</sub> CO <sub>3</sub>	20	97.2	99.1
6	Na <sub>2</sub> CO <sub>3</sub>	50	92.0	98.9
7	<sup>n</sup> Bu <sub>3</sub> N	30	91.8	99.4
8	NaHCO <sub>3</sub>	30	97.1	99.6

**Reaction conditions:** 4'-BAP:  $0.399 \text{ kmol/m}^3$ , n-BA:  $0.602 \text{ kmol/m}^3$ , Base:  $0.6 \text{ kmol/m}^3$ , TBAB:  $0.74 \text{ kmol/m}^3$ , Catalyst precursor I:  $8.51 \times 10^{-5} \text{ kmol/m}^3$ , Solvent: NMP, Total Volume:  $2.5 \times 10^{-5} \text{ m}^3$ , Temp: 423 K.

The use of strong bases like sodium hydroxide and potassium hydroxide gave < 3% product formation. Both these bases led to the dehalogenation of the halide. Acetophenone was formed from 4'BAP via dehalogenation. Acrylic acid and n-butanol were the decomposition products of the butyl acrylate. Sodium bicarbonate was a better base than sodium carbonate, leading to a 97 % conversion of 4'-BAP in 30 minutes as compared to 92 % conversion with sodium carbonate in 50 minutes. Sodium acetate was a better base than sodium bicarbonate, giving a 98.9 % conversion in 20 minutes. The product

concentration formed during the course of the reaction with different sodium bases is shown in Figure 2.13.

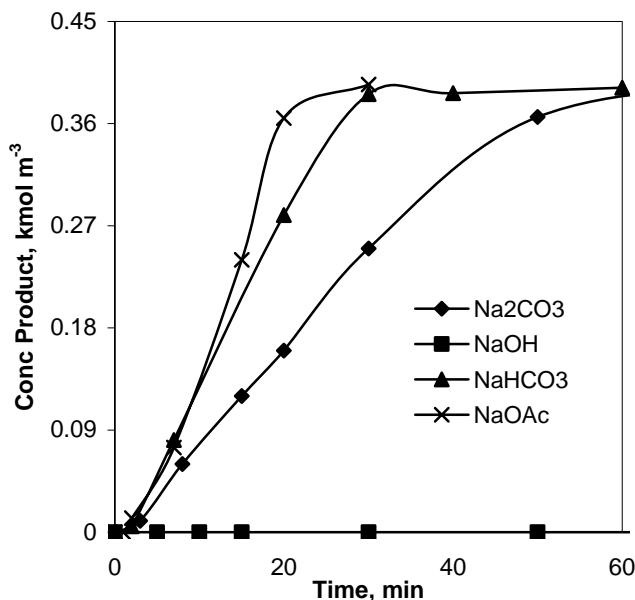


**Figure 2.13:** Effect of different sodium bases on the rate of Heck reaction

**Reaction conditions:** 4'-BAP:  $0.399 \text{ kmol/m}^3$ , n-BA:  $0.602 \text{ kmol/m}^3$ , Base:  $0.6 \text{ kmol/m}^3$ , TBAB:  $0.74 \text{ kmol/m}^3$ , Catalyst precursor I:  $8.51 \times 10^{-5} \text{ kmol/m}^3$ , Solvent NMP, Total Volume:  $2.5 \times 10^{-5} \text{ m}^3$ , Temp: 423K.

Potassium bases gave better activity compared to their respective sodium counterparts. Potassium acetate gave the best conversion amongst all the bases screened. This may be attributed to better solubility of the potassium bases in the organic solvents as compared to sodium bases. n-Tributylamine although active, gave inferior conversions than acetate and bicarbonate bases.

Sodium and potassium acetate remain the most commonly used bases for the Heck reaction. In this study, though, potassium acetate gave the highest conversion of 4'-BAP, it was not considered for the kinetic studies (Chapter 3) due to its hygroscopic nature.

### 2.3.6. Effect of quaternary ammonium salts on the Heck reaction

The Heck reaction of 4'-bromoacetophenone with n-butyl acrylate was carried out with different quaternary ammonium salt promoters. Both the anion and the cation of the ammonium salts were varied. When the anion of the quaternary ammonium salt promoter was varied, the rates observed were in the order  $I < Br < Cl$  as shown in Figure 2.14.

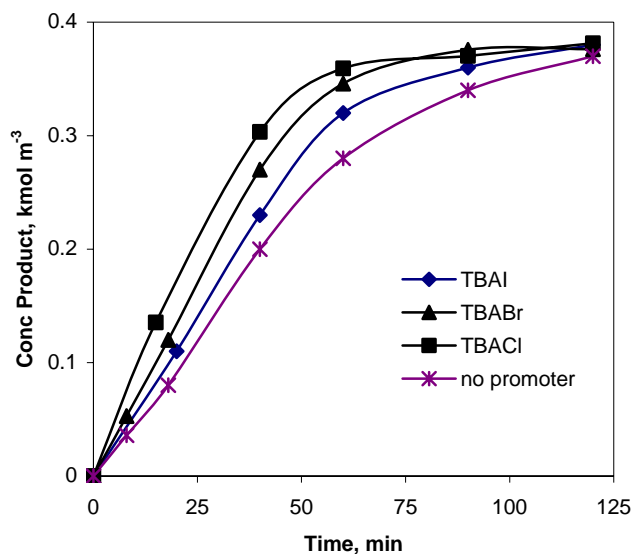
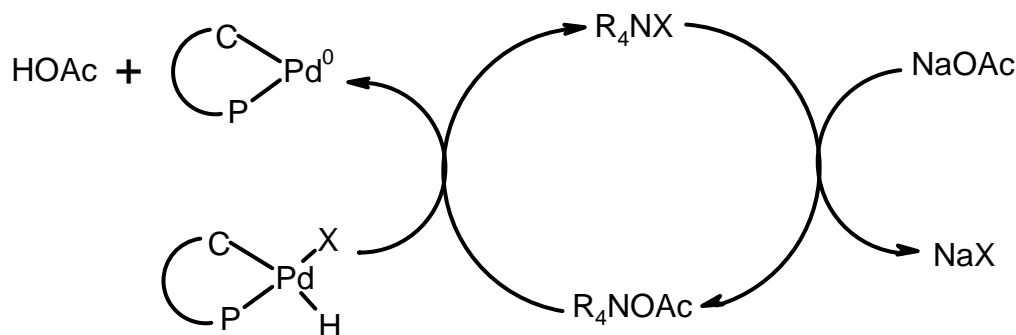


**Figure 2.14:** Effect of quaternary ammonium salt promoters on the rate of Heck reaction  
*Reaction conditions:* 4'-BAP:  $0.399 \text{ kmol/m}^3$ , n-BA:  $0.602 \text{ kmol/m}^3$ , NaOAc:  $0.6 \text{ kmol/m}^3$ ,  $Bu_4NX$ :  $0.74 \text{ kmol/m}^3$ , Catalyst precursor **1**:  $8.51 \times 10^{-5} \text{ kmol/m}^3$ , Solvent NMP, Total Volume:  $2.5 \times 10^{-5} \text{ m}^3$ , Temp: 423K.

This effect was similar to that observed by Jeffery<sup>13</sup> wherein, he carried out the Heck reaction of iodobenzene with different olefins. In the reaction mixture,  $R_4NX$  ionizes to give  $R_4N^+$  and  $X^-$ . These ions then interact with NaOAc to give NaX and  $R_4NOAc$ . The rate of formation of  $R_4NOAc$  will depend on the tendency of the halide to react with sodium to form NaX. This tendency will vary in the following order  $Cl > Br > I$ <sup>14</sup>. Therefore, when  $R_4NCl$  is added as a promoter, it will readily react with the base NaOAc to give  $R_4NOAc$ . Hence, the rate of formation of  $R_4NOAc$  will be greater for  $R_4NCl$  than  $R_4NBr$ , which will in turn be greater than that for  $R_4NI$ . The rate of Heck reaction will then also depend on the concentration of  $R_4NOAc$  as it will act as a more effective abstractor of

the HX than NaOAc. To investigate this hypothesis, a reaction was carried out with  $\text{Bu}_4\text{NOAc}$  as the base. For this reaction no other base or promoter was added.  $\text{Bu}_4\text{NOAc}$  acted both as a promoter as well as the base. The concentration of  $\text{Bu}_4\text{NOAc}$  taken was equal to the concentration of the base in the standard reaction. The reaction rates obtained with this base were higher than those obtained with other organic or inorganic bases even in the presence of quaternary ammonium halide promoter. The reaction was complete (> 99% conversion) in 17 minutes as compared to best of 20 minutes obtained for other bases. As per the literature, one of the roles of the quaternary ammonium salt is also to act as a phase transfer agent by enhancing the solubility of the inorganic base<sup>15</sup>. This might take place by formation of soluble weak base,  $\text{R}_4\text{NOAc}$ . On abstracting HX from the palladium in the catalytic cycle this will form  $\text{R}_4\text{NX}$  and HOAc. The  $\text{R}_4\text{NX}$  will again react with NaOAc to give  $\text{R}_4\text{NOAc}$  and NaX. Thus a steady supply of  $\text{R}_4\text{NOAc}$  base will be maintained (Scheme 2.5).



Scheme 2.5

The other role that  $\text{R}_4\text{NOAc}$  can play is to stabilize the underligated Pd(0) species during the reaction. The halide of the  $\text{R}_4\text{NX}$  can enter the coordination sphere of the palladium that will reduce the formation of palladium metal clusters. The quaternary ammonium salt can also increase the rate of the oxidative addition step by increasing the electron density on the palladium atom<sup>16</sup>.

The effect of the variation of the alkyl chain of the quaternary ammonium salt promoters is shown in Figure 2.15. It was observed that the rates initially increased as the chain length increased and then the rates decreased. The order of reactivity was  $\text{CH}_3\text{CH}_2 <$

$\text{CH}_3(\text{CH}_2)_3 < \text{CH}_3(\text{CH}_2)_5 > \text{CH}_3(\text{CH}_2)_7$ . The rates obtained with tetraoctylammonium bromide were lower than for the reaction without any promoter.

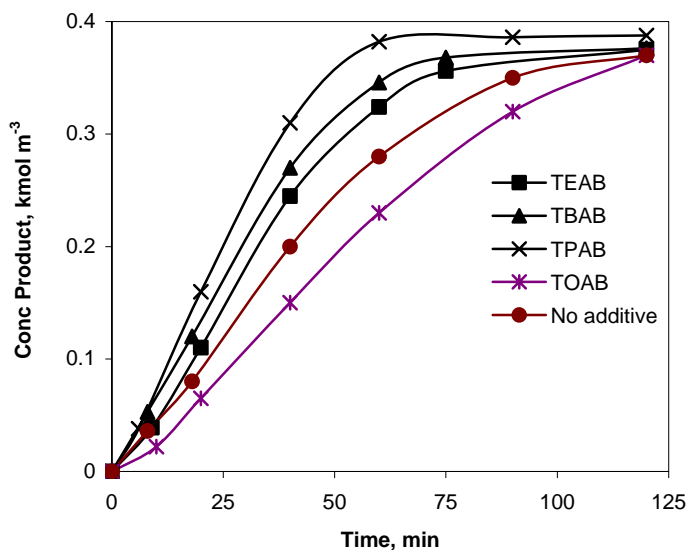


**Figure 2.15:** Effect of quaternary ammonium salt promoters on the rate of Heck reaction  
*Reaction conditions:* 4'-BAP:  $0.399 \text{ kmol/m}^3$ , n-BA:  $0.602 \text{ kmol/m}^3$ , NaOAc:  $0.6 \text{ kmol/m}^3$ ,  
*Bu<sub>4</sub>NX:*  $0.74 \text{ kmol/m}^3$ , Catalyst precursor **1**:  $8.51 \times 10^{-5} \text{ kmol/m}^3$ , Solvent NMP, Total  
*Volume:*  $2.5 \times 10^{-5} \text{ m}^3$ , Temp: 423K.

This can be explained on the basis of the stabilization of  $\text{R}_4\text{N}^+$  cation. The higher ability of the alkyl group to give electrons to nitrogen atom will lead to the formation of more stable  $\text{R}_4\text{N}^+$  and lead to a promoting effect as mentioned earlier. This ability of the alkyl group will increase with the increase in the length of the alkyl chain and thereby, the increase in the reaction rates as observed.

## 2.4. Conclusions

The screening of various palladium complex catalysts for the Heck reaction showed that the complexes formed with the phosphine free ligands catalyzed the reaction and gave complete conversions but were less active than the phosphine containing ligands. Presence of electron withdrawing substituents on the aryl halide and the olefin gave higher reaction rate than those obtained for unsubstituted substrates or with the substrates having electron



donating substituents. Both inorganic and organic bases were found to be active for Heck reactions. Presence of quaternary ammonium salts increased the reaction rates.

## 2.5. References

- 1 a) Yao, Q.; Kinney, E. P.; Yang, Z. *J. Org. chem.* **2003**, 68, 7528 b) Beletskaya, I. P.; Kashin, A. N.; Karlstedt, N. B.; Mitin, A. V.; Cheprakov, A. V.; Kazankov, G. M. *J. Organomet. Chem.* **2002**, 622, 89
- 2 a) Reetz, M. T.; Lohmer, G.; Schwickardi, R. *Angew. Chem. Int. Ed.* **1998**, 37, 481 b) Veelak, J.; Storch, J.; Czakoova, M.; Cermak, J. *J. Mol. Catal. A; Chem.* **2004**, 222, 121 c) Ozdemir, I.; Cetinkaya, B.; Demir, S. *J. Mol. Catal. A; Chem.* **2004**, 208, 109 d) Herrmann, W. A.; Ofele, K.; Preysing, D. V.; Schneider, S. K. *J. Organomet. Chem.* **2003**, 687, 229
- 3 a) Gruber, A. S.; Zim, D.; Ebeling, G.; Monteiro, A. L.; Dupont, J. *Org. Lett.* **2000**, 2, 9, 1287 b) Consorti, C. S.; Ebeling, G.; Flores, F. R.; Rominger, F.; Dupont, J. *Adv. Synth. Catal.* **2004**, 346, 617 c) Takenaka, K.; Uozumi, Y. *Adv. Synth. Catal.* **2004**, 346, 1693 d) Miyazaki, F.; Yamaguchi, K.; Shibasaki, M. *Tetrahedron Lett.* **1999**, 40, 7379 e) Jung, I. G.; Son, S. U.; Park, K. H.; Chung, K. C.; Lee, J. W.; Chung, Y. K. *Organometallics* **2003**, 22, 4715 f) Huang, M. H.; Liang, L. C. *Organometallics* **2004**, 23, 2813
- 4 Herrmann, W. A.; Brossmer, C.; Reisinger, C-P.; Riermeier, T. H.; Ofele, K.; Beller, M. *Chem. Eur. J.* **1997**, 3 1357
- 5 a) Parshall, G.; Ittel, S. D. *Homogeneous Catalysis: The Applications and Chemistry of Soluble Transition-Metal Complexes*, 2nd ed. John Wiley & Sons, New York, **1992** b) Littke, A. F.; Fu, G. C. *J. Org. Chem.* **1999**, 64, 10 c) Vries, A. H. M.; Mulders, J. M. C. A.; Mommers, J. H. M.; Henderickx, H. J. W.; Vries, J. G. *Org. Lett.* **2003**, 5, 3285
- 6 a) Phan, N. T. S.; Sluys, M. V. D.; Jones, C. W. *Adv. Synth. Catal.* **2006**, 348, 609 Reference for dimer to monomer b) Rosner T.; Bars J. L.; Pfaltz A.; Blackmond D. G. *J. Am. Chem. Soc.* **2001**, 123, 1848 c) Stambuli, J. P.; Kuwano, R.; Hartwig, J. F. *Angew. Chem. Int. Ed.* **2002**, 41, 4746
- 7 a) Zhao, F. g.; Bhanage, B. M.; Shirai, M.; Arai, M. *J. Mol. Catal. A; Chem.* **1999**, 142, 383 b) de Meijere, A.; Meyer, F. E. *Angew. Chem., Int. Ed. Engl.* **1994**, 33, 2379 c) Cabri, W.; Candiani, I. *Acc. Chem. Res.* **1995**, 28, 2 d) Kelkar, A. A.; Hanaoka, T.; Kubota, Y.; Sugi, Y. *Catal. Lett.* **1994**, 29, 69 e) Ohrai, K.; Kondo, K.; Sodeoka, M.; Shibasaki, M. *J. Am. Chem. Soc.* **1994**, 116, 11737
- 8 Asselt, R. V.; Vrieze, K.; Elsevier, C. J. *J. Organomet. Chem.* **1994**, 480, 27
- 9 a) Hammett, L. P. *J. Am. Chem. Soc.* **1937**, 59, 96 b) Hammett, L. P. *Chem. Rev.* **1935**, 17, 125 c) Benhaddon, R.; Czernecki, S.; Ville, G.; Zegar, A. *Organometallics*, **1988**, 7, 2435 d) Fristrup, P.; Qument, S. L.; Tanner, D.; Norrby, P-O. *Organometallics*, **2004**, 23, 6160 e) Consorti, C. S.; Flores, F. R.; Dupont, J. *J. Am. Chem. Soc.* **2005**, 127, 12054
- 10 a) Spencer, A. J. *Organomet. Chem.* **1983**, 258, 101 b) Feuerstein, M.; Doucet, H.; Santelli, M. *Synlett* **2001**, 12, 1280
- 11 Thorn, D. L.; Hoffmann, R. *J. Am. Chem. Soc.* **1978**, 100, 2079

- 
- 12 Cabri, W.; Candini, I.; Bedeschi, A.; Santi, R. *J. Org. Chem.* **1993**, 58, 7421
- 13 Jeffery, T. *Tetrahedron* **1996**, 52, 10113
- 14 a) Hill, J. W.; Petrucci, R. H. *General Chemistry*, 2nd edition, p 524-527, Prentice Hall, **1999** b) *Handbook of Chemistry and Physics*, 27th edition, Chemical Rubber Publishing Co., Cleveland, Ohio, **1943**
- 15 a) Jeffery, T. *J. Chem. Soc., Chem. Commun.* **1984**, 19, 1287 b) Jeffery, T. *Tetrahedron Lett.* **1985**, 26, 2667 c) Jeffery, T.; Galland, J. C. *Tetrahedron Lett.* **1994**, 35, 4103 d) Jeffery, T. *Tetrahedron Lett.* **1994**, 35, 3051
- 16 Beletskaya, I. P.; Cheprakov, A. V. *Chem. Rev.* **2000**, 100, 3009

*Chapter 3:*

*Kinetics of Heck Vinylation of 4'-  
Bromoacetophenone with n-Butyl acrylate  
Using P-C Palladacycle Catalyst*

### 3.1. Introduction

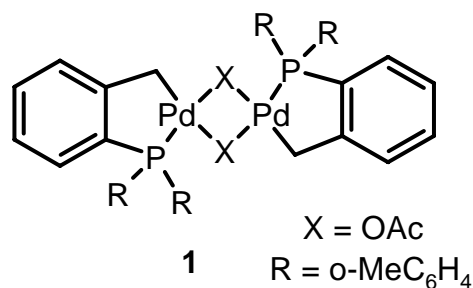
In the three and a half decades of Heck chemistry, a phenomenal amount of data has been published however, in spite of the developments taking place in the field of Heck chemistry and catalysts, not much work has been reported on the detailed kinetic analysis<sup>1-6</sup>. A kinetic study is important to understand the influence of the reaction parameters on the rate. It is also useful in understanding the mechanism of the reaction and in reactor modeling. The Heck reaction involving use of acrylates as an olefin source are very important, as the products are industrially useful cinnamates. The cinnamates obtained are used as UV absorbers, antioxidants, and as intermediates in perfumery, pharmaceutical, and dye industry<sup>7-9</sup>. To understand the kinetics and mechanism of such an industrially important reaction the vinylation of 4'-bromoacetophenone with n-butyl acrylate was investigated in the temperature range of 403–433 K. The effect of concentrations of catalysts, 4'-bromoacetophenone, n-butyl acrylate, NaOAc, and tetrabutylammonium bromide on the rate of reaction was studied. The rate was found to be first order with respect to 4'-BAP, fractional order with the catalyst, and first order tending to zero order with NaOAc concentration. The rates passed through a maximum with variation of TBAB and n-butyl acrylate concentrations. The rate data were analyzed to propose an empirical model. A mechanistic model was also developed and was found to be in good agreement with the experimental data.

### 3.2. Experimental Section

#### 3.2.1. Chemicals and Apparatus

Palladium acetate and tri (o-tolyl) phosphine were purchased from Aldrich Chemical Co. 4'-Bromoacetophenone, sodium acetate, n-butyl acrylate, tetrabutylammonium bromide, and 1-methyl 2-pyrrolidinone (NMP) were purchased from s-d Fine and Loba Chemicals and used as received. The palladacycle catalyst precursor **1** (Scheme 3.1) was synthesized as described in Chapter 2 Section 2.2.3 (complex **1**). The reactions were carried out in a 50 ml 2-necked stirred glass reactor fitted with a condenser, immersed in an oil bath held at a desired temperature. The stirring was by means of a magnetic stirrer. The analysis of the contents of the reaction mixture was done using

Agilent 6850A gas chromatograph, on an HP-I capillary column of 30 m length (stationary phase methyl siloxane) and a Flame Ionization Detector. The analysis was carried out using a temperature program between 80 to 250°C.



**Scheme 3.1**

### 3.2.2. General procedure for Heck reaction

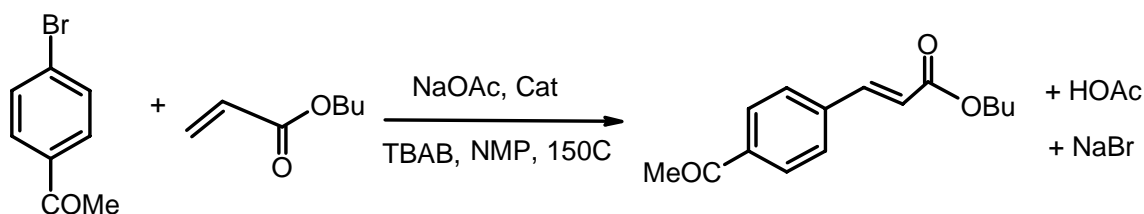
In a typical experiment, 10 mmol of 4'-bromoacetophenone (4'-BAP), 15 mmol *n*-butyl acrylate (*n*-BA), 15 mmol sodium acetate, 2 mmol tetrabutylammonium bromide (TBAB), and 2  $\mu\text{mol}$  palladacycle catalyst precursor **1** were taken in a 50 ml 2-necked stirred glass reactor maintained under nitrogen atmosphere. This was then immersed in an oil bath pre-heated to the required temperature. The reaction was then started by switching the stirrer on. Samples were withdrawn at regular intervals, filtered (to remove base and salt formed) and analyzed for conversion of 4'-bromoacetophenone and (E)-Butyl-3-(4-acetylphenyl)acrylate formation with respect to time. The analysis of the reaction mixture showed the formation of a single product which was isolated, identified, and characterized according to the procedure given in Chapter 2 Section 2.2.4.

When the catalyst was directly added to the reaction mixture, an induction period of approximately 3 minutes was observed. Since the induction period would vary with the variation in reaction parameters, it was necessary to carry out the reaction under the conditions wherein no induction period would be observed. When the catalyst was added from a previously prepared solution in NMP (after warming the solution to 50°C), no induction period was observed. The induction period is due to the time required for the formation of the active catalytic species from the catalyst precursor. In case of pre treated

catalyst, the active catalytic species is already formed and hence the induction period is no longer observed. For kinetic analysis the reactions were carried out for short durations such that the conversion of the 4'-bromoacetophenone was less than 20% to ensure differential conditions. The catalyst solution was prepared in the solvent used, prior to the reaction. From this catalyst solution, the quantity corresponding to the amount of catalyst required was added to the reaction mixture. The initial rates of the reaction were calculated from the plots of formation of (E)-Butyl-3-(4-acetylphenyl)acrylate product as a function of time.

### 3.3. Effect of reaction parameter variation on the rate of reaction

A few preliminary experiments were carried out on the vinylation of 4'-bromoacetophenone with n-butyl acrylate, using palladacycle **1** as the catalyst precursor in presence of TBAB as a promoter, to assess the material balance of reactants/products. A typical concentration-time profile for the reaction is presented in Figure 3.1. The consumption of 4'-BAP and n-butyl acrylate, and the formation of (E)-Butyl-3-(4-acetylphenyl)acrylate was monitored by GC. The consumption of 4'-BAP and n-butyl acrylate was found to be stoichiometrically consistent with the formation of (E)-Butyl-3-(4-acetylphenyl)acrylate according to the Scheme 3.2, in all the experiments. In the range of conditions employed during these studies, > 96 % material balance was observed. Only (E)-Butyl-3-(4-acetylphenyl)acrylate (BAcA) was formed under the reaction conditions.



Scheme 3.2

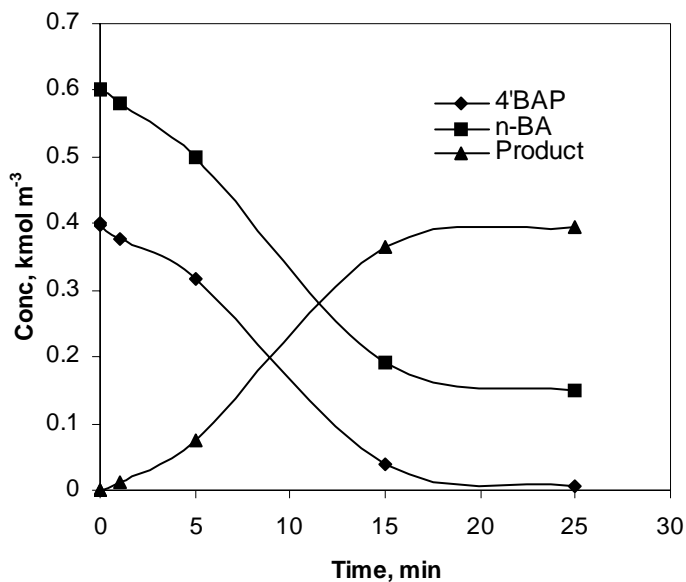


**Figure 3.1:** A typical Concentration- Time profile for the vinylation of 4'-BAP with n-BA at 423 K (standard reaction)

**Reaction conditions:** 4'-BAP:  $0.399 \text{ kmol/m}^3$ , n-BA:  $0.602 \text{ kmol/m}^3$ , NaOAc:  $0.6 \text{ kmol/m}^3$ , TBAB:  $0.074 \text{ kmol/m}^3$ , Catalyst precursor **1**:  $8.51 \times 10^{-5} \text{ kmol/m}^3$ , Solvent: NMP, Total Volume:  $2.5 \times 10^{-5} \text{ m}^3$ , Temp: 423 K.

Following the preliminary reactions for the material balance, the kinetics of vinylation of 4'-bromoacetophenone with n-butyl acrylate was studied using palladacycle **1** catalyst precursor in the presence of sodium acetate base and tetrabutylammonium bromide promoter. For this study, several experiments were carried out in the range of conditions shown in Table 3.1. The initial rates were calculated from the observed data on the formation of (E)-Butyl-3-(4-acetylphenyl)acrylate as a function of time. The rate of reaction was calculated from the slope of the product formed vs. time plot. The dependence of the rate on the various parameters was investigated at four different temperatures. The results showing the influence of different reaction parameters on the rate of the reaction and the kinetic modeling are discussed below.

**Table 3.1:** Range of conditions investigated for kinetic study

Concentration of catalyst ( $\text{kmol m}^{-3}$ )	$4.26 \times 10^{-5}$ to $2.55 \times 10^{-4}$
Concentration of 4'-bromoacetophenone ( $\text{kmol m}^{-3}$ )	0.1 to 0.75
Concentration of n-butyl acrylate ( $\text{kmol m}^{-3}$ )	0.25 to 1.1
Concentration of base ( $\text{kmol m}^{-3}$ )	0.1 to 1.1
Concentration of TBAB ( $\text{kmol m}^{-3}$ )	0.03 to 0.2
Temperature (K)	403 to 433

### 3.3.1. Effect of catalyst concentration on the rate of reaction

The effect of the concentration of the catalyst precursor (palladacycle **1**) on the rate was studied at constant 4'-BAP, n-BA, NaOAc, and TBAB concentrations of  $0.399 \text{ kmol/m}^3$ ,  $0.602 \text{ kmol/m}^3$ ,  $0.6 \text{ kmol/m}^3$ , and  $0.074 \text{ kmol/m}^3$ , respectively at four different temperatures ranging from 403 K to 433 K. A concentration time profile was obtained for each experiment. A typical plot of the product formation with respect to time at 423 K is shown in Figure 3.2.

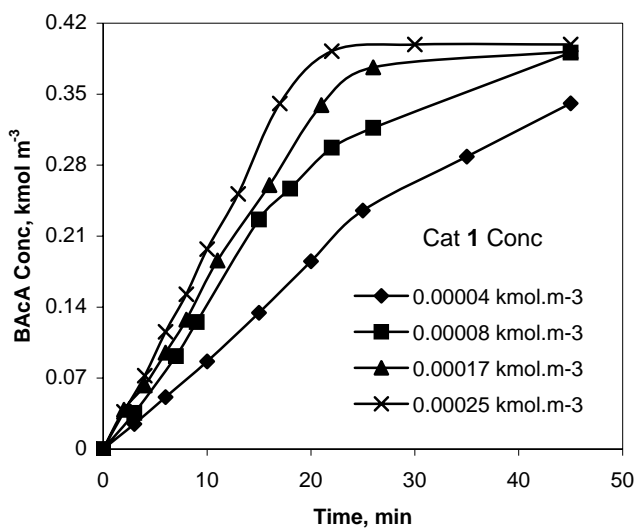


**Figure 3.2:** A typical plot for the product formation at 423 K with different initial concentrations of catalyst precursor

**Reaction conditions:** 4'-BAP:  $0.399 \text{ kmol/m}^3$ , n-BA:  $0.602 \text{ kmol/m}^3$ , NaOAc:  $0.6 \text{ kmol/m}^3$ , TBAB:  $0.074 \text{ kmol/m}^3$ , Catalyst precursor **1**, Solvent: NMP, Total Volume:  $2.5 \times 10^{-5} \text{ m}^3$ , Temp: 423 K.



The initial rate of product formation was calculated from the CT profile graph. This was done by considering the initial part of the curve, which represented the 4'-BAP conversions of less than 20% to ensure differential conditions. The rate of product formation was obtained from the slope of the curve. In the region of low 4'-BAP conversion levels the plot of product formation vs. time was essentially linear. The plots of the product formation as the function of time for the initial periods of the reaction are given in Figures 3.3 to 3.6 for the temperatures 403, 413, 423 and 433 K respectively.

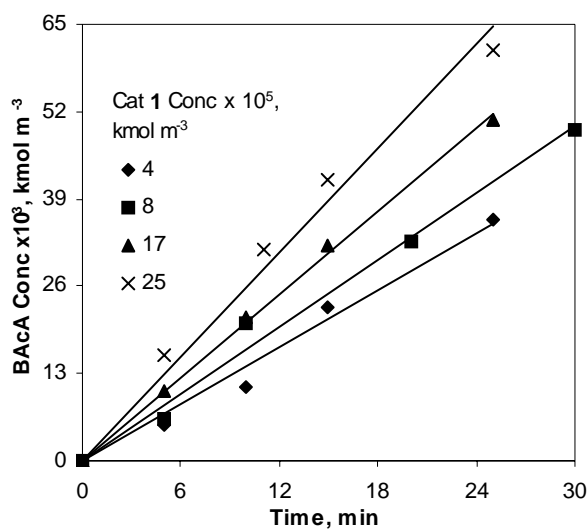


**Figure 3.3:** Plot of the product formation as a function of time for different initial concentrations of the catalyst precursor **1** at 403 K

**Reaction conditions:** 4'-BAP:  $0.399 \text{ kmol/m}^3$ , *n*-BA:  $0.602 \text{ kmol/m}^3$ , NaOAc:  $0.6 \text{ kmol/m}^3$ , TBAB:  $0.074 \text{ kmol/m}^3$ , Catalyst precursor **1**, Solvent: NMP, Total Volume:  $2.5 \times 10^{-5} \text{ m}^3$ , Temp: 403 K

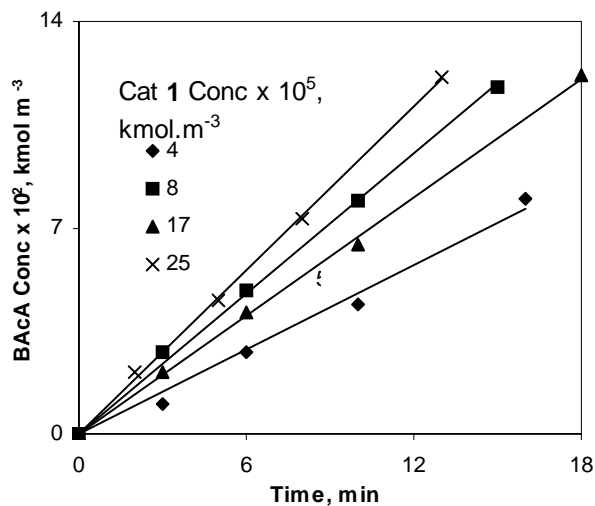


**Figure 3.4:** Plot of the product formation as a function of time for different initial concentrations of the catalyst precursor **1** at 413 K

*Reaction conditions:* 4'-BAP:  $0.399 \text{ kmol/m}^3$ , n-BA:  $0.602 \text{ kmol/m}^3$ , NaOAc:  $0.6 \text{ kmol/m}^3$ , TBAB:  $0.074 \text{ kmol/m}^3$ , Catalyst precursor **1**, Solvent: NMP, Total Volume:  $2.5 \times 10^{-5} \text{ m}^3$ , Temp: 413 K

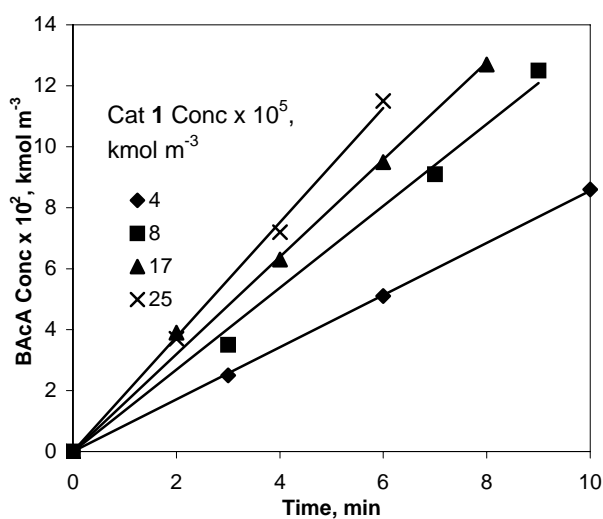


**Figure 3.5:** Plot of the product formation as a function of time for different initial concentrations of the catalyst precursor **1** at 423 K

*Reaction conditions:* 4'-BAP:  $0.399 \text{ kmol/m}^3$ , n-BA:  $0.602 \text{ kmol/m}^3$ , NaOAc:  $0.6 \text{ kmol/m}^3$ , TBAB:  $0.074 \text{ kmol/m}^3$ , Catalyst precursor **1**, Solvent: NMP, Total Volume:  $2.5 \times 10^{-5} \text{ m}^3$ , Temp: 423 K

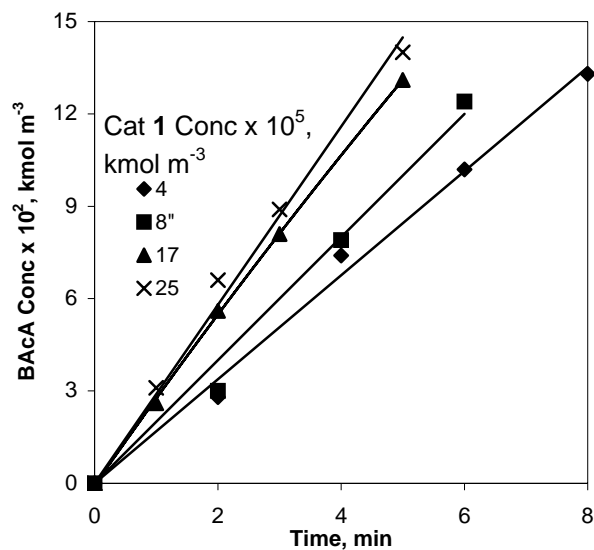


**Figure 3.6:** Plot of the product formation as a function of time for different initial concentrations of the catalyst precursor **1** at 433 K

**Reaction conditions:** 4'-BAP:  $0.399 \text{ kmol/m}^3$ , n-BA:  $0.602 \text{ kmol/m}^3$ , NaOAc:  $0.6 \text{ kmol/m}^3$ , TBAB:  $0.074 \text{ kmol/m}^3$ , Catalyst precursor **1**, Solvent: NMP, Total Volume:  $2.5 \times 10^{-5} \text{ m}^3$ , Temp: 433 K

The initial rates of the reactions were calculated from the slopes of the plots of the product formation vs. time. The plot of the initial rates as a function of catalyst concentration is presented in Figure 3.7.

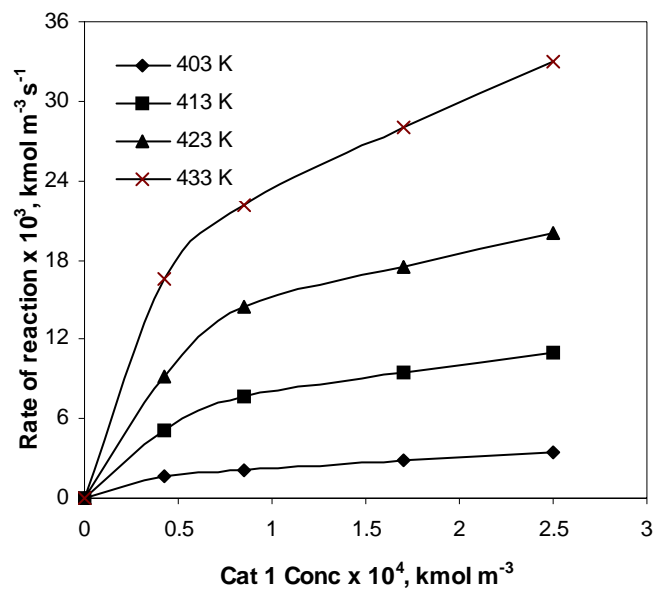
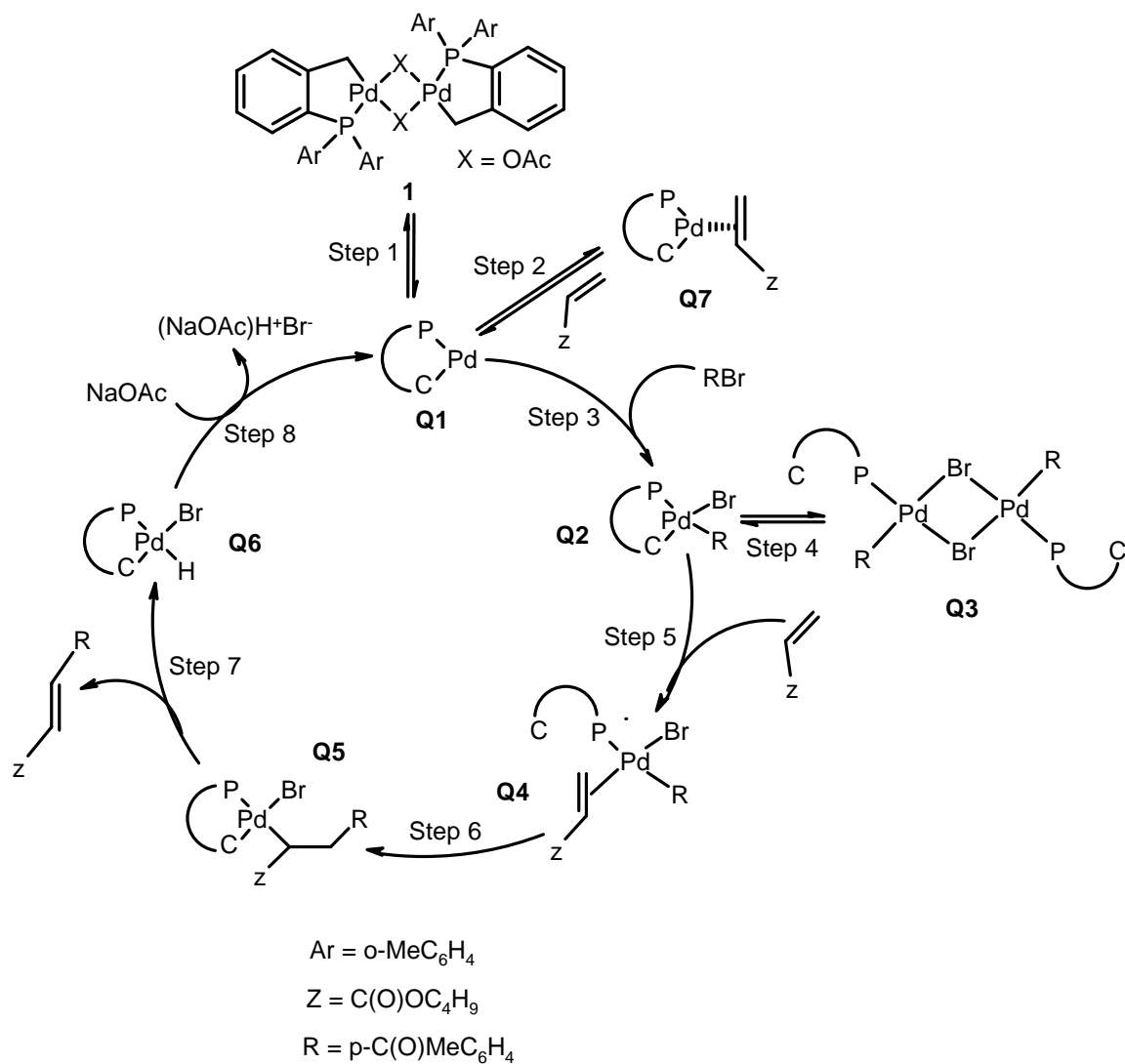


**Figure 3.7:** Plot of the initial rate vs. concentration of catalyst precursor **1** at different temperatures

**Reaction conditions:** 4'-BAP: 0.399 kmol/m<sup>3</sup>, n-BA: 0.602 kmol/m<sup>3</sup>, NaOAc: 0.6 kmol/m<sup>3</sup>, TBAB: 0.074 kmol/m<sup>3</sup>, Catalyst precursor **1**, Solvent: NMP, Total Volume: 2.5 x 10<sup>-5</sup> m<sup>3</sup>

It was observed that the rate increased with an increase in the catalyst concentration, in the range under investigation. The rate showed a fractional order dependence on the concentration of the catalyst as shown in Figure 3.7. This is in agreement with the earlier reports on Pd catalyzed Heck reactions<sup>1,4</sup>. This trend can be attributed to the formation of a dimeric species, Q3, shown in Scheme 3.3. This species exists in equilibrium with the monomeric species and is inactive for the Heck reaction. The formation of this type of dimeric species has also been reported in the case of ligand free palladium catalysed Heck reactions where the concentration of the catalyst precursor added is very small<sup>10,11</sup>. This dimeric species acts as a reservoir for the catalytically active monomeric species. As the catalyst concentration is increased more of the dimeric species is likely to form. Hence, the enhancement in the concentration of the active catalyst species available for the reaction is not proportional to the increase in the concentration of the catalyst precursor. Thus the increase in the observed reaction rates is not first order as would be expected, but instead shows a half order dependence on the catalyst concentration as would be observed from the equilibrium deactivation as shown in the mechanism (Scheme 3.3, Step 4). It should also be

noted that the catalyst precursor is a dimer, which will dissociate to a monomeric species in equilibrium. This may also contribute to the fractional order observed with respect to the catalyst concentration.



Scheme 3.3

### 3.3.2. Effect of p-bromo acetophenone concentration on the rate of reaction

The effect of 4'-bromoacetophenone concentration on the activity was studied at constant n-BA, palladacycle **1** as the catalyst precursor, NaOAc, and TBAB concentrations of  $0.602 \text{ kmol/m}^3$ ,  $8.511 \times 10^{-5} \text{ kmol/m}^3$ ,  $0.6 \text{ kmol/m}^3$ , and  $0.074 \text{ kmol/m}^3$ , respectively, in a temperature range of 403-433 K. A concentration time profile was obtained for each experiment with different initial concentrations of 4'BAP.

The initial rates of product formation for different initial concentrations of 4'-bromoacetophenone were calculated from the CT profile plots as described earlier. The plots of the product formation as the function of time for the initial periods of the reaction are given in Figures 3.8 to 3.11 for the temperatures 403, 413, 423 and 433 K respectively.

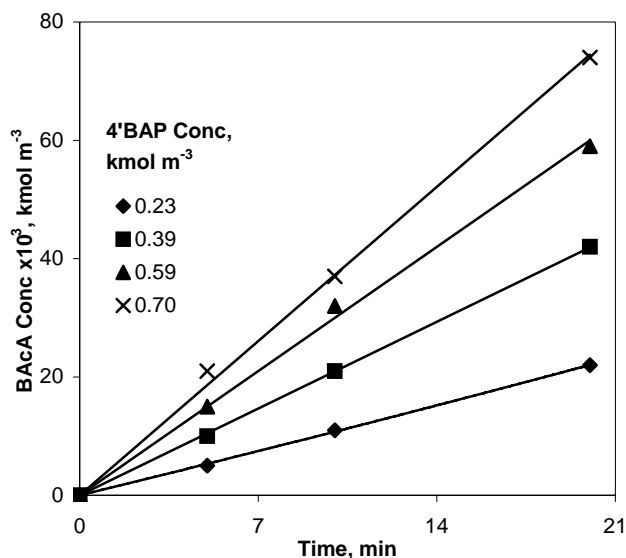


**Figure 3.8:** Plot of the product formation as a function of time for different initial concentrations of 4'BAP at 403 K

**Reaction conditions:** 4'-BAP, n-BA:  $0.602 \text{ kmol/m}^3$ , NaOAc:  $0.6 \text{ kmol/m}^3$ , TBAB:  $0.074 \text{ kmol/m}^3$ , Catalyst precursor **1**:  $8.51 \times 10^{-5} \text{ kmol/m}^3$ , Solvent: NMP, Total Volume:  $2.5 \times 10^5 \text{ m}^3$ , Temp: 403 K

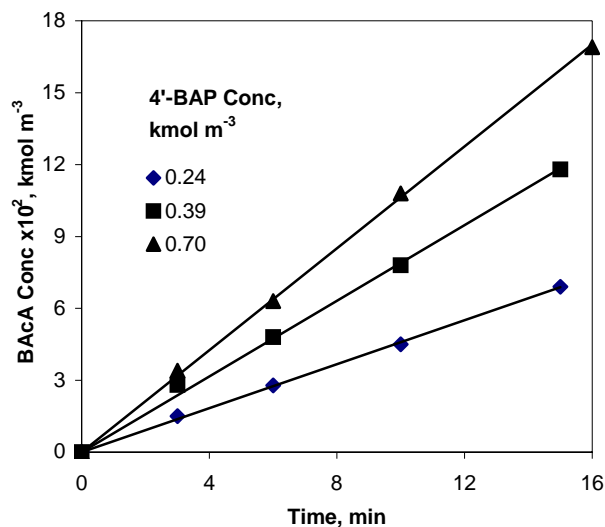


**Figure 3.9:** Plot of the product formation as a function of time for different initial concentrations of 4'BAP at 413 K

**Reaction conditions:** 4'-BAP,  $n$ -BA:  $0.602 \text{ kmol/m}^3$ , NaOAc:  $0.6 \text{ kmol/m}^3$ , TBAB:  $0.074 \text{ kmol/m}^3$ , Catalyst precursor **I**:  $8.51 \times 10^{-5} \text{ kmol/m}^3$ , Solvent: NMP, Total Volume:  $2.5 \times 10^5 \text{ m}^3$ , Temp: 413 K

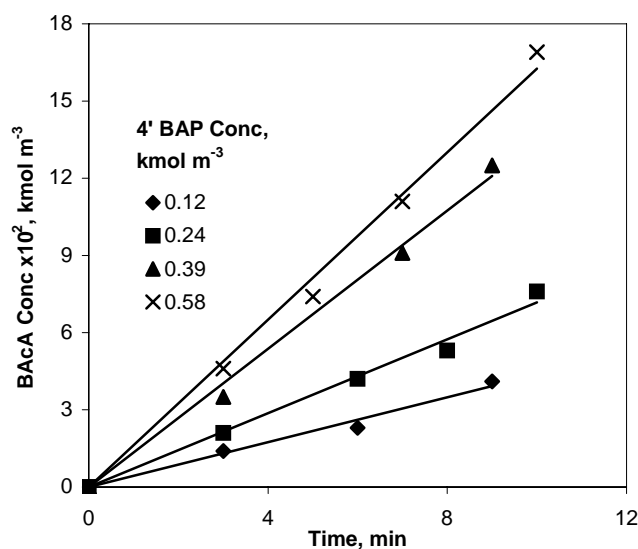


**Figure 3.10:** Plot of the product formation as a function of time for different initial concentrations of 4'BAP at 423 K

**Reaction conditions:** 4'-BAP,  $n$ -BA:  $0.602 \text{ kmol/m}^3$ , NaOAc:  $0.6 \text{ kmol/m}^3$ , TBAB:  $0.074 \text{ kmol/m}^3$ , Catalyst precursor **I**:  $8.51 \times 10^{-5} \text{ kmol/m}^3$ , Solvent: NMP, Total Volume:  $2.5 \times 10^5 \text{ m}^3$ , Temp: 423 K

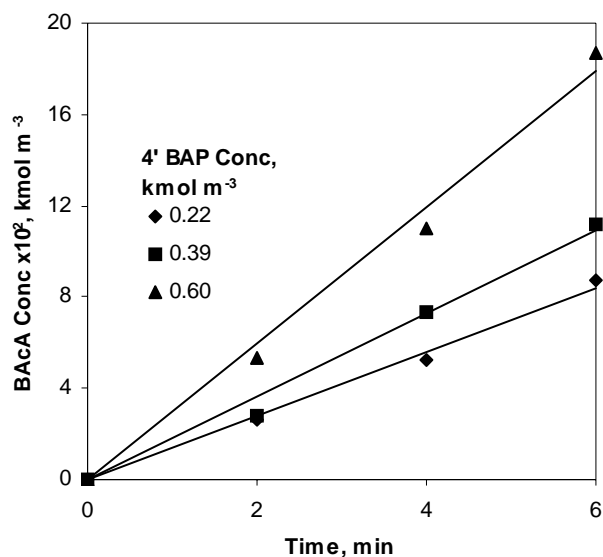


**Figure 3.11:** Plot of the product formation as a function of time for different initial concentrations of 4'BAP at 433 K

**Reaction conditions:** 4'-BAP,  $n$ -BA:  $0.602 \text{ kmol/m}^3$ , NaOAc:  $0.6 \text{ kmol/m}^3$ , TBAB:  $0.074 \text{ kmol/m}^3$ , Catalyst precursor **1**:  $8.51 \times 10^{-5} \text{ kmol/m}^3$ , Solvent: NMP, Total Volume:  $2.5 \times 10^{-5} \text{ m}^3$ , Temp: 433 K

The initial rates of the reactions were calculated from the slopes of the plots of the product formation vs. time. The plot of the initial rates as a function of 4'-bromoacetophenone concentration is presented in Figure 3.12.



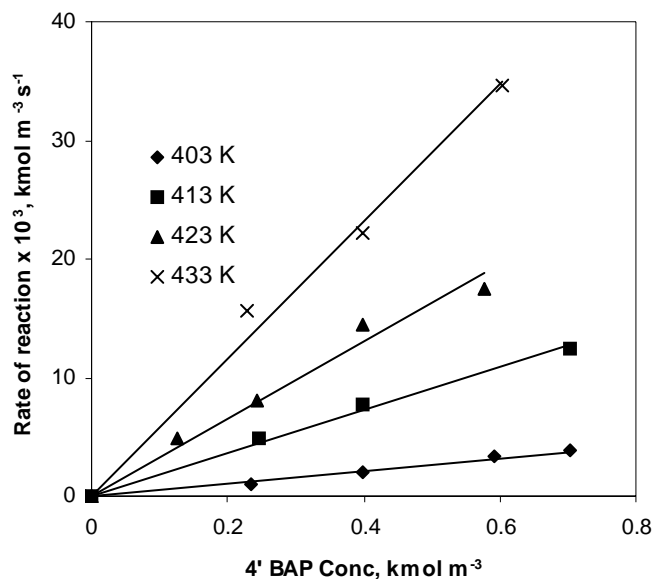


**Figure 3.12:** Plot of the initial rate vs. 4' BAP concentration at different temperatures

**Reaction conditions:** 4'-BAP, *n*-BA: 0.602 kmol/m<sup>3</sup>, NaOAc: 0.6 kmol/m<sup>3</sup>, TBAB: 0.074 kmol/m<sup>3</sup>, Catalyst precursor 1: 8.51 x 10<sup>-5</sup> kmol/m<sup>3</sup>, Solvent: NMP, Total Volume: 2.5 x 10<sup>-5</sup> m<sup>3</sup>

The rate was found to increase linearly with the increase in the concentration of 4'-BAP. This is to be expected as the ArX oxidatively adds to the catalytic species Q1 in the catalytic cycle shown in Scheme 3.3 (Step 3). The oxidative addition proceeds as a concerted step, where the C-Br bond cleavage is perfectly synchronized with the formation of Pd-C and Pd Br bond<sup>12,13</sup>. The strength of the C-X bond determines the rate of oxidative addition. This step is usually considered to be the rate-determining step in the Heck catalytic cycle<sup>14</sup>. As the concentration of the 4'-BAP increases it leads to enhanced generation of the active species and hence the linear dependence on the 4'-BAP concentration is observed. This observation is similar to an earlier report by Zhao et al<sup>1</sup> for the kinetics of Heck reaction of iodobenzene with methyl acrylate with Pd(OAc)<sub>2</sub>/PPh<sub>3</sub> as the catalyst precursor. Dupont et al<sup>5</sup> report saturation kinetics (first order at lower concentration and zero order at higher concentration) for PhI concentration for the reaction of iodobenzene with *n*-BA. Blackmond et al<sup>4</sup> report a zero order dependence on the halide concentration for the reaction of *p*-bromobenzaldehyde with *n*-BA, however, as is

expected, any zero order reaction essentially will be a positive order in the lower concentration range.

### 3.3.3. Effect of n-butyl acrylate concentration on the rate of reaction

The effect of n-butyl acrylate concentration was studied at constant 4'-BAP, catalyst precursor **1**, NaOAc, and TBAB concentrations of  $0.399 \text{ kmol/m}^3$ ,  $8.511 \times 10^{-5} \text{ kmol/m}^3$ ,  $0.6 \text{ kmol/m}^3$ , and  $0.074 \text{ kmol/m}^3$ , respectively, in the temperature range of 403-433 K. A concentration time profile was obtained for each experiment with different initial concentrations of n-butyl acrylate.

The initial rates of product formation for different initial concentrations of n-butyl acrylate were calculated from the CT profile plots as described earlier. The plots of the product formation as the function of time for the initial periods of the reaction are given in Figures 3.13 to 3.16 for the temperatures of 403, 413, 423 and 433 K respectively.

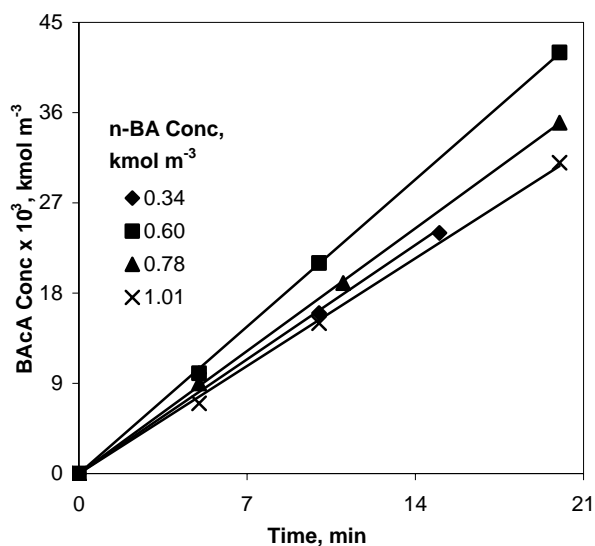


**Figure 3.13:** Plot of the product formation as a function of time for different initial concentrations of n-BA at 403 K

**Reaction conditions:** 4'-BAP:  $0.399 \text{ kmol/m}^3$ , n-BA, NaOAc:  $0.6 \text{ kmol/m}^3$ , TBAB:  $0.074 \text{ kmol/m}^3$ , Catalyst precursor **1**:  $8.51 \times 10^{-5} \text{ kmol/m}^3$ , Solvent: NMP, Total Volume:  $2.5 \times 10^5 \text{ m}^3$ , Temp: 403 K

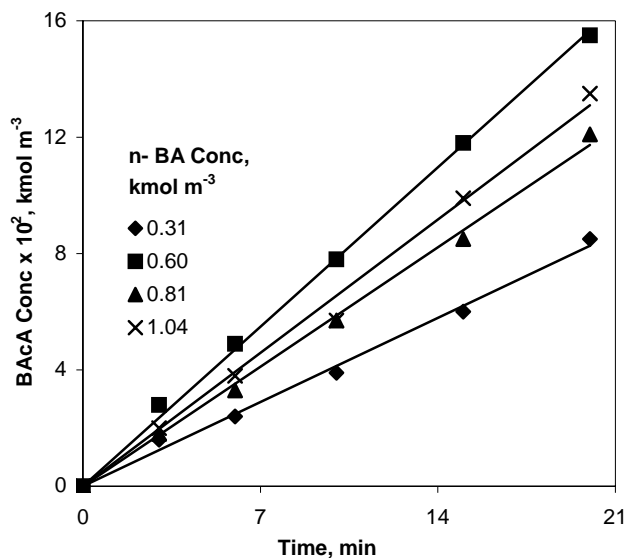


**Figure 3.14:** Plot of the product formation as a function of time for different initial concentrations of n-BA at 413 K

**Reaction conditions:** 4'-BAP:  $0.399 \text{ kmol/m}^3$ , n-BA, NaOAc:  $0.6 \text{ kmol/m}^3$ , TBAB:  $0.074 \text{ kmol/m}^3$ , Catalyst precursor I:  $8.51 \times 10^{-5} \text{ kmol/m}^3$ , Solvent: NMP, Total Volume:  $2.5 \times 10^5 \text{ m}^3$ , Temp: 413 K

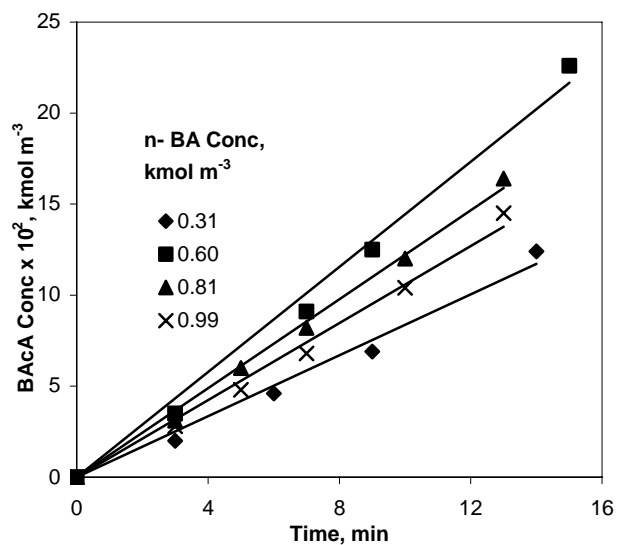


**Figure 3.15:** Plot of the product formation as a function of time for different initial concentrations of n-BA at 423 K

**Reaction conditions:** 4'-BAP:  $0.399 \text{ kmol/m}^3$ , n-BA, NaOAc:  $0.6 \text{ kmol/m}^3$ , TBAB:  $0.074 \text{ kmol/m}^3$ , Catalyst precursor I:  $8.51 \times 10^{-5} \text{ kmol/m}^3$ , Solvent: NMP, Total Volume:  $2.5 \times 10^5 \text{ m}^3$ , Temp: 423 K

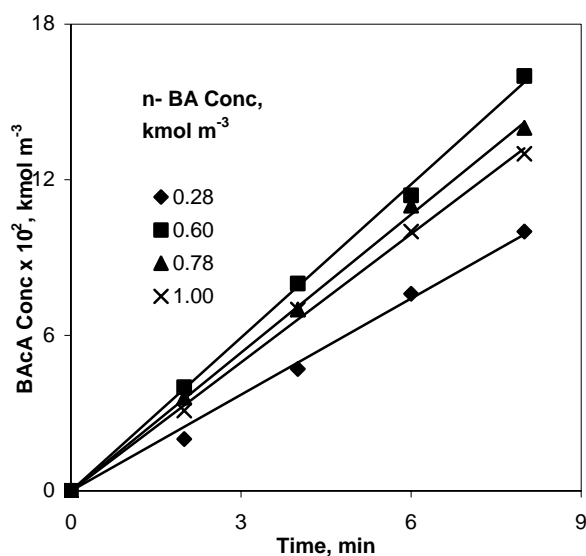


**Figure 3.16:** Plot of the product formation as a function of time for different initial concentrations of n-BA at 433 K

**Reaction conditions:** 4'-BAP:  $0.399 \text{ kmol/m}^3$ , n-BA, NaOAc:  $0.6 \text{ kmol/m}^3$ , TBAB:  $0.074 \text{ kmol/m}^3$ , Catalyst precursor I:  $8.51 \times 10^{-5} \text{ kmol/m}^3$ , Solvent: NMP, Total Volume:  $2.5 \times 10^{-5} \text{ m}^3$ , Temp: 433 K

The initial rates of the reactions were calculated from the slopes of the plots of the product formation vs. time. The plot of the initial rates as a function of n-butyl acrylate concentration is presented in Figure 3.17.

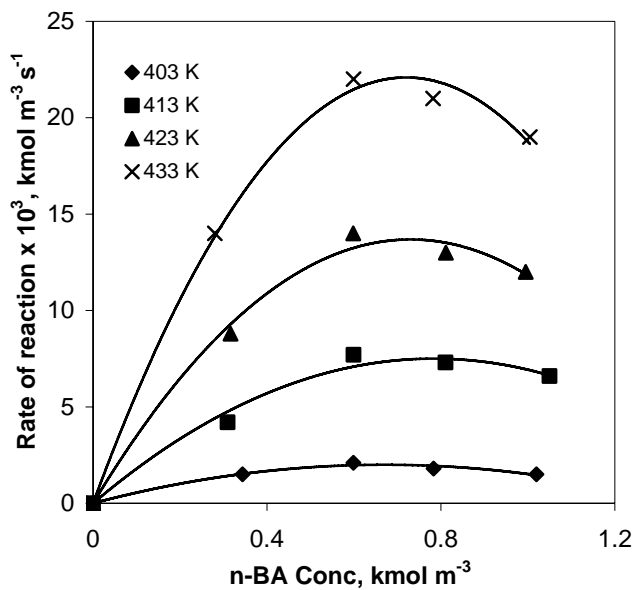


**Figure 3.17:** Plot of the initial rate vs. n-BA concentration at different temperatures

**Reaction conditions:** 4'-BAP:  $0.399 \text{ kmol/m}^3$ , n-BA, NaOAc:  $0.6 \text{ kmol/m}^3$ , TBAB:  $0.074 \text{ kmol/m}^3$ , Catalyst precursor 1:  $8.51 \times 10^{-5} \text{ kmol/m}^3$ , Solvent: NMP, Total Volume:  $2.5 \times 10^{-5} \text{ m}^3$

The rate of the reaction showed a complex dependence on n-BA concentration and passed through a maximum. Initially, first order dependence was observed with the acrylate concentration (in the lower concentration range  $< 0.6 \text{ kmol/m}^3$ ) and then, after attaining a maximum, the rates decreased marginally with increasing concentration of the olefin. This is the first time a negative order dependence of the rate on concentrations of n-BA has been observed in Heck reactions. In earlier studies Dupont et al<sup>5</sup> reported saturation kinetics with respect to n-BA concentration for the reaction of iodobenzene with n-BA, whereas, Blackmond et al<sup>4</sup> reported a first order dependence on the olefin concentration for the reaction of p-bromobenzaldehyde with n-BA using N-C palladacycle catalyst. The olefin concentration range used in the present study was higher than that used in the earlier studies. This might be one of the reasons why the decrease in the reaction rate with increase in olefin concentrations was not observed in the earlier studies.

The olefin addition to the catalyst complex Q2 leads to the formation of a  $\pi$  complex Q4 (Step 5, Scheme 3.3) in an equilibrium reaction which then leads to the formation of  $\sigma$  complex Q5 (Step 6, Scheme 3.3). This happens by the migratory insertion of the  $\pi$  bonded olefin between the Pd-C bond formed during the oxidative addition step. A  $\beta$ -hydrogen elimination then leads to the final product formation (Step 7, Scheme 3.3).

It has been reported that the presence of high concentrations of olefins leads to the formation of species Q7 (Step 2, Scheme 3.3), which is inactive for the reaction, leading to the reversible removal of the catalyst from the Heck catalytic cycle<sup>15</sup>. This leads to a decrease in the active catalyst available for the reaction and hence a drop in rate at higher n-butyl acrylate concentration is observed.

#### **3.3.4. Effect of NaOAc concentration on the rate of reaction**

The effect of base concentration on the vinylation of 4'-BAP with n-BA was studied at constant 4'-BAP, n-BA, catalyst precursor **1**, and TBAB concentrations of 0.399 kmol/m<sup>3</sup>, 0.602 kmol/m<sup>3</sup>, 8.511 x 10<sup>-5</sup> kmol/m<sup>3</sup>, and 0.074 kmol/m<sup>3</sup>, respectively, in a temperature range of 403-433 K. A concentration time profile was obtained for each experiment with different initial concentrations of sodium acetate at four different temperatures.

The initial rates of product formation for different initial concentrations of sodium acetate were calculated from the CT profile plots as described earlier. The plots of the product formation as the function of time for the initial periods of the reaction are given in Figures 3.18 to 3.21 for the temperatures 403, 413, 423 and 433 K respectively

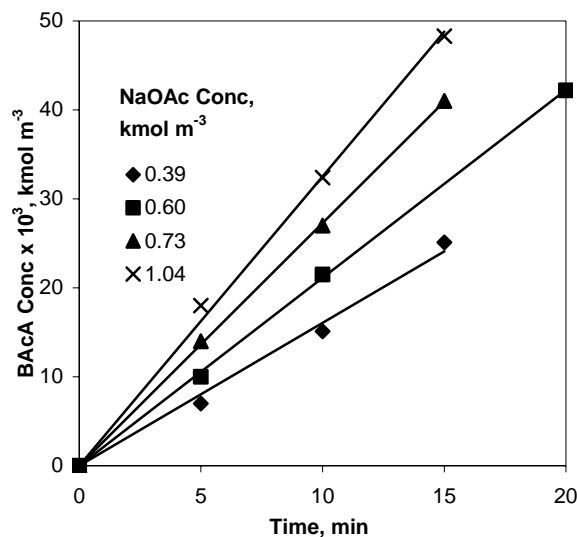


**Figure 3.18:** Plot of the product formation as a function of time for different initial concentrations of NaOAc at 403 K

**Reaction conditions:** 4'-BAP:  $0.399 \text{ kmol/m}^3$ , n-BA:  $0.602 \text{ kmol/m}^3$ , NaOAc, TBAB:  $0.074 \text{ kmol/m}^3$ , Catalyst precursor **1**:  $8.51 \times 10^{-5} \text{ kmol/m}^3$ , Solvent: NMP, Total Volume:  $2.5 \times 10^{-5} \text{ m}^3$ , Temp: 403 K

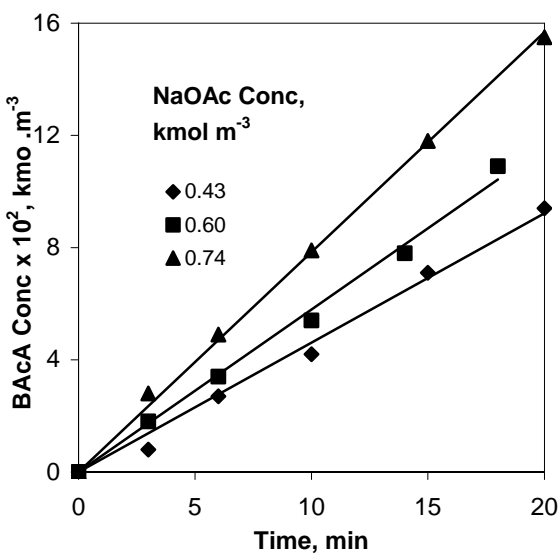


**Figure 3.21:** Plot of the product formation as a function of time for different initial concentrations of NaOAc at 413 K

**Reaction conditions:** 4'-BAP:  $0.399 \text{ kmol/m}^3$ , n-BA:  $0.602 \text{ kmol/m}^3$ , NaOAc, TBAB:  $0.074 \text{ kmol/m}^3$ , Catalyst precursor **1**:  $8.51 \times 10^{-5} \text{ kmol/m}^3$ , Solvent: NMP, Total Volume:  $2.5 \times 10^{-5} \text{ m}^3$ , Temp: 413 K

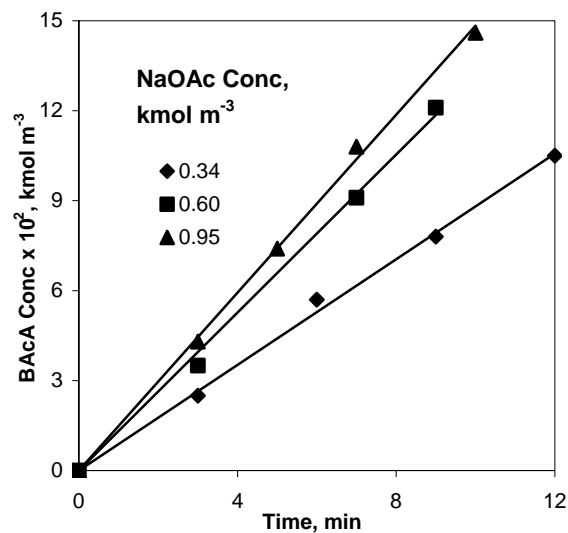


**Figure 3.21:** Plot of the product formation as a function of time for different initial concentrations of NaOAc at 423 K

**Reaction conditions:** 4'-BAP:  $0.399 \text{ kmol/m}^3$ , n-BA:  $0.602 \text{ kmol/m}^3$ , NaOAc, TBAB:  $0.074 \text{ kmol/m}^3$ , Catalyst precursor I:  $8.51 \times 10^{-5} \text{ kmol/m}^3$ , Solvent: NMP, Total Volume:  $2.5 \times 10^{-5} \text{ m}^3$ , Temp: 423 K

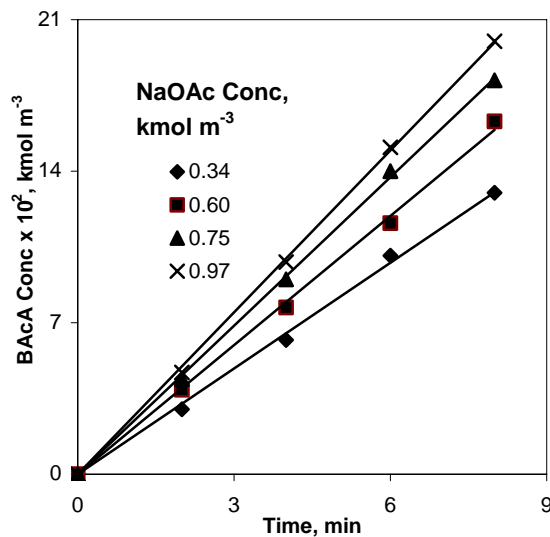


**Figure 3.21:** Plot of the product formation as a function of time for different initial concentrations of NaOAc at 433 K

**Reaction conditions:** 4'-BAP:  $0.399 \text{ kmol/m}^3$ , n-BA:  $0.602 \text{ kmol/m}^3$ , NaOAc, TBAB:  $0.074 \text{ kmol/m}^3$ , Catalyst precursor I:  $8.51 \times 10^{-5} \text{ kmol/m}^3$ , Solvent: NMP, Total Volume:  $2.5 \times 10^{-5} \text{ m}^3$ , Temp: 433 K



The initial rates of the reactions were calculated from the slopes of the plots of the product formation vs. time. The plot of the initial rates as a function of sodium acetate concentration is presented in Figure 3.22.

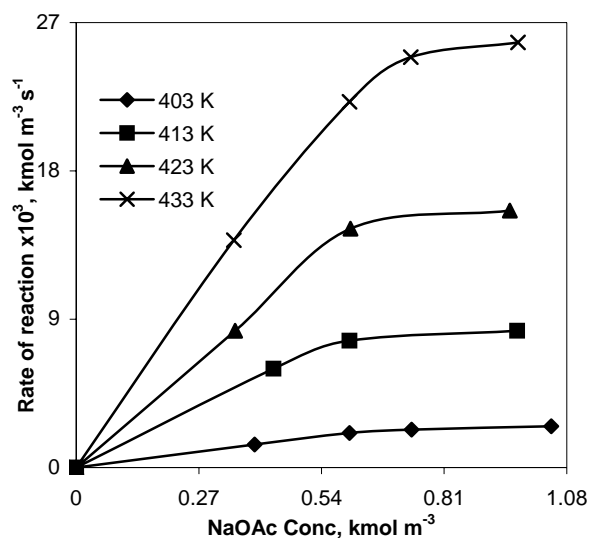


**Figure 3.22:** Plot of the initial rate vs. NaOAc concentration at different temperatures

**Reaction conditions:** 4'-BAP:  $0.399 \text{ kmol/m}^3$ , n-BA:  $0.602 \text{ kmol/m}^3$ , NaOAc, TBAB:  $0.074 \text{ kmol/m}^3$ , Catalyst precursor 1:  $8.51 \times 10^{-5} \text{ kmol/m}^3$ , Solvent: NMP, Total Volume:  $2.5 \times 10^{-5} \text{ m}^3$

The rate showed a linear dependence on NaOAc concentration in the lower concentration range ( $< 0.8 \text{ kmol/m}^3$ ). With further increase in NaOAc concentration the rate increased marginally with a near zero order dependence. Earlier reports by Dupont et al<sup>5</sup> showed a zero order dependence on the base concentration. Zhao et al<sup>1</sup> reported the rates passing through a maximum as the concentration of the base (triethylamine) was increased.

The base is required for the regeneration of the active catalytic species by abstraction of HBr from the species Q6 as shown in Step 8 of Scheme 3.3. As the concentration of the base increases, a faster regeneration of active catalytic species takes place leading to an increase in the rate as observed. Further increase in the base concentration above a certain value does not lead to any additional enhancements in the

rate. This could be due to the solubility limitation of NaOAc in NMP at higher base concentration.

### 3.3.5. Effect of TBAB concentration on the rate of reaction

The effect of tetrabutylammonium bromide concentration on the rate of the reaction was studied at constant 4'-BAP, n-BA, catalyst precursor **1**, and NaOAc concentrations of  $0.399 \text{ kmol/m}^3$ ,  $0.602 \text{ kmol/m}^3$ ,  $8.511 \times 10^{-5} \text{ kmol/m}^3$ , and  $0.6 \text{ kmol/m}^3$ , respectively, in a temperature range of 403-433 K. A concentration time profile was obtained for each experiment with different initial concentrations of tetrabutylammonium bromide at four different temperatures.

The initial rates of product formation for different initial concentrations of tetrabutylammonium bromide were calculated from the CT profile plots as described earlier. The plots of the product formation as the function of time for the initial periods of the reaction are given in Figures 3.23 to 3.26 for the temperatures 403, 413, 423 and 433 K respectively

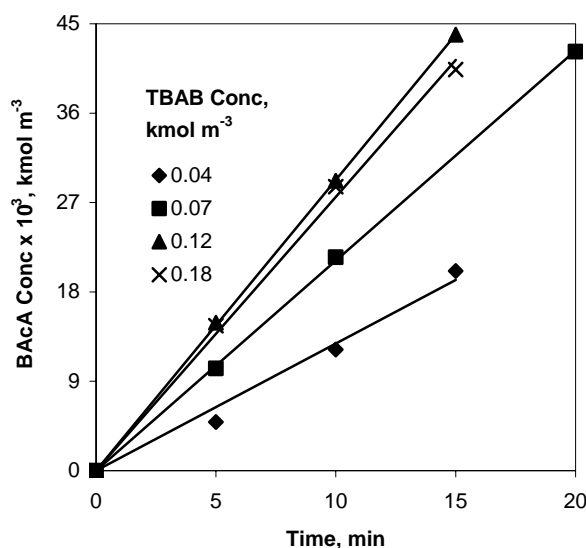


**Figure 3.23:** Plot of the product formation as a function of time for different initial concentrations of TBAB at 403 K

**Reaction conditions:** 4'-BAP:  $0.399 \text{ kmol/m}^3$ , n-BA:  $0.602 \text{ kmol/m}^3$ , NaOAc:  $0.602 \text{ kmol/m}^3$ , TBAB, Catalyst precursor **1**:  $8.51 \times 10^{-5} \text{ kmol/m}^3$ , Solvent: NMP, Total Volume:  $2.5 \times 10^{-5} \text{ m}^3$ , Temp: 403 K

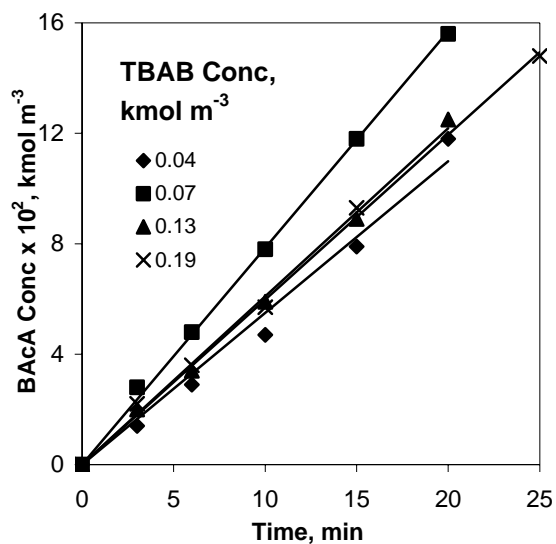


**Figure 3.24:** Plot of the product formation as a function of time for different initial concentrations of TBAB at 413 K

*Reaction conditions:* 4'-BAP:  $0.399 \text{ kmol/m}^3$ , n-BA:  $0.602 \text{ kmol/m}^3$ , NaOAc:  $0.602 \text{ kmol/m}^3$ , TBAB, Catalyst precursor **I**:  $8.51 \times 10^{-5} \text{ kmol/m}^3$ , Solvent: NMP, Total Volume:  $2.5 \times 10^{-5} \text{ m}^3$ , Temp: 413 K

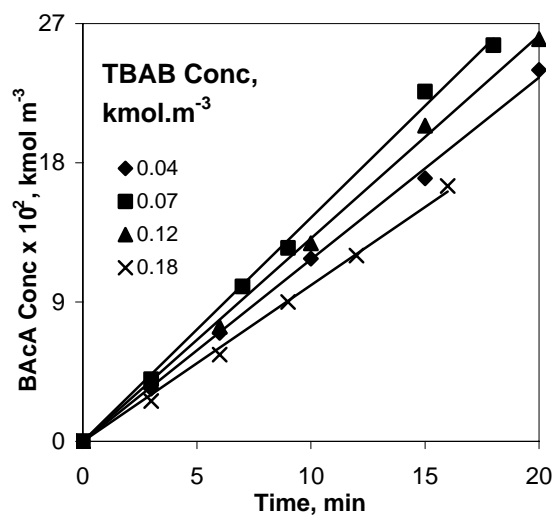


**Figure 3.25:** Plot of the product formation as a function of time for different initial concentrations of TBAB at 423 K

*Reaction conditions:* 4'-BAP:  $0.399 \text{ kmol/m}^3$ , n-BA:  $0.602 \text{ kmol/m}^3$ , NaOAc:  $0.602 \text{ kmol/m}^3$ , TBAB, Catalyst precursor **I**:  $8.51 \times 10^{-5} \text{ kmol/m}^3$ , Solvent: NMP, Total Volume:  $2.5 \times 10^{-5} \text{ m}^3$ , Temp: 423 K

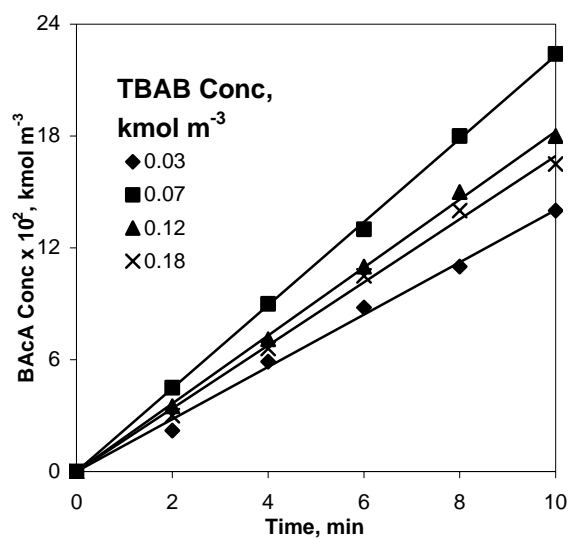


**Figure 3.26:** Plot of the product formation as a function of time for different initial concentrations of TBAB at 433 K

**Reaction conditions:** 4'-BAP:  $0.399 \text{ kmol/m}^3$ , n-BA:  $0.602 \text{ kmol/m}^3$ , NaOAc:  $0.602 \text{ kmol/m}^3$ , TBAB, Catalyst precursor **I**:  $8.51 \times 10^{-5} \text{ kmol/m}^3$ , Solvent: NMP, Total Volume:  $2.5 \times 10^{-5} \text{ m}^3$ , Temp: 433 K

The initial rates of the reactions were calculated from the slopes of the plots of the product formation vs. time. The plot of the initial rates as a function of sodium acetate concentration is presented in Figure 3.27.

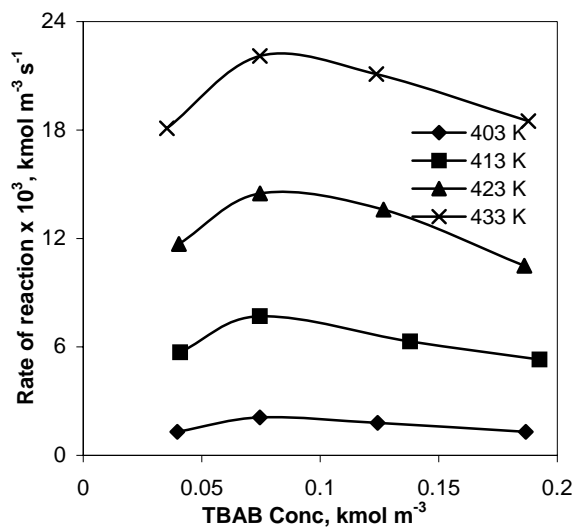


**Figure 3.27:** Plot of the initial rate vs. NaOAc concentration at different temperatures

**Reaction conditions:** 4'-BAP:  $0.399 \text{ kmol/m}^3$ , n-BA:  $0.602 \text{ kmol/m}^3$ , NaOAc:  $0.602 \text{ kmol/m}^3$ , TBAB, Catalyst precursor **I**:  $8.51 \times 10^{-5} \text{ kmol/m}^3$ , Solvent: NMP, Total Volume:  $2.5 \times 10^{-5} \text{ m}^3$

Quaternary ammonium salts were used as promoters for the first time by Jeffery<sup>16-19</sup>. He showed a marked improvement in the reaction rates by the addition of these promoters. Under these conditions, Jeffery was even able to carry out the Heck reaction with aryl iodides at room temperatures. The Heck reaction carried out with quaternary ammonium salts are thus known as the Jeffery protocol.

The rates passed through a maximum as the concentration of tetrabutylammonium bromide was increased. TBAB is known to play diverse roles in the reaction mechanism. It acts as a phase transfer agent<sup>17</sup> in order to increase the solubility of NaOAc in NMP. At higher concentrations of TBAB this can lead to enhanced solubility of NaOAc in NMP making it viscous (experimentally observed), thereby reducing the rates. TBAB can also act as a promoter to increase the rate of oxidative addition by increasing the electron density on the palladium atom due to the formation of more electron rich anionic Pd(0) species, as reported by Amatore and Jutand<sup>20</sup>. It can also act as a stabilizing additive to increase the lifetime of underligated Pd(0) species. The bromide of the TBAB can enter the coordination sphere of the palladium and form a stable complex that can prevent collisions between the Pd(0) species and thus reduce the possibility of formation of metal clusters<sup>12</sup>. It

has been reported earlier that the addition of quaternary ammonium salts enhances the life time of the palladacycle catalyst precursor **1**<sup>21</sup>. However, at higher TBAB concentrations this may reduce the reaction rates as vacant metal orbitals may not be available for the oxidative addition step. The exact nature of the influence of TBAB on the reaction rate cannot be restricted to a single effect but is rather a combination of all the effects mentioned earlier.

### 3.4. Kinetic Analysis

#### 3.4.1. Empirical rate models and model discrimination

The kinetic data obtained earlier was used to develop a rate equation for the Heck reaction of 4'-bromo acetophenone and n-butyl acrylate. Based on the observed trends, a variety of empirical models were examined, and the best model was selected based on the criterion of the least average error between predicted and experimental rates ( $\Phi_{\min}$ ) which is defined as:

$$\Phi_{\min} = \sum_{i=1}^n (R_{\text{EXP}} - R_{\text{PRE}})^2 \quad \text{Eq 3.1}$$

Where  $R_{\text{EXP}}$  is the observed rate of reaction and  $R_{\text{PRE}}$  is the predicted rate obtained by using the respective models.

The rate parameters  $k$ ,  $K_B$ ,  $K_C$ , and  $K_D$  were evaluated for 403, 413, 423, and 433 K by fitting the experimental rate data with Models I to V using non linear regression analysis and an optimisation routine based on Marquardt's method<sup>22</sup>. The values of the rate parameters for different temperatures are presented in Table 3.2.

The values of  $\Phi_{\min}$  suggest the extent of fit of the kinetic models used (lower value of the  $\Phi_{\min}$  shows the best fit).

$$R = \frac{k[A][B][C][D][Q]}{(1 + K_B[B]^2)(1 + K_C[C])(1 + K_D[D]^2)} \quad \text{Model I}$$

$$R = \frac{k[A][B][C][D][Q]^{0.5}}{(1 + K_B[B]^2)(1 + K_C[C])(1 + K_D[D]^2)} \quad \text{Model II}$$

$$R = \frac{k[A][B][C][D][Q]^{0.5}}{(1 + K_B[B])(1 + K_C[C])(1 + K_D[D])} \quad \text{Model III}$$

$$R = \frac{k[A][B][C][D][Q]^{0.5}}{(1 + K_B[B]^2)(1 + K_C[C])(1 + K_D[D])} \quad \text{Model IV}$$

$$R = \frac{k[A][B][C][D][Q]^{0.5}}{(1 + K_B[B]^2)(1 + K_D[D]^2)} \quad \text{Model V}$$

Model I was rejected as it gave negative values for the equilibrium constants. Model V gave very high value for  $\Phi_{\min}$  and hence was rejected. Models III and IV gave the  $\Phi_{\min}$  value higher than model II. In addition, on comparison of the predicted values of the rates using these three models, it was observed that overall prediction using model II was closest to the experimental values. Model II gave overall lowest values for  $\Phi_{\min}$ . This model thus turned out to be superior amongst all the models considered.

The following model was found to best fit the data at all the temperatures studied.

$$R = \frac{k[A][B][C][D][Q]^{0.5}}{(1 + K_B[B]^2)(1 + K_C[C])(1 + K_D[D]^2)} \quad \text{Model II}$$

Where R is the rate of reaction, expressed in  $\text{kmol/m}^3/\text{s}$ , [A] is the concentration of p-bromo acetophenone ( $\text{kmol/m}^3$ ), [B] is the concentration of n-butyl acrylate ( $\text{kmol/m}^3$ ), [C] is the concentration of NaOAc ( $\text{kmol/m}^3$ ), [D] is the concentration of TBAB ( $\text{kmol/m}^3$ ), and [Q] is the concentration of the palladacycle catalyst precursor **1** ( $\text{kmol/m}^3$ ). k is the rate constant, and  $K_B$ ,  $K_C$  and  $K_D$  are equilibrium constants. The values of the constants

obtained using Model II are presented in Table 3.2 and the fits obtained are presented in Figures 3.28 to 3.32. It can be seen that the experimental data are in good agreement with the predicted rates.

**Table 3.2:** Values of kinetic parameters at different temperatures

Mod	Temp, K	K	K <sub>B</sub>	K <sub>C</sub>	K <sub>D</sub>	Φ <sub>min</sub> × 10 <sup>4</sup>
I	403	9.36 × 10 <sup>3</sup>	3.03	0.60	1.17 × 10 <sup>2</sup>	0.16
	413	1.26 × 10 <sup>3</sup>	0.04	-0.47	-1.13 × 10 <sup>2</sup>	24.64
	423	5.17 × 10 <sup>4</sup>	1.86	0.91	91.81	10.08
	433	9.91 × 10 <sup>4</sup> (m <sup>3</sup> /kmol) <sup>5</sup>	2.31 (m <sup>3</sup> /kmol) <sup>2</sup>	0.76 (m <sup>3</sup> /kmol)	1.26 × 10 <sup>2</sup> (m <sup>3</sup> /kmol) <sup>2</sup>	21.51
II	403	1.09 × 10 <sup>2</sup>	1.90	1.18	1.48 × 10 <sup>2</sup>	0.01
	413	4.11 × 10 <sup>2</sup>	2.01	1.23	1.54 × 10 <sup>2</sup>	0.19
	423	8.06 × 10 <sup>2</sup>	2.08	1.29	1.58 × 10 <sup>2</sup>	1.23
	433	1.37 × 10 <sup>3</sup> (m <sup>3</sup> /kmol) <sup>4.5</sup>	2.28 (m <sup>3</sup> /kmol) <sup>2</sup>	1.31 (m <sup>3</sup> /kmol)	1.63 × 10 <sup>2</sup> (m <sup>3</sup> /kmol) <sup>2</sup>	2.07
III	403	5.14 × 10 <sup>2</sup>	3.13	1.05	59.19	0.06
	413	2.41 × 10 <sup>3</sup>	3.33	1.35	75.63	0.56
	423	5.77 × 10 <sup>3</sup>	3.89	1.22	86.71	2.42
	433	1.47 × 10 <sup>4</sup> (m <sup>3</sup> /kmol) <sup>4.5</sup>	4.35 (m <sup>3</sup> /kmol)	1.31 (m <sup>3</sup> /kmol)	1.28 × 10 <sup>2</sup> (m <sup>3</sup> /kmol)	2.34
IV	403	2.77 × 10 <sup>2</sup>	1.49	1.07	59.45	0.05
	413	1.27 × 10 <sup>3</sup>	1.66	1.12	75.03	0.46
	423	3.09 × 10 <sup>3</sup>	2.04	1.22	88.98	2.07
	433	7.59 × 10 <sup>3</sup> (m <sup>3</sup> /kmol) <sup>4.5</sup>	2.29 (m <sup>3</sup> /kmol) <sup>2</sup>	1.29 (m <sup>3</sup> /kmol)	1.31 × 10 <sup>2</sup> (m <sup>3</sup> /kmol)	2.45
V	403	2.556	1.17		1.48 × 10 <sup>2</sup>	0.33
	413	97.55	1.37		1.54 × 10 <sup>2</sup>	4.69
	423	1.87 × 10 <sup>2</sup>	1.73		1.63 × 10 <sup>2</sup>	18.01
	433	3.58 × 10 <sup>2</sup> (m <sup>3</sup> /kmol) <sup>4.5</sup>	2.34 (m <sup>3</sup> /kmol) <sup>2</sup>		1.73 × 10 <sup>2</sup> (m <sup>3</sup> /kmol) <sup>2</sup>	31.08



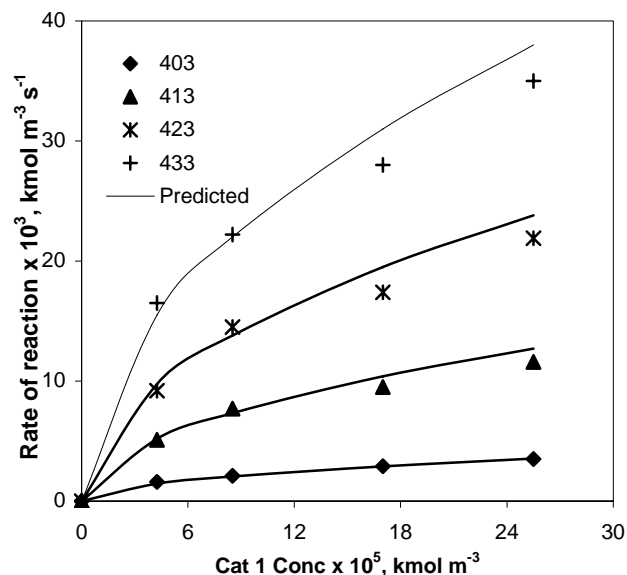


**Figure 3.28:** Effect of catalyst precursor **1** concentration on the reaction rates

*Reaction conditions:* 4'-BAP:  $0.399 \text{ kmol/m}^3$ , *n*-BA:  $0.602 \text{ kmol/m}^3$ , NaOAc:  $0.6 \text{ kmol/m}^3$ , TBAB:  $0.074 \text{ kmol/m}^3$ , Catalyst precursor **1**, solvent NMP, Total Volume:  $2.5 \times 10^{-5} \text{ m}^3$

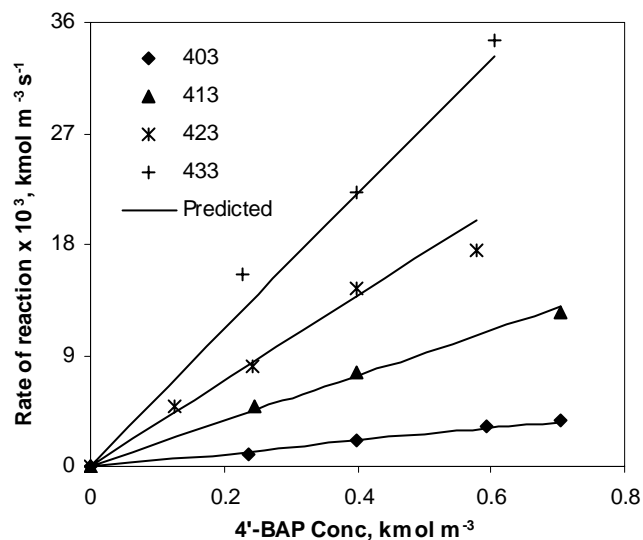


**Figure 3.29:** Effect of 4'-bromo acetophenone concentration on the reaction rates

*Reaction conditions:* 4'-BAP, *n*-BA:  $0.602 \text{ kmol/m}^3$ , NaOAc:  $0.6 \text{ kmol/m}^3$ , TBAB:  $0.074 \text{ kmol/m}^3$ , Catalyst precursor **1**:  $8.51 \times 10^{-5} \text{ kmol/m}^3$ , solvent NMP, Total Volume:  $2.5 \times 10^{-5} \text{ m}^3$

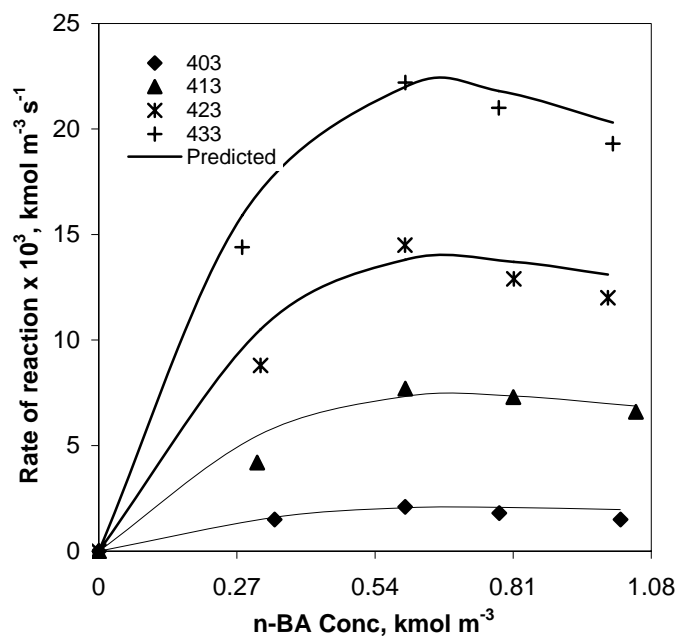


**Figure 3.30:** Effect of n-butyl acrylate concentration on the reaction rates

*Reaction conditions:* 4'-BAP  $0.399 \text{ kmol/m}^3$ , n-BA, NaOAc:  $0.6 \text{ kmol/m}^3$ , TBAB:  $0.074 \text{ kmol/m}^3$ , Catalyst precursor **I**:  $8.51 \times 10^{-5} \text{ kmol/m}^3$ , solvent NMP, Total Volume:  $2.5 \times 10^{-5} \text{ m}^3$

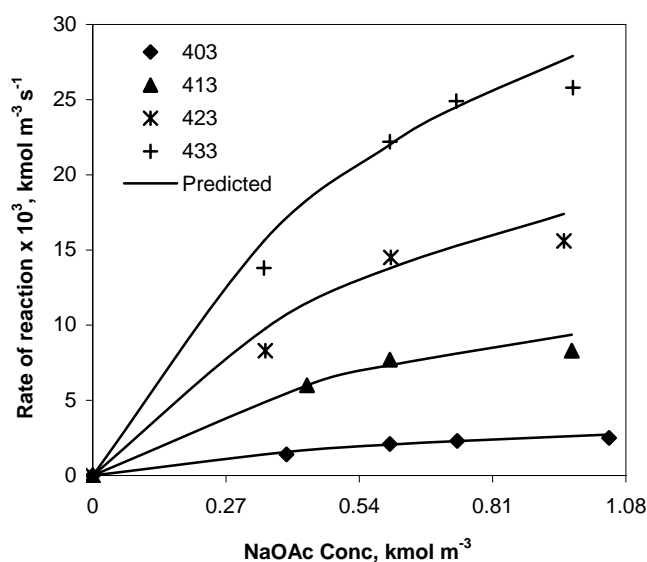


**Figure 3.31:** Effect of NaOAc concentration on the reaction rates

*Reaction conditions:* 4'-BAP  $0.399 \text{ kmol/m}^3$ , n-BA:  $0.6 \text{ kmol/m}^3$ , NaOAc, TBAB:  $0.074 \text{ kmol/m}^3$ , Catalyst precursor **I**:  $8.51 \times 10^{-5} \text{ kmol/m}^3$ , solvent NMP, Total Volume:  $2.5 \times 10^{-5} \text{ m}^3$

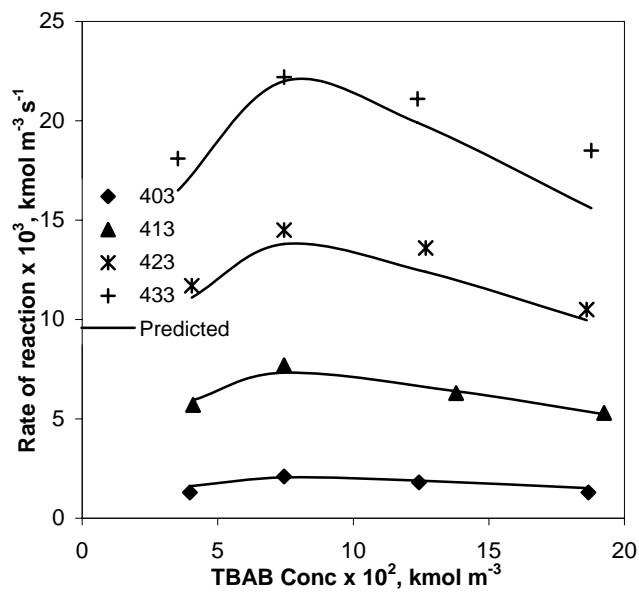


**Figure 3.32:** Effect of TBAB concentration on the reaction rates

**Reaction conditions:** 4'-BAP: 0.399 kmol/m<sup>3</sup>, n-BA: 0.602 kmol/m<sup>3</sup>, NaOAc: 0.6 kmol/m<sup>3</sup>, TBAB, Catalyst precursor I:  $8.51 \times 10^{-5}$  kmol/m<sup>3</sup>, solvents NMP, Total Volume:  $2.5 \times 10^{-5}$  m<sup>3</sup>

A comparison of the experimental rates with the predicted rates using model II is also shown on Figure 3.33, which too indicates a very good agreement between experiments and predictions. The average percent error between the experimental and predicted data was 1.12 %. The activation energy for this model was calculated to be 114.49 kJ/mol based on the Arrhenius plot (Figure 3.34). The dependence of  $K_B$ ,  $K_C$ , and  $K_D$  on temperature was also studied and is shown in Figure 3.35 for Model II. These constants were found to be a mild function of temperatures.

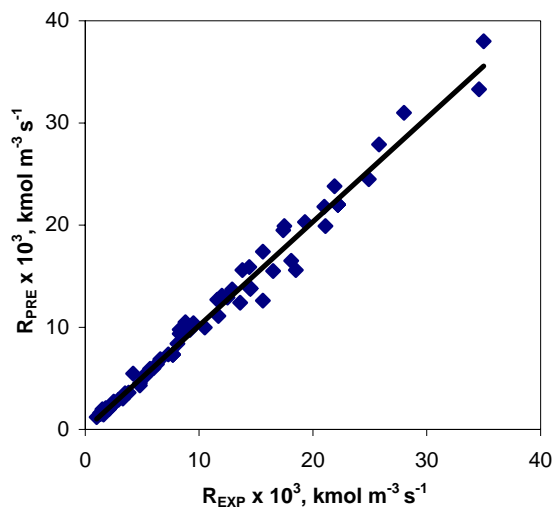


**Figure 3.33:** Comparison of experimental rates and rates predicted using model II

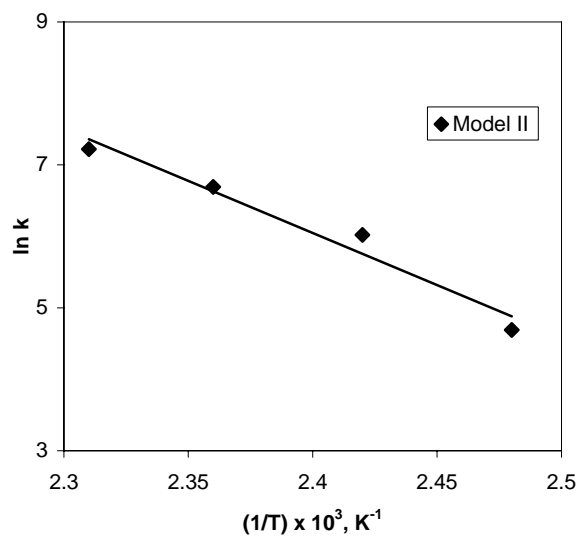


**Figure 3.34:** Temperature dependence of rate constant ( $k$ ) (Arrhenius plot)

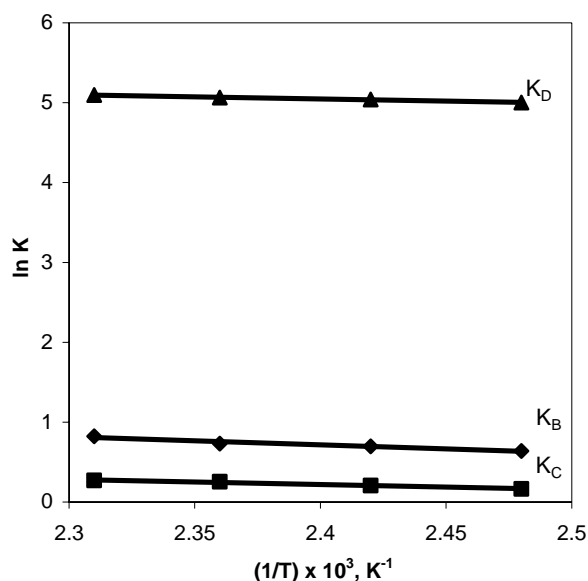


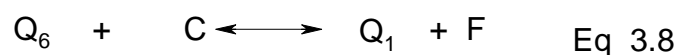
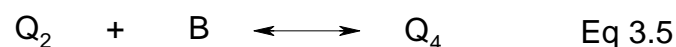
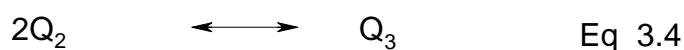
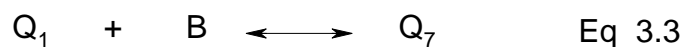
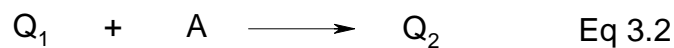
**Figure 3.35:** Temperature dependence of equilibrium constants  $K_B$ ,  $K_C$  and  $K_D$  obtained using Model II

### 3.4.2. Mechanistic rate models and model discrimination

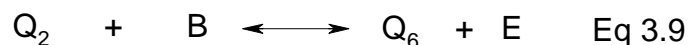
The empirical models are the mathematical models based on the reaction data obtained. These models provide a useful insight on the reaction behaviour. Apart from dealing with the empirical models it is also important to derive the reaction rates based on the mechanism of the reaction. These models allow for the data to be examined based on the reaction mechanism. Keeping this in mind rate equations were derived based on the reported reaction mechanism for the Heck reactions (Scheme 3.3). Different steps in the Heck catalytic cycle were considered to be rate determining and rate equations were derived for each case. While deriving the rate expressions following assumptions were made: i) all the reaction steps are in equilibrium except the rate determining step ii) for the initial rates, the concentrations of the products is very low and hence can be neglected and iii) all the rearrangement steps are fast and can be combined with other steps. For derivation of models following three cases were considered based on three different rate determining steps.

### 3.4.2.1. Oxidative addition of aryl halide to Pd as the rate determining step

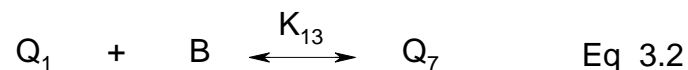
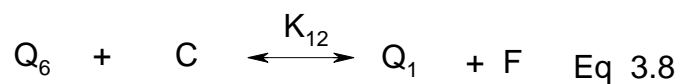
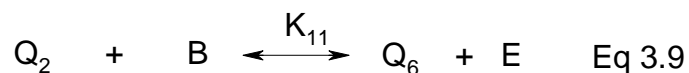
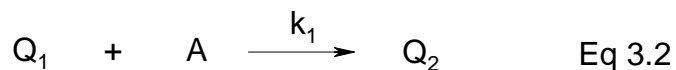
When the oxidative addition of the 4'-bromoacetophenone to palladium is considered the rate determining step, then, based on scheme 3.3 the mechanism can be expressed in terms of the following equations:



Equations 3.5, 3.6, and 3.7 can be combined to give the following equation:



For deriving the rate expression the above equations can be condensed to give the set of following equations.



Where Q is the total catalyst present in the reaction mixture and  $Q_1$ ,  $Q_2$ ,  $Q_3$ ,  $Q_4$ ,  $Q_5$ ,  $Q_6$ , and  $Q_7$  are the various catalytic intermediates present in the reaction mixture. A represents 4'-bromoacetophenone, B represents n-butyl acrylate, C represents NaOAc, E represents the Heck vinylated product, and F represents HBr abstracted by the base.  $K_{11}$ ,  $K_{12}$ , and  $K_{13}$  are the equilibrium constants and  $k_1$  is the reaction constant. The rate of the reaction can then be expressed by the following equation:

$$R = k_1[Q_1][A] \quad \text{Eq 3.10}$$

The total concentration of the catalyst (Q) is given as:

$$[Q] = [Q_1] + [Q_2] + [Q_6] + [Q_7] \quad \text{Eq 3.11}$$

For the Initial rates, the concentrations of E and F are very small and hence can be neglected. Expressing  $Q_2$ ,  $Q_6$ , and  $Q_7$  in terms of  $Q_1$  we get

$$[Q_6] = \frac{[Q_1]}{K_{12}[C]}$$

$$[Q_7] = K_{13}[Q_1][B]$$

$$[Q_2] = \frac{[Q_1]}{K_{11}K_{12}[B][C]}$$

On substituting these values in equation 3.11, the following expression is obtained:

$$\begin{aligned}
[Q] &= [Q_1 + \frac{[Q_1]}{K_{12}[C]} + \frac{[Q_1]}{K_{11}K_{12}[B][C]} + K_{13}[Q_1][B]] \\
&= [Q_1] \left[ 1 + \frac{1}{K_{12}[C]} + \frac{1}{K_{11}K_{12}[B][C]} + K_{13}[B] \right] \\
&= [Q_1] \left[ \frac{K_{11}K_{12}[B][C] + K_{11}[B] + 1 + K_{11}K_{12}K_{13}[B]^2[C]}{K_{11}K_{12}[B][C]} \right] \\
\Rightarrow [Q_1] &= \frac{K_{11}K_{12}[B][C][Q]}{K_{11}K_{12}[B][C] + K_{11}[B] + 1 + K_{11}K_{12}K_{13}[B]^2[C]}
\end{aligned}$$

Substituting  $K_{11}K_{12} = K_{1a}$ ,  $K_{11}K_{12}K_{13} = K_{1b}$

$$[Q_1] = \frac{K_{1a}[B][C][Q]}{K_{1a}[B][C] + K_{11}[B] + 1 + K_{1b}[B]^2[C]}$$

This value of  $Q_1$  is then substituted in equation 3.10

$$R = \frac{k_1 K_{1a} [A][B][C][Q]}{K_{1a}[B][C] + K_{11}[B] + 1 + K_{1b}[B]^2[C]}$$

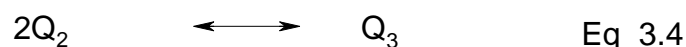
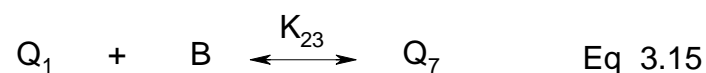
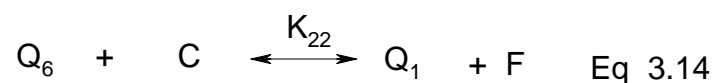
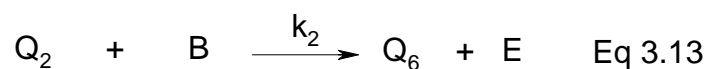
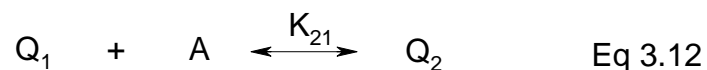
Again substituting  $k_1 K_{1a} = k_1'$  in this equation and taking into consideration the formation of the dimer (eq 3.4) the final rate expression is obtained as

$$R = \frac{k_1' [A][B][C][Q]^{0.5}}{K_{1a}[B][C] + K_{11}[B] + 1 + K_{1b}[B]^2[C]} \quad \text{Model VI}$$



### 3.4.2.2. Olefin insertion in the Pd-C bond as the rate determining step

If we consider insertion of n-butyl acrylate in the Pd-C bond as the rate determining step then the mechanism can be expressed in terms of the following equations:



Where Q is the total catalyst present in the reaction mixture and  $Q_1$ ,  $Q_2$ ,  $Q_3$ ,  $Q_6$ , and  $Q_7$  are the various catalytic intermediates present in the reaction mixture. A represents 4'-bromoacetophenone, B represents n-butyl acrylate, C represents NaOAc, E represents the Heck vinylated product, and F represents HBr abstracted by the base.  $K_{21}$ ,  $K_{22}$ , and  $K_{23}$  are the equilibrium constants and  $k_2$  is the reaction constant.

The rate of the reaction can then be expressed by the following equation:

$$R = k_2[Q_2][B] \quad \text{Eq 3.16}$$

The total concentration of the catalyst (Q) is given as:

$$[Q] = [Q_1] + [Q_2] + [Q_6] + [Q_7] \quad \text{Eq 3.17}$$

For the Initial rates, the concentrations of E and F are very small and hence can be neglected. Expressing  $Q_1$ ,  $Q_6$ , and  $Q_7$  in terms of  $Q_2$  we get

$$[Q_1] = \frac{[Q_2]}{K_{21}[A]}$$

$$[Q_6] = \frac{[Q_2]}{K_{21}K_{22}[A][C]}$$

$$[Q_7] = \frac{K_{23}[Q_2][B]}{K_{21}[A]}$$

Substituting these values in equation 3.17 we get

$$\begin{aligned} [Q] &= [Q_2] + \frac{[Q_2]}{K_{21}[A]} + \frac{[Q_2]}{K_{21}K_{22}[A][C]} + \frac{K_{23}[Q_2][B]}{K_{21}[A]} \\ &= [Q_2] \left[ 1 + \frac{1}{K_{21}[A]} + \frac{1}{K_{21}K_{22}[A][C]} + \frac{K_{23}[B]}{K_{21}[A]} \right] \\ &= [Q_2] \left[ \frac{K_{21}K_{22}[A][C] + K_{22}[C] + 1 + K_{22}K_{23}[B][C]}{K_{21}K_{22}[A][C]} \right] \\ \Rightarrow [Q_2] &= \frac{K_{21}K_{22}[A][C][Q]}{1 + K_{22}[C] + K_{21}K_{22}[A][C] + K_{22}K_{23}[B][C]} \end{aligned}$$

Substituting this value in equation 3.16 gives us

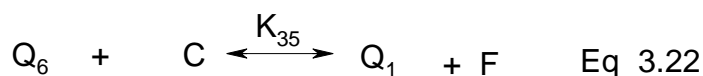
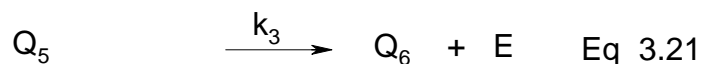
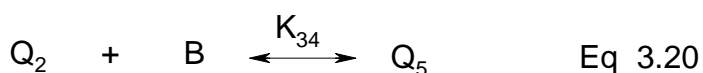
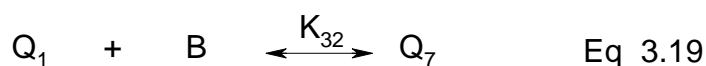
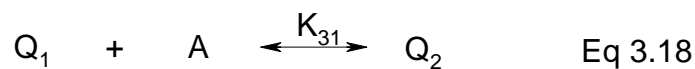
$$R = \frac{k_2 K_{21}K_{22}[A][B][C][Q]}{1 + K_{22}[C] + K_{21}K_{22}[A][C] + K_{22}K_{23}[B][C]}$$

Substituting  $K_{21}K_{22} = K_{2a}$ , and  $K_{22}K_{23} = K_{2b}$ ,  $k_2K_{21}K_{22} = k_2'$  and taking into account the dimer formation (Eq 3.4) the final rate is expressed as

$$R = \frac{k_2' [A][B][C][Q]}{1 + K_{22}[C] + K_{2a}[A][C] + K_{2b}[B][C]} \quad \text{Model VII}$$

### 3.4.2.3. $\beta$ -Hydride elimination as the rate determining step

If  $\beta$ -hydride elimination and Heck vinylation product formation is considered as the rate determining step then the mechanism of Heck reactions can be expressed in terms of the following equations:



Where Q is the total catalyst present in the reaction mixture and  $Q_1$ ,  $Q_2$ ,  $Q_3$ ,  $Q_5$ ,  $Q_6$ , and  $Q_7$  are the various catalytic intermediates present in the reaction mixture. A represents 4'-bromoacetophenone, B represents n-butyl acrylate, C represents NaOAc, E represents the Heck vinylated product, and F represents the HBr abstracted by the base.  $K_{31}$ ,  $K_{32}$ ,  $K_{34}$ , and  $K_{35}$  are the equilibrium constants and  $k_3$  is the reaction constant.

The rate of the reaction can then be expressed by the following equation:

$$R = k_3[Q_5] \quad \text{Eq 3.23}$$

The total concentration of the catalyst (Q) is given as:

$$[Q] = [Q_1] + [Q_2] + [Q_5] + [Q_6] + [Q_7] \quad \text{Eq 3.24}$$

For the Initial rates, the concentrations of E and F are very small and hence can be neglected. Expressing  $Q_1$ ,  $Q_2$ ,  $Q_6$ , and  $Q_7$  in terms of  $Q_5$  we get

$$[Q_1] = \frac{[Q_5]}{K_{31}K_{34}[A][B]}$$

$$[Q_7] = \frac{K_{32}[Q_5]}{K_{31}K_{34}[A]}$$

$$[Q_2] = \frac{[Q_5]}{K_{34}[B]}$$

$$[Q_6] = \frac{[Q_5]}{K_{31}K_{34}K_{35}[A][B][C]}$$

Substituting these values in equation 3.24

$$\Rightarrow [Q_5] = \frac{K_{31}K_{34}K_{35}[A][B][C][Q]}{K_{35}C + K_{32}K_{35}[B][C] + K_{31}K_{35}[A][C] + 1 + K_{31}K_{34}K_{35}[A][B][C]}$$

Substituting this value in equation 3.23

$$R = \frac{k_3 K_{31} K_{34} K_{35} [A][B][C] [Q]}{K_{35}C + K_{32} K_{35} [B][C] + K_{31} K_{35} [A][C] + 1 + K_{31} K_{34} K_{35} [A][B][C]}$$

Substituting  $k_3'K_{31}K_{34}K_{35} = k_3'$ ,  $K_{32}K_{35} = K_{3a}$ ,  $K_{31}K_{35} = K_{3b}$ ,  $K_{31}K_{34}K_{35} = K_{3c}$  and taking into account the dimer formation (eq 3.4) we get the final rate expression as

$$R = \frac{k_3' [A][B][C][Q]^{0.5}}{1 + K_{35}[C] + K_{3a}[B][C] + K_{3b}[A][C] + K_{3c}[A][B][C]} \quad \text{Model VIII}$$

### 3.4.2.4. Comparison of different mechanistic rate models

The values of the rate constants and equilibrium constants obtained using the mechanistic models are given in Tables 3.3 to 3.5. The three mechanistic models were discriminated on the basis of  $\Phi_{\min}$  value and also on the basis of the prediction of the rates. The least value of  $\Phi_{\min}$  was obtained for the model VI which corresponds to the oxidative addition of ArX as the rate determining step. The rates predicted by this model were in good agreement with the experimental rates. The comparison of the experimental rates and the rates predicted using model VI is shown in Figure 3.37. The average error between the experimental and predicted rates was found to be 1.16 %. The activation energy for model VI was found to be 122.44 kJ/mol based on the Arrhenius plot (Figure 3.36).

**Table 3.3:** Values of kinetic parameters at different temperatures using model VI

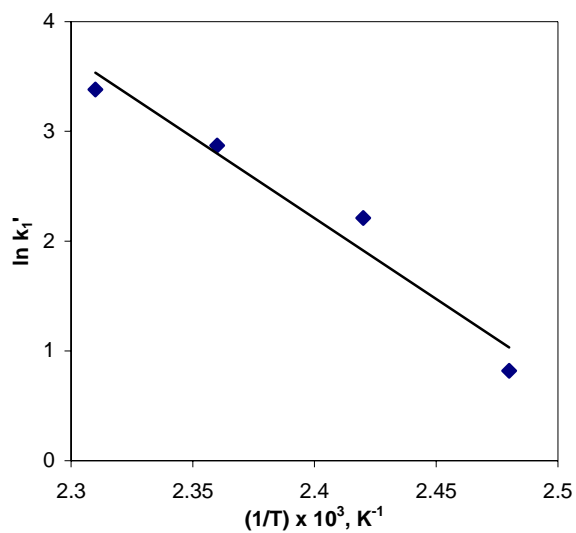
Temp, K	$k_1'$ ( $\text{m}^3/\text{kmol}$ ) <sup>4.5</sup>	$K_{1a}$ ( $\text{m}^3/\text{kmol}$ ) <sup>2</sup>	$K_{11}$ ( $\text{m}^3/\text{kmol}$ )	$K_{1b}$ ( $\text{m}^3/\text{kmol}$ ) <sup>3</sup>	$\Phi_{\min} \times 10^5$
403	2.27	$3.42 \times 10^{-4}$	$4.19 \times 10^{-5}$	2.26	0.32
413	9.12	$2.64 \times 10^{-4}$	$2.30 \times 10^{-5}$	3.07	1.79
423	17.67	$1.93 \times 10^{-4}$	$1.01 \times 10^{-5}$	3.42	6.91
433	29.51	$9.25 \times 10^{-5}$	$9.13 \times 10^{-6}$	3.73	0.99

**Table 3.4:** Values of kinetic parameters at different temperatures using model VII

Temp, K	$k_2'$ ( $\text{m}^3/\text{kmol}$ ) <sup>4.5</sup>	$K_{22}$ ( $\text{m}^3/\text{kmol}$ )	$K_{2a}$ ( $\text{m}^3/\text{kmol}$ ) <sup>2</sup>	$K_{2b}$ ( $\text{m}^3/\text{kmol}$ ) <sup>2</sup>	$\Phi_{\min} \times 10^5$
403	4.25	$3.44 \times 10^{-4}$	$4.19 \times 10^{-5}$	4.96	0.41
413	13.46	$6.86 \times 10^{-4}$	$2.30 \times 10^{-5}$	4.09	3.17
423	21.86	$9.87 \times 10^{-4}$	$1.01 \times 10^{-5}$	3.26	12.67
433	29.81	$1.25 \times 10^{-3}$	$9.13 \times 10^{-6}$	2.35	36.29

**Table 3.5:** Values of kinetic parameters at different temperatures using model VIII

Temp K	$k_3'$ ( $\text{m}^3/\text{kmol}$ ) <sup>4.5</sup>	$K_{35}$ ( $\text{m}^3/\text{kmol}$ )	$K_{3a}$ ( $\text{m}^3/\text{kmol}$ ) <sup>2</sup>	$K_{3b}$ ( $\text{m}^3/\text{kmol}$ ) <sup>2</sup>	$K_{3c}$ ( $\text{m}^3/\text{kmol}$ ) <sup>3</sup>	$\Phi_{\min}$ $\times 10^5$
403	4.25	$7.69 \times 10^{-5}$	4.96	$2.92 \times 10^{-4}$	$5.59 \times 10^{-4}$	0.41
413	13.25	$9.48 \times 10^{-5}$	4.00	$4.72 \times 10^{-4}$	$3.84 \times 10^{-4}$	3.17
423	21.62	$1.25 \times 10^{-4}$	3.19	$5.69 \times 10^{-4}$	$2.18 \times 10^{-4}$	12.72
433	29.82	$3.18 \times 10^{-4}$	2.35	$7.21 \times 10^{-4}$	$1.15 \times 10^{-4}$	30.26

**Figure 3.36:** Temperature dependence of the rate constant ( $k_1'$ ) for mechanistic model VI

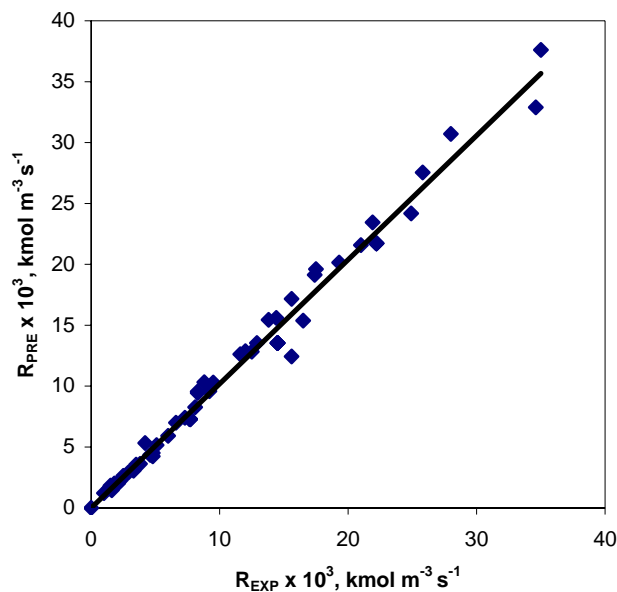


**Figure 3.37:** Comparison of the experimental rates and the rates predicted using model VI

If TBAB is not considered for proposing the empirical model, it is evident that the empirical model II and the mechanistic model VI are similar.

### 3.5. Conclusions

The kinetics of vinylation of 4'-bromoacetophenone with n-butylacrylate with palladacycle catalyst precursor **1** was studied in NMP as solvent, NaOAc as base, and in presence of TBAB promoter. The effect of different parameters *viz* concentration of the substrates, catalyst, base, and TBAB on the rate of the reaction was investigated in a temperature range of 403-433 K. The rate data were fitted to various empirical and mechanistic rate models. Amongst the empirical models the following model was found to predict the rates in good agreement with experimental values.

$$R = \frac{k[A][B][C][D][Q]^{0.5}}{(1 + K_B[B]^2) (1 + K_C[C]) (1 + K_D[D]^2)} \quad \text{Model II}$$

The best prediction of the rates was obtained with the following mechanistic model.

$$R = \frac{k_1' [A][B][C][Q]^{0.5}}{K_{1a} [B][C] + K_{11}[B] + 1 + K_{1b} [B]^2[C]} \quad \text{Model VI}$$

Based on the mechanistic model, it can be concluded that the oxidative addition of 4'-bromoacetophenone to the palladacycle catalyst precursor **1** is the rate determining step under the reaction conditions employed.

### 3.6. References

1. Zhao, F. G.; Bhanage, B. M.; Shirai, M.; Arai, M. *Reaction Kinetics Development Catal. Procedures* . **1999**, 427
2. Zhao, F.; Bhanage, B. M.; Shirai, M.; Arai, M. *J. Mol. Catal. A: Chem.* **1999**, 142, 383
3. Van Strijdonck, G. P. F.; Boele, M. D. K.; Kamer, P. C. J.; de Vries, J. G.; van Leeuwen, P. W. N. M. *Eur. J. Inorg. Chem.* **1999**, 1073
4. Rosner T.; Bars J. L.; Pfaltz A.; Blackmond D. G. *J. Am. Chem. Soc.* **2001**, 123, 1848
5. Consorti, C. S.; Flores, F. R.; Dupont, J. *J. Am. Chem. Soc.* **2005**, 127, 12054
6. Zhao F. G.; Bhanage B. M.; Shirai M.; Arai M. *Stud. Surf. Sci. Catal.* **1999**, 122, 427
7. Blaser, H. U.; Indolese, A.; Naud, F.; Nettekoven, U.; Schnyder, A. *Adv. Synth. Catal.* **2004**, 346, 1583
8. Gabre, D. *Ullmann's Encyclopaedia of Industrial Chemistry* **1992**, 7, 99
9. Dounay, A. B.; Overman, L. E. *Chem. Rev.* **2003**, 103, 2945
10. Stambuli, J. P.; Kuwano, R.; Hartwig, J. F. *Angew. Chem. Int. Ed.* **2002**, 41, 4746
11. Phan, N. T. S.; Sluys, M. V. D.; Jones, C. W. *Adv. Synth. Catal.* **2006**, 348, 609
12. Beletskaya, I. P.; Cheprakov, A. V. *Chem. Rev.* **2000**, 100, 3009
13. Fauvarque, J. F.; Pfluger, F. J. *Organomet. Chem.* **1981**, 208, 419
14. Crisp, G. T. *Chem. Soc. Rev.* **1998**, 27, 427
15. Amatore, C.; Carre, E.; Jutand, A.; Medjour, Y. *Organometallics* **2002**, 21, 4540
16. Jeffery, T. *J. Chem. Soc., Chem. Commun.* **1984**, 19, 1287
17. Jeffery, T. *Tetrahedron Lett.* **1985**, 26, 2667
18. Jeffery, T.; Galland, J. C. *Tetrahedron Lett.* **1994**, 35, 4103
19. Jeffery, T. *Tetrahedron Lett.* **1994**, 35, 3051
20. Amatore, C.; Jutand, A. *J. Organomet. Chem.* **1999**, 576, 254
21. Herrmann, W. A.; Brossmer, C.; Ofele, K.; Reisinger, C. P.; Priermeier, T.; Beller, M.; Fischer, H. *Angew. Chem. Int. Ed. Engl.* **1995**, 34, 1844
22. Marquardt, D. W. *J. Soc. Ind. Appl. Math.* **1963**, 11, 431



*Chapter 4:*

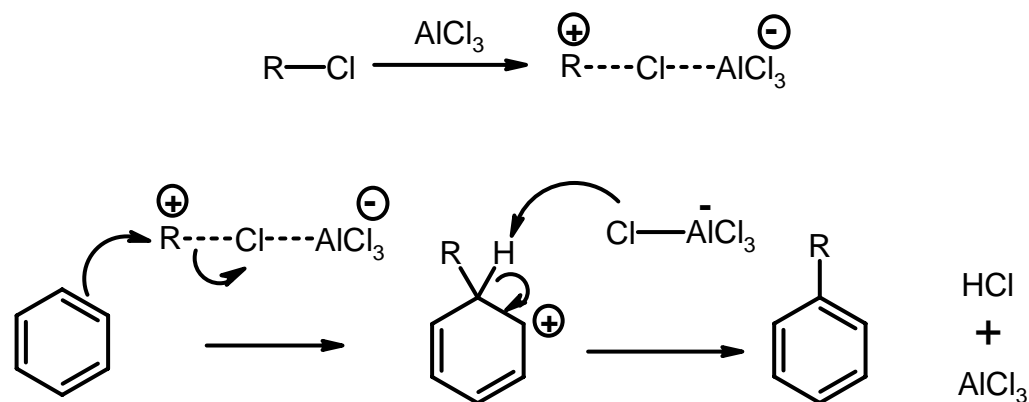
*Studies on Lewis Acid Promoted*

*Heck Reactions*

#### 4.1. Introduction

The role of promoters and co-catalysts in homogeneous catalysis to tailor the performance of catalysts is well known. These could be either ligands or simple molecules which can influence the catalyst/catalytic cycle, making it more efficient. For instance,  $\text{CH}_3\text{I}$  has been efficiently applied as a promoter for Monsanto/BP process for carbonylation of alcohols<sup>1</sup>. Ligands like  $\text{PPh}_3$  have also been used to obtain efficient processes like the LP oxo process for the hydroformylation of olefins<sup>2</sup>. The role of promoters in the Heck reactions has so far not been investigated in enough detail. In the mid 1980's Jeffery reported that the addition of quaternary ammonium salts increased the rates and overall yields of the Heck reaction<sup>3</sup>. These quaternary ammonium salts need to be employed in large quantities (up to 20 mol% of the substrate) as the primary mode for rate enhancement is via both phase transfer action (solubilizing the inorganic base in the solvent) and by stabilization of the palladium<sup>4</sup>. Under these conditions Jeffery was able to carry out the coupling reactions of iodoarenes with acrylates at room temperature. In another report by Bozell et al<sup>5</sup> nickel co-catalysts jointly with alkali metals have been used to activate the relatively inert chloroarenes using palladium catalysts. The enhancement is due to the conversion of small quantities of the chloroarene to the iodo derivative, which is more active. Apart from these there have not been any reports of substances that can act as promoters to enhance the reaction rates.

The role of Lewis acids to assist the polarization of the alkane-halogen bond in Friedel Crafts chemistry is well known (Scheme 4.1)<sup>6</sup>. The carbon atom of alkyl halides is electrophilic but not sufficiently so, as to affect the substitution of an aromatic species. To carry out the substitution of an aromatic species under Friedel Crafts reaction conditions the presence of a Lewis acid is required.



Scheme 1

The reaction of alkyl halides with Lewis acids has been demonstrated by the exchange of radioactive bromine from  $\text{AlBr}_3^*$  into  $\text{C}_2\text{H}_5\text{Br}$  on mixing and isolation. Isolation of solid 1:1 complexes like  $\text{CH}_3\text{Br}^-\text{AlBr}_3^+$  has also been achieved at low temperatures<sup>7</sup>. In some cases, where the alkyl group is capable of forming a stable carbocation (e.g. with  $\text{Me}_3\text{C}-\text{Br}$ ), it is probable that the attacking electrophile is then the actual carbocation,  $[\text{Me}_3\text{C}]^+$ , as part of an ion pair  $[\text{Me}_3\text{C}]^+[\text{AlBr}_4]^-$ . But in most of the cases the attacking electrophile is a polarized complex  $\text{R}^{\delta+}-\text{ClFeCl}_3^{\delta-}$ . The degree of polarization depends on the alkyl group R and the Lewis acid employed. The order of effectiveness of Lewis acids is  $\text{AlCl}_3 > \text{FeCl}_3 > \text{BF}_3 > \text{TiCl}_3 > \text{ZnCl}_2 > \text{SnCl}_4$  for Friedel Crafts alkylation reactions<sup>6</sup>.

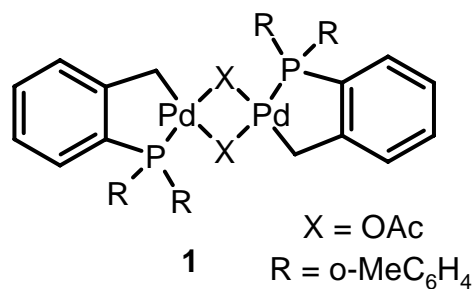
Since the Heck reaction also involves similar activation of the aryl – halogen bond, the presence of Lewis acids is expected to influence the rate of reaction.  $\text{AlCl}_3$  and  $\text{ZnCl}_2$  have been used previously in Heck reactions, at the concentrations comparable to that of the substrates, but with no significant improvement in the rate of reaction<sup>8</sup>. A detailed investigation was carried out to study the effect of Lewis acids on the Heck reactions. For this study, the following Lewis acids were selected:  $\text{AlCl}_3$ ,  $\text{FeCl}_3$ ,  $\text{TiCl}_4$ ,  $\text{ZnCl}_2$ ,  $\text{SnCl}_4$ ,  $\text{SnCl}_2$ , and  $\text{LiCl}$ . The influence of different Lewis acids on the rates of the Heck reactions at different concentrations has been investigated. The effect of Lewis acids has been studied with different catalyst precursors, haloarenes, olefins, and bases. The influence of Lewis acids on the rate of reaction has been explained based on the activation

energy. A probable mechanism, taking into account all the experimental observations, has also been proposed.

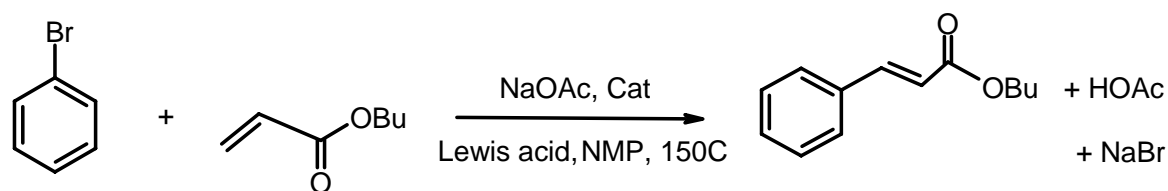
## 4.2. Experimental

### *General procedure for Heck reaction*

In a typical experiment 10 mmol bromobenzene, 15 mmol n-butyl acrylate, 15 mmol sodium acetate,  $2 \times 10^{-3}$  mmol palladium complex catalyst **1** (shown in Scheme 4.2), and  $1.4 \times 10^{-3}$  mmol  $\text{FeCl}_3$  were taken in a 50ml 2-necked glass reactor equipped with a condenser, magnetic stirrer, and a septum to facilitate the withdrawal of the samples. This was then immersed in an oil bath pre-heated to the required temperature. On attainment of the temperature (2 minutes) the reaction was started by switching the stirrer on. Samples were withdrawn at regular time intervals and analyzed by GC for conversion of bromobenzene and cinnamate formation (Scheme 4.3). The reactions were carried out for 2 hours. The initial turnover frequency (TOF) was calculated based on the formation of the product in the first 20 minutes of reaction, for comparison between the rates of different reactions.



**Scheme 4.2**



**Scheme 4.3**

### 4.3. Effect of different Lewis acids on the rate of reaction

In order to demonstrate the promoting effect of Lewis acids, the experiments on vinylation of bromobenzene with n-butyl acrylate were conducted in the presence of sodium acetate as a base and palladium complex **1** as the catalyst precursor. In the preliminary experiments, in order to test the effect of different Lewis acids, a catalytic amount of a particular Lewis acid (1:1 ratio with palladium) was added to the reaction mixture. It was found that apart from AlCl<sub>3</sub> all the Lewis acids screened, were able to enhance the rate of reaction to varying extents (Table 4.1).

**Table 4.1:** Effect of Lewis acids on the rate of Heck reactions

No.	Lewis Acid	Initial TOF (min <sup>-1</sup> )	% Enhancement
1	None	32	-
2	AlCl <sub>3</sub>	32	0
3	LiCl	44	37.5
4	TiCl <sub>4</sub>	46	43.7
5	SnCl <sub>4</sub>	48	50
6	SnCl <sub>2</sub>	49	53.1
7	ZnCl <sub>2</sub>	51	59.3
8	FeCl <sub>3</sub>	96	200

**Reaction conditions:** Bromobenzene: 0.399 kmol/m<sup>3</sup>, n-butyl acrylate: 0.602 kmol/m<sup>3</sup>, NaOAc: 0.6 kmol/m<sup>3</sup>, Catalyst precursor **1**: 8.51 x 10<sup>-5</sup> kmol/m<sup>3</sup>, Solvent: NMP, Total Volume: 2.5 x 10<sup>-5</sup> m<sup>3</sup>, Temp: 423 K, Lewis acid: 8.51 x 10<sup>-5</sup> kmol/m<sup>3</sup>

With AlCl<sub>3</sub> no noticeable enhancement in the reaction rate was observed. Further to this the effect of concentration of Lewis acid was studied in order to arrive at the optimum concentration of Lewis acid required to achieve the highest activity. The results of these optimization studies are presented below..

### 4.3.1. Effect of LiCl addition on the rate of reaction

The concentration of LiCl was varied between 0 to  $1.7 \times 10^{-4} \text{ kmol/m}^3$  (i.e. LiCl: Pd ratio of 0 to 2). The results are presented in Figure 4.1.

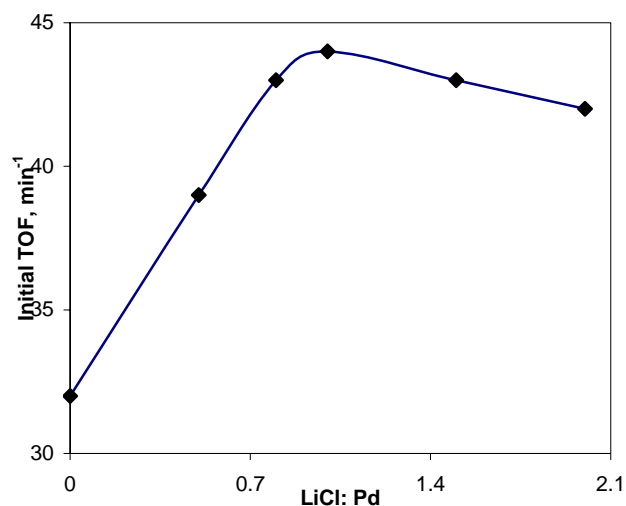


**Figure 4.1:** Influence of LiCl on the activity in Heck reaction

**Reaction conditions:** Bromobenzene:  $0.399 \text{ kmol/m}^3$ , *n*-butyl acrylate:  $0.602 \text{ kmol/m}^3$ , NaOAc:  $0.6 \text{ kmol/m}^3$ , Catalyst precursor 1:  $8.51 \times 10^{-5} \text{ kmol/m}^3$ , Solvent: NMP, Total Volume:  $2.5 \times 10^{-5} \text{ m}^3$ , Temp: 423 K, LiCl: (0 to  $1.7 \times 10^{-4} \text{ kmol/m}^3$ )

It was observed that addition of even a small amount of LiCl ( $1 \times 10^{-3} \text{ mmol}$ , LiCl: Pd ratio of 0.5) was able to increase the rate of the reaction by 20 %. When the amount of LiCl added was increased to  $1.7 \times 10^{-3} \text{ mmol}$  (i.e. 80 % of the palladium), a further enhancement in the reaction rate was observed. At this concentration of LiCl, enhancement in the rate was around 40%. With further increase in LiCl the rate passed through a maximum at a LiCl: Pd ratio of 0.8:1, and then fell slightly. The rate was however still higher than the unpromoted reaction even at a LiCl: Pd ratio of 2:1.

### 4.3.2. Effect of TiCl<sub>4</sub> addition on the rate of reaction

The effect of TiCl<sub>4</sub> concentration variation on the reaction rates was investigated. The results obtained are presented in Figure 4.2.

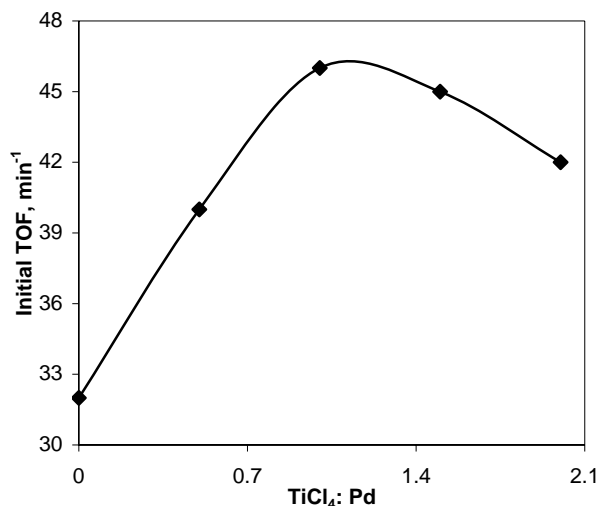


**Figure 4.2:** Influence of TiCl<sub>4</sub> on the activity of Heck reaction

**Reaction conditions:** Bromobenzene:  $0.399 \text{ kmol/m}^3$ , *n*-butyl acrylate:  $0.602 \text{ kmol/m}^3$ , NaOAc:  $0.6 \text{ kmol/m}^3$ , Catalyst precursor **1**:  $8.51 \times 10^{-5} \text{ kmol/m}^3$ , Solvent: NMP, Total Volume:  $2.5 \times 10^{-5} \text{ m}^3$ , Temp: 423 K, TiCl<sub>4</sub>: (0 to  $1.7 \times 10^{-4} \text{ kmol/m}^3$ )

As in the case of LiCl, it was observed that the enhancement in the reaction rate took place even on addition of small amount of TiCl<sub>4</sub>. The concentration of TiCl<sub>4</sub> was varied between 0 to  $1.7 \times 10^{-4} \text{ kmol/m}^3$  (TiCl<sub>4</sub>: Pd range of 0 to 2). The maximum enhancement in the rate of reaction observed was 44% of the standard reaction on addition of  $8.51 \times 10^{-5} \text{ kmol/m}^3$  of TiCl<sub>4</sub>, which was a molar ratio of 1:1 with respect to palladium. When the amount of TiCl<sub>4</sub> was further increased, a drop in the rates was seen. But even at the TiCl<sub>4</sub> to palladium ratio of 2:1 the rate of the reaction was higher than that of the reaction without any Lewis acid.

#### 4.3.3. Effect of ZnCl<sub>2</sub> addition on the rate of reaction

For this study the concentration of ZnCl<sub>2</sub> was varied between 0 to  $1.7 \times 10^{-4} \text{ kmol/m}^3$  (ZnCl<sub>2</sub>: Pd range of 0 to 2). The results obtained for this study are presented in Figure 4.3.

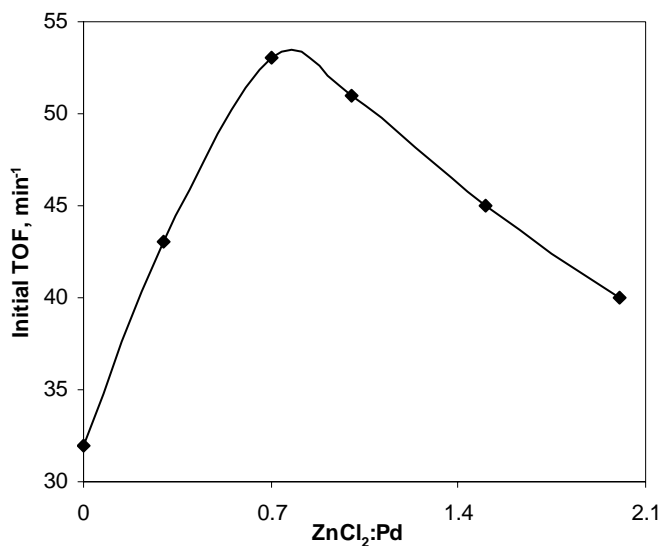


**Figure 4.3:** Influence of ZnCl<sub>2</sub> on the activity of Heck reaction

**Reaction conditions:** Bromobenzene:  $0.399 \text{ kmol/m}^3$ , *n*-butyl acrylate:  $0.602 \text{ kmol/m}^3$ , NaOAc:  $0.6 \text{ kmol/m}^3$ , Catalyst precursor **1**:  $8.51 \times 10^{-5} \text{ kmol/m}^3$ , Solvent: NMP, Total Volume:  $2.5 \times 10^{-5} \text{ m}^3$ , Temp: 423 K, ZnCl<sub>2</sub>: (0 to  $1.7 \times 10^{-4} \text{ kmol/m}^3$ )

The maximum enhancement in the rate of reaction of 65% was obtained at the ZnCl<sub>2</sub> to palladium ratio of 0.75:1. The rates initially increased and then decreased with the increase in ZnCl<sub>2</sub> concentration. As seen for LiCl and TiCl<sub>4</sub> the rate of reaction was always higher than that of the standard reaction on addition of ZnCl<sub>2</sub>. In case of ZnCl<sub>2</sub> as the Lewis acid additive, the maximum enhancement in the reaction rate was observed for the ZnCl<sub>2</sub>: Pd molar ratio of 0.75:1.

#### 4.3.4. Effect of SnCl<sub>2</sub> addition on the rate of reaction

For studying the influence of SnCl<sub>2</sub> on the reaction rate the concentration of SnCl<sub>2</sub> was varied between 0 to  $1.7 \times 10^{-4} \text{ kmol/m}^3$  (SnCl<sub>2</sub>: Pd range of 0 to 2). The results obtained are shown in Figure 4.4.



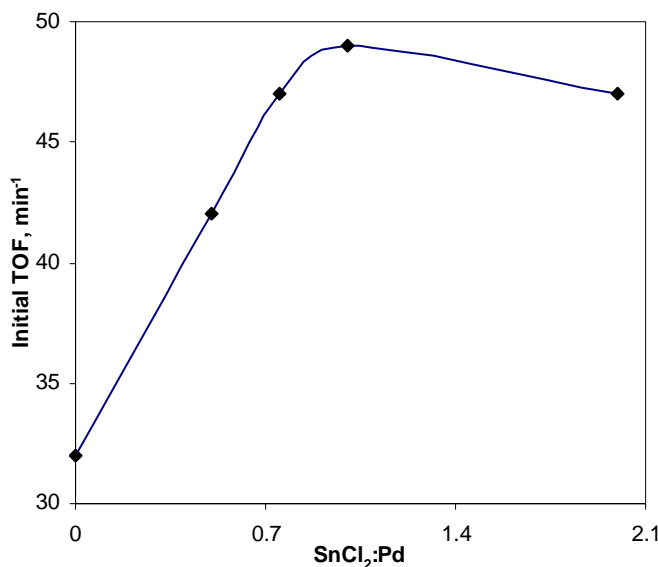


**Figure 4.4:** Influence of SnCl<sub>2</sub> on the activity of Heck reaction

**Reaction conditions:** Bromobenzene:  $0.399 \text{ kmol/m}^3$ , *n*-butyl acrylate:  $0.602 \text{ kmol/m}^3$ , NaOAc:  $0.6 \text{ kmol/m}^3$ , Catalyst precursor **1**:  $8.51 \times 10^{-5} \text{ kmol/m}^3$ , Solvent: NMP, Total Volume:  $2.5 \times 10^{-5} \text{ m}^3$ , Temp: 423 K, SnCl<sub>2</sub>: (0 to  $1.7 \times 10^{-4} \text{ kmol/m}^3$ )

Addition of  $2.1 \times 10^{-3} \text{ mmol}$  of SnCl<sub>2</sub> to the reaction mixture led to the maximum rate enhancement of 53% which corresponds to the SnCl<sub>2</sub> to palladium ratio of 1:1. After reaching this value the rate dropped to 47% above that of standard reaction when the SnCl<sub>2</sub> concentration was increased to  $4.2 \times 10^{-3} \text{ mmol}$  (SnCl<sub>2</sub>: Pd molar ratio of 2:1). At all the concentrations of SnCl<sub>2</sub> a rate enhancement over the standard reaction was observed.

#### 4.3.5. Effect of SnCl<sub>4</sub> addition on the rate of reaction

For the study of effect of SnCl<sub>4</sub> on the reaction rate, the concentration of SnCl<sub>4</sub> was varied between 0 to  $1.7 \times 10^{-4} \text{ kmol/m}^3$ , corresponding to SnCl<sub>4</sub>: Pd molar ratio in the range of 0 to 2. The results are presented in Figure 4.5.

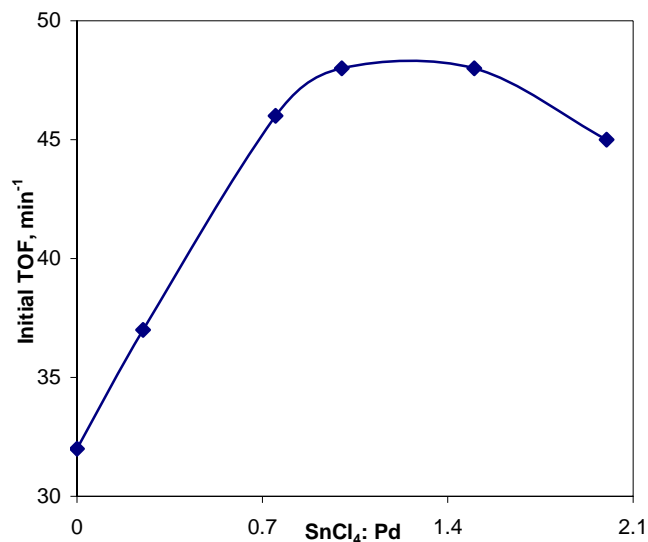


**Figure 4.5:** Influence of SnCl<sub>4</sub> on the activity of Heck reaction

**Reaction conditions:** Bromobenzene:  $0.399 \text{ kmol/m}^3$ , *n*-butyl acrylate:  $0.602 \text{ kmol/m}^3$ , NaOAc:  $0.6 \text{ kmol/m}^3$ , Catalyst precursor **1**:  $8.51 \times 10^{-5} \text{ kmol/m}^3$ , Solvent: NMP, Total Volume:  $2.5 \times 10^{-5} \text{ m}^3$ , Temp: 423 K, SnCl<sub>4</sub>: (0 to  $1.7 \times 10^{-4} \text{ kmol/m}^3$ )

The maximum rate enhancement of 50 % was observed in the SnCl<sub>4</sub> concentration range of  $8.51 \times 10^{-5} \text{ kmol/m}^3$  to  $1.7 \times 10^{-4} \text{ kmol/m}^3$  (SnCl<sub>4</sub> to Pd ratio in the range of 1 to 1.2). After reaching a maximum the reaction rates then fell with further increase in the SnCl<sub>4</sub> concentration. At all the concentration of SnCl<sub>4</sub> the rate of reaction was higher than that of the standard reaction having no Lewis acid.

#### 4.3.6. Effect of FeCl<sub>3</sub> addition on the rate of reaction

The effect of FeCl<sub>3</sub> addition to the reaction mixture was investigated by varying the FeCl<sub>3</sub> concentration between 0 to  $1.7 \times 10^{-4} \text{ kmol/m}^3$  (FeCl<sub>3</sub>: Pd ratio range of 0 to 2). As seen in Figure 4.6 a maximum in the rate is observed.

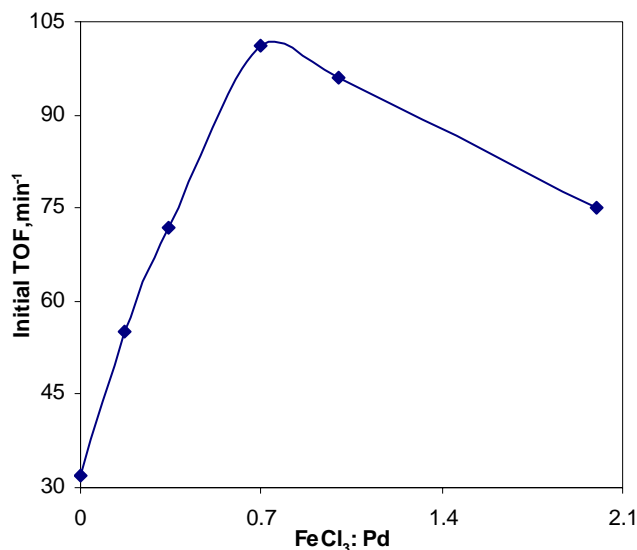


**Figure 4.6:** Influence of FeCl<sub>3</sub> on the activity of Heck reaction

**Reaction conditions:** Bromobenzene:  $0.399 \text{ kmol/m}^3$ , *n*-butyl acrylate:  $0.602 \text{ kmol/m}^3$ , NaOAc:  $0.6 \text{ kmol/m}^3$ , Catalyst precursor **1**:  $8.51 \times 10^{-5} \text{ kmol/m}^3$ , Solvent: NMP, Total Volume:  $2.5 \times 10^{-5} \text{ m}^3$ , Temp: 423 K, FeCl<sub>3</sub>: (0 to  $1.7 \times 10^{-4} \text{ kmol/m}^3$ )

At FeCl<sub>3</sub> to Pd ratio of 0.7:1 the rate enhancement was 215% over the unpromoted reaction. The influence of FeCl<sub>3</sub> addition was much stronger than that of the other Lewis acids screened. On addition of just  $1.48 \times 10^{-5} \text{ kmol/m}^3$  of FeCl<sub>3</sub> (FeCl<sub>3</sub>: Pd ratio of 0.17: 1), the rate enhancement achieved was 87 % over that of the standard reaction. This was much higher than the best enhancements obtained from any of the earlier studied Lewis acids in this work. After achieving the maximum rate enhancement, the rates fell with increase in the FeCl<sub>3</sub> concentration as observed with all Lewis acids.

#### 4.3.7. Effect of AlCl<sub>3</sub> addition on the rate of reaction

When the Lewis acid, AlCl<sub>3</sub>, was added to the reaction mixture, there was no enhancement in the reaction rate. The rate of the reaction remained almost same as that of the standard reaction.

### 4.3.8. Comparison of the effect of different Lewis acids on the reaction rate

After screening the Lewis acids and studying the concentration variation of all the Lewis acids, a comparison of the effect of Lewis acids on the reaction rate was carried out at the optimum concentration of each Lewis acid. A comparison of the effect of Lewis acids on the rates of reaction is shown in Figure 4.7.

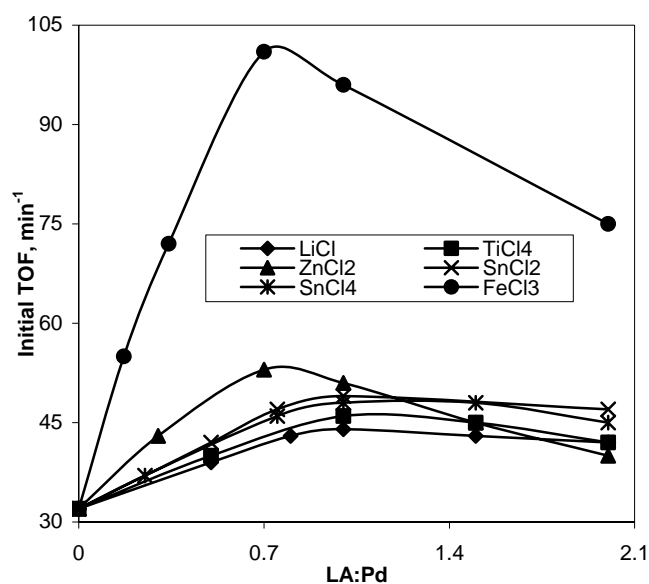


**Figure 4.7:** Influence of different Lewis acids and their concentration on the activity of Heck reaction

**Reaction conditions:** Bromobenzene:  $0.399 \text{ kmol/m}^3$ , *n*-butyl acrylate:  $0.602 \text{ kmol/m}^3$ , NaOAc:  $0.6 \text{ kmol/m}^3$ , Catalyst precursor 1:  $8.51 \times 10^{-5} \text{ kmol/m}^3$ , Solvent: NMP, Total Volume:  $2.5 \times 10^{-5} \text{ m}^3$ , Temp: 423 K, Lewis acids: LiCl, TiCl<sub>4</sub>, SnCl<sub>2</sub>, SnCl<sub>4</sub>, ZnCl<sub>2</sub>, FeCl<sub>3</sub>

The comparison of the initial TOFs obtained at the optimum concentration of each Lewis acid is shown in Figure 4.8.

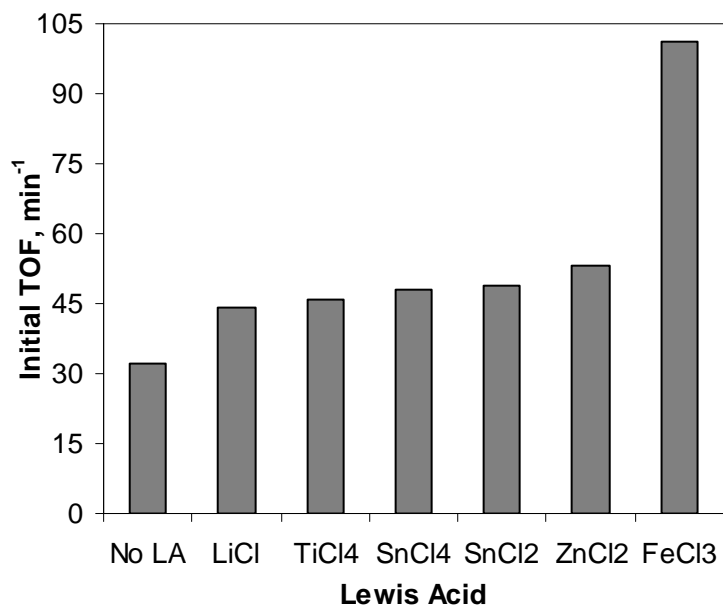


**Figure 4.8:** Effect of different Lewis acids on the rate of the Heck reaction

**Reaction conditions:** Bromobenzene:  $0.399 \text{ kmol/m}^3$ , *n*-butyl acrylate:  $0.602 \text{ kmol/m}^3$ , NaOAc:  $0.6 \text{ kmol/m}^3$ , Catalyst precursor **1**:  $8.51 \times 10^{-5} \text{ kmol/m}^3$ , Solvent: NMP, Total Volume:  $2.5 \times 10^{-5} \text{ m}^3$ , Temp: 423 K, Lewis acid: (LiCl:  $6.8 \times 10^{-5} \text{ kmol/m}^3$ , TiCl<sub>4</sub>:  $8.51 \times 10^{-5} \text{ kmol/m}^3$ , SnCl<sub>2</sub>:  $8.51 \times 10^{-5} \text{ kmol/m}^3$ , SnCl<sub>4</sub>:  $8.5 \times 10^{-5} \text{ kmol/m}^3$ , ZnCl<sub>2</sub>:  $6.5 \times 10^{-5} \text{ kmol/m}^3$ , FeCl<sub>3</sub>:  $5.93 \times 10^{-5} \text{ kmol/m}^3$ )

The formation of product as a function of time at the optimum concentration of each Lewis acid is presented in Figure 4.9. This clearly shows that high initial rates were obtained with FeCl<sub>3</sub>.

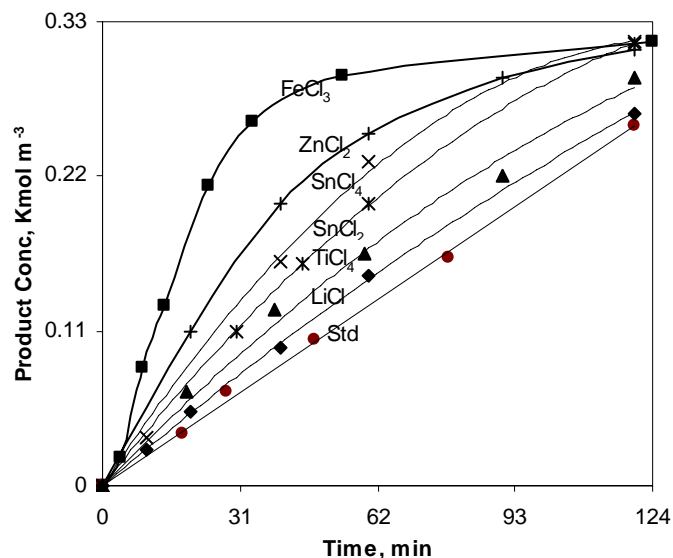


**Figure 4.9:** Influence of different Lewis acids on the activity of Heck reaction

**Reaction conditions:** Bromobenzene:  $0.399 \text{ kmol/m}^3$ , *n*-butyl acrylate:  $0.602 \text{ kmol/m}^3$ , NaOAc:  $0.6 \text{ kmol/m}^3$ , Catalyst precursor 1:  $8.51 \times 10^{-5} \text{ kmol/m}^3$ , Solvent: NMP, Total Volume:  $2.5 \times 10^{-5} \text{ m}^3$ , Temp: 423 K, Lewis acid: (LiCl:  $6.8 \times 10^{-5} \text{ kmol/m}^3$ , TiCl<sub>4</sub>:  $8.51 \times 10^{-5} \text{ kmol/m}^3$ , SnCl<sub>2</sub>:  $8.51 \times 10^{-5} \text{ kmol/m}^3$ , SnCl<sub>4</sub>:  $8.5 \times 10^{-5} \text{ kmol/m}^3$ , ZnCl<sub>2</sub>:  $6.5 \times 10^{-5} \text{ kmol/m}^3$ , FeCl<sub>3</sub>:  $5.93 \times 10^{-5} \text{ kmol/m}^3$ )

From this figure it is evident that, while the promoting effect on catalytic activity was observed for all the promoters used, except AlCl<sub>3</sub>, FeCl<sub>3</sub> was by far the best in terms of enhancing the reaction rates. The trend observed regarding the enhancement in activity obtained with different Lewis acids was similar to their order of effectiveness for Friedel Crafts alkylation reactions<sup>4,5</sup>. This could imply that the role of Lewis acids is similar to the Friedel Crafts chemistry which is to assist in the polarization of the arene-halogen bond. Lewis acids like FeCl<sub>3</sub> and ZnCl<sub>2</sub> were able to polarize the C-X bond better and hence led to greater rate enhancements compared to Lewis acids like LiCl and TiCl<sub>4</sub>. The only exception turned out to be AlCl<sub>3</sub>, which did not give any rate enhancement in spite of being the most active Lewis acid for Friedel Crafts alkylation reactions.

The moisture content of the reaction mixture was generally in the range of 700-1000 ppm, which was high enough for hydrolysing AlCl<sub>3</sub>. Hence to understand whether

moisture plays a role in enhancing the activity, it was decided to carry out the reactions under anhydrous conditions (<50 ppm water). This would also answer whether the inactivity of  $\text{AlCl}_3$  was due to  $\text{AlCl}_3$  being converted to  $\text{Al}(\text{OH})_3$  by the moisture present in the reaction mixture. For this purpose, NMP solvent, bromobenzene, and n-butyl acrylate were dried using the standard procedures<sup>9</sup> just prior to the reaction and used immediately. Under these anhydrous conditions the reaction in presence of  $\text{FeCl}_3$  gave the same results as the anhydrous Heck reaction in absence of any Lewis acid under similar conditions. Use of  $\text{AlCl}_3$  as the Lewis acid under these conditions also did not lead to any enhancement in the reaction rate. These experiments show that the presence of moisture was necessary for the rate enhancements to be observed with Lewis acid promoters. Thus the actual species responsible for the rate enhancement might not be the Lewis acid as such, but a hydrated Lewis acid species like  $\text{FeCl}_3 \cdot x\text{H}_2\text{O}$ . This type of hydrated species is not possible with  $\text{AlCl}_3$ .  $\text{AlCl}_3$  does not form a hydrated species in presence of moisture, but instead reacts with water to form  $\text{Al}(\text{OH})_3$ , and hence no rate enhancement is observed. Even in the Friedel Crafts chemistry,  $\text{AlCl}_3$  is ineffective in the presence of water<sup>10</sup>.

A set of experiments were carried out with increasing amount of water added to the reaction mixture in order to study the influence of water concentration. The results are presented in Figure 4.10a. When water was added to the anhydrous reaction mixture, the reaction rate increased. The increase was more dramatic for the reactions carried out in presence of  $\text{FeCl}_3$ . At 500 ppm water, the rate of the reaction in presence of  $\text{FeCl}_3$  was twice that of the rate in absence of  $\text{FeCl}_3$ . The maximum enhancement of three times was obtained in presence of 1000 ppm water. At the water content higher than this, though the reaction rates increased, the rate enhancement observed on addition of  $\text{FeCl}_3$  more or less remained constant. From these experiments it was concluded that the presence of 1000 ppm moisture was necessary to obtain the optimum rate enhancement on addition of  $\text{FeCl}_3$ .

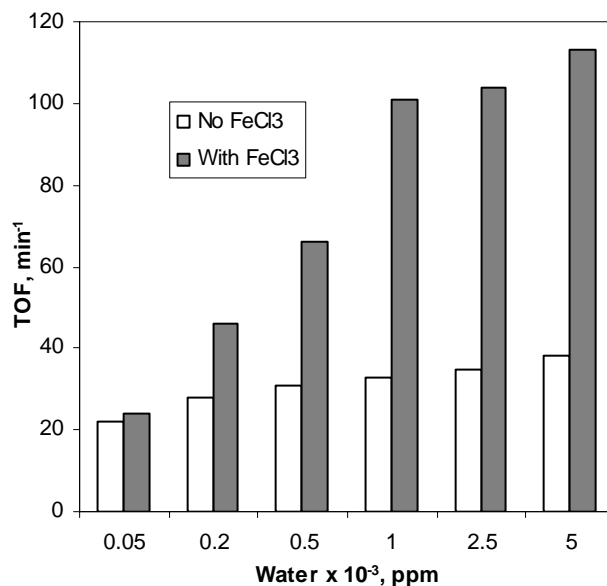


**Figure 4.10a:** Effect of FeCl<sub>3</sub> on the reaction rate in presence of water

**Reaction conditions:** Bromobenzene:  $0.399 \text{ kmol/m}^3$ , *n*-butyl acrylate:  $0.602 \text{ kmol/m}^3$ , NaOAc:  $0.6 \text{ kmol/m}^3$ , Catalyst precursor 1:  $8.51 \times 10^{-5} \text{ kmol/m}^3$ , Solvent: NMP, Total Volume:  $2.5 \times 10^{-5} \text{ m}^3$ , Temp: 423 K, FeCl<sub>3</sub>:  $5.93 \times 10^{-5} \text{ kmol/m}^3$  (FeCl<sub>3</sub>: Pd ratio of 0.7:1), Water

It has already been mentioned that the presence of hydrated FeCl<sub>3</sub> is required to promote the reaction. The maximum increase in the reaction rate on addition of FeCl<sub>3</sub> is observed when the amount of water reaches 1000 ppm, and any further increase in the amount of water leads to only a marginal rate enhancement commensurate with that of unpromoted reaction (Figure 4.10b). At 1000 ppm water the optimum concentration of hydrated FeCl<sub>3</sub> in NMP solvent is probably achieved and any further increase in water beyond 1000 ppm does not cause any major rate enhancement.



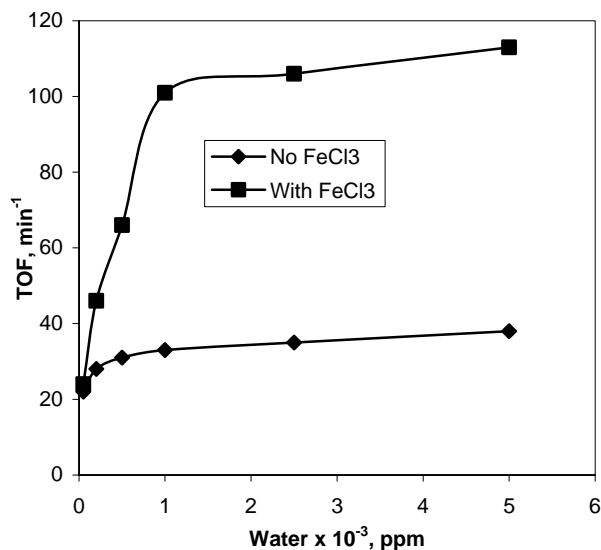


**Figure 4.10b:** Effect of FeCl<sub>3</sub> on the reaction rate in presence of water

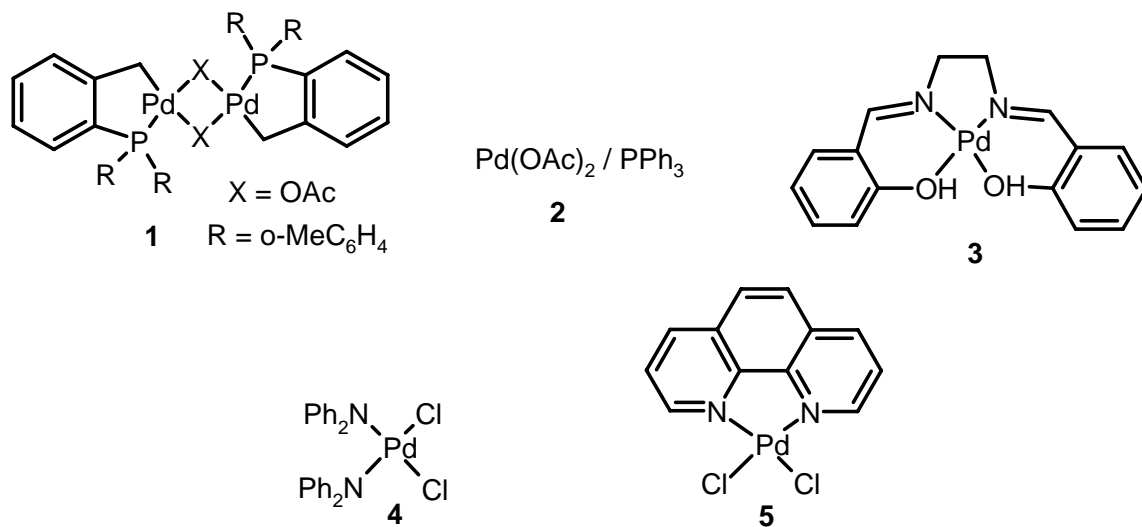
**Reaction conditions:** Bromobenzene:  $0.399 \text{ kmol/m}^3$ , *n*-butyl acrylate:  $0.602 \text{ kmol/m}^3$ , NaOAc:  $0.6 \text{ kmol/m}^3$ , Catalyst precursor **1**:  $8.51 \times 10^{-5} \text{ kmol/m}^3$ , Solvent: NMP, Total Volume:  $2.5 \times 10^{-5} \text{ m}^3$ , Temp: 423 K, FeCl<sub>3</sub>:  $5.93 \times 10^{-5} \text{ kmol/m}^3$  (FeCl<sub>3</sub>: Pd ratio of 0.7:1), Water

#### 4.4. Influence of FeCl<sub>3</sub> on the rate of reaction

To further validate the experimental results, FeCl<sub>3</sub> was used as a promoter for Heck reaction under different conditions.

##### 4.4.1. Effect of FeCl<sub>3</sub> on the rate of reaction with different palladium catalyst precursors

In order to further investigate the role of FeCl<sub>3</sub> on the reaction rates, a study was carried out wherein, different catalyst precursors were used. Each catalyst precursor represented a different class of palladium catalyst for the Heck reaction. The different catalyst precursors, Pd(OAc)<sub>2</sub>/PPh<sub>3</sub>, phosphapalladacycle, palladium complexes having N-O chelating ligand, palladium complexes with monodentate nitrogen ligands, and with bidentate N-N chelating ligands were tested (Scheme 4.4). The results obtained are presented in Figure 4.11.



Scheme 4.4

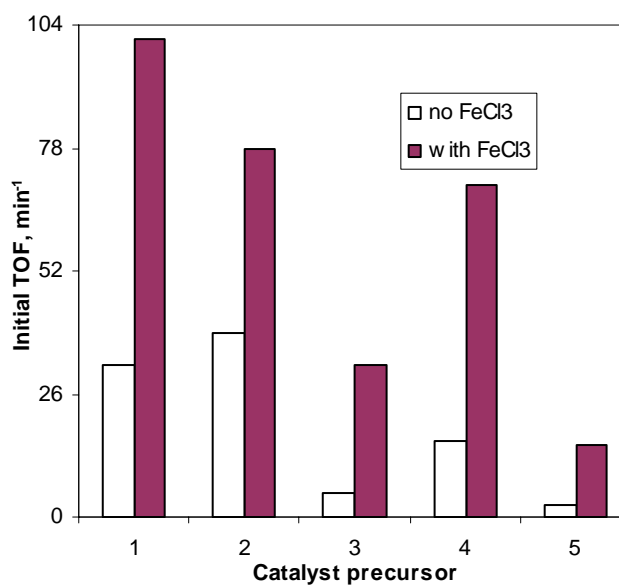


**Figure 4.11:** Influence of  $\text{FeCl}_3$  on the activity of Heck reaction with different catalyst precursors

**Reaction conditions:** Bromobenzene:  $0.399 \text{ kmol/m}^3$ , *n*-butyl acrylate:  $0.602 \text{ kmol/m}^3$ , NaOAc:  $0.6 \text{ kmol/m}^3$ , Catalyst precursor:  $8.51 \times 10^{-5} \text{ kmol/m}^3$ , Solvent: NMP, Total Volume:  $2.5 \times 10^{-5} \text{ m}^3$ , Temp: 423 K,  $\text{FeCl}_3$ :  $5.93 \times 10^{-5} \text{ kmol/m}^3$  ( $\text{FeCl}_3$ : Pd ratio of 0.7:1)

$\text{FeCl}_3$  was found to promote the rate of the reaction irrespective of the palladium catalyst precursor used. In case of  $\text{Pd}(\text{OAc})_2/\text{PPh}_3$  catalyst precursor, a rate enhancement of 100% was observed on addition of  $\text{FeCl}_3$ . The effect was even more pronounced in the case of catalyst precursor **4** [ $\text{PdCl}_2(\text{NPh}_2)_2$ ]. On addition of  $\text{FeCl}_3$  to this catalyst precursor, the initial TOF increased from 16 per min to 70 per min (rate enhancement of 337%). When the effect of  $\text{FeCl}_3$  on the reaction rate was tested for the catalyst precursors with still lower inherent activity for the Heck reaction, the results were even more fascinating. With the catalyst precursor **3** (having N-O chelating ligand) the increase in initial TOF of 5 per min to 32 per min was observed (rate enhancement of 540%). When palladium catalyst precursor **5** [ $\text{PdCl}_2(\text{Phen})$ ] was used the initial TOF increased from 2.5 per min to 15 per min (rate enhancement of 508%). Though these TOFs appear small in comparison with that of palladium phosphine complexes, the ability of  $\text{FeCl}_3$  to enhance the reaction rate of less active systems is worth considering.

These results show that the use of  $\text{FeCl}_3$  was beneficial for all the catalysts screened. Another fact that was evident was that the less efficient the catalyst precursor for Heck reaction, more the rate enhancement obtained by the addition of  $\text{FeCl}_3$ . The efficiency of the Pd catalyst for Heck reaction depends on its ability to oxidatively add the aryl halide. Another factor affecting the efficiency of the catalyst is the ease with which it can facilitate the migratory insertion of the olefin.  $\text{FeCl}_3$  can help in both these accounts. It can polarize the C-X bond thus making it easier for the palladium to cleave it during the oxidative addition step.  $\text{FeCl}_3$  can also remove the electron density from the olefin by complexing with it, thus making it more reactive for the Heck reaction. This ability of  $\text{FeCl}_3$  has been discussed in greater detail in the later part of the chapter.

#### **4.4.2. Effect of $\text{FeCl}_3$ on the rate of reaction at different temperatures**

The role of  $\text{FeCl}_3$  for the vinylation of bromobenzene with n-butyl acrylate using the catalyst precursor **1** was studied at different temperatures. The results obtained are presented in Figure 4.12. At 140°C there was an increase of 235% in the reaction rate over the unpromoted reaction. The increase in the rate was 215% and 159% at 150°C and 160°C respectively. This shows that as the temperature increases, the rate enhancement by  $\text{FeCl}_3$

decreases. This is to be expected because at higher temperatures, higher energy is available for the breaking of C-X bond, and hence the effect of FeCl<sub>3</sub> is less evident. Whereas, at lower temperatures FeCl<sub>3</sub> addition becomes more important as it is able to weaken the C-X bond and make it active towards oxidative addition. Thus, the role of FeCl<sub>3</sub> in increasing the rate of reaction is more evident at lower temperatures.

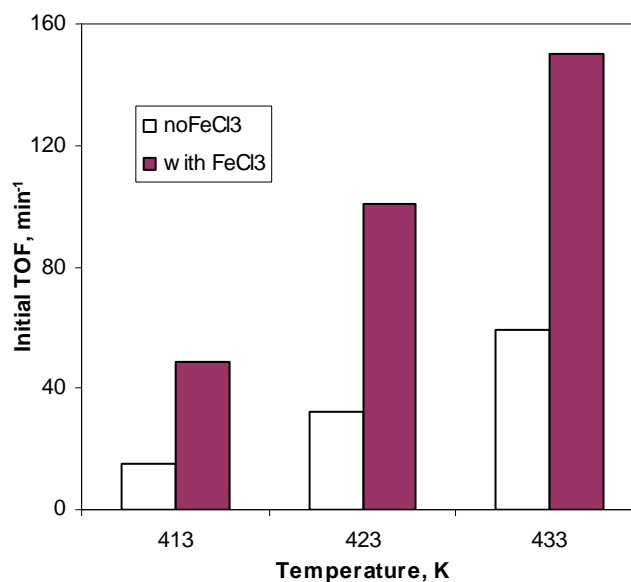


**Figure 4.12:** Influence of FeCl<sub>3</sub> on the activity of Heck reaction at different temperatures  
*Reaction conditions:* Bromobenzene: 0.399 kmol/m<sup>3</sup>, n-butyl acrylate: 0.602 kmol/m<sup>3</sup>, NaOAc: 0.6 kmol/m<sup>3</sup>, Catalyst precursor 1: 8.51 × 10<sup>-5</sup> kmol/m<sup>3</sup>, Solvent: NMP, Total Volume: 2.5 × 10<sup>-5</sup> m<sup>3</sup>, FeCl<sub>3</sub>: 5.93 × 10<sup>-5</sup> kmol/m<sup>3</sup>

Based on the results obtained at different temperatures, activation energies for the reactions with and without FeCl<sub>3</sub> were calculated (Figure 4.13). Since all the parameters at different temperatures are kept constant, ln k will be a function of activity. Hence the relative measure of activation energy can be calculated based on the plot of ln of activity versus the inverse of the temperature. The activation energy without the presence of FeCl<sub>3</sub> was calculated to be 103.61 kJ/mol, whereas, the activation energy for the reactions in presence of FeCl<sub>3</sub> was found to be 85.19 kJ/mol. From this data it is clearly

evident that the Lewis acid increases the rate of the reaction by lowering the activation energy.

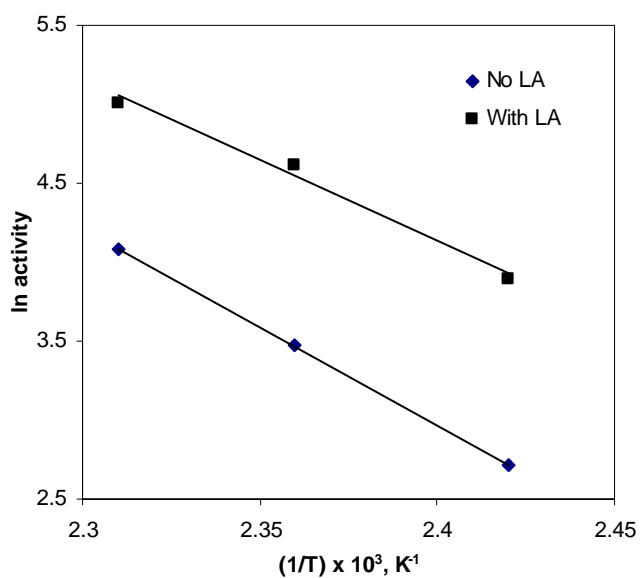


**Figure 4.13:** Temperature dependence of activity (Arrhenius plot)

#### 4.4.3. Effect of $\text{FeCl}_3$ on the rates of reactions with different bases

The effect of  $\text{FeCl}_3$  addition on the rate of reaction in presence of different bases was studied. For this, the reactions were carried out in the presence of organic, as well as, inorganic bases. The results are presented in Figure 4.14 and Table 4.2.

**Table 4.2:** Screening of olefins and bases

No	Olefin	Base	Product	Initial TOF, min <sup>-1</sup>	
				No FeCl <sub>3</sub>	With FeCl <sub>3</sub>
1	Methyl acrylate	NaOAc	Methyl cinnamate	57	160
2	Ethyl acrylate	NaOAc	Ethyl cinnamate	41	126
3	n-Butyl acrylate	NaOAc	n-Butyl cinnamate	32	101
4	Styrene	NaOAc	Stilbene*	75	148
5	n-Butyl acrylate	NaHCO <sub>3</sub>	n-Butyl cinnamate	111	136
6	n-Butyl acrylate	Na <sub>2</sub> CO <sub>3</sub>	n-Butyl cinnamate	35	51
7	n-Butyl acrylate	KOAc	n-Butyl cinnamate	113	251

**Reaction conditions:** Bromobenzene:  $0.399 \text{ kmol/m}^3$ , Olefin:  $0.602 \text{ kmol/m}^3$ , Base:  $0.6 \text{ kmol/m}^3$ , Catalyst precursor 1:  $8.51 \times 10^{-5} \text{ kmol/m}^3$ , Solvent: NMP, Total Volume:  $2.5 \times 10^{-5} \text{ m}^3$ , Temp: 423 K, FeCl<sub>3</sub>:  $5.93 \times 10^{-5} \text{ kmol/m}^3$

\* (*trans* + *cis*) Stilbene

The positive effect of FeCl<sub>3</sub> addition on the rate enhancement was seen to varying extent for all the inorganic bases tested. Initial TOF increase of 35 per min to 51 per min (45%), 32 per min to 101 per min (215%), 111 per min to 136 per min (22%), and 87 per min to 190 per min (118%) were observed with sodium carbonate, sodium acetate, sodium bicarbonate, and potassium acetate bases, respectively.

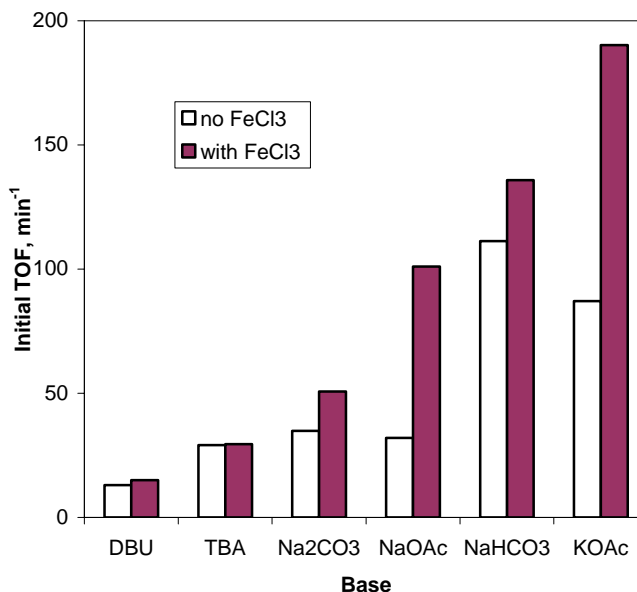


**Figure 4.14:** Influence of FeCl<sub>3</sub> on the activity of Heck reaction with different bases

**Reaction conditions:** Bromobenzene:  $0.399 \text{ kmol/m}^3$ , *n*-butyl acrylate:  $0.602 \text{ kmol/m}^3$ , Base:  $0.6 \text{ kmol/m}^3$ , Catalyst precursor 1:  $8.51 \times 10^{-5} \text{ kmol/m}^3$ , Solvent: NMP, Total Volume:  $2.5 \times 10^{-5} \text{ m}^3$ , Temp: 423 K, FeCl<sub>3</sub>:  $5.93 \times 10^{-5} \text{ kmol/m}^3$  (DBU: 1,8-diazabicyclo[5.4.0]undec-7-ene(1,5-5), TBA: *n*-tributyl amine)

As a general trend, the less active bases showed more rate enhancement on addition of FeCl<sub>3</sub>. Another interesting observation was that no rate enhancement was observed with the organic bases like TBA and DBU. Lewis acids are electrophilic in nature and can accept electrons. In case of organic bases like TBA and DBU, the lone pair of electrons present on nitrogen atom can participate in bonding with the Lewis acids. Thus, no FeCl<sub>3</sub> is available for polarizing the C-X bond of the aryl halide and hence, no enhancement in the rates is observed when organic bases are used. This is consistent with the Friedel Crafts chemistry, where the alkylation of the compounds containing nitrogen with free electron pair gives very poor results<sup>4</sup>.

#### 4.4.4. Effect of FeCl<sub>3</sub> on the rates of reactions with different olefins

Influence of FeCl<sub>3</sub> on the reaction rate was studied for the following olefins: methyl acrylate, ethyl acrylate, n-butyl acrylate, and styrene. The results obtained are presented in Table 4.2 and Figure 4.15.

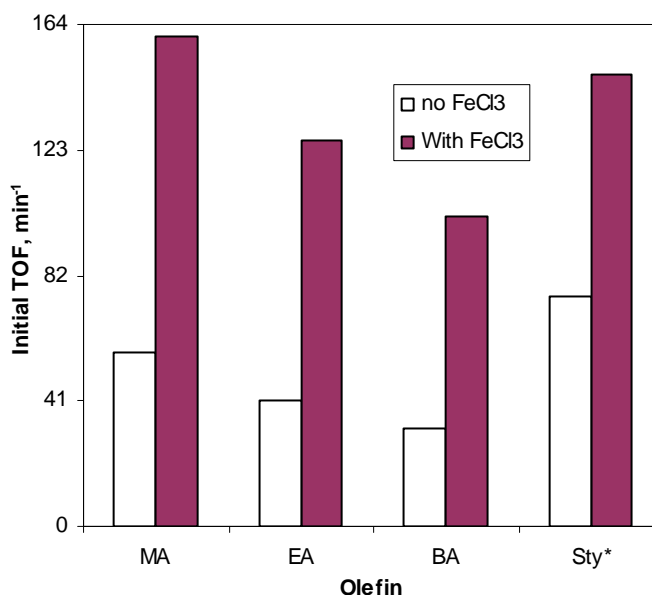


**Figure 4.15:** Influence of FeCl<sub>3</sub> on the activity of Heck reaction with different olefins

**Reaction conditions:** Bromobenzene:  $0.399 \text{ kmol/m}^3$ , Olefin:  $0.602 \text{ kmol/m}^3$ , NaOAc:  $0.6 \text{ kmol/m}^3$ , Catalyst precursor 1:  $8.51 \times 10^{-5} \text{ kmol/m}^3$ , Solvent: NMP, Total Volume:  $2.5 \times 10^{-5} \text{ m}^3$ , Temp: 423 K, FeCl<sub>3</sub>:  $5.93 \times 10^{-5} \text{ kmol/m}^3$  (\* sum of cis and trans stilbene)

On addition of FeCl<sub>3</sub> the initial TOF increased from 57 per min to 160 per min (180%), 41 per min to 126 per min (207%), 32 per min to 101 per min (215%), and 75/min to 158 per min (97%) for the reactions with methyl acrylate, ethyl acrylate, n-butyl acrylate, and styrene. Here too it was observed that the quantum of enhancement in the reaction rate was lesser for the olefins that were inherently more reactive. Methyl acrylate, which has the fastest reaction rate without FeCl<sub>3</sub> among the acrylates tested, gave the least enhancement in the rate on addition of FeCl<sub>3</sub>. Ethyl acrylate had the next best rate enhancement, while n-butyl acrylate gave the maximum enhancement of 215% on addition of FeCl<sub>3</sub>. In case of styrene, an intrinsically active olefin for Heck reactions (TOF 75 per



min), addition of  $\text{FeCl}_3$  gave 97% rate enhancement, which is much less compared to other olefins.

#### 4.4.5. Effect of $\text{FeCl}_3$ on the rates of reactions with different aryl halides

The magnitude of enhancement in the reaction rate was also found to depend on the nature of aryl halide.  $\text{FeCl}_3$  was able to enhance the reaction rates for chloro, bromo, as well as iodo arenes. The results are presented in Figure 4.16.

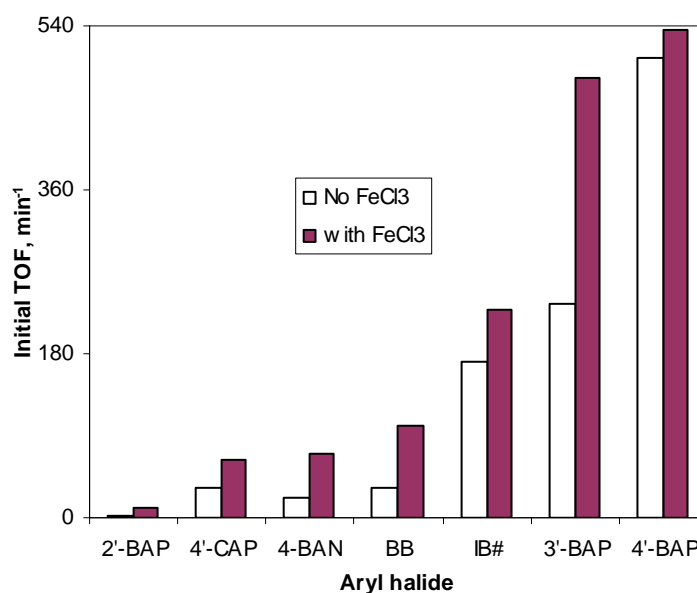


**Figure 4.16:** Influence of  $\text{FeCl}_3$  on the activity of Heck reaction with different aryl halides

**Reaction Conditions:** Aryl halide:  $0.399 \text{ kmol/m}^3$ , *n*-butyl acrylate:  $0.602 \text{ kmol/m}^3$ , NaOAc:  $0.6 \text{ kmol/m}^3$ , Catalyst precursor I:  $8.51 \times 10^{-5} \text{ kmol/m}^3$ , Solvent: NMP, Total Volume:  $2.5 \times 10^{-5} \text{ m}^3$ , Temp: 423 K,  $\text{FeCl}_3$ :  $5.93 \times 10^{-5} \text{ kmol/m}^3$

**# Reaction Conditions:**  $0.198 \text{ kmol/m}^3$ , BA:  $0.300 \text{ kmol/m}^3$ , NaOAc:  $0.301 \text{ kmol/m}^3$ , Catalyst precursor I:  $8.51 \times 10^{-5} \text{ kmol/m}^3$ , Solvent: NMP, Total Volume:  $2.5 \times 10^{-5} \text{ kmol/m}^3$ , Temp: 423 K,  $\text{FeCl}_3$ :  $5.93 \times 10^{-5} \text{ kmol/m}^3$ .

BAP: Bromoacetophenone, CAP: Chloroacetophenone, BAN: Bromoanisole, IB: Iodobenzene, BB: Bromobenzene

In case of bromobenzene the rate was found to increase by almost three times in the presence of  $\text{FeCl}_3$ . The initial rates were enhanced by almost two times in case of 4'-chloroacetophenone but the overall reaction did not proceed beyond 30 % conversions in both the cases - with or without  $\text{FeCl}_3$ . Good rate enhancements were observed for the vinylation of 3'-bromoacetophenone (TOF increased from 234 per min to 438 per min i.e. 97% increase in the rate) in presence of  $\text{FeCl}_3$ . The rates for 2'-bromoacetophenone were low as this is an intrinsically inactive system for the Heck vinylation reactions. In this case too the rate enhancement of 284% was observed, though the overall reaction rate remained very low (the increase in initial TOF from 3 per min to 11 per min). For 4'-bromoanisole, the initial TOF increased from 22 per min to 70 per min (rate enhancement of 223%). In case of iodobenzene, the initial TOF increased from 172 per min to 228 per min (enhancement in the rate by 56%). In case of vinylation of 4'-bromoacetophenone, a very active substrate for these reactions, the presence of  $\text{FeCl}_3$  resulted in only a minor enhancement in the rate (6%). This trend again conforms to the trends observed earlier wherein, the magnitude of rate enhancement on addition of  $\text{FeCl}_3$  is lower when the system itself is more reactive. Whereas, in case of 4'-bromoanisole (a less reactive substrate for Heck reaction), the rate enhancement of 223% was observed on addition of  $\text{FeCl}_3$ .

For the more reactive aryl halides, already enough concentration of easily cleavable C-X bonds is available. Hence, addition of  $\text{FeCl}_3$  does not have a very profound effect. But, in case of less active aryl halides (where the C-X bond is not easily cleavable),  $\text{FeCl}_3$  weakens the C-X bond and facilitates oxidative addition. Thus, the rate enhancement in such cases is very high. When the reactive system is made less reactive, by decreasing the temperature, the effect of  $\text{FeCl}_3$  becomes significant.

Interestingly, when 4'-nitrobromobenzene and 4'-bromoaniline were used as aryl halides, no enhancement in the reaction rate was observed on addition of  $\text{FeCl}_3$ . This can be attributed to the presence of lone pair of electrons on the nitrogen atom of 4'-bromoaniline and on the oxygen atom of the 4'-bromonitrobenzene. This lone pair of electrons can be donated to  $\text{FeCl}_3$  thus making it unavailable for the interaction with the C-X bond of aryl halide. This is similar to the observations made during the screening of the

bases, where too no enhancement in the rates was observed when organic bases with free lone pair of electrons on nitrogen atom, were used.

#### 4.5. Comparison of the promoting effect of FeCl<sub>3</sub> with tetrabutylammonium bromide

In order to compare the rate enhancements observed with Lewis acid promoters over the commonly used quaternary ammonium salt promoters, few experiments were carried out with tetrabutylammonium bromide in presence and absence of FeCl<sub>3</sub>. The experiments were carried out at the normally employed concentrations of TBAB (20 mol% of aryl halide) and also at a concentration comparable to that of FeCl<sub>3</sub> used in this study (~ 0.02 mol% of aryl halide). The results obtained are presented in Figure 4.17.

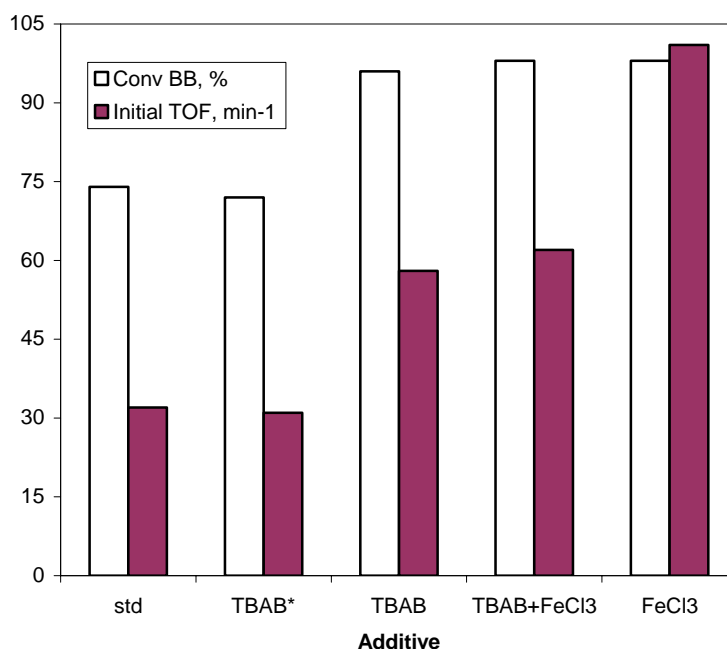


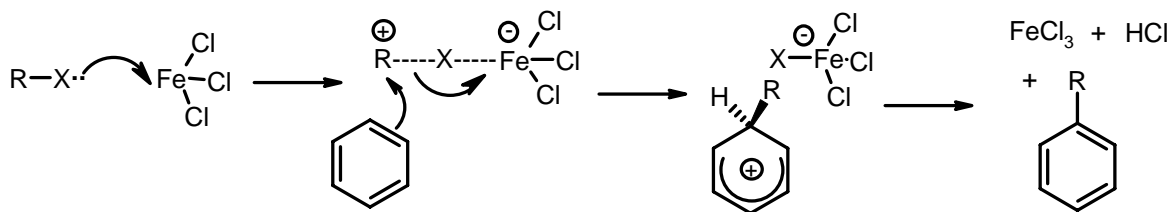
**Figure 4.17:** Comparison of influence of FeCl<sub>3</sub> and TBAB on the activity of Heck reaction  
*Reaction Conditions:* Bromobenzene: 0.399 kmol/m<sup>3</sup>, *n*-Butyl acrylate: 0.602 kmol/m<sup>3</sup>, NaOAc: 0.6 kmol/m<sup>3</sup>, FeCl<sub>3</sub>: 5.93 × 10<sup>-5</sup> kmol/m<sup>3</sup>, TBAB: 0.08 kmol/m<sup>3</sup>, Catalyst precursor I: 8.51 × 10<sup>-5</sup> kmol/m<sup>3</sup>, Solvent: NMP, Total Volume: 2.5 × 10<sup>-5</sup> m<sup>3</sup>, Temp: 423 K, Time: 2 Hours. \* TBAB: 5.93 × 10<sup>-5</sup> kmol/m<sup>3</sup>

For promoting the Heck reaction, tetrabutylammonium bromide needs to be added in large amounts (~ 20 mol% of the aryl halide). This becomes amply evident from the Figure 4.17. Addition of catalytic amounts of TBAB (0.014 mol% of the aryl halide), did not lead to any change in the reaction rate or the conversions obtained after 2 hours of reaction. When the amount of TBAB was increased to that reported in the literature (20 mol% of the aryl halide), the initial TOF increased to 58 per min (rate enhancement of 81%) as compared to the initial TOF of 32 per min for the reaction without any promoter. Whereas, catalytic amount of  $\text{FeCl}_3$  (0.014 mol% of aryl halide) was able to increase the initial TOF to 101 per min (rate enhancement of 215%). When TBAB and  $\text{FeCl}_3$  were taken together for the reaction (TBAB: 20 mol%,  $\text{FeCl}_3$ : 0.014mol% of aryl halide), the rates obtained were marginally better than those obtained with TBAB alone. Though both the promoters led to similar conversions at the end of 2 hour reaction period, the difference was starkly visible in the initial reaction rates represented by TOF.

A small amount of TBAB is just not sufficient for enhancing the reaction rates, as the amount is sufficient neither to dissolve NaOAc nor to stabilize the palladium complex. Hence, a relatively larger quantity of TBAB is required to make its role significant. When TBAB and  $\text{FeCl}_3$  are taken together, the rates remain comparable to those obtained with TBAB alone. This can be explained by taking into consideration the interaction of  $\text{FeCl}_3$  with TBAB.  $\text{FeCl}_3$  is electrophilic and hence, can accept the electrons from bromide ion of TBAB. Thus, free  $\text{FeCl}_3$  is no longer available for interaction with aryl halide or the olefin and the rates observed are essentially the same as observed with TBAB alone.

#### **4.6. Understanding the mode of action of Lewis acid promoters**

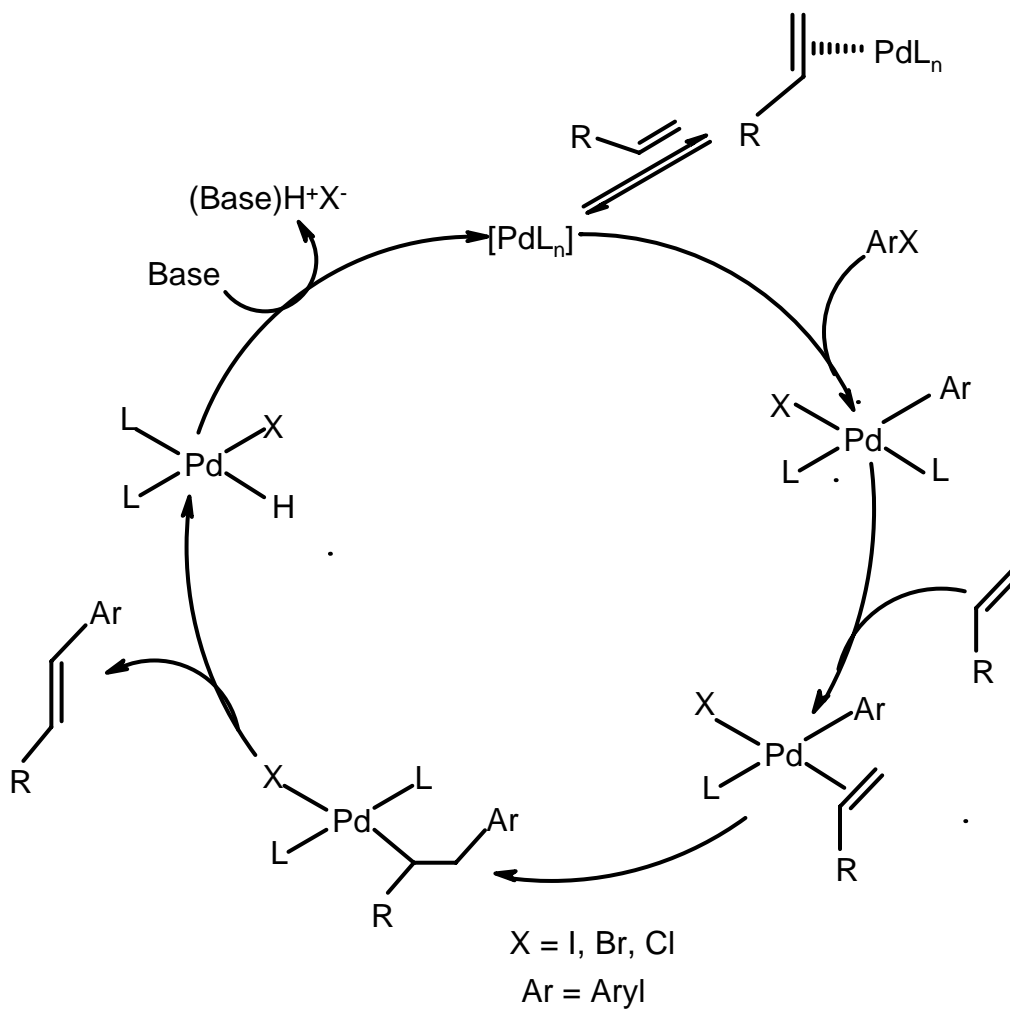
In Friedel Crafts alkylation, the halogen atom can interact with the Lewis acid through its lone pair of electrons. This leads to partial bond formation between the halogen atom and the metal atom of the Lewis acid. The alkyl halogen bond is polarized with a partial positive charge on the alkyl group and a partial negative charge on the Lewis acid. This interaction weakens the alkyl-halogen bond, which can then be cleaved rather easily (Scheme 4.5)<sup>5</sup>.



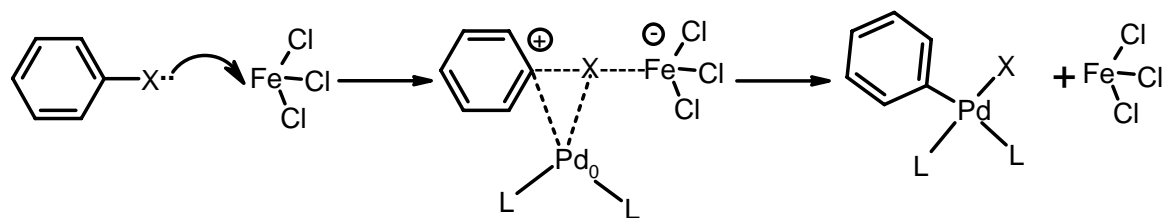
Scheme 4.5

It is very likely that the Lewis acids can interact in a similar way with the aryl halide in the Heck reaction. Lewis acids can polarize the aryl-halogen bond and can facilitate the oxidative addition of aryl halide to palladium. Another source of electrons available for Lewis acid to interact with is the olefin. It is possible that  $\text{FeCl}_3$  interacts with the olefin and draws away the electron density from it thereby making it more reactive towards Heck coupling. A general mechanism for the Heck reactions is presented in Scheme 4.6<sup>11</sup>. The mechanistic cycle of the Heck reaction involves the following basic steps which are common for all the different mechanisms suggested for these reactions: i) oxidative addition of aryl halide to catalytic palladium species ii) migratory insertion of the olefin into the palladium carbon bond iii)  $\beta$ -hydride elimination and release of the coupling product and iv) reductive elimination promoted by base to regenerate the active palladium species.

Generally in Heck reactions, the oxidative addition step is considered to be the rate determining step<sup>12</sup>. Any process that can facilitate this addition will lead to an increase in the rate of this step and consequently in the rate of the reaction. Similar to the Friedel Crafts alkylation, Lewis acids can interact with the halogen atom of the aryl halide through its lone pair of electrons. Thus Lewis acids can draw away the electron density from the aryl-halogen bond and polarize it. This polarization of the aryl-halogen bond will reduce the strength of this bond and make it easy to cleave. This will reduce the activation energy of the oxidative addition step and make the reaction faster. The activation energy of the  $\text{FeCl}_3$  promoted reaction was found to be approximately 18 kJ/mol lower than that of the unpromoted reaction (Figure 4.12). This type of speculated interaction is shown in Scheme 4.7. This polarized aryl halide can then oxidatively add to palladium (0) species to give the palladium (II) species.  $\text{FeCl}_3$  is regenerated and is free for the next cycle.



Scheme 4.6



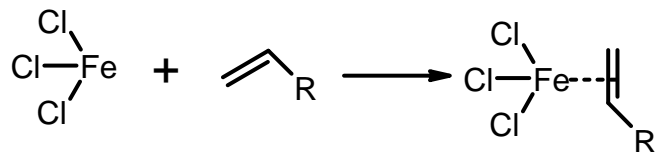
Scheme 4.7

The substituents present on the aromatic ring will have a profound effect on this step. Electron donating substituents like Me and OMe present on the ring increase the electron density on the ring, compensating for the electron density removed from the ring by the electronegative halogen atom. It becomes more difficult for palladium to oxidatively add such aryl halides, which in turn leads to the lower rates for Heck reaction of these halides<sup>13</sup>. The addition of Lewis acid solves this problem. Lewis acids interact with the electron pair of the halogen and thus reduce the overall electron density on the aromatic ring. This makes the C-X bond labile and a large enhancement in the reaction rate is observed (e.g. 223% for 4'-bromoanisole).

Electron withdrawing substituents like COMe and CHO present on the aromatic ring reduce the electron density on the ring. This makes it easier for them to undergo oxidative addition to the palladium. When Lewis acid is added to the reaction mixture then the electron density is further reduced by the interaction of Lewis acids with halogen electrons. But this influence is not as strong as that in case of electron donating substituents. Hence, though the addition of Lewis acids enhances the reaction rates in this case too, the enhancement is not as marked as in the earlier case of electron donating substituents (e.g. 97% for 3'-bromoacetophenone and 6% for 4'-bromoacetophenone).

However, the enhancement in the reaction rates for aryl halides with electron withdrawing substituents can be made more evident on addition of Lewis acids if the temperature of the reaction is reduced. At lower temperatures, the oxidative addition is slow as not sufficient energy is available to cleave the aryl-halogen bond. Addition of Lewis acid reduces the activation energy of the reaction (Figure 4.13), thus facilitating the reaction at lower temperatures. The cleavage of this bond now requires lower energy. Thus, the increase in the rate observed on addition of Lewis acids at lower temperatures is more pronounced (in case of 4'-bromoacetophenone magnitude of rate enhancement increases from 6% at 423 K to 114% at 413 K).

Apart from interacting with the aryl halides, the Lewis acids can also interact with the olefins. Lewis acids can bind to the olefin and thus remove the electron density from the olefin (Scheme 4.8).



Scheme 4.8

The effect of Lewis acid on the reactivity will depend on the R group of the olefin. The interaction of Lewis acid with the olefin will decrease as the electron density on the olefin reduces. The rate of the Heck reaction is faster for olefins with electron withdrawing R groups than for electron donating R groups. So the effect of Lewis acid on the rate of reaction will be more pronounced for the olefin having electron donating R group. The argument for this is similar to that for influence of Lewis acids on aryl halides. Thus, the rate enhancement observed on addition of  $\text{FeCl}_3$  to the Heck reaction of methyl acrylate (180%) is lower than that for ethyl acrylate (207%), which in turn is lower than that of n-butyl acrylate (215%). This follows because, as the length of the alkyl chain in the acrylate increases, the electronegativity of the oxygen atoms will be satisfied by the alkyl chain and the electrons forming the  $\pi$  bond will be available for interaction with the Lewis acid.

It is also possible that the Lewis acids can interact with the palladium catalysts and remove them from the active catalytic cycle. To illustrate this phenomenon, the reaction of 4'-bromoacetophenone was carried out at high Lewis acid concentration. The initial rates obtained were lesser than those obtained for the reaction without any Lewis acid. But the interesting observation was that the reaction practically stops after 20 minutes giving 40% conversion (Figure 4.18). This clearly shows that at higher concentrations,  $\text{FeCl}_3$  probably interacts with the palladium species in some way to deactivate it for the Heck reaction. Hence, the concentration of Lewis acid requires to be carefully optimized so that the rate enhancing effect takes precedence over the rate decreasing effect.



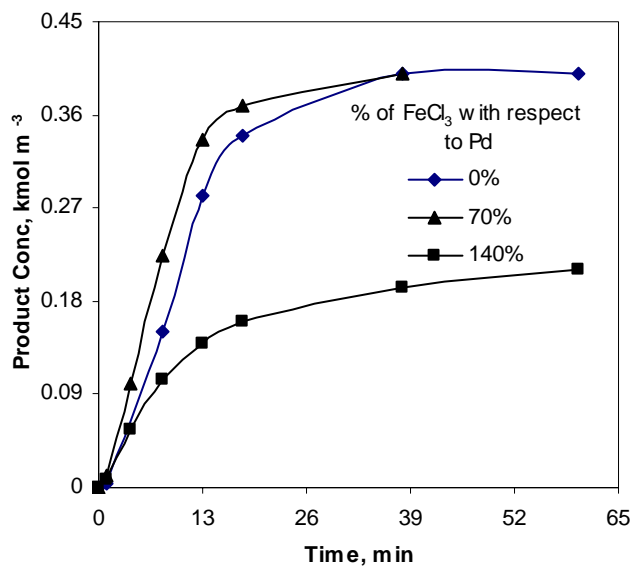
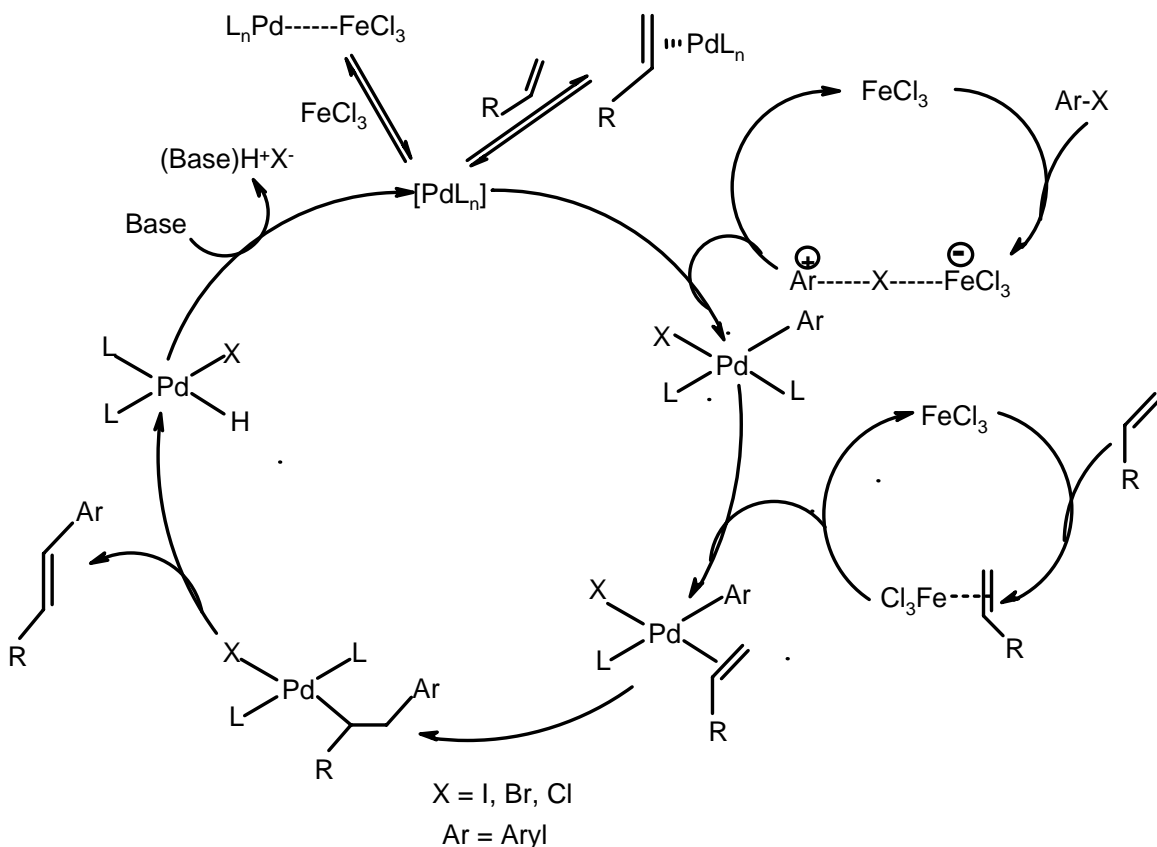


**Figure 4.18:** Influence of FeCl<sub>3</sub> concentration on the reaction

**Reaction Conditions:** 4'-Bromoacetophenone:  $0.399 \text{ kmol/m}^3$ , *n*-Butyl acrylate:  $0.602 \text{ kmol/m}^3$ , NaOAc:  $0.6 \text{ kmol/m}^3$ , Catalyst precursor **1**:  $8.51 \times 10^{-5} \text{ kmol/m}^3$ , Solvent: NMP, Total Volume:  $2.5 \times 10^{-5} \text{ m}^3$ , Temp: 423 K

A following reaction mechanism (Scheme 4.9) is proposed for the Heck reaction with palladium catalysts in presence of Lewis acids like FeCl<sub>3</sub>.



Scheme 4.9

#### 4.7. Conclusions

A new and very effective class of promoters for the Heck reactions was investigated in this study. The Lewis acid promoters were found to be a cheap and better alternate for the conventionally used quaternary ammonium salt promoters. A remarkable enhancement in the rate of palladium catalyzed Heck reactions was achieved by introduction of catalytic amounts of Lewis acids, like  $\text{FeCl}_3$ . This effect was demonstrated for a variety of bases, alkenes, aryl halides and palladium catalysts. It has been shown that the Lewis acids enhance the rate of reaction by reducing the activation energy. A mechanism, taking into account all the probable routes by which Lewis acids can influence the reaction rates, has also been proposed. Although the exact nature of the interaction of the Lewis acids with the substrate needs further elucidation, this strategy can nevertheless be applied to enhance the activities for Heck reactions. The same methodology may also be applicable for improving the yields of less active substrates.

## 4.8. References

- 1 a) Roth, J.; Craddock, J.; Hershmann, A.; Paulik, F. *Chemtech.* **1971**, 600 b) Roth, J. F. *Platinum Met. Rev.* **1975**, 19, 12 c) Paulik, F. E.; Roth, J. F. *Chem. Commun.* **1968**, 1578 d) Dekleva, T.; Forster, D. *Adv. Catal.* **1986**, 34, 81 e) Adamson, G. W.; Daly, J. J.; Forster, D. *J. Organomet. Chem.* **1974**, 71, C17 f) Garland, C. S.; Giles, M. F.; Sunley, J. G. *Eur. Pat.* 643034, **1995** g) Garland, C. S.; Giles, M. F.; Poole, A. d.; Sunley, J. G. *Eur. Pat.* 728726, **1994**
- 2 a) BASF AG, *Hydrocarbon Process* **1977**, 11, 135 b) BASF AG, *Hydrocarbon Process* **1977**, 11, 172
- 3 a) Jeffery, T. *J. Chem. Soc. Chem. Commun.* **1984**, 1287 b) Jeffery, T. *Tetrahedron Lett.* **1985**, 26, 2667 c) Jeffery, T. *Tetrahedron Lett.* **1994**, 35, 3051 d) Jeffery, T. *Tetrahedron Lett.* **1994**, 35, 4103 e) Jeffery, T. *Tetrahedron* **1996**, 52, 10113
- 4 Beletskaya, I. P.; Cheprakov, A. V. *Chem. Rev.* **2000**, 100, 3009
- 5 Bozell, J. J.; Vogt, C. E. *J. Am. Chem. Soc.* **1988**, 110, 2655
- 6 Smith, M. B. March, J. *March's Advanced Organic Chemistry: Reactions, Mechanisms, and Structures*, 5th Ed. Wiley-Interscience Publication, John Wiley and sons, Inc., USA, **2001**, 707-711
- 7 Sykes, P. *A Guidebook to Mechanisms in Organic Chemistry*, 6th Ed. Orient Longman Pvt. Ltd. New Delhi **1970**, 141-143
- 8 a) Iyer, S.; Ramesh, C. *Tetrahedron Lett.* **2000**, 41, 8981 b) Iyer, S.; Kulkarni, G. M.; Ramesh, C. *Tetrahedron Lett.* **2004**, 60, 2163
- 9 Armarego, W. L. F.; Chai, C. L. L. *Purification of Laboratory Chemicals*, 5<sup>th</sup> Ed. Butterworth Heinemann, Elsevier Science (USA) **2003**
- 10 a) Kobayashi, S.; Nagayama, S.; Busujima, T. *J. Am. Chem. Soc.* **1998**, 120, 8287 b) Kobayashi, S. *Synlett* **1994**, 689 c) Kobayashi, S. *Lanthanides: Chemistry and Use in Organic Synthesis* Springer: Berlin, **1999**
- 11 a) Amatore, C.; Jutand, A. *J. Organomet. Chem.* **1999**, 576, 254 b) Strijdonck, G. P. F.; Boele, M. D. K.; Kamer, P. C. J.; de Vries, J. G.; Leeuwen, P. W. N. M. *Eur. J. Inorg. Chem.* **1999**, 1073 c) Bohm, V. P. W.; Herrmann, W. A. *Chem. Eur. J.* **2001**, 2, 4191 d) Crisp, G. T. *Chem. Soc. Rev.* **1998**, 27, 427
- 12 Sundermann, A.; Uzan O.; Martin, J. M. L. *Chem. Eur. J.* **2001**, 7, 1703
- 13 a) Cabri, W.; Candiani, I.; DeBernardinis, S.; Francalanci, F.; Penco, S.; Santi, R. *J. Org. Chem.* **1991**, 56, 5796 b) Cabri, W.; Candiani, I. *Acc. Chem. Res.* **1995**, 28, 2

*Chapter 5:*

*Synthesis and Characterization of Ossified  
Palladium Complexes and Their Application  
to Heck Reaction*

## 5.1. Introduction

Although homogeneous catalysts dominate the basic research being carried out worldwide, they are industrially not lucrative due to the difficulties associated with catalyst product separation and catalyst recycle. To overcome this issue, one of the approaches is heterogenisation of catalyst by the synthesis of heterogeneous catalyst complexes, or the immobilization of the homogeneous catalyst complexes on the solid supports. Homogeneous catalyst complexes can be immobilized on either inorganic supports or on soluble polymer supports that can be precipitated at the end of the reaction. Various techniques like tethering<sup>1</sup>, encapsulation<sup>2</sup>, binding to functionalized polymers<sup>3</sup>, formation of dendritic complexes<sup>4</sup>, Supported Liquid Phase Catalysts (SLPC)<sup>5</sup>, etc. have been used for the immobilization of the homogeneous palladium complexes for application to Heck reactions. In this chapter, a recently developed technique for immobilizing the homogeneous complexes, termed “ossification<sup>6</sup>”, has been applied for the synthesis of catalyst precursors for the Heck reaction.

The term ossification is borrowed from the biology, where it refers to the process of formation of osseous tissue from the simple water soluble precursors, leading to the formation of insoluble biomaterials such as bones, coral reefs, and shells which are known for their strength and durability. The process of ossification, proposed here involves the synthesis of catalytically active material, which is inherently insoluble, by the process similar to that described earlier for the formation of robust insoluble biomaterials from simpler molecules and ions. To achieve this, the organometallic complexes are made soluble in water by the introduction of a non-coordinating anionic functionality such as sulphonate ( $-\text{SO}_3^-$ ), to the ligand/s of the complex, reported in detail in the literature<sup>7</sup>. These ligands, thus derivatized, can then be precipitated as solid material by treatment with heavier group II A cations like barium ( $\text{Ba}^{2+}$ ) and strontium ( $\text{Sr}^{2+}$ ). These cations form salts which are inherently insoluble in water, acids, and most of the organic solvents, and are high melting solids. Thus, molecular solids having their catalytically active transition-metal-centered environments intact can be obtained via a novel process described as “ossification” of metal complexes. A schematic representation of the ossification of metal complexes is given in Figure 5.1.

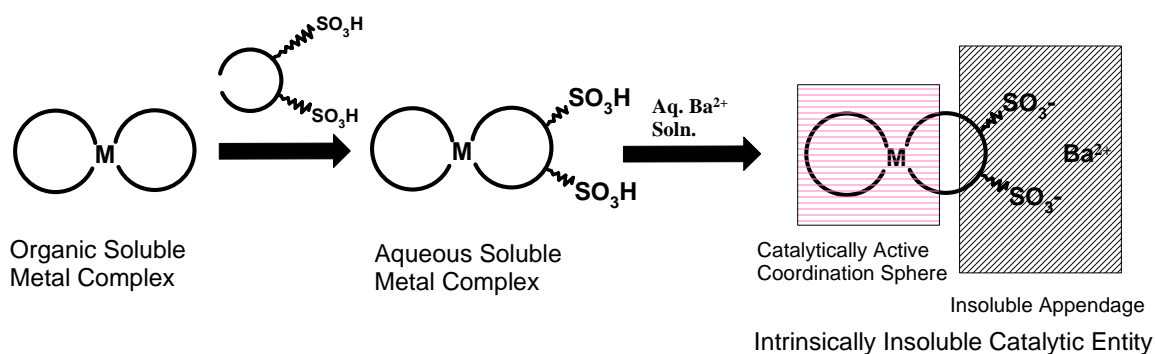


**Figure 5.1:** Schematic representation of Ossification of metal complexes

This technique of immobilization of homogeneous catalysts, namely the ossification has been demonstrated in this chapter. The heterogenisation of palladium complexes having a hemi-labile chelating N-N or N-O ligand, followed by their application as catalysts for the Heck reaction of aryl halides with olefins has been studied. A thorough characterization of the new catalyst materials using powder X-ray diffraction study (XRD), <sup>31</sup>P cross-polarized magic-angle spinning nuclear magnetic resonance spectroscopy (<sup>31</sup>P CP-MAS NMR), X-ray photoelectron spectroscopy (XPS), scanning electron microscopy (SEM), elemental microanalysis, BET surface area analysis etc. has been presented. Recycle studies showing the stability and true heterogeneity of the catalysts have been demonstrated and screening of the substrates and bases has been carried out.

## 5.2. Experimental

### 5.2.1. Materials

All the materials required for the experimental work in this chapter were procured from the following sources. Palladium acetate, Pd(OAc)<sub>2</sub>; palladium chloride, PdCl<sub>2</sub>; triphenylphosphine, PPh<sub>3</sub>; *p*-toluenesulphonic acid monohydrate (TsOH); picolinic acid (pycaH); 2-acetylpyridine (acpy); pyridine-2-carboxyaldehyde (pycald); bipyridine (bipy); aryl halides; olefins; were procured from Aldrich, USA, and used as obtained. Barium nitrate, Ba(NO<sub>3</sub>)<sub>2</sub> was obtained from s.d. Fine Chemicals, India. Sulphuric acid, H<sub>2</sub>SO<sub>4</sub>; phosphorous pentoxide, P<sub>2</sub>O<sub>5</sub>; sodium hydroxide, NaOH; hydrochloric acid, HCl; sodium bicarbonate, NaHCO<sub>3</sub>; anhydrous sodium sulphate, Na<sub>2</sub>SO<sub>4</sub>; sodium acetate (NaOAc); sodium carbonate, Na<sub>2</sub>CO<sub>3</sub>; tributylamine (TBA); chloroform, CHCl<sub>3</sub>; n-hexane; diethyl

ether, methyl ethyl ketone, N-methyl-pyrrolidinone (NMP); N,N-dimethyl formamide (DMF); etc. were procured from Merck, India. Nitrogen and argon gases were supplied by Indian Oxygen Limited, Mumbai.

### 5.2.2. Synthesis of Triphenylphosphine trisulphonate, sodium salt (TPPTS-Na)

TPPTS was prepared by sulphonation of Triphenylphosphine using oleum following the literature procedure<sup>7</sup>. Firstly, 66 % oleum was synthesized by distillation of H<sub>2</sub>SO<sub>4</sub> over anhydrous P<sub>2</sub>O<sub>5</sub>. In a typical oleum synthesis, 500 g anhydrous P<sub>2</sub>O<sub>5</sub> was taken in a round-bottom flask, and 400 ml concentrated H<sub>2</sub>SO<sub>4</sub> was added with stirring over a period of 2 hours. The mixture was heated till the solid dissolved and mixture started fuming. On further heating, SO<sub>3</sub> fumes emanated which were condensed using an air-condenser and collected in a jar containing 45 ml concentrated H<sub>2</sub>SO<sub>4</sub>, till the total volume was 148 ml. Thus, the oleum obtained was ~ 66%..

In the next step, 200 g (~100ml) concentrated H<sub>2</sub>SO<sub>4</sub> was taken in the sulphonation vessel (a water-jacketed stirred glass reactor); to it 50 g PPh<sub>3</sub> was added slowly over a period of 2 h at 283 K. To this solution, 280 g 66% oleum was added carefully with continuous stirring for efficient mixing and heat dissipation. The mixture was stirred for 76 h after the completion of oleum addition at a constant temperature of 295 K. After completion of the reaction, the temperature was lowered to 273 K and the contents were diluted using 50 ml degassed distilled water slowly so that temperature did not exceed 278 K followed by further 500 ml distilled water. To this, a 50% NaOH solution was added with stirring to neutralize the mixture under a controlled temperature not exceeding 278 K. The solid Na<sub>2</sub>SO<sub>4</sub> formed during neutralization was removed by filtration. After further concentration of the filtrate in a rotary evaporator, 2 liters of methanol were added to further precipitate Na<sub>2</sub>SO<sub>4</sub> as a white solid. The methanol-water solution was then refluxed for two hours which led to further precipitation of white Na<sub>2</sub>SO<sub>4</sub>, which was removed by filtration. The supernatant liquor (after the removal of all solid Na<sub>2</sub>SO<sub>4</sub>) was evaporated to dryness to get sodium salt of TPPTS as a white powder. This white solid was dissolved in minimum volume of water and re-precipitated by adding ethanol to obtain pure TPPTS (> 99 %). This was dried under high vacuum and stored under argon.

### 5.2.3. Syntheses of Palladium complexes

A number of palladium complexes having hemi-labile N-O or N-N chelating ligands, were synthesized as follows.

#### 5.2.3.1. Pd(pyca)(PPh<sub>3</sub>)(OTs) complex

The Pd(pyca)(PPh<sub>3</sub>)(OTs) complex was prepared by the literature procedure<sup>8</sup>. In a typical synthesis, 0.5 g Pd(OAc)<sub>2</sub> (2.225 mmol), 0.274 g pyridine-2-carboxylic acid (2.225 mmol), 0.846 g *p*-toluenesulphonic acid (4.45 mmol) and 1.168 g triphenylphosphine (4.45 mmol) were taken in a minimum volume of chloroform in a round-bottomed flask and were vigorously shaken at room temperature for few minutes until all the components dissolved completely and the solution turned bright yellow. The product was isolated as a yellow oily mass by addition of *n*-hexane to the chloroform solution and vigorous shaking for 10 minutes. The oily material was washed with *n*-hexane and then with diethyl ether a number of times. Applying vacuum led to the formation of a yellow fluffy solid. For elemental and spectroscopic analysis, the complex was purified by re-precipitation from chloroform.

#### 5.2.3.2. Pd(acpy)(PPh<sub>3</sub>)(OTs) complex

A similar procedure as that described above in section 5.2.3.1. was used. 0.2 g Pd(OAc)<sub>2</sub> (0.89 mmol), 0.108 g 2-acetyl pyridine (0.89 mmol), 0.338 g *p*-toluenesulphonic acid (1.78 mmol) and 0.468 g PPh<sub>3</sub> (1.78 mmol) in chloroform were vigorously stirred at room temperature until all the components dissolved completely and the solution turned yellow. The product was isolated as a yellow oil by adding *n*-hexane. The oily product was washed several times with *n*-hexane and diethyl ether and was kept under vacuum forming a yellow fluffy solid, which was purified by re-precipitation from chloroform.

#### 5.2.3.3. Pd(pycald)(PPh<sub>3</sub>)(OTs) complex

A similar procedure as that described above in section 5.2.3.1. was followed. 0.2 g Pd(OAc)<sub>2</sub> (0.89 mmol), 0.095 g pyridine-2-carboxaldehyde (0.89 mmol), 0.338 g *p*-toluenesulphonic acid (1.78 mmol) and 0.468 g PPh<sub>3</sub> (1.78 mmol) in chloroform were vigorously shaken at room temperature until all the components dissolved completely and

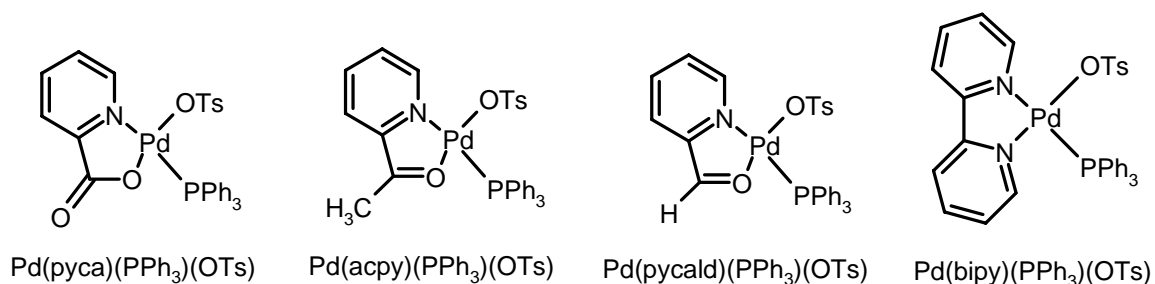


the solution turned yellow. The complex was isolated as yellow thick oil by adding *n*-hexane. The oily product was washed several times with *n*-hexane and diethyl ether and was kept under vacuum forming a yellow fluffy solid, which was purified by re-precipitation from chloroform.

#### 5.2.3.4. Pd(bipy)(PPh<sub>3</sub>)(OTs) complex

A procedure similar to that described in earlier section was followed for the synthesis of this complex. 0.2 g Pd(OAc)<sub>2</sub> (0.89 mmol), 0.139 g 2,2'-Bipyridine (0.89 mmol), 0.338 g *p*-toluenesulphonic acid (1.78 mmol) and 0.468 g PPh<sub>3</sub> (1.78 mmol) in chloroform were vigorously stirred under room temperature until all the components dissolved completely and the solution turned yellow. The complex was isolated as a yellow oil by addition of *n*-hexane. The oily product was washed several times with *n*-hexane and diethyl ether and was kept under vacuum forming a yellow fluffy solid, which was purified by re-precipitation from chloroform.

The structures of these four complexes are shown in Scheme 5.1.

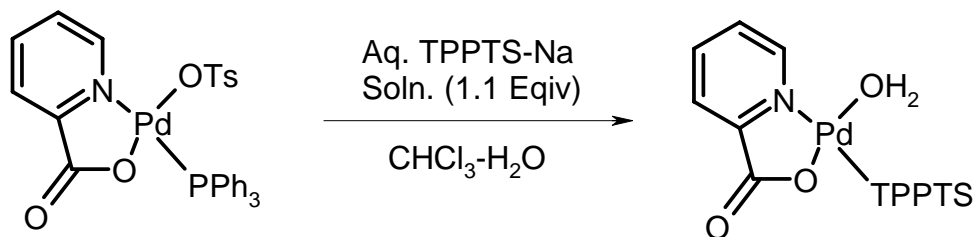


**Scheme 5.1**

#### 5.2.4. Synthesis of aqueous-soluble complexes

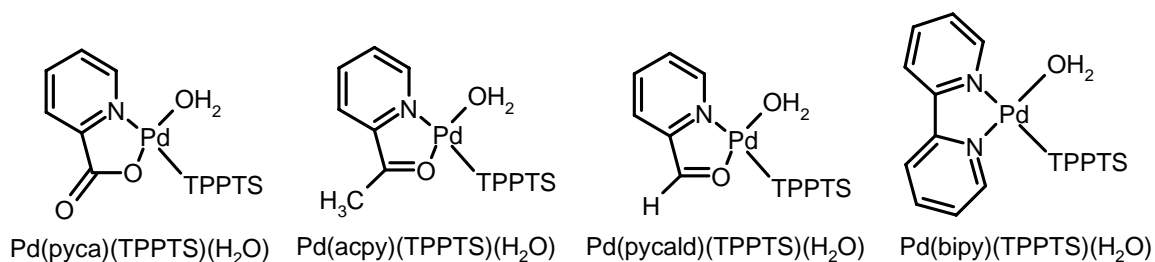
For converting the complexes having N-N and N-O hemi-labile ligands (namely pyca, acpy, pycald and bipy) into water soluble complexes, a common protocol was followed as reported in the literature<sup>9</sup>. Since each of these complexes contains only one phosphine ligand coordinated to the palladium centre, only a slight excess of the free TPPTS was added. The particular complex was dissolved in 10 ml chloroform and shaken vigorously with a solution of 1.1 equivalents of TPPTS in 6 ml distilled, degassed water in a separatory funnel. The yellow color of the CHCl<sub>3</sub> layer disappeared and the aqueous layer

became yellow in color indicating the formation of the aqueous soluble complex by substitution of the  $\text{PPh}_3$  by TPPTS at the Pd-centre as shown in Scheme 5.2.



**Scheme 5.2**

The aqueous layer was allowed to separate well and then removed, followed by washing with 5ml portions of fresh  $\text{CHCl}_3$  thrice to remove any organic soluble precursor. The aqueous solution of the catalyst was flushed with argon and preserved under argon. The other three aqueous-soluble complexes were synthesized similarly. For the next step, i.e. ossification, the same solution was used. But the pure water-soluble complex can be obtained by precipitation, on the addition of methanol as faint yellow solid. The solid was filtered under argon, washed with methanol and dried under vacuum to yield a yellow fine powder. The probable structures of the four aqueous-soluble complexes thus prepared are shown in Figure 5.3.



**Scheme 5.3**

### 5.2.5. Ossification of palladium complexes

The protocol adopted for ossification of the metal complexes is based on a simple approach of precipitation of insoluble salts of sulphonated-ligand coordinated to the transition metal centers. Since,  $\text{BaSO}_4$  and  $\text{SrSO}_4$  are well-known insoluble materials in water and almost all organic solvents,  $\text{Ba}^{2+}$  was used for ossification. To an excess

saturated solution of  $\text{Ba}(\text{NO}_3)_2$  (15 ml) in degassed de-ionized water, taken in a double-necked round bottomed flask, the aqueous solution of the Pd-complex prepared as mentioned earlier was added drop wise, with vigorous stirring at ambient temperature ( $\sim 298\text{K}$ ). The entire procedure was carried out under argon atmosphere. Immediate appearance of pale yellow precipitate was observed. Slow addition of the metal complex with good agitation was required to prevent rapid agglomeration of the precipitate. After complete addition, the mixture was stirred for 10 h at ambient temperature, to completely precipitate the solid. The material was then separated by filtration as a pale yellow solid. The solid was washed with copious amount of water to remove all  $\text{Ba}^{2+}$  adhering to the precipitated solid (since  $\text{Ba}^{2+}$  was used in excess), till the washings were found to be free of barium. The solid was then washed with acetone to remove any organic moieties. It was dried in air and then Soxhlet extracted with water and acetone successively, for 16 hours each. The catalyst material was obtained as a free-flowing pale yellow powder after drying in air. This process of ossification was used for all the palladium complexes synthesized earlier. The four different ossified palladium complexes were designated as ossified  $\text{Pd}(\text{pyca})(\text{TPPTS})$  – Catalyst 1A, ossified  $\text{Pd}(\text{acpy})(\text{TPPTS})$  – Catalyst 1B, ossified  $\text{Pd}(\text{pycald})(\text{TPPTS})$  – Catalyst 1C and  $\text{Pd}(\text{bipy})(\text{TPPTS})$  – Catalyst 1D respectively, and the catalysts have been henceforth referred to as mentioned above.

#### 5.2.6. General procedure for recycling the catalyst for Heck reaction

Iodobenzene 2.4 mmol, n-butyl acrylate 3.0 mmol, sodium acetate 3.0 mmol, and ossified palladium catalyst 5 mg (Pd content: 0.33 % w/w) were taken in N,N-dimethyl formamide (total volume 10 ml) solvent in a 20 ml single neck glass reactor, equipped with a reflux condenser and a stirrer, under nitrogen atmosphere. The reactor was immersed in an oil bath pre heated to the desired temperature. The reaction was carried out for 30 minutes, after which, the reaction mixture was cooled and allowed to settle. A sample was withdrawn for analysis by GC (as described in Chapter 2) in order to determine the conversion of iodobenzene and the selectivity towards the Heck vinylation product. The solution was decanted and the solid residue washed twice with methanol to remove the unreacted base and the salt formed during the reaction. The left over traces of methanol were removed under vacuum. Fresh substrates, base, and solvent was added to the

recovered catalyst and the reaction was carried out to investigate the activity of the recycled catalyst.

### 5.2.7. General procedure for screening of substrates and bases for Heck reaction

Iodobenzene 2.44 mmol, n-butyl acrylate 3.0 mmol, NaOAc 3.0 mmol, and ossified palladium catalyst 10 mg (Pd content: 0.33% w/w) were taken in DMF solvent (total volume 20 ml) in 50 ml 2 necked glass reactor, under nitrogen atmosphere. The glass reactor was equipped with a reflux condenser, a magnetic stirrer, and a septum to withdraw the intermediate reaction samples. The reactor was immersed in an oil bath pre heated to the desired temperature. The reaction was carried out for different time durations depending on the substrates used. Reaction samples were withdrawn at regular intervals with the help of a hypodermic syringe to be analyzed by GC.

## 5.3. Results and discussions

The results obtained from the characterizations as well as the various catalytic experiments are described in this section. The catalyst entities were characterized by using numerous techniques.

### 5.3.1. Characterization of the Catalysts

#### 5.3.1.1. $^{31}\text{P}$ Cross-Polarized Magic Angle Spinning NMR Spectroscopy

The solid state NMR experiments were performed for establishing the novel concept of immobilization. In principle, the single phosphorous atom of the phosphine ligand present in the chosen Pd-complexes should show a definite chemical shift in the pure form. The existence of the *cis-trans* equilibrium between the isomers may not be visible in the solid state NMR spectra due to the partial quenching of the molecular dynamics and line-broadening in solid state due to static anisotropic interactions. Variation of the position of the chemical shift is likely whenever electron-mobility is operating in the complex from any source, which may be due to the introduction of substituents in the present ligand, or a new ligand. The  $^{31}\text{P}$  signal for the pure Pd(pyca)(PPh<sub>3</sub>)(OTs) complex appears at  $\delta_{\text{iso}}$  33.44 ppm (Figure 5.2A) wherein, the anisotropic and dipolar coupling are averaged to zero by the magic-angle spinning. However, the  $^{31}\text{P}$ -NMR signal for the water-soluble complex

$\text{Pd}(\text{pyca})(\text{TPPTS})(\text{H}_2\text{O})$  in  $\text{D}_2\text{O}$  appeared at 35.31 and 36.13 ppm, which are justifiable by the fact that the presence of the electron-withdrawing sulfonate functionality,  $-\text{SO}_3\text{H}$  on the P-atom causes the change in its electronic environment and thus the chemical shift position in the NMR spectrum. Also, the liquid phase spectrum demonstrated the presence of the *cis-trans* isomers in liquid phase.

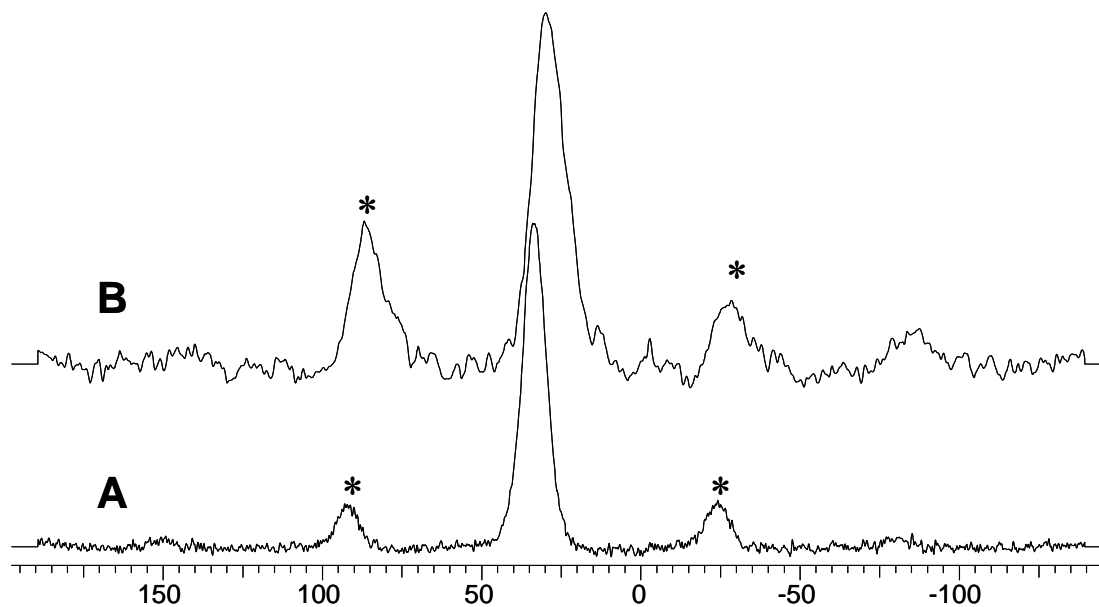


**Figure 5.2:**  $^{31}\text{P}$  CP-MAS NMR spectra of the catalysts: A-  $\text{Pd}(\text{Pyca})(\text{PPh}_3)(\text{OTS})$  complex, B- ossified  $\text{Pd}(\text{Pyca})(\text{TPPTS})(\text{H}_2\text{O})$  using  $\text{Ba}^{2+}$  ions. \* in the spectra indicate the side bands at 7 kHz

The  $^{31}\text{P}$  signal for the solid ossified  $\text{Pd}(\text{pyca})(\text{TPPTS})(\text{H}_2\text{O})$  complex occurs at  $\delta_{\text{iso}}$  29.83 ppm as a single peak as shown in Figure 5.2. We observe an upfield shift of the position of the signal due to the P-atom in the ossified  $\text{Pd}(\text{pyca})(\text{TPPTS})$  complex. This upfield shift of the signal may be attributed to the formation of the Ba-sulphonate ion-pair by the ionic interaction of the  $\text{SO}_3^-$  with the  $\text{Ba}^{2+}$  cations. The ionic interaction of the anionic sulphonate moiety of the TPPTS coordinated to the Pd-centre, with the  $\text{Ba}^{2+}$  cation, quenches the electron withdrawing effect of the  $-\text{SO}_3^-$  on the phenyl rings and subsequently on the P-atom which thus appears at a lower ppm on the  $^{31}\text{P}$  NMR spectrum. Also, the formation of a Ba-sulphonate lattice may impart some environmental effect to this upfield shift. These spectra confirm the formation of the ossified complex with the retention of the structure of the parent coordination environment in the Pd-complex. Also,

the integrity of the complex was maintained during the ossification process, which may be concluded from the absence of the peak at  $\delta_{\text{iso}} - 2.85$  ppm which corresponds to the free  $\text{Ba}_3(\text{TPPTS})_2$  type species. This might have been observed either by the disintegration of the Pd-complex during the ossification process, or presence of any free excess TPPTS in the aqueous solution of the complex prior to ossification, giving rise to the free  $\text{Ba}_3(\text{TPPTS})_2$  peak. The  $^{31}\text{P}$  CP-MAS NMR spectra of the other Pd-complexes with different ligands (Figure 5.3) show similar patterns of chemical shifts with slightly different  $\delta$ -values.

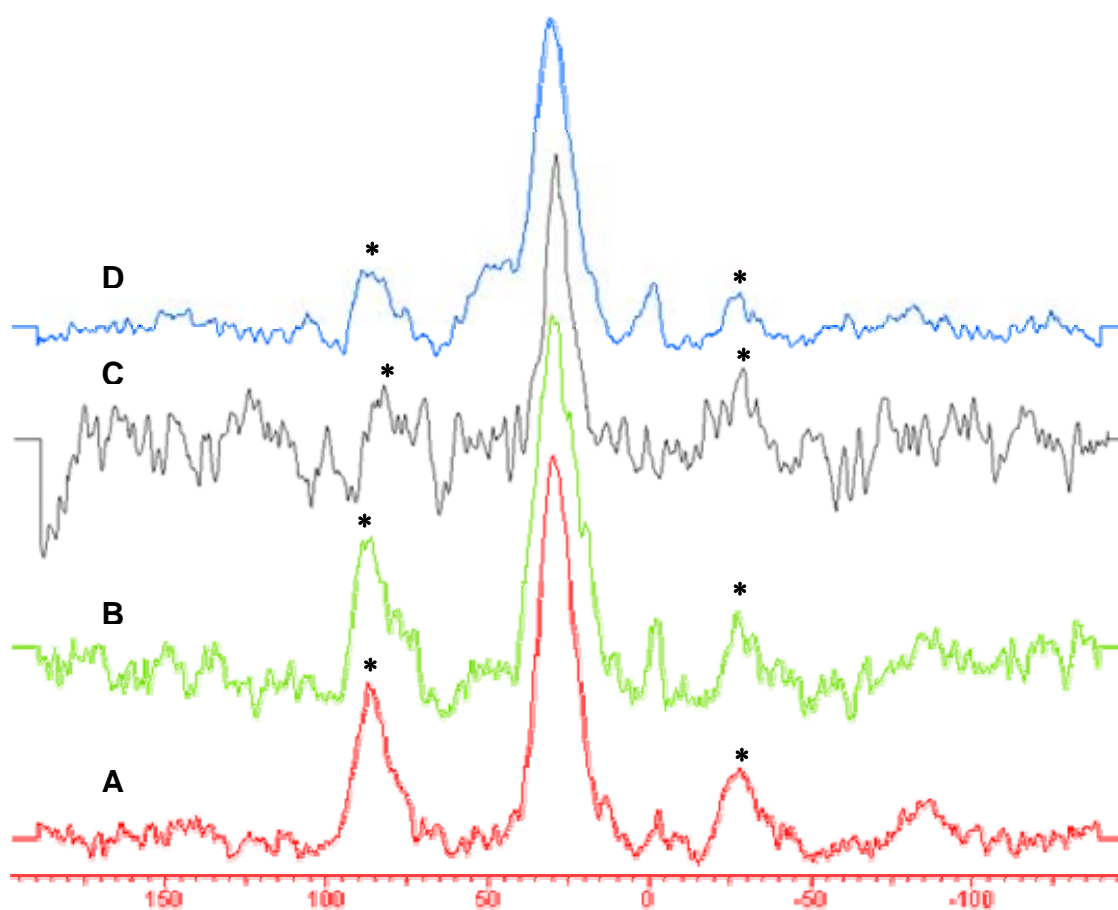


**Figure 5.3:**  $^{31}\text{P}$  CP-MAS NMR Spectra of the ossified catalysts using  $\text{Ba}^{2+}$  ions, (A) Ossified  $\text{Pd}(\text{pyca})(\text{TPPTS})$  complex, (B) Ossified  $\text{Pd}(\text{Acpy})(\text{TPPTS})$  complex, (C) Ossified  $\text{Pd}(\text{Pycald})(\text{TPPTS})$  complex, (D) Ossified  $\text{Pd}(\text{Bipy})(\text{TPPTS})$  complex. \* in the spectra indicate the side bands at 7kHz.

This variation of the chemical shift values may be attributed to the change in the stereo-electronic environments around the Pd-centre in the said complexes due to the different chelating ligands present in them. Of the ligands selected in the Pd-complexes for ossification, the order of nucleophilicity is Pyca > Acpy > Pycald > Bipy. Eventually, the  $^{31}\text{P}$  CP-MAS NMR chemical shift values ( $\delta_{\text{iso}}$ ) of their ossified Pd-complexes show a trend in the reverse order as 29.83, 30.23, 30.74 and 30.90 ppm respectively as shown in Figure 5.3 A to D. This order may be justified as follows. The phosphine ligand being TPPTS in all the complexes, the effect of the nucleophilicity of the other ligands in the palladium complexes is reflected on the respective chemical shifts. More the nucleophilicity of the ligand more the transfer of electron density to the Pd-atom. Subsequently, more electron density is transmitted to the P-atom by the  $\tilde{\pi}$  acceptor property of the triphenylphosphine ligand, using the  $d\pi - d\pi$  back bonding. Thus the P-atom of Ba-[Pd(Pyca)(TPPTS)] moiety will resonate at an upfield position in comparison to the Ba-[Pd(Bipy)(TPPTS)] species, which is exactly as observed in the spectra. The  $^{31}\text{P}$  CPMAS NMR studies clearly illustrated that the ossified palladium complexes maintained the stereoelectronic orientation of the original Pd-complexes throughout the ossification process and after ossification, the complexes retained their Pd-centres intact, as required for the catalytic cycle to operate. This also established our protocol of ossification, and further emphasized the stability of the ossified Pd-complexes under aerial and moisture-laden conditions, in contrary to the pristine Pd-complexes which were quite air and moisture-sensitive, and decomposed to black mass on prolonged exposure to air or moisture.

### 5.3.1.2. Powder X-Ray Diffraction

The powder X-ray diffraction is another important tool for the characterization of the materials prepared by the ossification technique. The Ba-sulphonate formed may be anticipated of having similarity in the powder XRD pattern of that of the inorganic  $\text{BaSO}_4$  salt, as the functionalities are same, but since the sulphonate ion concerned in the ossification methodology is a functionalized one (bearing phenyl rings attached to a P-atom, for TPPTS), the relative intensity of the principle peaks *may* differ from the pure inorganic salt, due to the variation in the unit cell dimensions caused by the difference in

the size with the pure  $\text{SO}_4^{2-}$  anion. The powder XRD will also be instrumental in determining the nature of the solid as amorphous or crystalline.

With this logical background, the XRD spectra for the ossified palladium complexes were recorded and the result for ossified Pd(pyca)(TPPTS) complex, using  $\text{Ba}^{2+}$  cations, i.e. Catalyst 1A is presented in Figure 5.4.

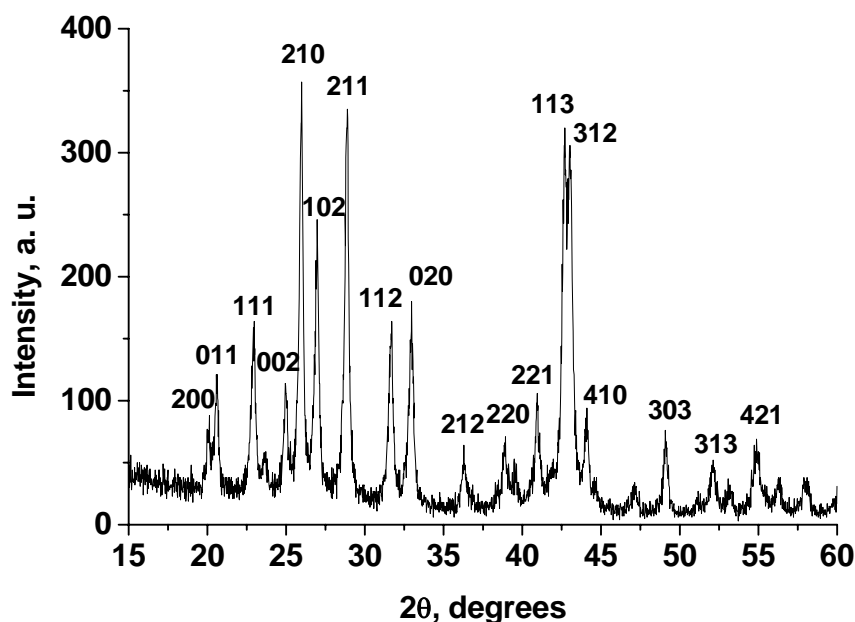


**Figure 5.4:** Powder XRD pattern of ossified Pd(pyca)(TPPTS) complex using  $\text{Ba}^{2+}$  cations. Numbers in the plot denote the different Miller indices for the respective Bragg's planes

The XRD pattern showed that the Ba-sulphonate ionic entity of the ossified complex (Catalyst 1A) had a similar constitution as that of the inorganic  $\text{BaSO}_4$ . The complete indexing of the pattern was performed for the ossified Pd-complex and it was observed that the Miller indices of all the peaks matched exactly that of  $\text{BaSO}_4$ . However, the intensity of some peaks showed dissimilarity, which was as expected for the barium salt of a functionalized sulphonate moiety. The peak with highest intensity was assigned for the Bragg's plane of 210, which is different from that of pure  $\text{BaSO}_4$ , where, the principle peak (considered 100% intensity) occurs for the plane 211. The other peaks also were consistent with the diffraction planes of the inorganic  $\text{BaSO}_4$  with respect to the peak positions. Hence, we can also speculate an orthorhombic unit cell for the ossified material by



calculating the  $d$ -values of the Bragg's planes as in the case of pure  $\text{BaSO}_4$ . Thus, the ossified palladium complex resembled the pure  $\text{BaSO}_4$  in X-ray diffraction pattern. This showed that the protocol conceived for the formation of the Ba-sulphonate ion-pair by the reaction of a functionalized sulphonate moiety with  $\text{Ba}^{2+}$  cation was established, and thus the immobilization of the metal complex in the form of a solid molecule is rationalized. The powder XRD characterization was also used to characterize the other ossified Pd-metal complexes prepared using  $\text{Ba}^{2+}$  cations. These materials (Catalyst 1B, 1C and 1D) also had the characteristic peaks for the Ba-sulphonate ion-pair similar to that of the ossified Pd-pyca complex (Catalyst 1A), as expected. The comparative results of the three different ossified palladium complexes, namely ossified Pd(acpy)(TPPTS) complex, ossified Pd(pycald)(TPPTS) complex and ossified Pd(bipy)(TPPTS) complex are presented in Figure 5.5. From the powder XRD data, it was clear that the postulated Ba-sulphonate ion pair was formed for all of the palladium complexes, while the differences in the relative intensities of the principle peaks in the spectra of the respective ossified complexes were also visible. This variation of the relative intensities of the principle peaks might be attributed to the difference in the nature of the different chelating ligand in each of them. The slight variation in the stereo-electronic contribution of the ligands was manifested in terms of the variation of the relative peak intensities. The steric as well as the electron-cloud environment of the different chelating ligands might influence the arrangements of the crystallographic planes of the Ba-sulphonate ion-pair, thus generating the dissimilarities in the intensities of the same peaks, for the four different ossified palladium complexes.

Thus, the powder XRD characterization of the ossified palladium complex catalysts had shown that the formation of the Ba-sulphonate ion-pair had occurred just as hypothesized, and the protocol of ossification is thus further consolidated.

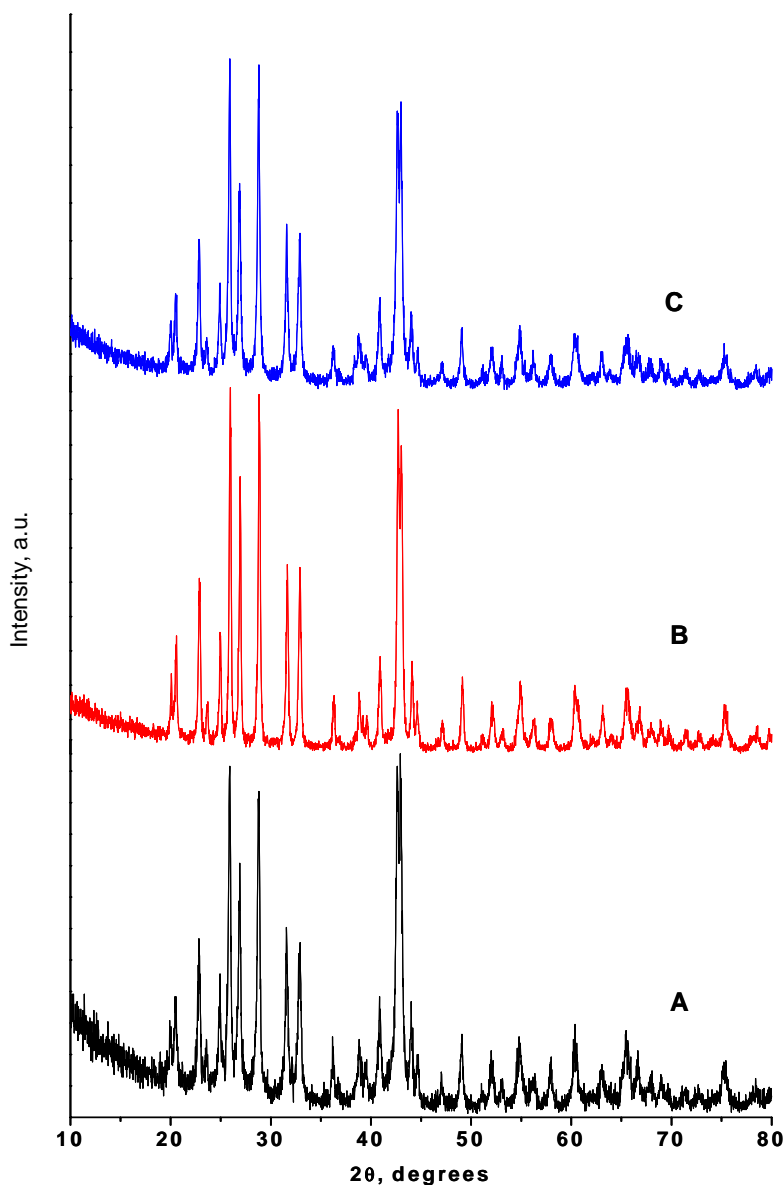


**Figure 5.5:** Powder XRD patterns of different ossified Pd complexes using  $Ba^{2+}$  ions: (A)  $Pd(acpy)(TPPTS)$  complex, (B)  $Pd(pycald)(TPPTS)$  complex, (C)  $Pd(bipy)(TPPTS)$  complex

### 5.3.1.3. X-Ray Photoelectron Spectroscopy

The X-ray photoelectron spectroscopy was used for the determination of the oxidation states of the respective elements present in the catalyst composites. The X-ray actually removes the core orbital electrons of the elements at specific binding energies, which are fingerprints for particular oxidation states of the element.

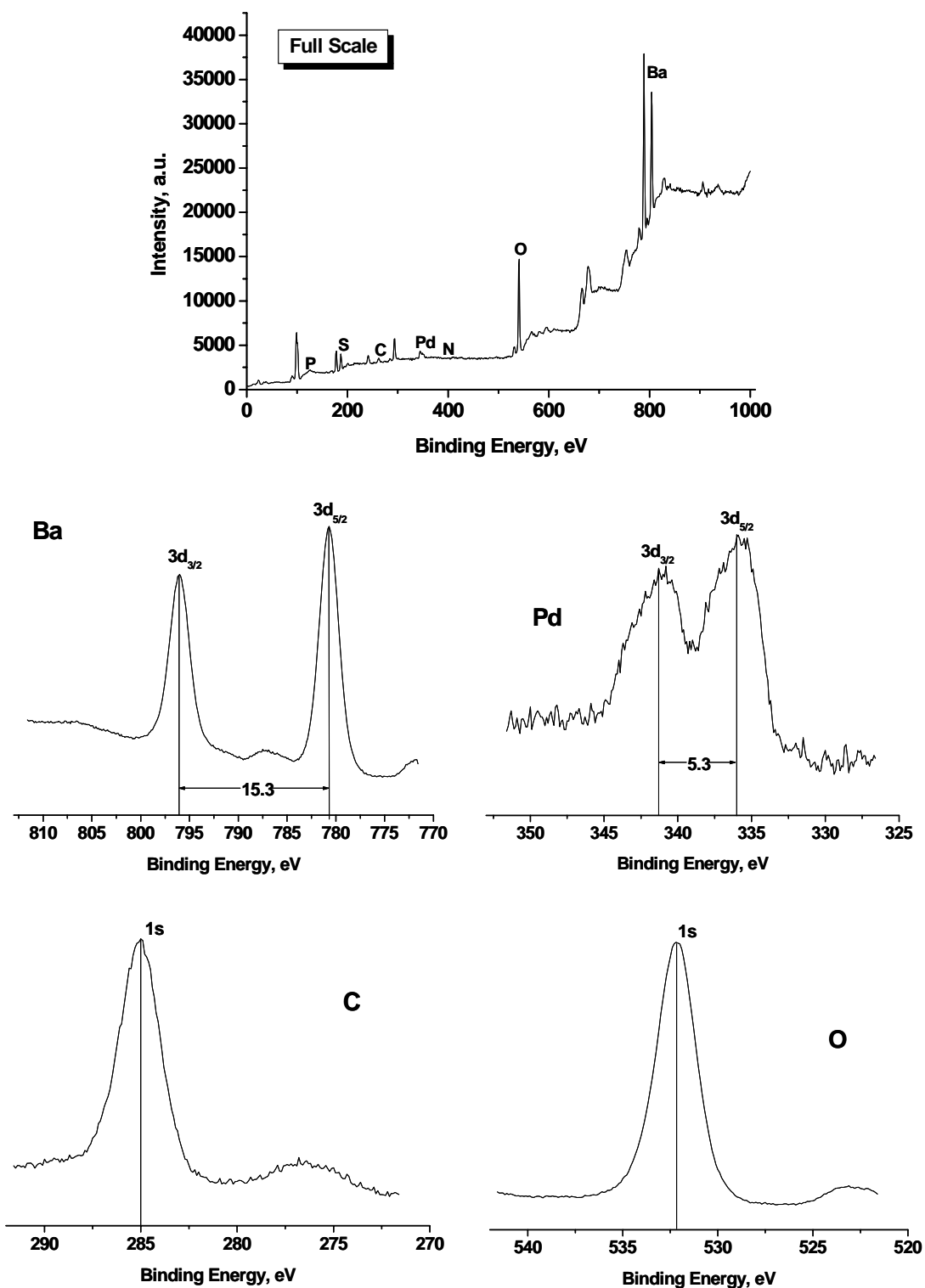
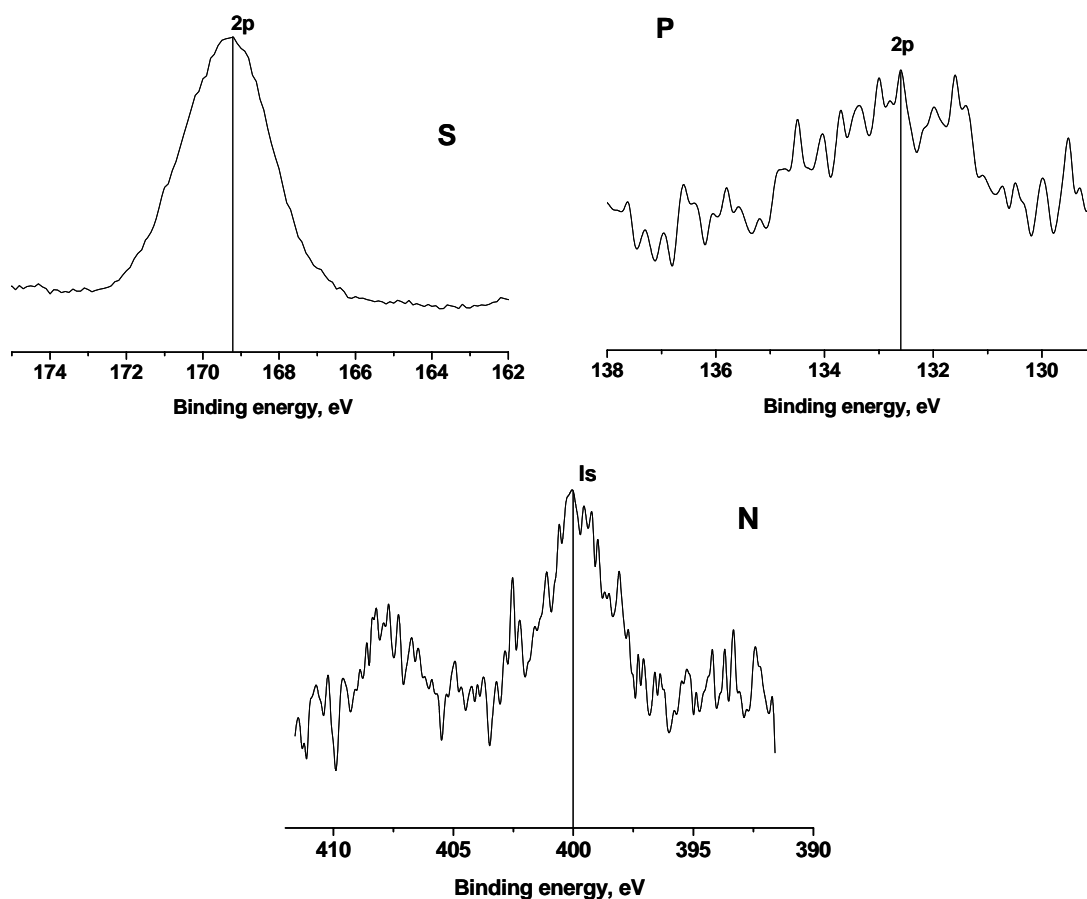


Figure 5.6: XPS data of ossified Pd(pyca)(TPPTS) complex i.e. Catalyst 1A



**Figure 5.6 (continued):** XPS data of ossified Pd(pyca)(TPPTS) complex i.e. Catalyst 1A

The XPS data also delivers some information about the immediate local electronic environment of the selected element incorporating the perturbation of the electron density due to the neighboring functional groups and/or ligands. The XPS spectra of the different elements present in ossified Pd(pyca)(TPPTS) complex, 1A using barium, is presented in Figure 5.6. The data for each element is corrected with respect to signal of the adventitious carbon at 285 eV. Based on the binding energies of the observed signals the different peaks were assigned to the different elements with different oxidation states. The full-scale spectrum shows peaks for almost all of the elements present in the catalyst 1A, but further intricate details are obtained by analyzing the individual peaks more precisely. The peaks at 796 and 780.7 eV correspond to the  $3d_{3/2}$  and  $3d_{5/2}$  states of  $Ba^{2+}$  oxidation state with the characteristic band gap of 15.3 eV. The absence of any further peaks for barium confirms

its presence in +2 oxidation state as  $\text{Ba}^{2+}$  ions in the solid catalyst 1A. The peaks at 341.3 and 336 eV are assigned to the  $3d_{3/2}$  and  $3d_{5/2}$  states of +2 oxidation state of palladium. A very interesting observation in this regard is that for pure  $\text{Pd}(\text{OAc})_2$  the  $3d_{5/2}$  state occurs at around 338.5 eV, while the palladium is in the same +2 oxidation state. The soft and resonating character of the  $\text{OAc}^-$  anion imparts lesser electron density to the Pd centre and hence Pd binding energy is slightly higher for  $\text{Pd}(\text{OAc})_2$ . For catalyst 1A, the pyridine-2-carboxylate anionic ligand can impart its electron density better onto the  $\text{Pd}^{2+}$  centre along with the other ligands, thus increasing the electron-cloud density over the Pd-atom, consequently, palladium appears at a lower binding energy (336 eV), than that for  $\text{Pd}(\text{OAc})_2$ . A characteristic band gap of 5.3 eV was also observed between the  $3d_{5/2}$  and  $3d_{3/2}$  signals of palladium for catalyst 1A. The binding energies of the other elements however matched very nicely with the electronic condition of the ossified complex. For instance, O 1s state occurs at 532.1 eV, which is similar to the +2 oxidation state of oxygen in an anion, e.g. carboxylate, or sulphonate; binding energy value for N 1s in catalyst 1A was 400 eV, which is slightly higher than the binding energy for N in pyridine (~398.7 eV) due to the chelation through the N-atom in the complex and consequent depletion of electron density. The binding energy values of sulphur 2p and phosphorous 2p were also observed to be matching with those of sulphonate group and coordinated phosphine moieties owing to the depletion of electron density while chelation to the metal centre. All these binding energy values indirectly confirm that the coordination pattern in the ossified  $\text{Pd}(\text{pyca})(\text{TPPTS})$  complex are intact as in the pure complex. Also, no degradation of the ligand/s was understandably detected during the ossification process as, if it were such, then the binding energies of the clue elements e.g. Pd, N, P etc would have been much different. The XPS data for the other three ossified complexes, namely catalyst 1B, 1C, and 1D respectively, are presented in Table 5.1 which also consistently match with the stereo-electronic variation of the respective ligands in them. Interestingly, the variations are best manifested in the binding energies of the clue elements as N, O and Pd. For example, in catalyst 1D, the presence of the bipyridyl ligand makes use of two N-atoms as highly electron-donating centres, which become electron-deficient thus increasing the binding energy value for N 1s. Consequently, the Pd atom becomes little more electron rich thus decreasing the binding energy for Pd  $3d_{5/2}$ .

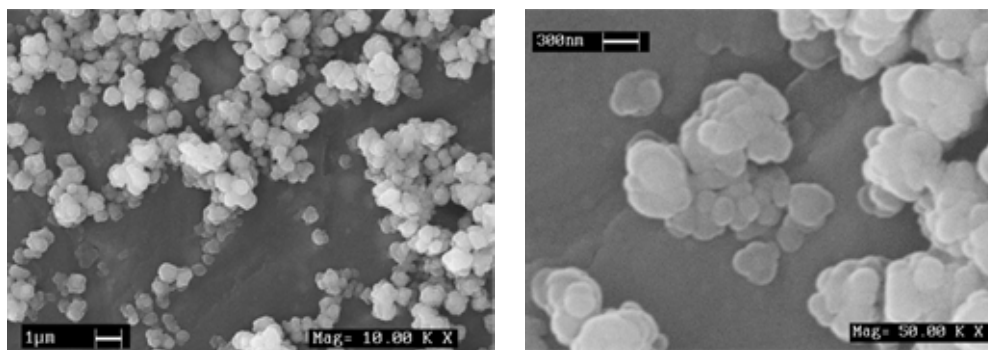
**Table 5.1:** XPS data for Catalyst 1B, 1C and 1D (values in eV)

<b>Elements Catalysts</b>	<b>Ba 3d<sub>5/2</sub></b>	<b>Pd 3d<sub>5/2</sub></b>	<b>O 1s</b>	<b>N 1s</b>	<b>P 2p</b>	<b>S 2p</b>
<b>Catalyst 1B</b>	780.5	336	532	400	132.6	169.3
<b>Catalyst 1C</b>	780.5	336	531.8	399.9	132.6	169.2
<b>Catalyst 1D</b>	780.6	335.9	531.9	400.8	132.5	169.2

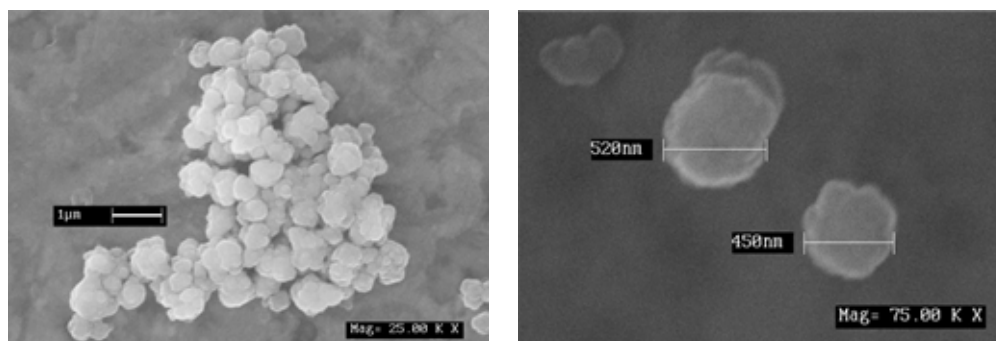
The x-ray photoelectronic spectra data thus delivers important evidence in support of the states of the individual atoms and stability of the complex during the course of the ossification process. The Pd-complexes were in the oxidation states as expected, and did not change during the synthesis of the catalyst materials.

#### 5.3.1.4. Scanning Electron Microscopy

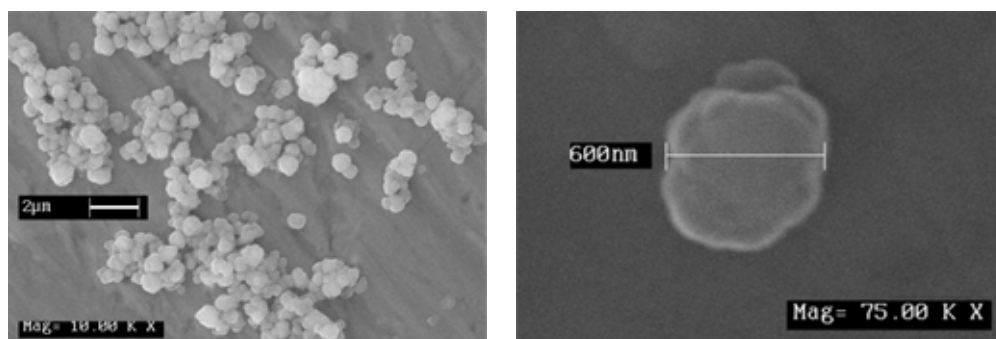
The morphological characterization of the ossified Pd-complexes was done by scanning electron microscopy (SEM), in terms of the size and shape of the solid particles and their particulate distribution. Taking ossified Pd(pyca)(TPPTS) complex i.e. catalyst 1A as the typical example for illustration of the characterization, it was observed that the material was in the form of irregular polyhedral particles of average diameter of about 450 nm. These particles were discrete and non-cohesive with distinct borders/ boundaries with more or less uniform particles of the said size. On a closer look, by applying magnification to a small grain of the catalyst, the particles seem to be macro-clusters of the solid catalyst molecules with regular sizes. The SEM images of the different ossified palladium complex catalyst entities such as, Pd(acpy)(TPPTS), Pd(pycald)(TPPTS), Pd(bipy)(PPh<sub>3</sub>)(OTs), using Ba<sup>2+</sup> cations are presented in the Figure 5.7. All of the catalyst composites showed similar kind of evenly dispersed irregular polyhedral particulate materials, which were actually clusters of the heterogeneous catalyst molecules. On further magnification, all the catalysts revealed discrete clusters of irregular shapes and of sizes varying from 450 nm to 600 nm on an average for the catalyst 1A, 1B, 1C and 1D.



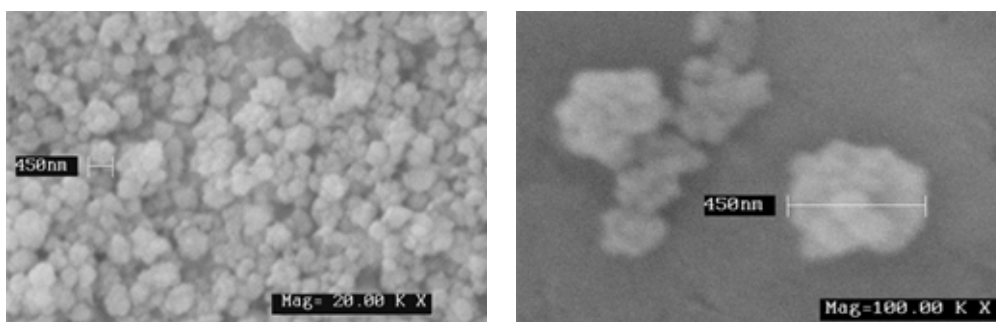
**Ossified [Pd(bvca)(TPPTS)] complex**



**Ossified [Pd(bio)(TPPTS)] complex**



**Ossified [Pd(acv)(TPPTS)] complex**



**Ossified [Pd(bvca)(TPPTS)] complex**

**Figure 5.7:** SEM images of the different ossified Pd-complex catalysts

However, the almost uniform size of the particles in each case may be attributed to the fact that the agitation of the synthesis mixture during the precipitation might be one of the size-dictating factors for the ossification procedure. The particles of average diameter ~450 to 600 nm were typically observed when the agitation of the synthesis mixture was around 600 rpm i.e. 10 Hz. However, when the agitation speed was lowered to 6.66 Hz, larger lumps of average particle diameter ~1 $\mu$ m were obtained. This further confirmed that the occurrence of a particular particle size might be due to the agitation effect of the reaction mixture at the time of precipitation from aqueous medium. The SEM micrographs also showed no existence of any smaller particles or fragments, which indicated that the clusters of the ossified complexes had grown uniformly during the synthesis procedure and also, they are resistant to the physical wear and tear that they are subjected to, while under high agitation during their preparation.

#### 5.3.1.5. Surface Area Measurements

The ossified palladium complexes were analyzed for the determination of the surface area of the composite matrices formed. It was important from the viewpoint of the activity of the catalyst, as the larger the surface area, greater is the accessibility of the reactants to the catalytic sites, and better is the activity. The surface area analyses of the ossified palladium complexes were done using N<sub>2</sub>-physisorption-desorption technique, using the BET formula. The results are presented in Table 5.2.

**Table 5.2:** BET surface area data for the ossified palladium complexes

Entry	Material	Surface area, m <sup>2</sup> g <sup>-1</sup>
1	Ossified Pd(pyca)(TPPTS) complex	18.6
2	Ossified Pd(acpy)(TPPTS) complex	17.1
3	Ossified Pd(pycald)(TPPTS) complex	11.9
4	Ossified Pd(bipy)(TPPTS) complex	18.7

It is observed from the data in Table 5.2 that the ossified Pd-complexes have quite low surface areas, not exceeding 20 m<sup>2</sup>g<sup>-1</sup>. Such low surface areas might be justified from



the fact that these materials were synthesized by simple precipitation technique, where the agglomeration might be a very common phenomenon. More importantly, the solubility of the Ba-sulphonates being very low (if considered similar to the sparingly soluble BaSO<sub>4</sub>), might lead to ultra-fast formation of the ion-pair precipitate, leading to agglomeration and consequently a low surface area. This is commensurate with the SEM data, which shows the irregular polyhedral clusters for all the four ossified complexes, with the average sizes of the particles ranging from 450 to 600 nm. The single-point adsorption-desorption studies also indicated that the particulate ossified materials catalyst 1A, 1B, 1C and 1D were non-porous in nature, as in that case, the respective surface areas would have been much higher. This also matched with the SEM analyses and thus, it may be concluded that the ossified palladium catalysts were non-porous robust solid clusters of uniform average size ranging from 450 to 600 nm in diameter, having surface areas in the range of 11 to 20 m<sup>2</sup>g<sup>-1</sup>.

#### 5.3.1.6. Palladium Content Analysis

All the ossified palladium complexes were analyzed for Pd-content using the atomic absorption spectroscopic (AAS) method. The samples of fixed weight were digested and dissolved in concentrated HNO<sub>3</sub> and were diluted to a fixed volume. Further AAS experiments were conducted using these solutions. The results of AAS analysis are presented in Table 5.3.

**Table 5.3:** Pd-content of different ossified Pd-complexes

Entry	Material	Pd-content, %
1	Ossified Pd(pyca)(TPPTS) complex	0.33
2	Ossified Pd(acpy)(TPPTS) complex	0.36
3	Ossified Pd(pycald)(TPPTS) complex	0.35
4	Ossified Pd(bipy)(TPPTS) complex	0.34

### 5.3.2. Heck reactions using Ossified Palladium Complexes:

#### 5.3.2.1. Recycle studies with different ossified complexes

After synthesis and characterization of the ossified palladium complexes, their applicability in the Heck reaction was investigated. A test reaction of the ossified 1A catalyst was carried out for the Heck vinylation reaction of iodobenzene with n-butyl acrylate in presence of sodium acetate base in N-methyl 2-pyrrolidinone solvent. The solution turned brown after 30 minutes of reaction. On recycling the solid catalyst precursor, a drastic fall in the conversion of iodobenzene was observed (95% to 72% to 47%). The use of the decanted liquid for the fresh reaction gave 35% conversion of iodobenzene in the similar time frame. The palladium content analysis of the liquid phase by Atomic Absorption Spectroscopy showed > 20% leaching of the metal.

Since NMP is usually associated with higher metal leaching than other solvents, it was decided to carry out the reaction in N,N-dimethyl formamide solvent which is reported to give lower leaching than NMP<sup>10</sup>. Using the same reaction conditions as described above, the reaction was carried out in DMF solvent. No color change was observed after 30 minutes of the reaction. GC analysis showed the reaction to be complete in 20 minutes. The concentration vs. time profile for this reaction is shown in Figure 5.8. A complete mass balance was obtained for the reaction. The AAS analysis of the liquid phase showed less than 1% palladium in the solution. On recycling the solid phase the leaching of the palladium in subsequent recycles was also less than 1%. The recycle of the liquid phase showed < 4 % conversion of iodobenzene. After carrying out initial test reactions a detailed recycle study was carried out. For carrying out the recycle study, the amount of the catalyst in the reaction mixture was reduced by half. The reaction was carried out for 30 minutes and no intermediate samples were withdrawn for analysis. The GC analysis was carried out for the final sample taken at the end of 30 minutes of the reaction. After the reaction, the catalyst precursor was recovered as described earlier and was used for the fresh reaction. The liquid phase was also recycled for the Heck reaction to check for the influence of small amount of palladium that was shown to have leached out in the first run. The results are shown in Figure 5.9.

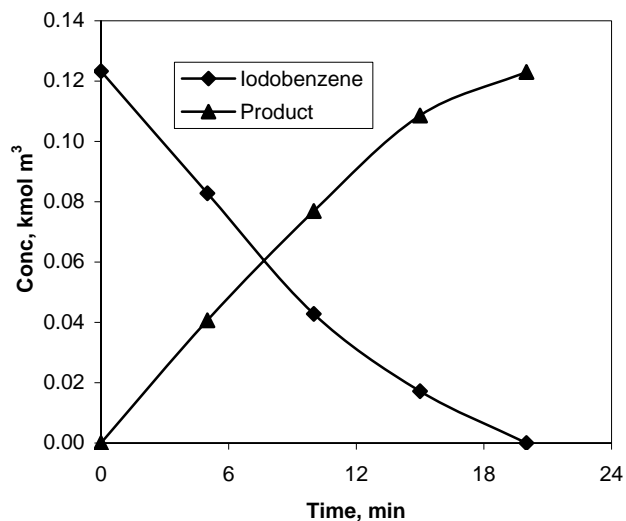


**Figure 5.8:** CT profile for the Heck reaction with ossified catalyst 1A

**Reaction conditions:** Iodobenzene:  $0.122 \text{ kmol/m}^3$ , *n*-Butyl acrylate:  $0.149 \text{ kmol/m}^3$ , NaOAc:  $0.151 \text{ kmol/m}^3$ , Ossified catalyst 1A:  $5 \times 10^{-7} \text{ kg/m}^3$  (Pd: 0.33% w/w), Solvent: DMF, Total Volume:  $2 \times 10^{-5} \text{ m}^3$ , Reflux

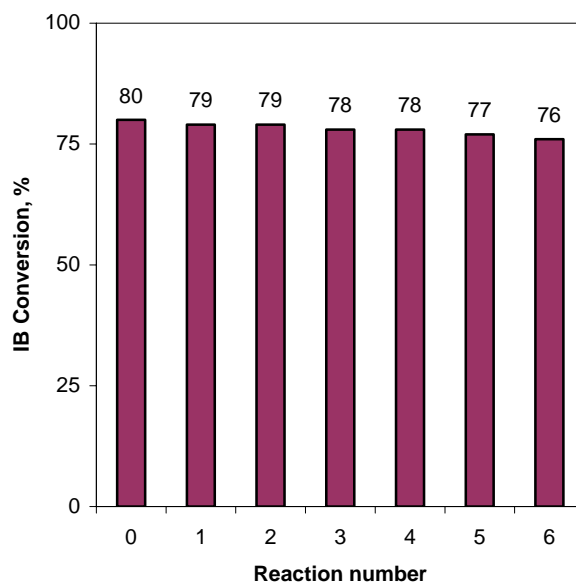


**Figure 5.9:** Recycle study with ossified catalyst 1A

**Reaction conditions:** Iodobenzene:  $0.24 \text{ kmol/m}^3$ , *n*-Butyl acrylate:  $0.301 \text{ kmol/m}^3$ , NaOAc:  $0.302 \text{ kmol/m}^3$ , Ossified catalyst 1A:  $5 \times 10^{-7} \text{ kg/m}^3$  (Pd: 0.33% w/w), Solvent: DMF, Total Volume:  $1 \times 10^{-5} \text{ kmol/m}^3$ , Time, 30 mins, Reflux

The fresh reaction gave 80% conversion of iodobenzene. This conversion fell to 79% for the first recycle run with the catalyst precursor. On further recycles, no major drop in the iodobenzene conversion was observed. The catalyst precursor was recycled 7 times (1 + 6). On recycling the liquid phase of the fresh reaction (run 0), ~ 4% conversion of iodobenzene was observed. When the liquid phase of the subsequent reaction (run 1) was recycled, trace amounts of n-butyl cinnamate were observed (< 2% iodobenzene conversion).

Recycle studies under the similar reaction conditions were carried out for other ossified palladium complexes (1B, 1C, 1D). The results are shown in Figures 5.10, 5.11, and 5.12.

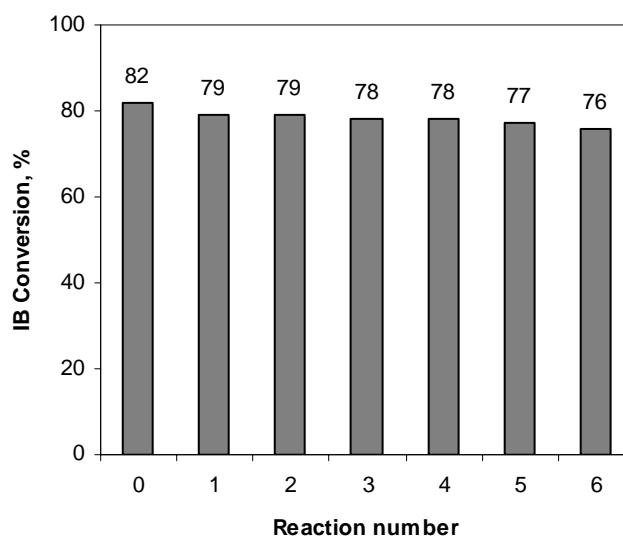


**Figure 5.10:** Recycle study with ossified 1C catalyst precursor

**Reaction conditions:** Iodobenzene:  $0.24 \text{ kmol/m}^3$ , n-Butyl acrylate:  $0.301 \text{ kmol/m}^3$ , NaOAc:  $0.302 \text{ kmol/m}^3$ , Ossified catalyst 1C:  $4.4 \times 10^{-7} \text{ kg/m}^3$  (Pd: 0.35% w/w), Solvent: DMF, Total Volume:  $1 \times 10^{-5} \text{ m}^3$ , Time, 30 mins, Reflux

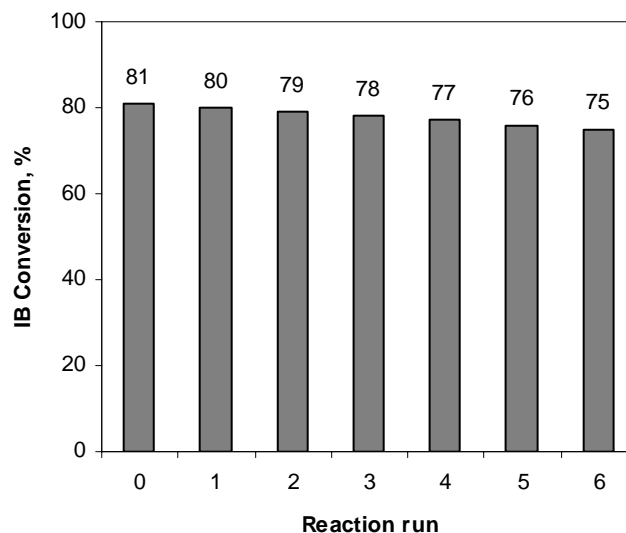


**Figure 5.11:** Recycle study with ossified catalyst 1B

**Reaction conditions:** Iodobenzene:  $0.24 \text{ kmol/m}^3$ , *n*-Butyl acrylate:  $0.301 \text{ kmol/m}^3$ , NaOAc:  $0.302 \text{ kmol/m}^3$ , Ossified catalyst 1B:  $5 \times 10^{-7} \text{ kg/m}^3$  (Pd: 0.36% w/w), Solvent: DMF, Total Volume:  $1 \times 10^{-5} \text{ m}^3$ , Time, 30 mins, Reflux

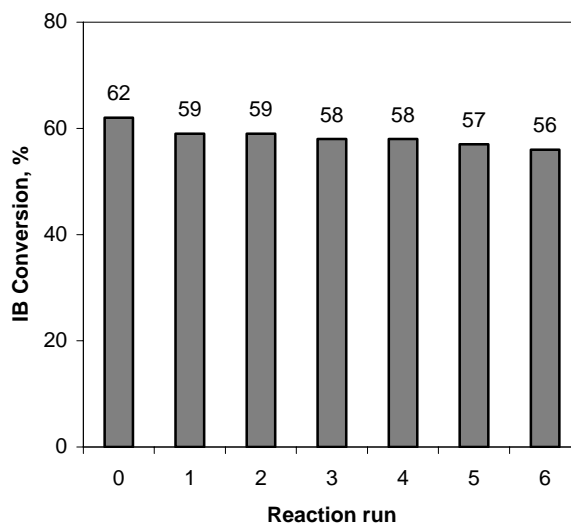


**Figure 5.12:** Recycle study with ossified catalyst 1D

**Reaction conditions:** Iodobenzene:  $0.24 \text{ kmol/m}^3$ , *n*-Butyl acrylate:  $0.301 \text{ kmol/m}^3$ , NaOAc:  $0.302 \text{ kmol/m}^3$ , Ossified catalyst 1D:  $6.3 \times 10^{-7} \text{ kg/m}^3$  (Pd: 0.34% -w/w), Solvent: DMF, Total Volume:  $1 \times 10^{-5} \text{ m}^3$ , Time, 60 mins, Reflux

There was a small fall in the conversions of iodobenzene on recycling the ossified catalyst precursors. All the catalysts were recycled 7 times and were found to retain their activity. The liquid phase was also recycled for all these catalyst precursors and was not found to give any significant conversions of iodobenzene ( $< 5\%$  for the recycle of the liquid phase of the fresh run and  $< 2\%$  for the recycle of the liquid phase of the subsequent runs). For these catalysts too the palladium content in the solution for the first run was in the range of 1-2 %. For subsequent recycle runs the amount of palladium leaching was less than 1% in all the cases.

### 5.3.2.2. Comparison of different ossified complexes

After testing these ossified palladium catalyst precursors for recyclability, a comparison of the activities of these catalysts was carried out. The results obtained are presented in Figure 5.13.

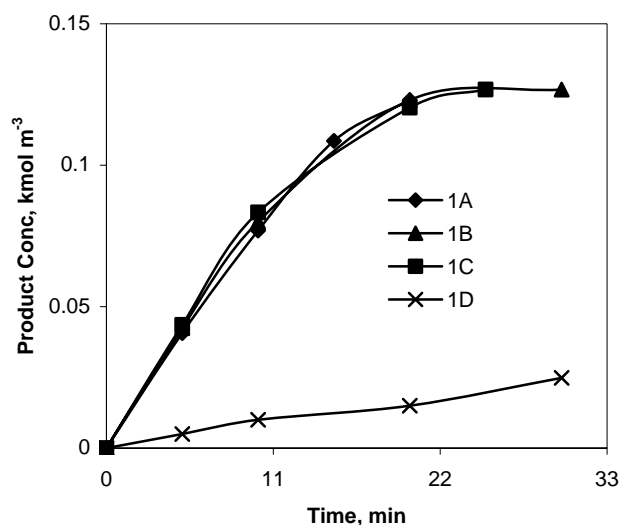


**Figure 5.13:** Comparison of different ossified palladium complexes in Heck reaction  
**Reaction conditions:** Iodobenzene:  $0.122 \text{ kmol/m}^3$ , *n*-Butyl acrylate:  $0.149 \text{ kmol/m}^3$ , NaOAc:  $0.151 \text{ kmol/m}^3$ , Ossified catalyst:  $5 \times 10^{-7} \text{ kg/m}^3$ , Solvent: DMF, Total Volume:  $2 \times 10^{-5} \text{ m}^3$ , Reflux

The results obtained with ossified palladium complexes 1A to 1C were similar. The reaction was complete in 20 minutes (>98% conversion of iodobenzene). When the ossified palladium complex 1D was used, the reaction was very slow. This can be attributed to the strong binding of the two nitrogen atoms to palladium. In the case of ossified complexes 1A to 1C the presence of oxygen provides for a labile ligand, which can dissociate and allow the palladium to oxidatively add to aryl halide. When the palladium is bound by two nitrogen atoms, there is no labile ligand present that can vacate a binding site for the oxidative addition of aryl halide to take place.

A Heck vinylation reaction of iodobenzene (49 mmol) with n-butyl acrylate (57.4 mmol) in presence of sodium acetate (57.4 mmol) and DMF solvent (total volume 35 ml) was carried out with ossified catalyst 1A 1.3 mg (Pd content: 0.33% w/w). The reaction was carried out as described in the experimental section. The concentration- time profile for the reaction showed that the catalyst was uniformly active throughout the reaction and there was no slowing down of the reaction rate. This observation further highlights the fact that the ossified catalyst was stable under the reaction conditions and did not deactivate during the course of the reaction. For this reaction, iodobenzene conversion of 79% was obtained after 48 hours of reaction time. This conversion corresponds to a TON of  $9.7 \times 10^5$  based on palladium mole%, and a TOF of  $2 \times 10^4 \text{ h}^{-1}$ . The results thus obtained are comparable to the best TON of  $1.05 \times 10^6$  reported with immobilized palladium complexes for Heck vinylation of iodobenzene with n-butyl acrylate using tributylamine as base<sup>11</sup>. This ossified palladium complex was used for the further studies on the Heck vinylation reactions.

### 5.3.2.3. Screening of bases for the Heck reaction

Effect of different organic and inorganic bases on the Heck reaction of iodobenzene with n-butyl acrylate was investigated. The results obtained are presented in Figure 5.14.

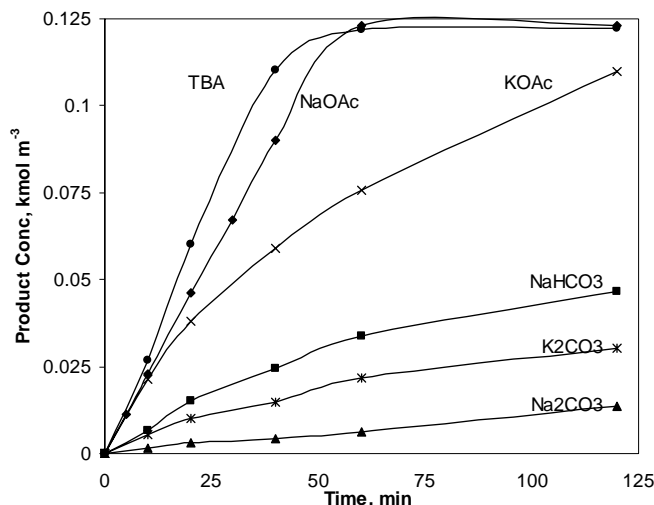


**Figure 5.14:** Effect of different bases on the Heck reaction using ossified 1A catalyst  
**Reaction conditions:** IB:  $0.122 \text{ kmol/m}^3$ , n-BA:  $0.149 \text{ kmol/m}^3$ , Base:  $0.151 \text{ kmol/m}^3$ ,  
 Ossified catalyst 1A:  $1.5 \times 10^{-7} \text{ kg/m}^3$  (Pd: 0.33% w/w), Solvent: DMF, Total Volume:  $2 \times 10^{-5} \text{ m}^3$ , Reflux

Carbonate and bicarbonate bases did not turn out to be good bases for these reactions under the reaction conditions studied. Potassium acetate gave better results than the carbonate bases. Sodium acetate was the best inorganic base for these reactions. Amongst the organic and inorganic bases screened, tri-butylamine gave the highest rates which were slightly higher than those obtained with sodium acetate.

#### 5.3.2.4. Screening of aryl halides for the Heck reaction

After the screening of bases, different aryl halides were screened for the Heck reaction with n-butyl acrylate in presence of NaOAc as base. Iodo, bromo and chloro arenes were screened for their reactivity in presence of the ossified catalyst 1A. No reaction was observed when the vinylation of 4'-chloroacetophenone with n-butyl acrylate was carried out. The results obtained with iodo and bromo arenes are presented in Figure 5.15.



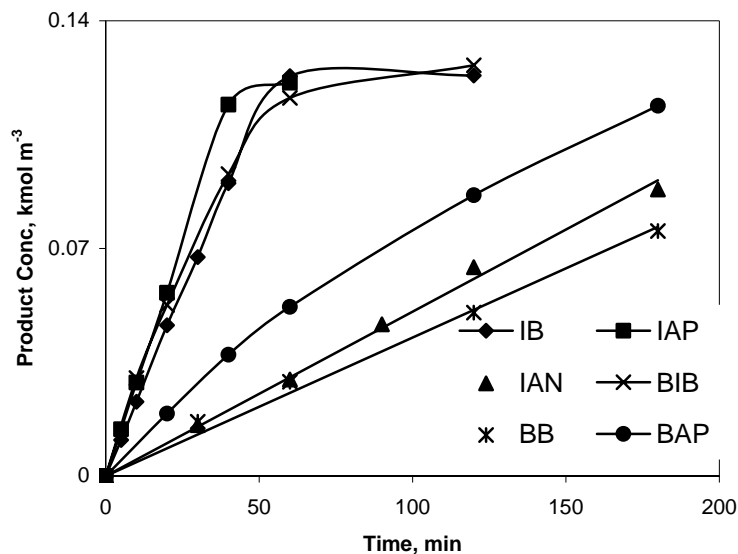


**Figure 5.15:** Activity of ossified catalyst 1A for Heck reaction of different aryl halides  
**Reaction conditions:** Aryl halide:  $0.122 \text{ kmol/m}^3$ , *n*-BA:  $0.149 \text{ kmol/m}^3$ , NaOAc:  $0.151 \text{ kmol/m}^3$ , Ossified catalyst 1A:  $1.5 \times 10^{-7} \text{ kg/m}^3$  (Pd: 0.33% w/w), Solvent: DMF, Total Volume:  $2 \times 10^{-5} \text{ m}^3$ , Reflux  
 IB: Iodobenzene, IAP: 4'-Iodoacetophenone, IAN: 4'-Iodoanisole, BIB: 4'-Bromoiodobenzene, BB: Bromobenzene, BAP: 4'-Bromoacetophenone

The arenes were chosen so as to study the effect of electron donating and electron withdrawing substituents on the aromatic ring. It was observed that the electron withdrawing substituents on the aromatic ring led to higher reaction rate, whereas, the presence of electron donating substituents on the aromatic ring decreased the rate of Heck reaction. These results were similar to those observed with homogeneous catalysts. Bromo arenes gave lower reaction rates than their iodo counterparts. This is to be expected in Heck reactions due to the easier cleavage of C-I bond as compared to C-Br bond for the oxidative addition step. When the reaction was carried out with 4-bromo iodobenzene, the vinylation occurred exclusively at the carbon atom bearing the iodo group. No product corresponding to double vinylation or the exclusive vinylation of carbon bearing the bromo group was observed.

### 5.3.2.5. Screening of olefins for the Heck reaction

Various olefins were screened for the Heck reaction with iodobenzene in presence of NaOAc as base using catalyst 1A. The results obtained are presented in Figure 5.16.

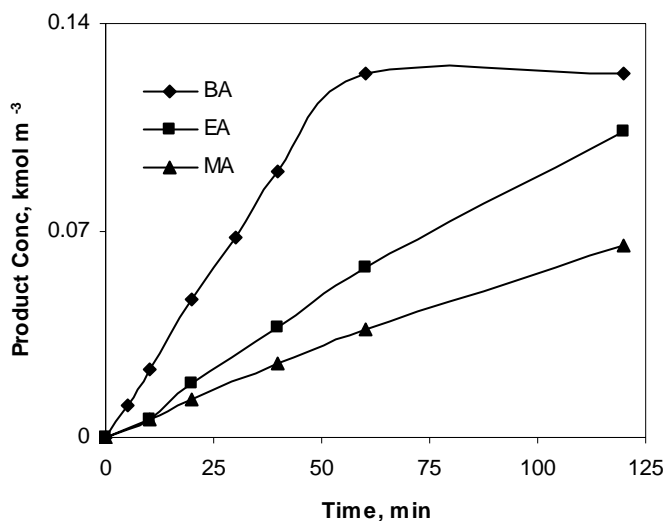
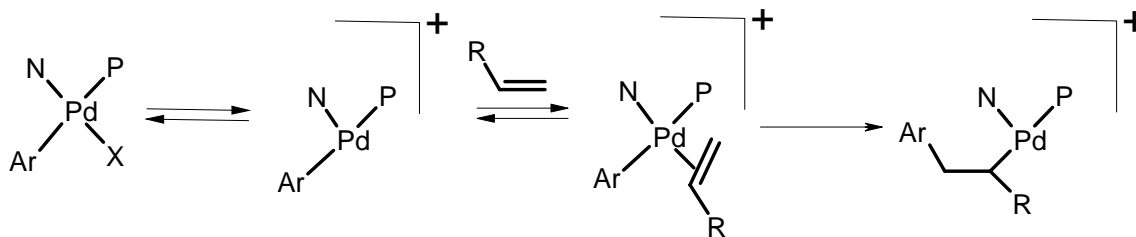


**Figure 5.16:** Activity of ossified catalyst 1A for Heck reaction of different olefins

**Reaction conditions:** IB:  $0.122 \text{ kmol/m}^3$ , Olefin:  $0.149 \text{ kmol/m}^3$ , NaOAc:  $0.151 \text{ kmol/m}^3$ , Ossified catalyst 1A:  $1.5 \times 10^{-7} \text{ kg/m}^3$  (Pd: 0.33% w/w), Solvent: DMF, Total Volume:  $2 \times 10^{-5} \text{ m}^3$ , Reflux

MA: Methyl acrylate, EA: Ethyl acrylate, BA: Butyl acrylate

Very low reaction rates were observed for the reaction of methyl and ethyl acrylates as compared to n-butyl acrylate. This was in total contrast to the results obtained in the case of homogeneous catalysts. This is similar to the earlier reports with the Pd- TPPTS complexes<sup>12</sup>. The olefin addition and insertion into the palladium complex during the catalytic reaction probably takes place by the cationic pathway (Scheme 5.4)<sup>13</sup>. Since the palladium complex is electron deficient, the olefins with higher electron density will react faster than the olefins with lower electron density. This is what is observed experimentally as n-butyl acrylate reacts faster than methyl acrylate.



Scheme 5.4

## 5.4. Conclusions

A novel approach to immobilize the palladium complexes termed “ossification” has been discussed in this chapter. Four different water soluble palladium complexes were synthesized and then precipitated using the ossification technique. These ossified catalysts were characterized using techniques like  $^{31}\text{P}$  Cp-MAS NMR, XRD, XPS, SEM etc. These catalysts were found to be active for Heck reactions, giving < 1% metal leaching during the reaction. The catalysts were recycled 7 times without any significant loss in activity. Various aryl halides, olefins, and bases were screened with these complexes. TON of  $9.7 \times 10^5$  based on the palladium mole% was obtained for the reaction of iodobenzene with n-butyl acrylate which was comparable to the best TON reported in the literature for Heck reactions using heterogeneous catalysts.

## 5.5. References

- 1 a) Yu, K.; Sommer, W.; Weck, M.; Jones, C. W. *J. Catal.* **2004**, 226, 101 b) Arellana, C. G.; Corma, A.; Iglesias, M.; Sanchez, F. *Adv. Synth. Catal.* **2004**, 346, 1758 c) Lagasi, M.; Moggi, P. *J. Mol. Catal. A: Chem.* **2002**, 182, 61 d) Zhao, S. F.; Zhou, R. X.; Zheng, X. M. *J. Mol. Catal. A: Chem.* **2004**, 211, 139 e) Cassol, C. C.; Umpierre, A. P.; Machado, G.; Wolke, S. I.; Dupont, J. *J. Am. Chem. Soc.* **2005**, 127, 3298 f) Yi, P.; Zhuangyu, Z.; Hongwen, H. *J. Mol. Catal.* **1990**, 62, 297
- 2 a) Yeung, L. K.; Crooks, R. M. *Nano Lett.* **2001**, 1, 1, 14 b) Djakovitch, L.; Heise, H.; Kohler, K. *J. Organomet. Chem.* **1999**, 584, 16 c) Price, K. E.; Mcquade, D. T. *Chem. Commun.* **2005**, 1714
- 3 a) Lin, C. A.; Luo, F. T. *Tetrahedron Lett.* **2003**, 44, 7565 b) Shokouhimehr, M.; Kim, J. H.; Lee, Y. S. *Synlett.* **2006**, 4, 618 c) Zhuangyu, Z.; Hongwen, H.; Yu, K. T. *React. Polym.* **1988**, 9, 249 d) Zhuangyu, Z.; Hongwen, H.; Yu, K. T. *React. Polym.* **1990**, 12, 229 e) McNamara, C. A.; King, F.; Bradley, M. *Tetrahedron Lett.* **2004**, 45, 8239 f) Bergbreiter, D. E. *Catalysis Today* **1998**, 42, 389
- 4 a) Retz, M. T.; Lohmer, G.; Schwickardi, R. *Angew. Chem. Int. Ed. Engl.* **1997**, 36, 1526 b) Smith, G. S.; Mapolie, S. P. *J. Mol. Catal. A: Chem.* **2004**, 213, 187

- 
- 5 a) Davis, M. E. *CHEMTECH* **1992**, 498 b) Tonks, L.; Anson, M. S.; Hellgardt, K.; Mirza, A. R.; Thompson, D. F.; Williams, J. M. J. *Tetrahedron Lett.* **1997**, 38, 4319 c) Anson, M. S.; Mirza, A. R.; Tonks, L.; Williams, J. M. J. *Tetrahedron Lett.* **1999**, 40, 7147
- 6 a) Chaudhari, R. V.; Mahajan, A. N. *US 7026266*, **2003** b) Sarkar, B. R.; Chaudhari, R. V. *J. Catal.* **2006**, 242, 231 c) Pagar, N. S.; Deshpande, R. M.; Chaudhari, R. V. *Catal. Lett.* **2006**, 110, 129
- 7 Bhanage B. M., Divekar S. S., Deshpande R. M., Chaudhari R. V., *Org. Process Res. Dev.* **2000**, 4(5), 342
- 8 Jayasree S., Seayad A., Chaudhari R. V., *Org. Lett.*, **2000**, 2(2), 203
- 9 Jayasree S., Seayad A., Chaudhari R. V., *Chem. Commun.*, **2000**, 1239
- 10 Phan, N. T. S.; Sluys, M. V. D.; Jones, C. W. *Adv. Synth. Catal.* **2006**, 348, 609
- 11 Tsai, F. Y.; Wu, C. L.; Mou, C. Y.; Chao, M. C.; Lin, H. P.; Liu, S. T.; *Tetrahedron Lett.* **2004**, 45, 7503
- 12 Bhanage, B. M.; Shirai, M.; Arai, M. *J. Mol. Catal. A: Chem.* **1999**, 145, 69
- 13 a) Ozawa, F.; Kubo, A.; Hayashi, T. *J. Am. Chem. Soc.* **1991**, 113, 1417 b) Cabri, W.; Candiani, I.; DeBernardinis, S.; Francalanci, F.; Penco, S.; Santi, R. *J. Org. Chem.* **1991**, 56, 5796 c) Sato, Y.; Sodeoka, M.; Shibasaki, M. *Chem. Lett.* **1990**, 10, 1953 d) Beletskaya, I. P.; Cheprakov, A. V. *Chem. Rev.* **2000**, 100, 3009

*Chapter 6:*

*Kinetics of Heck Vinylation of  
Iodobenzene with n-Butyl acrylate Using  
Ossified Pd(Pyca)(TPPTS) Catalyst*

## 6.1. Introduction

The literature on kinetics of Heck reactions using homogeneous catalysts is scanty and very few detailed studies have been done as discussed in Chapter 1, Section 1.6<sup>1-6</sup>. For Heck reactions using heterogeneous catalysts, there are practically no studies on the kinetics. The exact mechanism of the Heck reaction catalyzed by heterogeneous catalysts needs detailed investigation<sup>7-9</sup>. Whether the true catalytic species remains bound to the solid support during the reaction or whether the reaction is carried out by the leached catalytic species in a homogeneous phase still remains unanswered. Keeping this in mind a detailed kinetic study on the Heck vinylation of iodobenzene with n-butyl acrylate using sodium acetate base with the ossified Pd(Pyca)(TPPTS) catalyst was undertaken in the temperature range of 403–433 K. The effect of concentrations of catalyst, iodobenzene, n-butyl acrylate, and NaOAc on the rate of reaction was studied. The rate was found to be first order with respect to iodobenzene and catalyst concentration. The rates were first order tending to zero order with n-butyl acrylate and NaOAc concentration. A similar study using the analogous non-ossified catalyst was also undertaken in a DMF medium to compare the performance of the homogeneous catalyst. The rate data were analyzed to propose an empirical model. A mechanistic model was also developed and was found to be in good agreement with the experimental data.

## 6.2. Experimental

### General procedure for Heck reaction

Iodobenzene 2.4 mmol, n-butyl acrylate 3.0 mmol, NaOAc 3.0 mmol, and ossified palladium catalyst 5 mg (Pd: 0.33 % w/w) were taken in DMF solvent in a 50 ml 2 necked glass reactor under nitrogen atmosphere (total volume 20 ml). The glass reactor was equipped with a reflux condenser, a magnetic stirrer, and a septum to withdraw the intermediate reaction samples. The reactor was immersed in an oil bath preheated to the desired temperature. The reaction was then started by switching the stirrer on. Samples were withdrawn at regular intervals, filtered and analyzed for iodobenzene conversion and n-butyl cinnamate formed. Some reactions were carried out to complete conversion, following which the product was identified, isolated and characterized as described earlier (Chapter 2, Section 2.2).

For kinetic analysis the reactions were carried out for short durations such that the conversion of the iodobenzene was less than 20% to ensure differential conditions. The initial rates of the reaction were calculated from the plots of formation of the product n-butyl cinnamate as a function of time, in a region where the conversion of iodobenzene was less than 20%.

### 6.3. Preliminary experiments

A few preliminary experiments were carried out on the vinylation of iodobenzene with n-butyl acrylate, using ossified catalyst **1** to assess the material balance of reactants/products. A typical concentration-time profile for the reaction is presented in Figure 6.1. The consumption of iodobenzene and the formation of n-butyl cinnamate were monitored by GC. The consumption of iodobenzene was found to be stoichiometrically consistent with the formation of n-butyl cinnamate according to the Scheme 6.1 in all the experiments. Under all the conditions employed in these studies, there was more than 96 % material balance with respect to iodobenzene and n-butyl acrylate consumption and n-butyl cinnamate formation. Only a single product was formed under the reaction conditions.

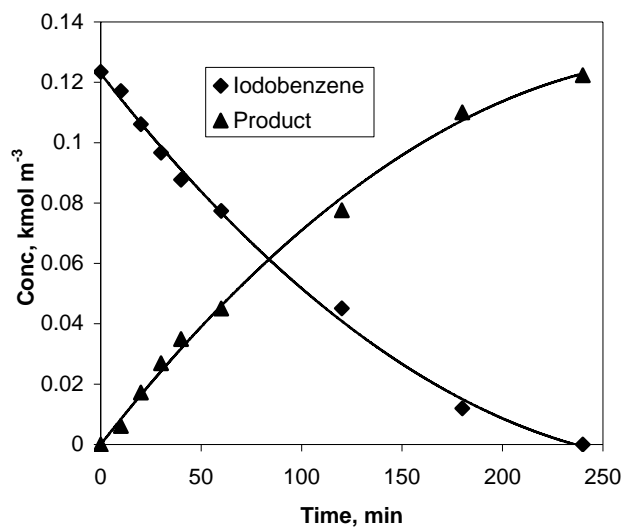
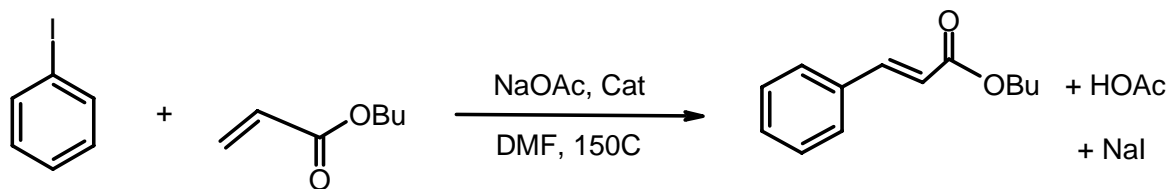
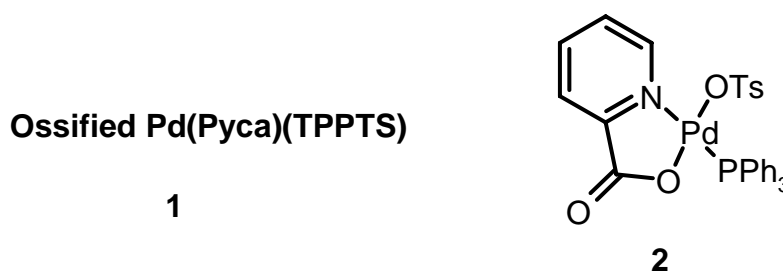


**Figure 6.1:** CT profile for the Heck reaction with ossified catalyst **1**

**Reaction conditions:** Iodobenzene:  $0.122 \text{ kmol/m}^3$ , n-Butyl acrylate:  $0.149 \text{ kmol/m}^3$ , NaOAc:  $0.151 \text{ kmol/m}^3$ , Ossified catalyst **1**:  $2.5 \times 10^{-7} \text{ kg/m}^3$  (Pd: 0.33 % w/w), Solvent: DMF, Temp: 423 K, Total Volume:  $2 \times 10^{-5} \text{ m}^3$



Scheme 6.1



Scheme 6.2

For the kinetic study, several experiments were carried out in the range of conditions shown in Table 6.1.

**Table 6.1:** Range of conditions investigated for kinetic study

Loading of ossified catalyst ( $\text{kg m}^{-3}$ ) (Pd: 0.33 % w/w)	$1 \times 10^{-7}$ to $5 \times 10^{-7}$
Concentration of iodobenzene ( $\text{kmol m}^{-3}$ )	0.0245 to 0.172
Concentration of n-butyl acrylate ( $\text{kmol m}^{-3}$ )	0.078 to 0.273
Concentration of sodium acetate ( $\text{kmol m}^{-3}$ )	0.091 to 0.305
Temperature (K)	403 to 423

The initial rates were calculated from the observed data on the formation of n-butyl cinnamate as a function of time. The rate of reaction was calculated from the slope of product formed vs. time plot. A typical plot of the formation of n-butyl cinnamate at different loadings of ossified catalyst **1** at 423 K used for the calculation of the rates is shown in Figure 6.2.



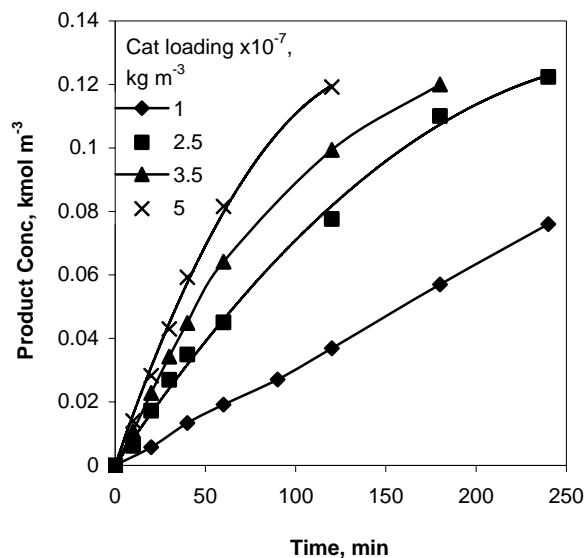


**Figure 6.2:** CT profile for the product formation at 423 K with different loading of ossified catalyst

**Reaction conditions:** Iodobenzene:  $0.122 \text{ kmol/m}^3$ , *n*-Butyl acrylate:  $0.149 \text{ kmol/m}^3$ , NaOAc:  $0.151 \text{ kmol/m}^3$ , Ossified catalyst I: (Pd: 0.33 % w/w), Solvent: DMF, Temp: 423 K, Total Volume:  $2 \times 10^{-5} \text{ m}^3$

The dependence of the rate on the various parameters was investigated at three different temperatures. The results showing the dependence of the rates on different parameters and the kinetic modeling of the observed data are discussed below.

### 6.3.1. Effect of catalyst concentration on the rate of reaction

The effect of the catalyst loading on the rate was studied at constant iodobenzene, *n*-butyl acrylate, and NaOAc concentrations of  $0.122 \text{ kmol/m}^3$ ,  $0.149 \text{ kmol/m}^3$ , and  $0.151 \text{ kmol/m}^3$  respectively, in the temperature range of 403 K to 423 K. A concentration time profile was obtained for each experiment. The profile for product formation at different loading of ossified catalyst at 423 K is presented in Figure 6.2. From the initial rates, a graph of initial rate vs. catalyst loading was plotted as shown in Figure 6.3.

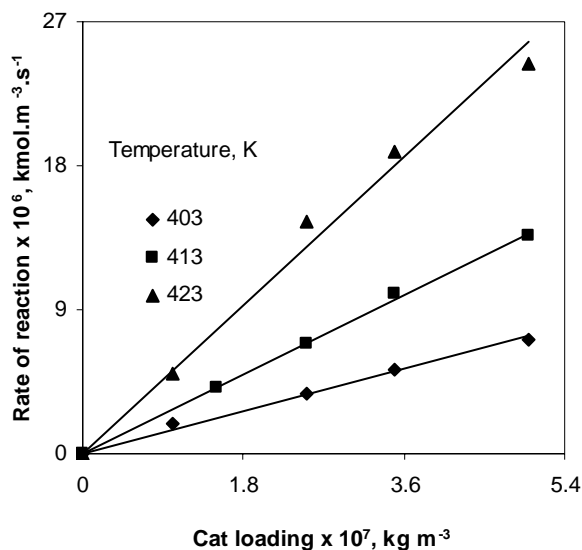


**Figure 6.3:** Plot of initial rate vs ossified catalyst **1** loading at different temperatures  
*Reaction conditions:* Iodobenzene:  $0.122 \text{ kmol/m}^3$ , *n*-Butyl acrylate:  $0.149 \text{ kmol/m}^3$ , NaOAc:  $0.151 \text{ kmol/m}^3$ , Ossified catalyst **1**: (Pd: 0.33 % w/w), Solvent: DMF, Total Volume:  $2 \times 10^{-5} \text{ m}^3$

Since the ossified Pd(Pyca)(TPPTS) catalyst has been investigated for the first time for the kinetics of Heck reactions, it was necessary to also understand the behavior of the catalyst for Heck reaction under homogeneous conditions. For this purpose, reactions were carried out using Pdpyca catalyst **2** at different concentrations under homogeneous conditions. The results obtained are presented in Figure 6.4.

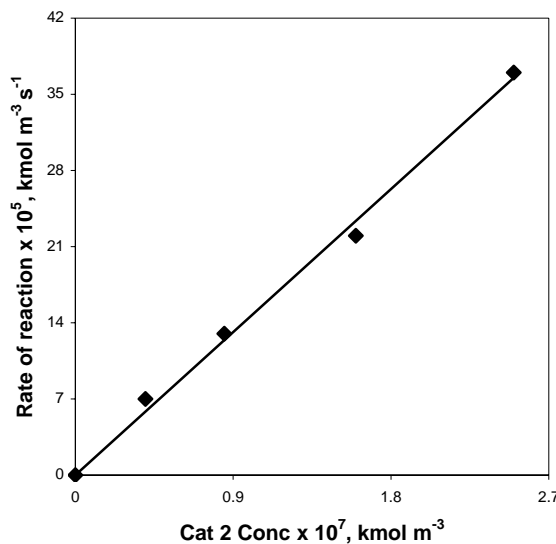


**Figure 6.4:** Plot of initial rate vs concentration of **2** at 423 K

**Reaction conditions:** Iodobenzene:  $0.122 \text{ kmol/m}^3$ , *n*-Butyl acrylate:  $0.149 \text{ kmol/m}^3$ , NaOAc:  $0.151 \text{ kmol/m}^3$ , Catalyst Precursor **2**, Solvent: DMF, Temperature: 423 K, Total Volume:  $2 \times 10^{-5} \text{ m}^3$

When the ossified catalyst **1** was used the rates showed a first order dependence on the catalyst concentration. This is to be expected because as the concentration of the catalyst increases, more and more of iodobenzene gets converted into the product. This trend was similar to that observed with the catalyst **2** under homogeneous reaction conditions. These trends were different than the trends observed for the Heck reaction with P-C and N-C palladacycle catalysts reported earlier<sup>4,9-10</sup>. In the P-C and N-C catalyst precursors, the rates showed a partial order dependence on the catalyst concentration due to the formation of a dimer that is inactive for the Heck reactions. This dimer is formed from the active monomeric species in equilibrium (Chapter 3, Scheme 3.3). For both the catalysts, the dimeric species is probably not formed in the present case and hence a first order is observed.

### 6.3.2. Effect of iodobenzene concentration on the rate of reaction

The effect of iodobenzene concentration on the activity was studied at constant n-BA and NaOAc concentrations of  $0.149 \text{ kmol/m}^3$  and  $0.151 \text{ kmol/m}^3$  respectively, at the catalyst **1** loading of  $2.5 \times 10^{-7} \text{ kg/m}^3$ , in a temperature range of 403-423 K. A concentration time profile was obtained for each experiment with different starting concentrations of iodobenzene.

The initial rate of product formation was calculated from the plot of n-butyl cinnamate formed vs time, considering the initial part of the curve, which represented the iodobenzene conversion of less than 20%. The results are presented in Figure 6.5.

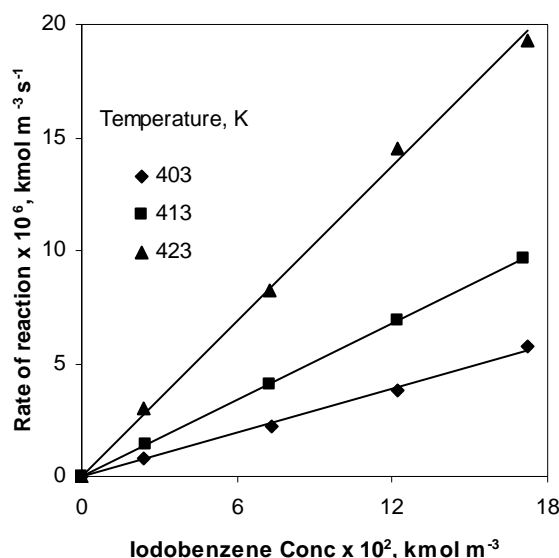


**Figure 6.5:** Plot of initial rate vs concentration of iodobenzene at different temperatures

**Reaction conditions:** Iodobenzene, n-Butyl acrylate:  $0.149 \text{ kmol/m}^3$ , NaOAc:  $0.151 \text{ kmol/m}^3$ , Ossified catalyst **1**:  $2.5 \times 10^{-7} \text{ kg/m}^3$  (Pd: 0.33 % w/w), Solvent: DMF, Total Volume:  $2 \times 10^{-5} \text{ m}^3$

The reactions were carried out at different initial concentrations of iodobenzene using catalyst **2** at 423 K in order to compare the trends observed using ossified catalyst with those observed under homogeneous conditions. The results obtained are presented in Figure 6.6.

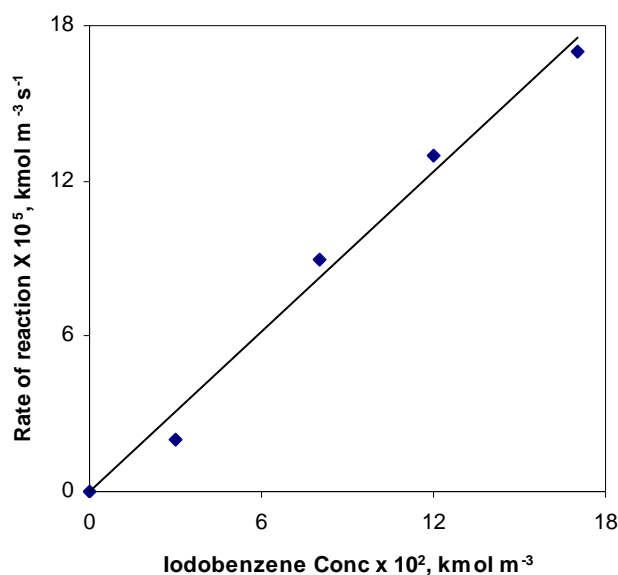
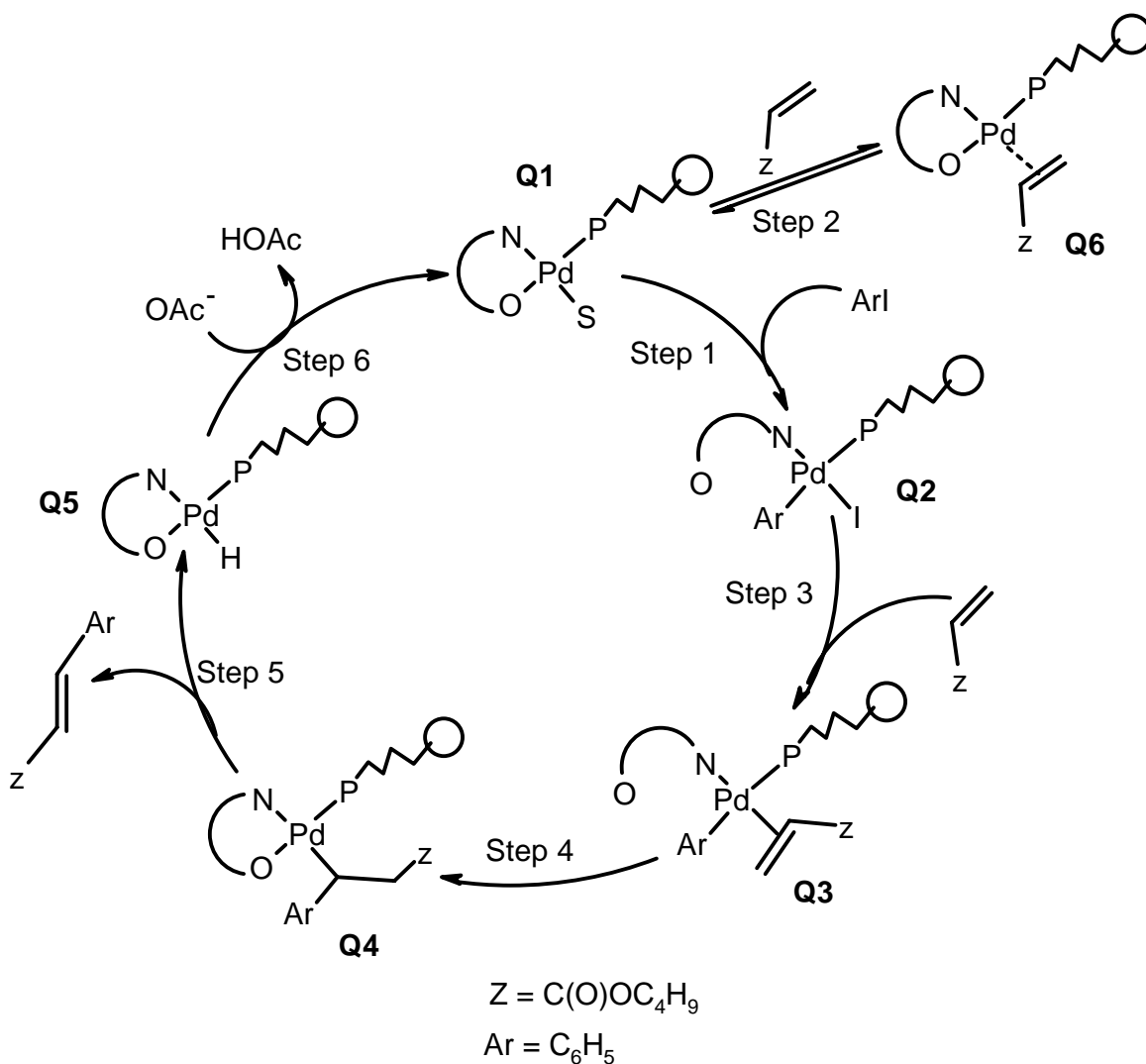


**Figure 6.6:** Plot of initial rate vs concentration of iodobenzene under homogeneous conditions at 423 K

**Reaction conditions:** Iodobenzene, *n*-Butyl acrylate:  $0.149 \text{ kmol/m}^3$ , NaOAc:  $0.151 \text{ kmol/m}^3$ , Catalyst precursor **2**:  $8.5 \times 10^{-8} \text{ kmol/m}^3$ , Solvent: DMF, Temperature: 423 K, Total Volume:  $2 \times 10^{-5} \text{ m}^3$

The rate was found to increase with the increase in the concentration of IB. The ArX moiety oxidatively adds to the catalytic species Q1 in the catalytic cycle shown in Scheme 6.3. The oxidative addition proceeds as a concerted step, where the C-I bond cleavage is perfectly synchronized with the formation of Pd-C and Pd I bonds<sup>11</sup>. This step is usually considered to be the rate-determining step in the catalytic cycle<sup>12</sup>. As the concentration of the IB increases it leads to more and more generation of the active species and hence the linear dependence on the IB concentration is observed. A similar trend was observed for the reaction with the catalyst precursor **2** under the homogeneous conditions. The earlier kinetic studies carried out using P-C palladacycle catalysts (Chapter 3) also gave the first order dependence of the rate on the concentration of aryl halide. These observations were similar to earlier report by Zhao et al<sup>1</sup> for the homogeneous kinetics of Heck reaction of iodobenzene with methyl acrylate using Pd(OAc)<sub>2</sub>/PPh<sub>3</sub> as the catalyst precursor. Dupont et al<sup>5</sup> report saturation kinetics (first order at lower concentration and

zero order at higher concentration) for  $\text{PhI}$  concentration for the reaction of iodobenzene with n-BA.



**Scheme 6.3**

### 6.3.3. Effect of n-butyl acrylate concentration on the rate of reaction

The effect of n-butyl acrylate concentration on the activity was studied at constant iodobenzene and NaOAc concentrations of  $0.122 \text{ kmol/m}^3$  and  $0.151 \text{ kmol/m}^3$  respectively, at ossified catalyst **1** loading of  $2.5 \times 10^{-7} \text{ kg/m}^3$  in a temperature range of 403-423 K. A

concentration time profile was obtained for each experiment with different starting concentrations of n-butyl acrylate. The results are shown in Figure 6.7.

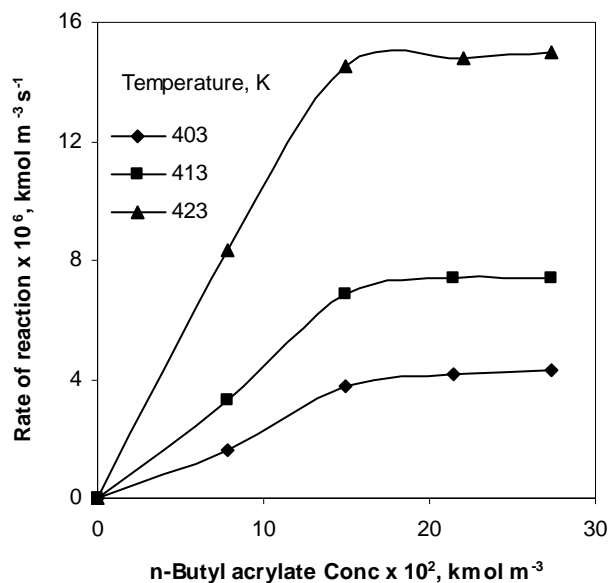


**Figure 6.7:** Plot of initial rate vs concentration of n-butyl acrylate at different temperatures  
**Reaction conditions:** Iodobenzene 0.122 kmol/m<sup>3</sup>, n-Butyl acrylate, NaOAc: 0.151 kmol/m<sup>3</sup>, Ossified catalyst **1**: 2.5 x 10<sup>-7</sup> kg/m<sup>3</sup> (Pd: 0.33 % w/w), Solvent: DMF, Total Volume: 2 x 10<sup>-5</sup> m<sup>3</sup>

The reactions were carried out at different initial concentrations of n-butyl acrylate using catalyst **2** in order to compare the trends observed using the ossified catalyst with those observed under homogeneous conditions. The results obtained are presented in Figure 6.8.

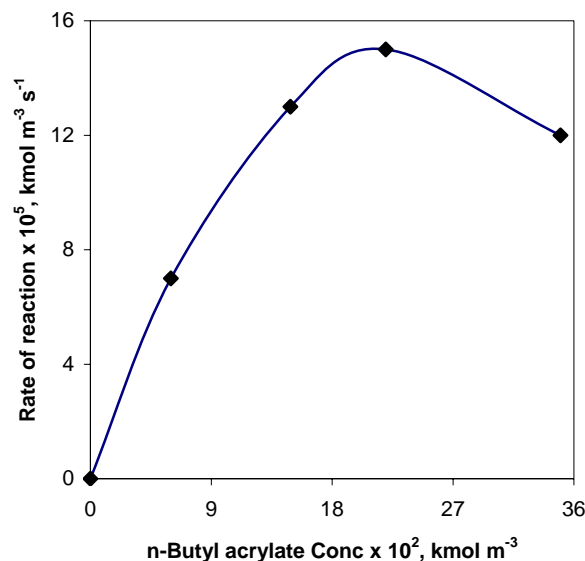


**Figure 6.8:** Plot of initial rate vs concentration of n-butyl acrylate under homogeneous conditions at 423 K

**Reaction conditions:** Iodobenzene:  $0.122 \text{ kmol/m}^3$ , n-Butyl acrylate, NaOAc:  $0.151 \text{ kmol/m}^3$ , Catalyst precursor **2**:  $8.5 \times 10^{-8} \text{ kmol/m}^3$ , Solvent: DMF, Temperature: 423 K, Total Volume:  $2 \times 10^{-5} \text{ kmol/m}^3$

The rates initially increased with the increase in n-butyl acrylate concentration ( $< 0.15 \text{ kmol/m}^3$ ) and then were constant for the reaction with the ossified palladium catalyst **1**. When the reaction was carried out under the homogeneous conditions with the catalyst precursor **2**, the rates initially increased with increase in n-butyl acrylate concentration ( $< 0.22 \text{ kmol/m}^3$ ) and then decreased. This behavior was similar to that observed when the reactions were carried out with P-C palladacycle catalyst as a precursor (Chapter 3).

#### 6.3.4. Effect of NaOAc concentration on the rate of reaction

The effect of variation of sodium acetate concentration on the activity was studied at constant iodobenzene and n-butyl acrylate concentrations of  $0.122 \text{ kmol/m}^3$  and  $0.149 \text{ kmol/m}^3$  respectively, at catalyst **1** loading of  $2.5 \times 10^{-7} \text{ kg/m}^3$  in a temperature range of 403-423 K. The results are shown in Figure 6.9.



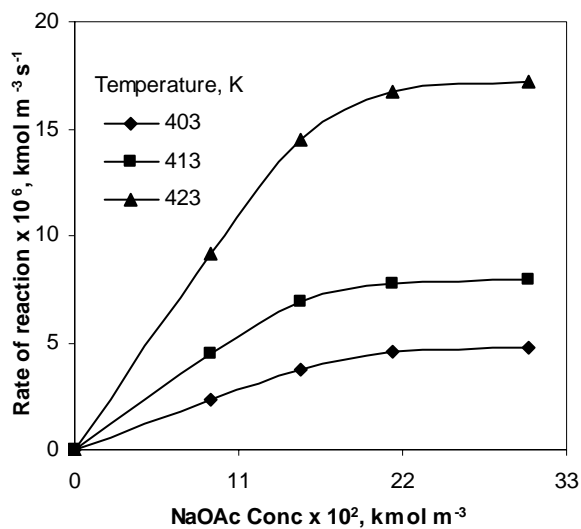


**Figure 6.9:** Plot of initial rate vs concentration of sodium acetate at different temperatures  
**Reaction conditions:** Iodobenzene  $0.122 \text{ kmol/m}^3$ , *n*-Butyl acrylate:  $0.149 \text{ kmol/m}^3$ , NaOAc, Ossified catalyst **1**:  $2.5 \times 10^{-7} \text{ kg/m}^3$  (Pd: 0.33 % w/w), Solvent: DMF, Total Volume:  $2 \times 10^{-5} \text{ m}^3$

The reactions were carried out at different initial concentrations of sodium acetate using catalyst **2** at 423 K in order to compare the trends observed using ossified catalyst with those observed under homogeneous conditions. The results are presented in Figure 6.10.

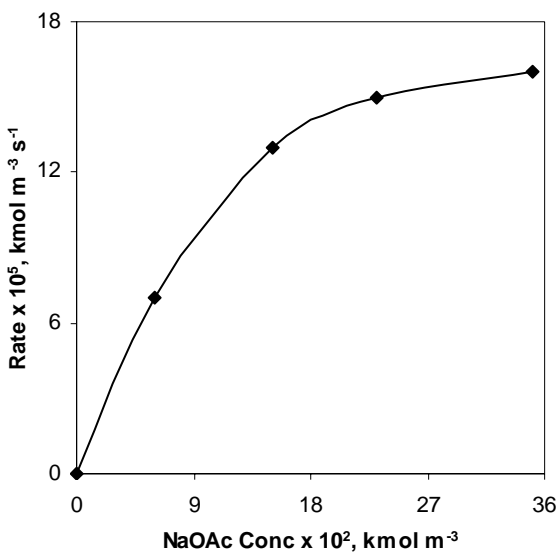


**Figure 6.10:** Plot of initial rate vs concentration of sodium acetate under homogeneous conditions at 423 K

**Reaction conditions:** Iodobenzene:  $0.122 \text{ kmol/m}^3$ , *n*-Butyl acrylate:  $0.149 \text{ kmol/m}^3$ , NaOAc, Catalyst precursor **2**:  $8.5 \times 10^{-8} \text{ kmol/m}^3$ , Solvent: DMF, Temperature: 423 K, Total Volume:  $2 \times 10^{-5} \text{ m}^3$

The rate showed a linear dependence on NaOAc concentration in the lower concentration range ( $< 0.2 \text{ kmol/m}^3$ ). With further increase in NaOAc concentration the rate increased marginally with a near zero order dependence. This was similar to the trends observed under homogeneous reaction conditions with catalyst precursor **2**. Even in the case of P-C palladacycle catalyst precursor, a similar trend was observed (Chapter 3). Earlier reports by Dupont et al<sup>5</sup> too find the rates to be zero order with respect to base concentration with N-C palladacycle under homogeneous reaction conditions. Zhao et al<sup>1</sup> have reported the rates passing through a maximum with increase in base concentration.

The base is required for the regeneration of the active catalytic species by abstraction of H from the species Q5 as shown in Step 6 of Scheme 6.3. As the concentration of the base increases, a faster regeneration of active catalytic species takes place leading to an increase in the rate as observed. Further increase in the base concentration above a certain value does not lead to any additional enhancements in the

rate. This could be due to the solubility limitation of NaOAc in the organic solvent (DMF) at higher base concentration.

## 6.4. Kinetic Analysis

### 6.4.1. Empirical rate models and model discrimination

The kinetic data obtained earlier was used to develop a rate equation for the Heck reaction of iodobenzene and n-butyl acrylate. Based on the observed trends, a variety of empirical models were examined, and the best model was selected based on the criterion of the least average error between predicted and experimental rates ( $\Phi_{\min}$ ) which is defined as:

$$\Phi_{\min} = \sum_{i=1}^n (R_{\text{EXP}} - R_{\text{PRE}})^2 \quad \text{Eq 6.1}$$

Where  $R_{\text{EXP}}$  is the observed rate of reaction and  $R_{\text{PRE}}$  is the predicted rate obtained by using the respective models.

The rate parameters  $k$ ,  $K_B$ , and  $K_C$  were evaluated at 403, 413, and 423 K by fitting the experimental rate data with equations I to VI using non linear regression analysis and an optimization routine based on Marquardt's method<sup>13</sup>. The values of the rate parameters at different temperatures are presented in Table 6.2.

The values of  $\Phi_{\min}$  suggest the extent of fit of the kinetic models used (least value of the  $\Phi_{\min}$  shows the best fit).

$$\begin{array}{rcl}
 R & = & \frac{k[A][B][C][Q]}{(1 + K_B[B]) (1 + K_C[C])} \quad \text{Model I} \\
 R & = & \frac{k[A][B][C][Q]}{(1 + (K_B[B])^2) (1 + (K_C[C])^2)} \quad \text{Model II} \\
 R & = & \frac{k[A][B][C][Q]}{(1 + (K_B[B])^2) (1 + K_C[C])} \quad \text{Model III} \\
 R & = & \frac{k[A][B][C][Q]}{(1 + K_B[B]) (1 + (K_C[C])^2)} \quad \text{Model IV} \\
 R & = & \frac{k[A][B][C][Q]}{1 + K_B[B]} \quad \text{Model V} \\
 R & = & \frac{k[A][B][C][Q]}{1 + K_C[C]} \quad \text{Model VI}
 \end{array}$$

Models V and VI gave very high values for  $\Phi_{\min}$  and hence were rejected. Models I to IV had comparable  $\Phi_{\min}$  values. On comparison of the predicted values of the rates using these four models, it was observed that overall prediction using model I was closest to the experimental values. This model thus turned out to be superior amongst all the models considered. The activation energy was calculated using Arrhenius plot (Table 6.2 and Figure 6.11).

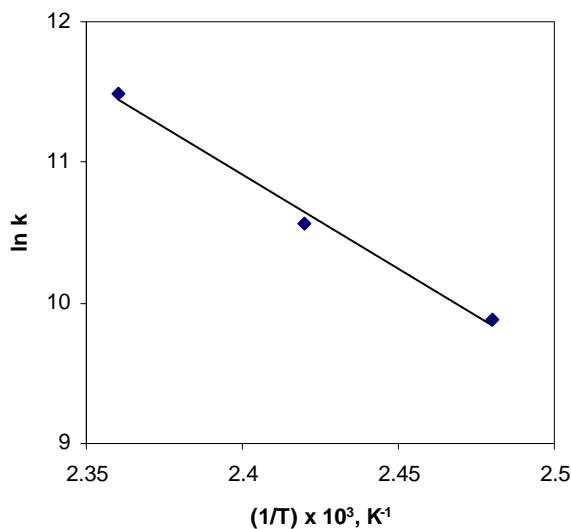


**Figure 6.11:** Temperature dependence of rate constant ( $k$ ) (Arrhenius plot)

The following model was found to best fit the data at all the temperatures studied.

$$R = \frac{k[A][B][C][Q]}{(1 + K_B[B])(1 + K_C[C])} \quad \text{Model I}$$

Where  $R$  is the rate of reaction, expressed in  $\text{kmol/m}^3/\text{s}$ ,  $[A]$  is the concentration of iodobenzene ( $\text{kmol/m}^3$ ),  $[B]$  is the concentration of n-butyl acrylate ( $\text{kmol/m}^3$ ),  $[C]$  is the concentration of NaOAc ( $\text{kmol/m}^3$ ), and  $[Q]$  is the loading of the ossified catalyst **1** ( $\text{kg/m}^3$ ).  $k$  is the rate constant, and  $K_B$  and  $K_C$  are equilibrium constants.

**Table 6.2:** Values of kinetic parameters at different temperatures

Mod	Temp, K	k	$K_B$	$K_C$	$\Phi_{\min} \times 10^4$
I	403	$1.96 \times 10^4$	7.37	4.98	$3.39 \times 10^{-12}$
	413	$3.86 \times 10^4$	8.45	5.19	$1.06 \times 10^{-11}$
	423	$9.70 \times 10^4$ ( $m^{12}/kg \text{ kmol}^3$ )	11.41 ( $m^3/\text{kmol}$ )	5.25 ( $m^3/\text{kmol}$ )	$3.31 \times 10^{-11}$
II	403	$8.71 \times 10^3$	3.81	3.07	$1.74 \times 10^{-12}$
	413	$1.61 \times 10^4$	4.02	3.10	$4.70 \times 10^{-12}$
	423	$3.39 \times 10^4$ ( $m^{12}/kg \text{ kmol}^3$ )	4.28 ( $m^3/\text{kmol}$ ) <sup>2</sup>	3.12 ( $m^3/\text{kmol}$ ) <sup>2</sup>	$2.07 \times 10^{-11}$
III	403	$1.28 \times 10^4$	3.76	5.39	$2.28 \times 10^{-12}$
	413	$2.39 \times 10^4$	3.98	5.51	$6.37 \times 10^{-12}$
	423	$5.12 \times 10^4$ ( $m^{12}/kg \text{ kmol}^3$ )	4.23 ( $m^3/\text{kmol}$ ) <sup>2</sup>	5.70 ( $m^3/\text{kmol}$ )	$2.49 \times 10^{-11}$
IV	403	$1.36 \times 10^4$	7.49	2.97	$2.94 \times 10^{-12}$
	413	$2.97 \times 10^4$	9.19	3.56	$7.68 \times 10^{-12}$
	423	$7.82 \times 10^4$ ( $m^{12}/kg \text{ kmol}^3$ )	12.63 ( $m^3/\text{kmol}$ )	4.01 ( $m^3/\text{kmol}$ ) <sup>2</sup>	$5.01 \times 10^{-11}$
V	403	$8.35 \times 10^3$	4.70		$1.32 \times 10^{-11}$
	413	$1.59 \times 10^4$	5.48		$5.49 \times 10^{-11}$
	423	$3.83 \times 10^4$ ( $m^{12}/kg \text{ kmol}^3$ )	7.73 ( $m^3/\text{kmol}$ )		$1.57 \times 10^{-10}$
VI	403	$4.65 \times 10^3$		4.99	$2.03 \times 10^{-11}$
	413	$8.31 \times 10^3$		5.19	$7.87 \times 10^{-11}$
	423	$1.67 \times 10^4$ ( $m^{12}/kg \text{ kmol}^3$ )		5.25 ( $m^3/\text{kmol}$ )	$2.87 \times 10^{-10}$

The fits obtained for the model I are presented in Figures 6.12 to 6.15.

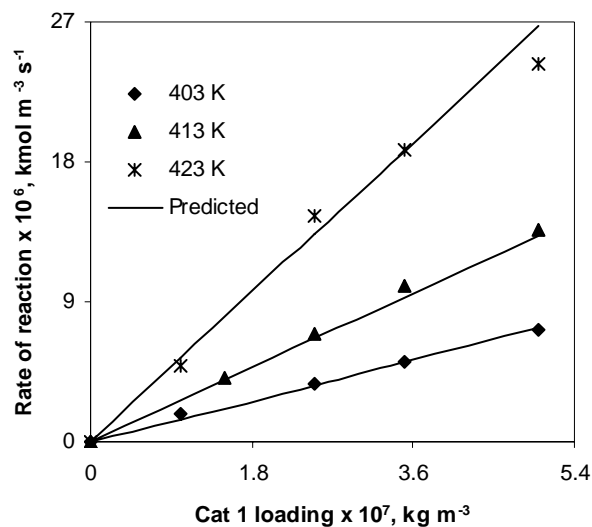


**Figure 6.12:** Plot of initial rate vs loading of ossified catalyst **1** at different temperatures  
*Reaction conditions:* Iodobenzene:  $0.122 \text{ kmol/m}^3$ , *n*-Butyl acrylate:  $0.149 \text{ kmol/m}^3$ , NaOAc:  $0.151 \text{ kmol/m}^3$ , Ossified catalyst **1**, Solvent: DMF, Total Volume:  $2 \times 10^{-5} \text{ m}^3$

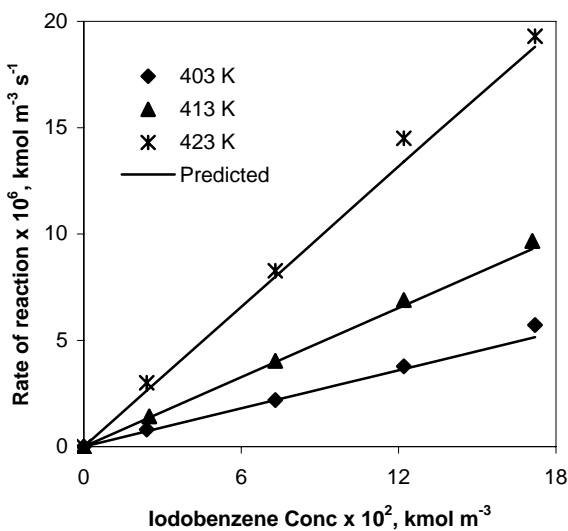


**Figure 6.13:** Plot of initial rate vs concentration of iodobenzene at different temperatures  
*Reaction conditions:* Iodobenzene, *n*-Butyl acrylate:  $0.149 \text{ kmol/m}^3$ , NaOAc:  $0.151 \text{ kmol/m}^3$ , Ossified catalyst **1**:  $2.5 \times 10^{-7} \text{ kg/m}^3$  (Pd: 0.33 % w/w), Solvent: DMF, Total Volume:  $2 \times 10^{-5} \text{ m}^3$

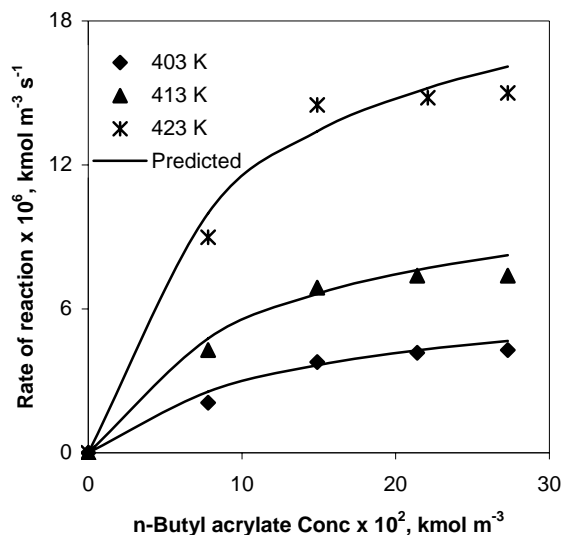


**Figure 6.14:** Plot of initial rate vs concentration of n-butyl acrylate at different temperatures

**Reaction conditions:** Iodobenzene  $0.122 \text{ kmol/m}^3$ , n-Butyl acrylate, NaOAc:  $0.151 \text{ kmol/m}^3$ , Ossified catalyst **I**:  $2.5 \times 10^{-7} \text{ kg/m}^3$  (Pd: 0.33 % w/w), Solvent: DMF, Total Volume:  $2 \times 10^{-5} \text{ m}^3$

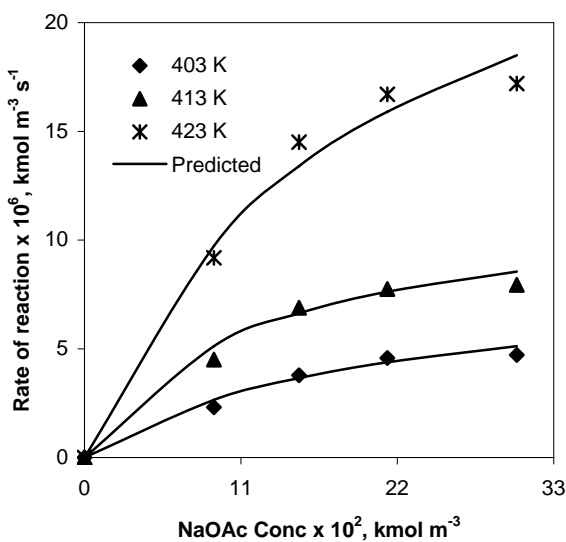


**Figure 6.15:** Plot of initial rate vs concentration of sodium acetate at different temperatures

**Reaction conditions:** Iodobenzene  $0.122 \text{ kmol/m}^3$ , n-Butyl acrylate:  $0.149 \text{ kmol/m}^3$ , NaOAc, Ossified catalyst **I**:  $2.5 \times 10^{-7} \text{ kg/m}^3$  (Pd: 0.33 % w/w), Solvent: DMF, Total Volume:  $2 \times 10^{-5} \text{ m}^3$



The rates predicted using model I were in very good agreement with the experimentally obtained rates as is evident for the Figures 6.12 to 6.15. A comparison of the experimental rates with the predicted rates using model I is also shown on Figure 6.16, which too indicates a very good agreement between experimental and predicted values. The average percent error between the experimental and predicted data was 1.06 %. The activation energy for this model was calculated to be 110.81 kJ/mol from the Arrhenius plot (Figure 6.11). The dependence of  $K_B$  and  $K_C$  on temperature was also studied and is shown in Figure 6.17 for Model I. The dependence of  $K_C$  on the temperature was marginal.

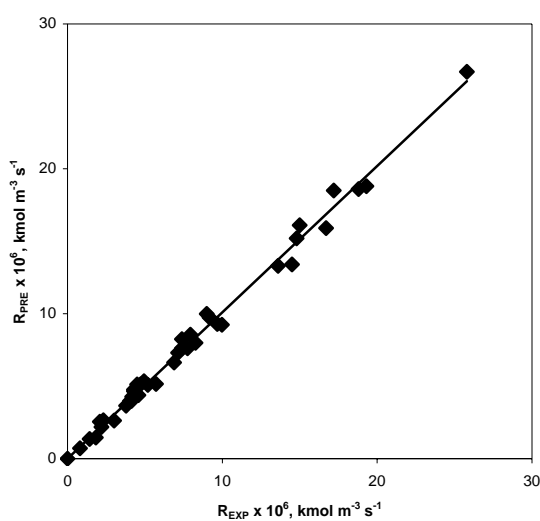


**Figure 6.16:** Comparison of experimental rates and rates predicted using model I

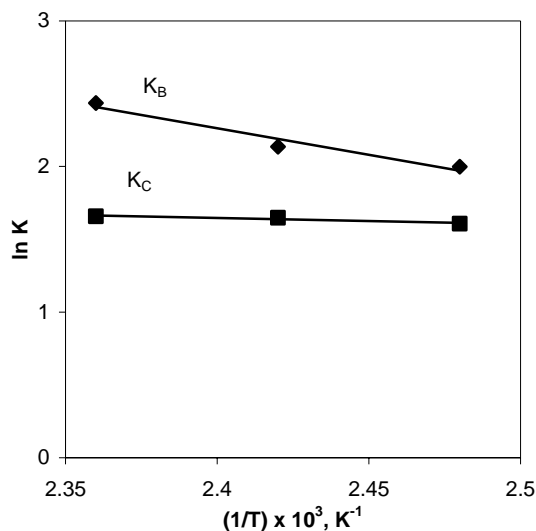


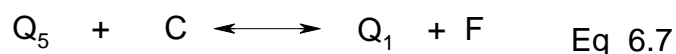
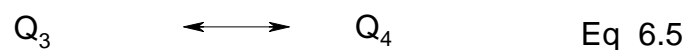
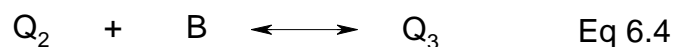
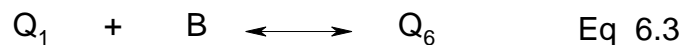
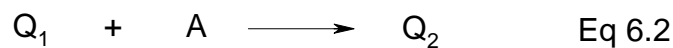
**Figure 6.17:** Temperature dependence of equilibrium constants  $K_B$  and  $K_C$

#### 6.4.2. Mechanistic rate models and model discrimination

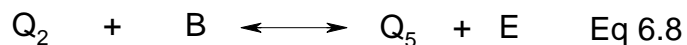
The empirical models are the mathematical models based on the reaction data obtained. These models provide a useful insight on the reaction behaviour. Apart from dealing with the empirical models it is also important to derive the reaction rate models based on the mechanism of the reaction. These models allow for the data to be examined based on the reaction mechanism. Keeping this in mind, rate equations were derived based on the reported reaction mechanism for the Heck reactions (Scheme 6.3). Different steps in the Heck catalytic cycle were considered to be rate determining steps and rate equations were derived for each case. While deriving the rate expressions, some assumptions were made. These are i) all the reaction steps are in equilibrium except the rate determining step ii) for the initial rates, the concentrations of the products is very low and hence can be neglected and iii) all the rearrangement steps are fast and can be clubbed with other steps. While considering the rate determining step and deriving the models following three cases were considered.

### 6.4.2.1. Oxidative addition of aryl halide to Pd as the rate determining step

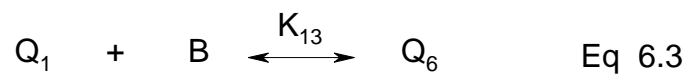
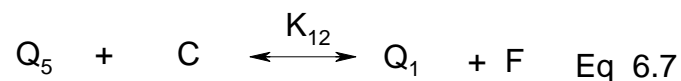
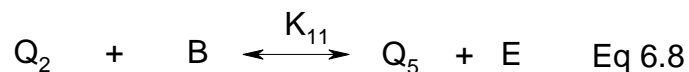
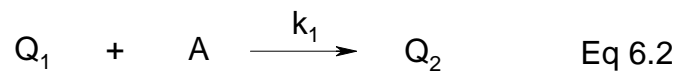
When the oxidative addition of the iodobenzene to palladium is considered the rate determining step, then, based on scheme 6.3 the mechanism can be expressed in terms of following equations:



Equations 6.4, 6.5, and 6.6 can be combined to give the following equation:



For deriving the rate expression the above equations can be condensed to give the set of following equations.



Where Q is the total catalyst concentration and  $Q_1$ ,  $Q_2$ ,  $Q_3$ ,  $Q_4$ ,  $Q_5$ , and  $Q_6$  are the various catalytic intermediates present in the reaction mixture. A represents iodobenzene, B represents n-butyl acrylate, C represents NaOAc, E represents the Heck vinylated product, and F represents HBr abstracted by the base.  $K_{11}$ ,  $K_{12}$ , and  $K_{13}$  are the equilibrium constants and  $k_1$  is the reaction constant.

The rate of the reaction can then be expressed by the following equation:

$$R = k_1[Q_1][A] \quad \text{Eq 6.9}$$

The total concentration of the catalyst (Q) is given as:

$$[Q] = [Q_1] + [Q_2] + [Q_5] + [Q_6] \quad \text{Eq 6.10}$$

For the Initial rates, the concentrations of E and F are very small and hence can be neglected. Expressing  $Q_2$ ,  $Q_5$ , and  $Q_6$  in terms of  $Q_1$  we get

$$[Q_5] = \frac{[Q_1]}{K_{12}[C]}$$

$$[Q_6] = K_{13}[Q_1][B]$$

$$[Q_2] = \frac{[Q_1]}{K_{11}K_{12}[B][C]}$$

On substituting these values in equation 6.10, the following expression is obtained:

$$\begin{aligned}
[Q] &= [Q_1] + \frac{[Q_1]}{K_{12}[C]} + \frac{[Q_1]}{K_{11}K_{12}[B][C]} + K_{13}[Q_1][B] \\
&= [Q_1] \left[ 1 + \frac{1}{K_{12}[C]} + \frac{1}{K_{11}K_{12}[B][C]} + K_{13}[B] \right] \\
&= [Q_1] \left[ \frac{K_{11}K_{12}[B][C] + K_{11}[B] + 1 + K_{11}K_{12}K_{13}[B]^2[C]}{K_{11}K_{12}[B][C]} \right] \\
\Rightarrow [Q_1] &= \frac{K_{11}K_{12}[B][C][Q]}{K_{11}K_{12}[B][C] + K_{11}[B] + 1 + K_{11}K_{12}K_{13}[B]^2[C]}
\end{aligned}$$

Substituting  $K_{11}K_{12} = K_{1a}$ ,  $K_{11}K_{12}K_{13} = K_{1b}$

$$[Q_1] = \frac{K_{1a}[B][C][Q]}{K_{1a}[B][C] + K_{11}[B] + 1 + K_{1b}[B]^2[C]}$$

This value of  $[Q_1]$  is then substituted in equation 6.9

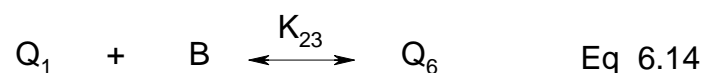
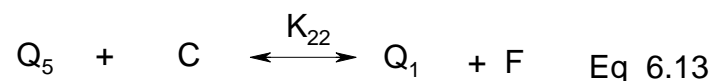
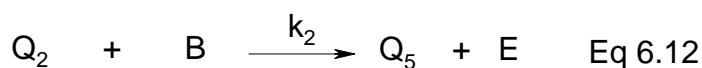
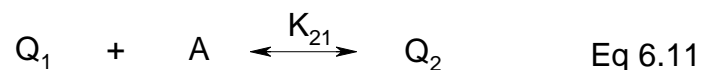
$$R = \frac{k_1 K_{1a} [A][B][C][Q]}{K_{1a}[B][C] + K_{11}[B] + 1 + K_{1b}[B]^2[C]}$$

Again substituting  $k_1 K_{1a} = k_1'$  in this equation the final rate expression is obtained as

$$R = \frac{k_1' [A][B][C][Q]}{1 + K_{11}[B] + K_{1a}[B][C] + K_{1b}[B]^2[C]} \quad \text{Model VII}$$

### 6.4.2.2. Olefin insertion in the Pd-C bond as the rate determining step

If we consider insertion of n-butyl acrylate in the Pd-C bond as the rate determining step then the mechanism can be expressed in terms of the following equations:



Where Q is the total catalyst concentration and  $Q_1$ ,  $Q_2$ ,  $Q_5$ , and  $Q_6$  are the various catalytic intermediates present in the reaction mixture. A represents iodobenzene, B represents n-butyl acrylate, C represents NaOAc, E represents the Heck vinylated product, and F represents HBr abstracted by the base.  $K_{21}$ ,  $K_{22}$ , and  $K_{23}$  are the equilibrium constants and  $k_2$  is the reaction constant.

The rate of the reaction can then be expressed by the following equation:

$$R = k_2[Q_2][B] \quad \text{Eq 6.15}$$

The total concentration of the catalyst [Q] is given as:

$$[Q] = [Q_1] + [Q_2] + [Q_5] + [Q_6] \quad \text{Eq 6.16}$$

For the Initial rates, the concentrations of E and F are very small and hence can be neglected. Expressing  $Q_1$ ,  $Q_5$ , and  $Q_6$  in terms of  $Q_2$  we get

$$[Q_1] = \frac{[Q_2]}{K_{21}[A]}$$

$$[Q_5] = \frac{[Q_2]}{K_{21}K_{22}[A][C]}$$

$$[Q_6] = \frac{K_{23}[Q_2][B]}{K_{21}[A]}$$

Substituting these values in equation 6.16 we get

$$\begin{aligned} [Q] &= [Q_2] + \frac{[Q_2]}{K_{21}[A]} + \frac{[Q_2]}{K_{21}K_{22}[A][C]} + \frac{K_{23}[Q_2][B]}{K_{21}[A]} \\ &= [Q_2] \left[ 1 + \frac{1}{K_{21}[A]} + \frac{1}{K_{21}K_{22}[A][C]} + \frac{K_{23}[B]}{K_{21}[A]} \right] \\ &= [Q_2] \left[ \frac{K_{21}K_{22}[A][C] + K_{22}[C] + 1 + K_{22}K_{23}[B][C]}{K_{21}K_{22}[A][C]} \right] \\ \Rightarrow [Q_2] &= \frac{K_{21}K_{22}[A][C][Q]}{1 + K_{22}[C] + K_{21}K_{22}[A][C] + K_{22}K_{23}[B][C]} \end{aligned}$$

Substituting this value in equation 6.15 gives us

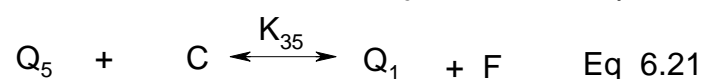
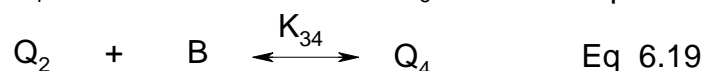
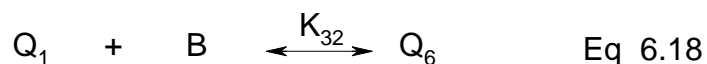
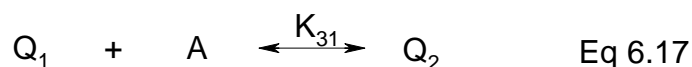
$$R = \frac{k_2 K_{21} K_{22} [A][B][C][Q]}{1 + K_{22}[C] + K_{21} K_{22} [A][C] + K_{22} K_{23} [B][C]}$$

Substituting  $K_{21}K_{22} = K_{2a}$ , and  $K_{22}K_{23} = K_{2b}$ ,  $k_2K_{21}K_{22} = k_2'$  the final rate is expressed as

$$R = \frac{k_2' [A][B][C][Q]}{1 + K_{22}[C] + K_{2a}[A][C] + K_{2b}[B][C]} \quad \text{Model VIII}$$

### 6.4.2.3. $\beta$ -Hydride elimination as the rate determining step

If  $\beta$ -hydride elimination and Heck product formation is considered as the rate determining step then the mechanism of Heck reactions can be expressed in terms of the following equations:



Where  $Q$  is the total catalyst concentration and  $Q_1$ ,  $Q_2$ ,  $Q_4$ ,  $Q_5$ , and  $Q_6$  are the various catalytic intermediates present in the reaction mixture.  $A$  represents iodobenzene,  $B$  represents *n*-butyl acrylate,  $C$  represents NaOAc,  $E$  represents the Heck vinylated product, and  $F$  represents the HBr abstracted by the base.  $K_{31}$ ,  $K_{32}$ ,  $K_{34}$ , and  $K_{35}$  are the equilibrium constants and  $k_3$  is the reaction constant.

The rate of the reaction can then be expressed by the following equation:

$$R = k_3[Q_4] \quad \text{Eq 6.22}$$

The total concentration of the catalyst  $[Q]$  is given as:

$$[Q] = [Q_1] + [Q_2] + [Q_4] + [Q_5] + [Q_6] \quad \text{Eq 6.23}$$

For the Initial rates, the concentrations of  $E$  and  $F$  are very small and hence can be neglected. Expressing  $Q_1$ ,  $Q_2$ ,  $Q_5$ , and  $Q_6$  in terms of  $Q_4$  we get



$$[Q_1] = \frac{[Q_4]}{K_{31}K_{34}[A][B]}$$

$$[Q_6] = \frac{K_{32}[Q_4]}{K_{31}K_{34}[A]}$$

$$[Q_2] = \frac{[Q_4]}{K_{34}[B]}$$

$$[Q_5] = \frac{[Q_4]}{K_{31}K_{34}K_{35}[A][B][C]}$$

Substituting these values in equation 6.23

$$\Rightarrow [Q_4] = \frac{K_{31}K_{34}K_{35}[A][B][C][Q]}{K_{35}C + K_{32}K_{35}[B][C] + K_{31}K_{35}[A][C] + 1 + K_{31}K_{34}K_{35}[A][B][C]}$$

Substituting this value in equation 6.22

$$R = \frac{k_3 K_{31} K_{34} K_{35} [A][B][C] [Q]}{K_{35}C + K_{32} K_{35} [B][C] + K_{31} K_{35} [A][C] + 1 + K_{31} K_{34} K_{35} [A][B][C]}$$

Substituting  $k_3'K_{31}K_{34}K_{35} = k_3'$ ,  $K_{32}K_{35} = K_{3a}$ ,  $K_{31}K_{35} = K_{3b}$ ,  $K_{31}K_{34}K_{35} = K_{3c}$  we get the final rate expression as

$$R = \frac{k_3' [A][B][C][Q]}{1 + K_{35}[C] + K_{3a}[B][C] + K_{3b}[A][C] + K_{3c}[A][B][C]} \quad \text{Model IX}$$

#### 6.4.2.4. Comparison of different mechanistic models

The values of the rate constants and equilibrium constants obtained using the mechanistic models are given in Tables 6.3 to 6.5. The three mechanistic models were

discriminated on the basis of  $\Phi_{\min}$  value and also on the basis of the prediction of the rates. The least value of  $\Phi_{\min}$  was obtained for the model VII which corresponded to the oxidative addition of ArX as the rate determining step. The rates predicted by this model were in good agreement with the experimental rates. The comparison of the experimental rates and the rates predicted using model VII is shown in Figure 6.18. The average error between the experimental and predicted rates was found to be 1.44 %. The activation energy for model VII was found to be 106.51 kJ/mol based on the Arrhenius plot (Figure 6.19).

**Table 6.3:** Values of kinetic parameters at different temperatures using model VII

Temp, K	$k_1'$ ( $\text{m}^3/\text{kmol}$ ) <sup>4</sup>	$K_{1a}$ ( $\text{m}^3/\text{kmol}$ ) <sup>2</sup>	$K_{11}$ ( $\text{m}^3/\text{kmol}$ )	$K_{1b}$ ( $\text{m}^3/\text{kmol}$ ) <sup>3</sup>	$\Phi_{\min} \times 10^{11}$
403	$1.12 \times 10^4$	40.06	1.32	$2.14 \times 10^{-4}$	0.33
413	$2.39 \times 10^4$	47.37	2.95	$2.16 \times 10^{-4}$	1.12
423	$5.21 \times 10^4$	52.89	3.37	$2.18 \times 10^{-4}$	3.31

**Table 6.4:** Values of kinetic parameters at different temperatures using model VIII

Temp, K	$k_2'$ ( $\text{m}^3/\text{kmol}$ ) <sup>4</sup>	$K_{22}$ ( $\text{m}^3/\text{kmol}$ )	$K_{2a}$ ( $\text{m}^3/\text{kmol}$ ) <sup>2</sup>	$K_{2b}$ ( $\text{m}^3/\text{kmol}$ ) <sup>2</sup>	$\Phi_{\min} \times 10^{11}$
403	$1.02 \times 10^4$	$1.36 \times 10^{-5}$	$1.09 \times 10^{-5}$	40.75	0.36
413	$2.21 \times 10^4$	$2.64 \times 10^{-5}$	$1.10 \times 10^{-5}$	57.09	0.92
423	$5.15 \times 10^4$	$3.93 \times 10^{-5}$	$1.12 \times 10^{-5}$	71.89	4.69

**Table 6.5:** Values of kinetic parameters at different temperatures using model IX

Temp K	$k_3'$ ( $\text{m}^3/\text{kmol}$ ) <sup>4</sup>	$K_{35}$ ( $\text{m}^3/\text{kmol}$ )	$K_{3a}$ ( $\text{m}^3/\text{kmol}$ ) <sup>2</sup>	$K_{3b}$ ( $\text{m}^3/\text{kmol}$ ) <sup>2</sup>	$K_{3c}$ ( $\text{m}^3/\text{kmol}$ ) <sup>3</sup>	$\Phi_{\min}$ $\times 10^{11}$
403	$1.02 \times 10^4$	$6.18 \times 10^{-3}$	40.93	$1.32 \times 10^{-5}$	$1.25 \times 10^{-5}$	0.36
413	$2.21 \times 10^4$	$4.26 \times 10^{-3}$	57.07	$1.36 \times 10^{-5}$	$1.26 \times 10^{-5}$	0.92
423	$5.15 \times 10^4$	$2.24 \times 10^{-3}$	71.85	$1.38 \times 10^{-5}$	$1.27 \times 10^{-5}$	4.69

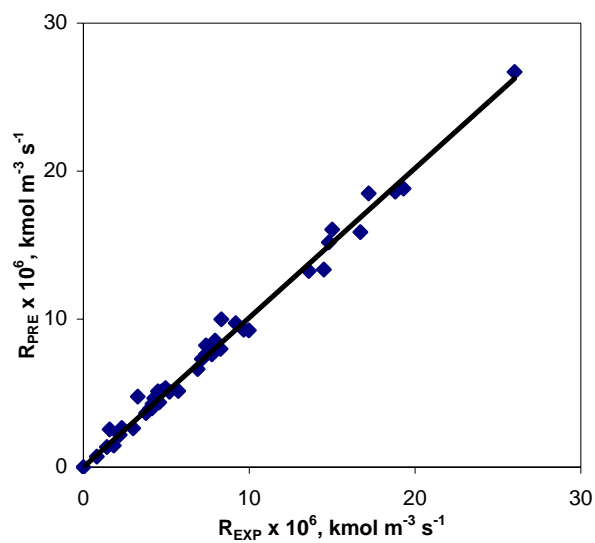


**Figure 6.18:** Comparison of experimental rates and rates predicted using model VII

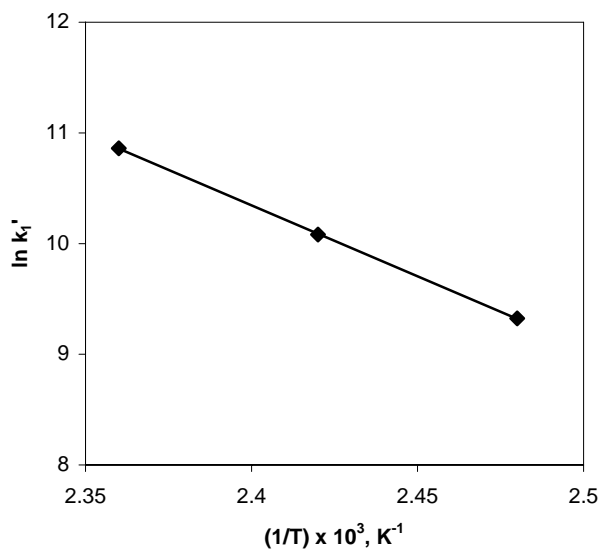


**Figure 6.19:** Temperature dependence of rate constant ( $k_1'$ ) for mechanistic model VII

## 6.5. Conclusions

The kinetics of vinylation of iodobenzene with n-butyl acrylate using ossified palladium catalyst **1** was studied in DMF as solvent and NaOAc as base. The effect of different parameters *viz* concentration of the substrates, catalyst, and base on the rate of the reaction was investigated in a temperature range of 403-423 K. The rate data were fitted to various empirical and mechanistic rate models. The following model amongst the empirical models was found to predict the rates in good agreement with experimental values.

$$R = \frac{k[A][B][C][Q]}{(1 + K_B[B]) (1 + K_C[C])} \quad \text{Model I}$$

The best prediction of the rates was obtained with the following mechanistic model.

$$R = \frac{k_1' [A][B][C][Q]}{1 + K_{11}[B] + K_{1a}[B][C] + K_{1b}[B]^2[C]} \quad \text{Model VII}$$

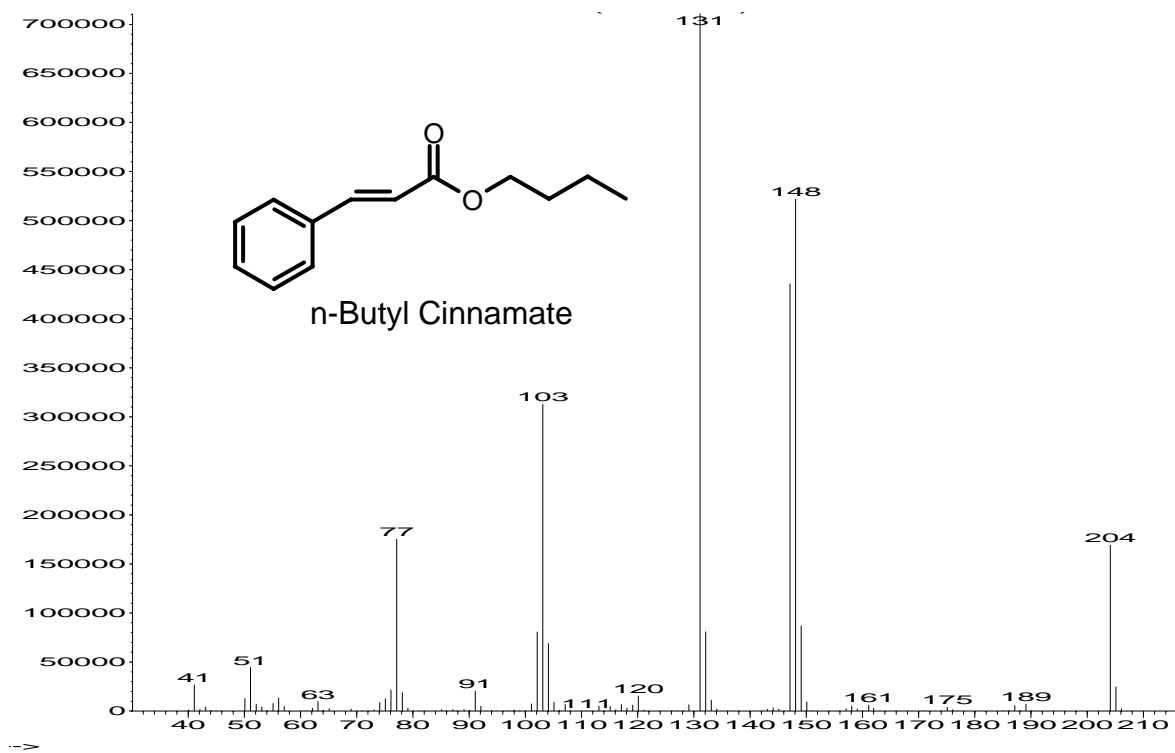
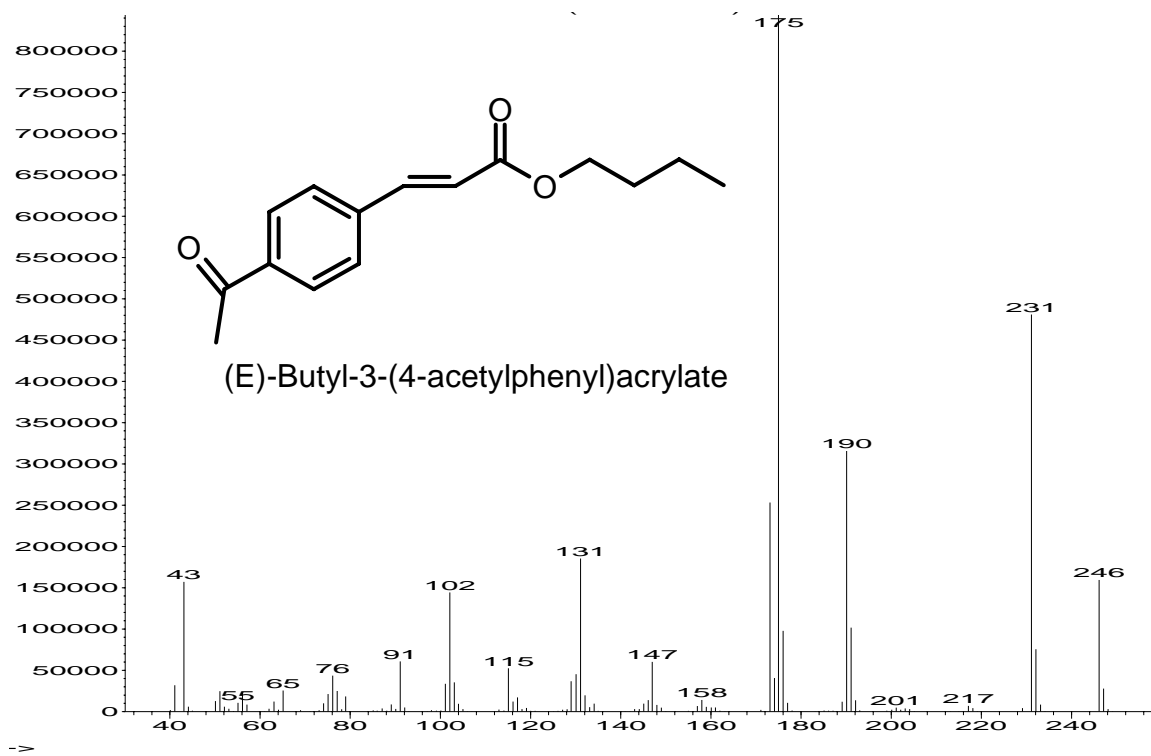
Based on the mechanistic model, it can be concluded that the oxidative addition of iodobenzene to the Pd is the rate determining step under the reaction conditions employed.

## 6.6. References

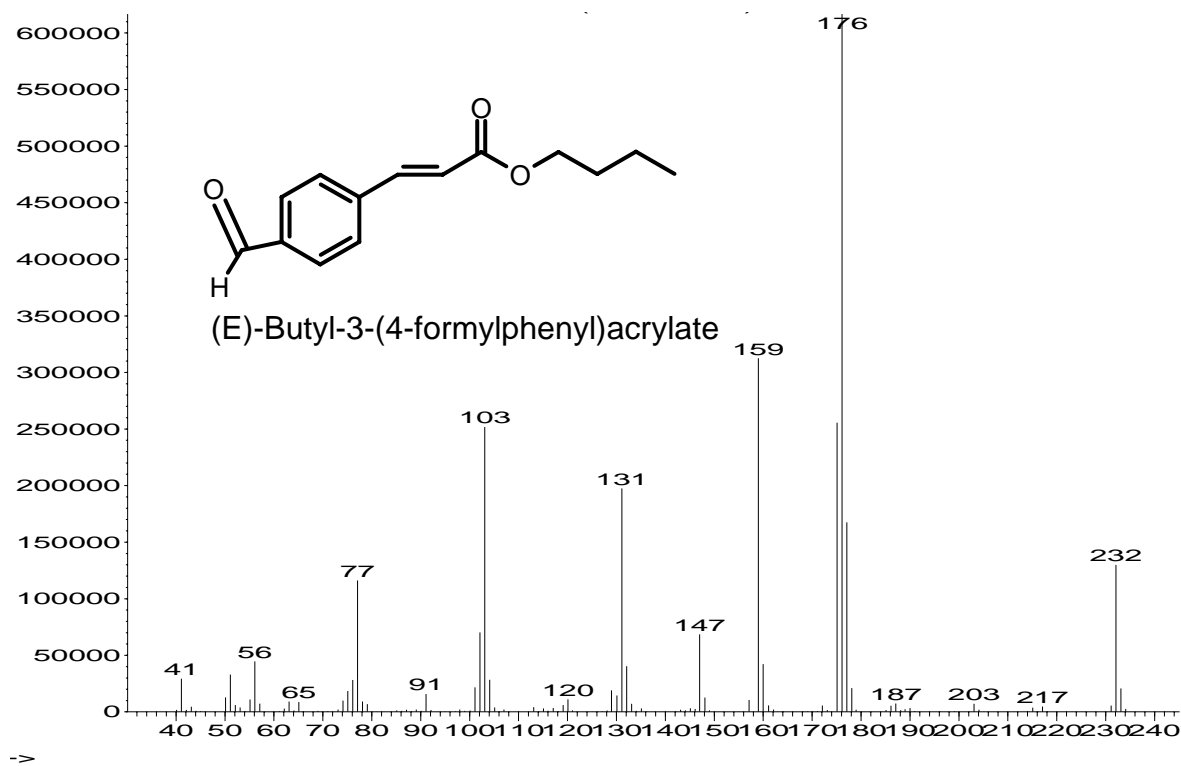
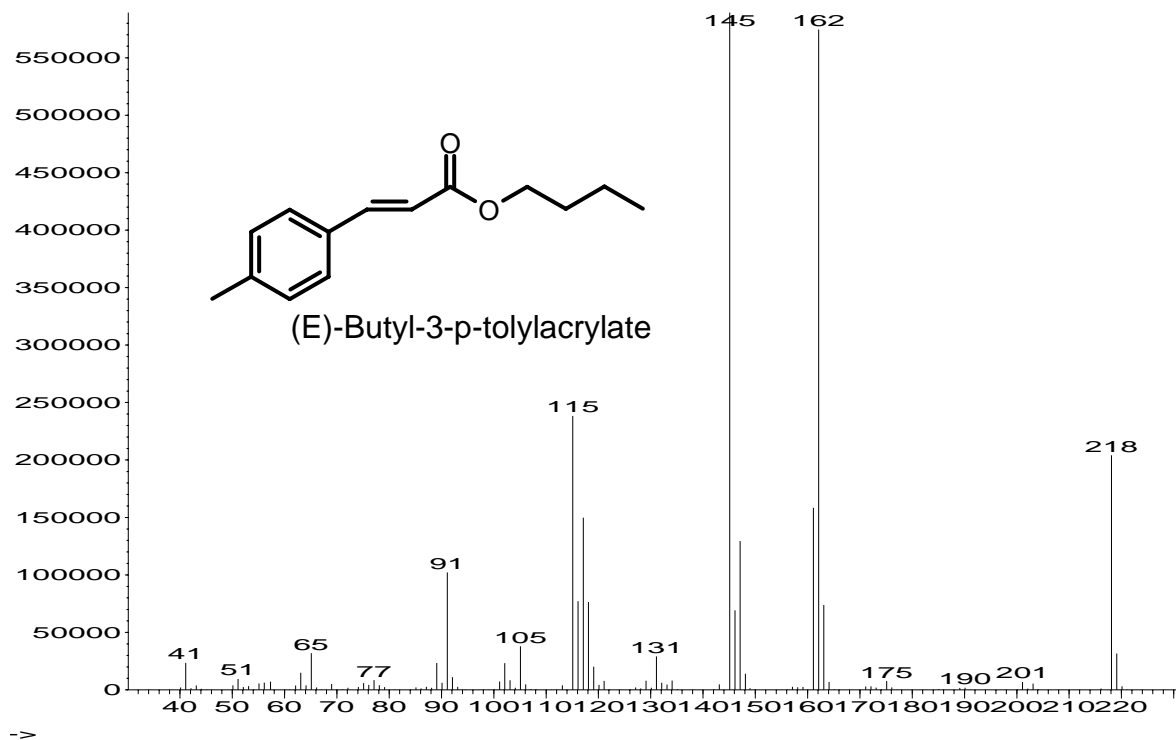
1. Zhao, F. G.; Bhanage, B. M.; Shirai, M.; Arai, M. *Reaction Kinetics Development Catal. Procedures* . **1999**, 427
2. Zhao, F.; Bhanage, B. M.; Shirai, M.; Arai, M. *J. Mol. Catal. A: Chem.* **1999**, 142, 383
3. Van Strijdonck, G. P. F.; Boele, M. D. K.; Kamer, P. C. J.; de Vries, J. G.; van Leeuwen, P. W. N. M. *Eur. J. Inorg. Chem.* **1999**, 1073
4. Rosner T.; Bars J. L.; Pfaltz A.; Blackmond D. G. *J. Am. Chem. Soc.* **2001**, 123, 1848
5. Consorti, C. S.; Flores, F. R.; Dupont, J. *J. Am. Chem. Soc.* **2005**, 127, 12054
6. Zhao F. G.; Bhanage B. M.; Shirai M.; Arai M. *Stud. Surf. Sci. Catal.* **1999**, 122, 427
7. Biffis, A.; Zecca, M.; Basato, M. *J. Mol. Catal. A: Chem.* **2001**, 173, 249
8. Sommer, W. J.; Yu, K.; Sears, J. S.; Ji, Y.; Zheng, X.; Davis, R. j.; Sherrill C. D.; Jones, C. W.; Weck, M. *Organometallics*, **2005**, 24, 4351
9. Phan, N. T. S.; Sluys, M. V. D.; Jones, C. W. *Adv. Synth. Catal.* **2006**, 348, 609
10. Stambuli, J. P.; Kuwano, R.; Hartwig, J. F. *Angew. Chem. Int. Ed.* **2002**, 41, 4746
11. Beletskaya, I. P. ; Cheprakov, A. V. *Chem. Rev.* **2000**, 100, 3009
12. Crisp, G. T. *Chem. Soc. Rev.* **1998**, 27, 427
13. Marquardt, D. W. *J. Soc. Ind. Appl. Math.* **1963**, 11, 431

# *Appendix*

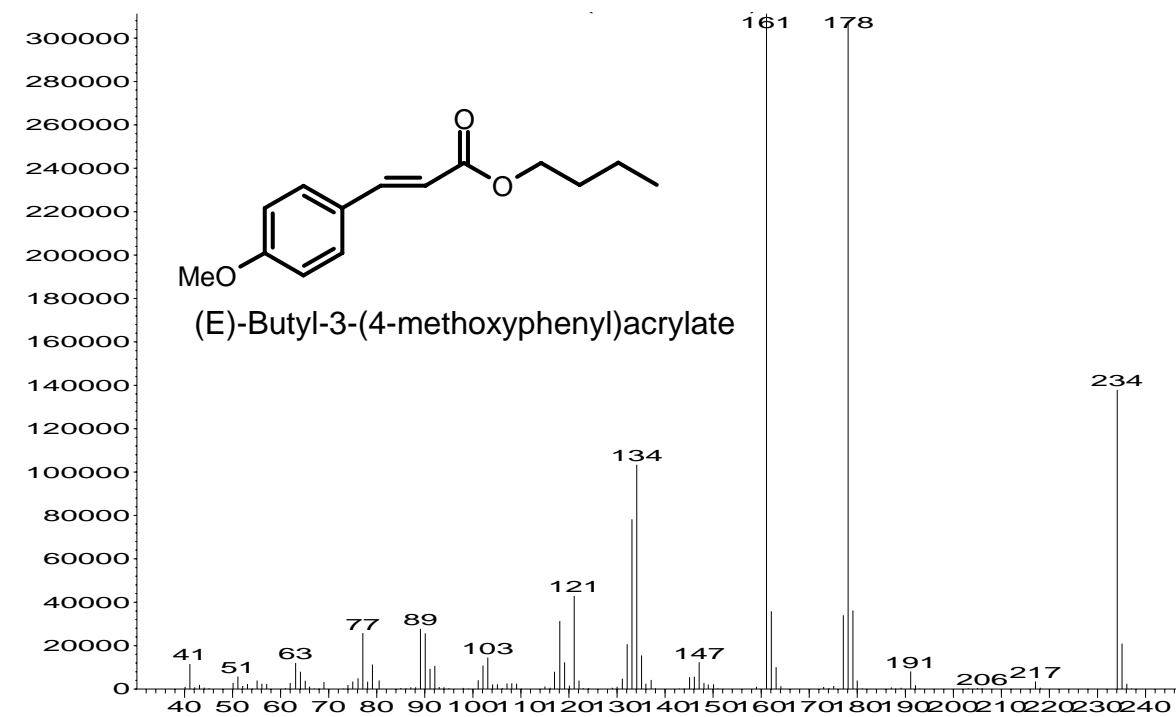
**Appendix 1.** MS data of the products obtained from Heck reaction of various substrates



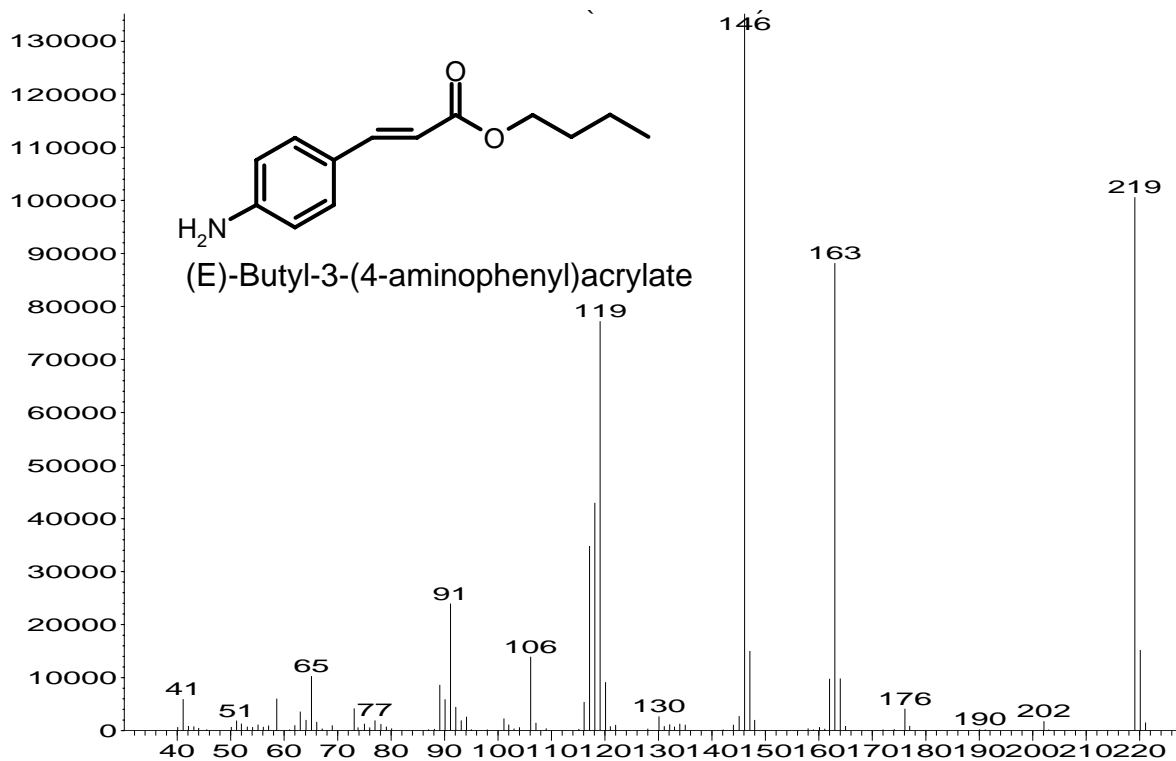
**Appendix 1 (Continued).** MS data of the products obtained from Heck reaction of various substrates



**Appendix 1 (Continued).** MS data of the products obtained from Heck reaction of various substrates



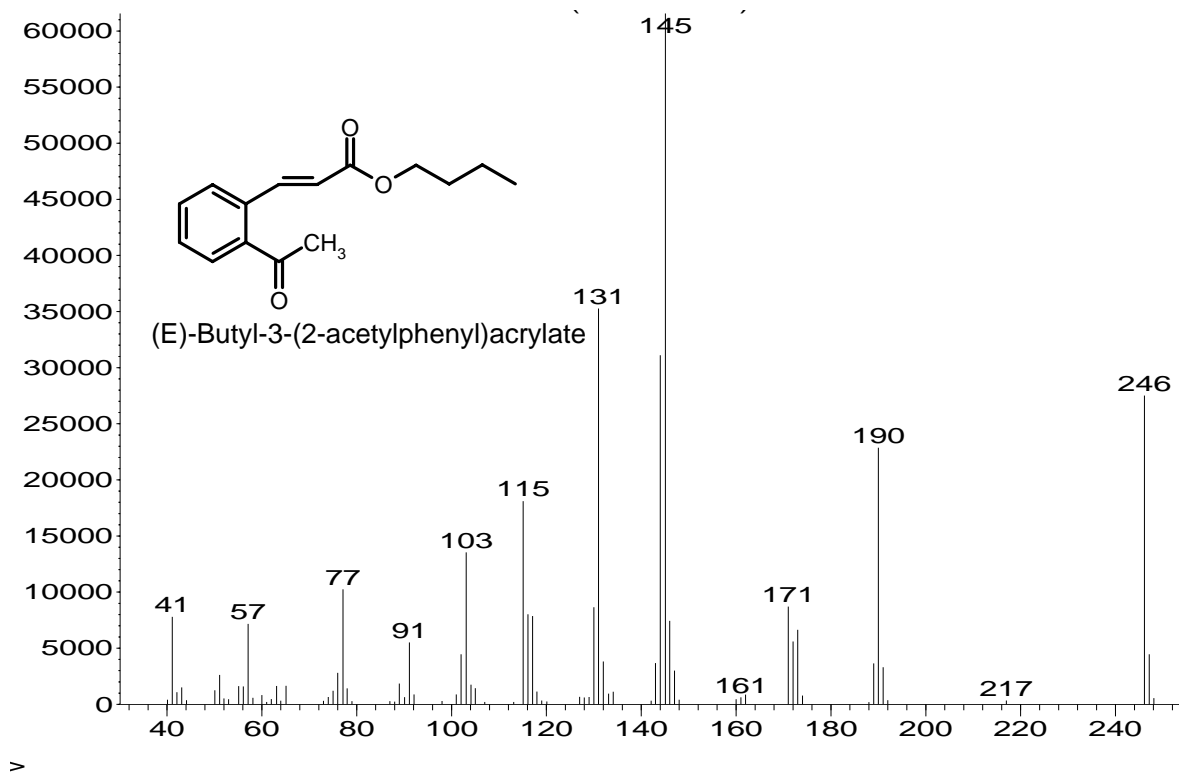
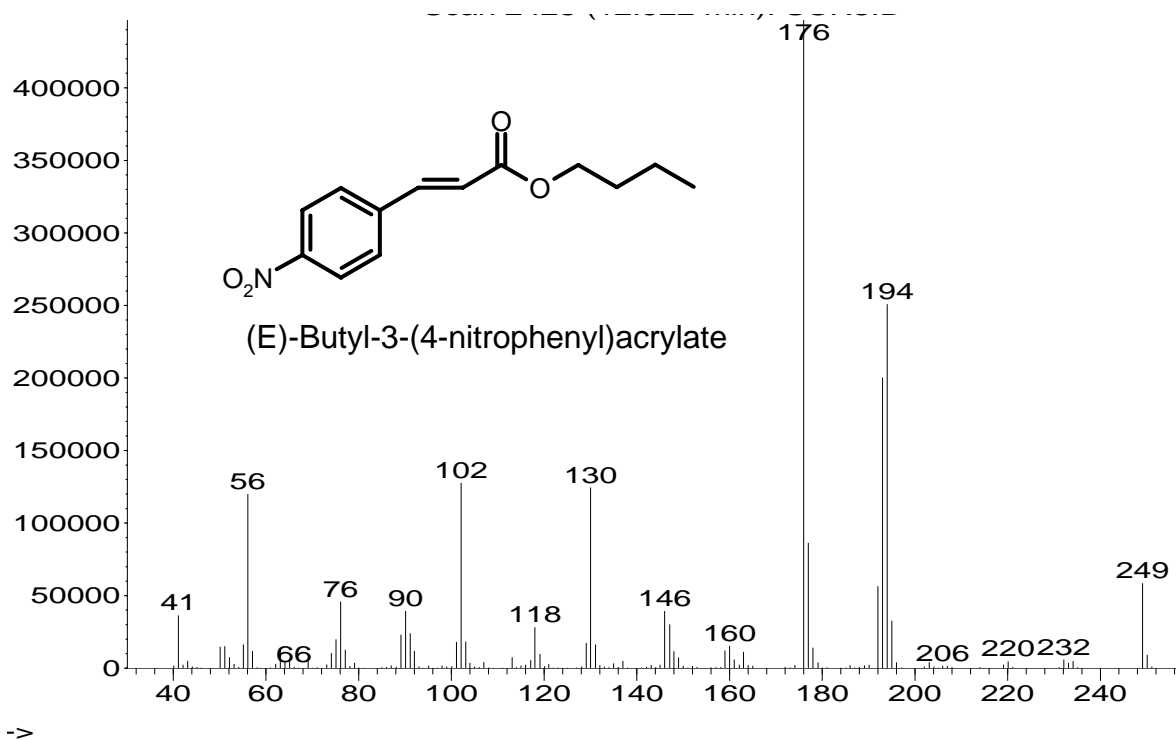
-->



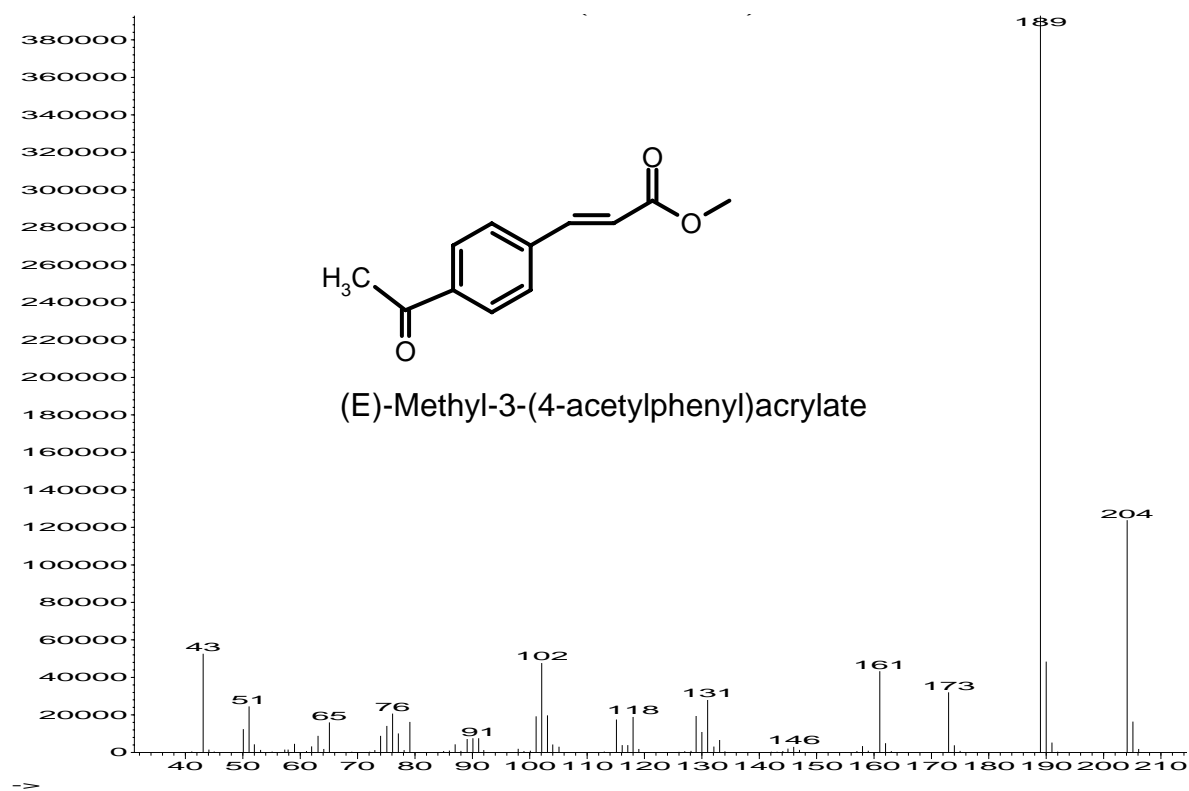
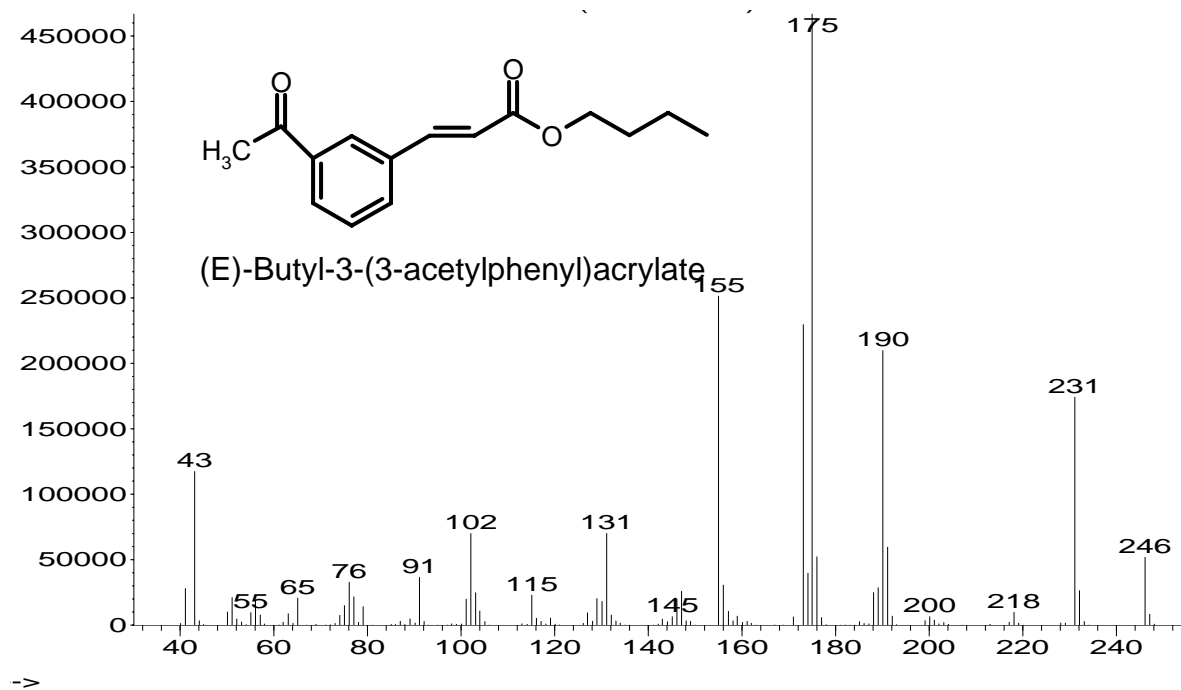
>



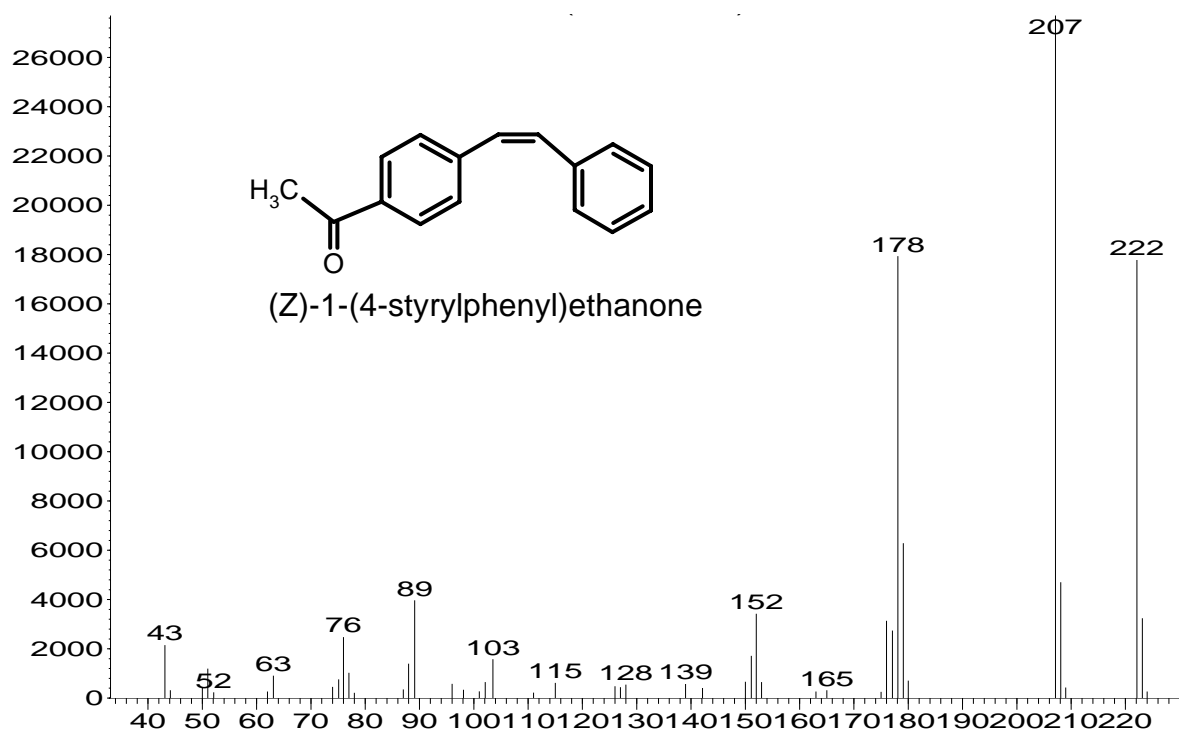
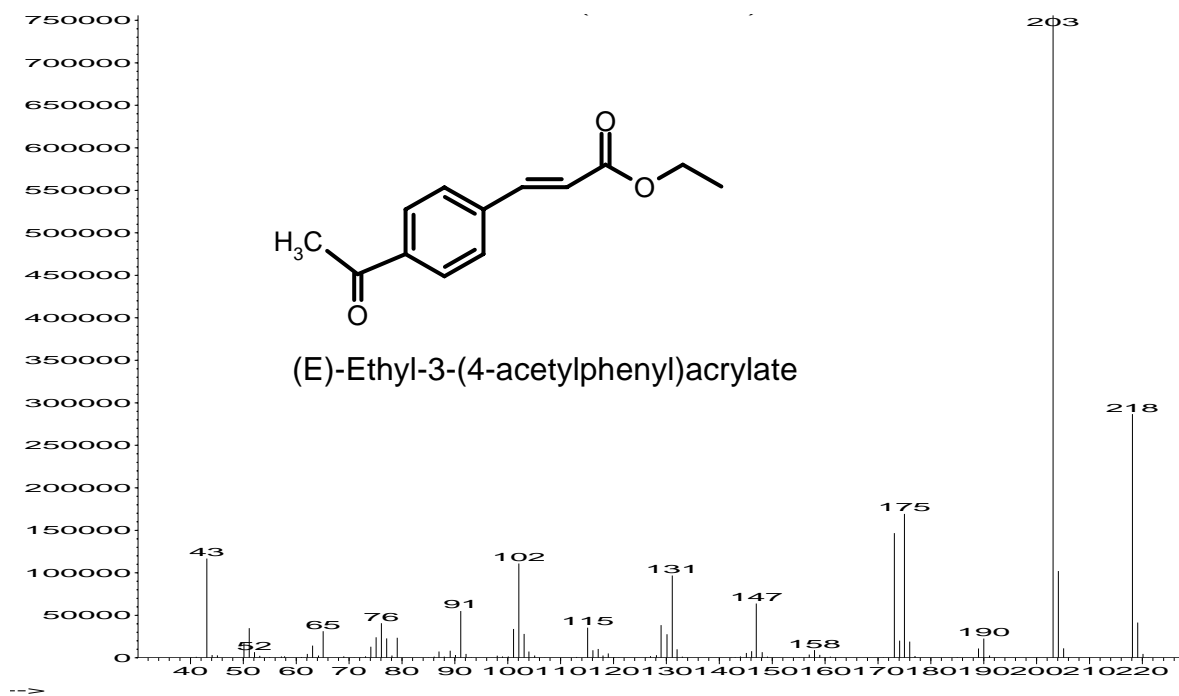
**Appendix 1 (Continued).** MS data of the products obtained from Heck reaction of various substrates



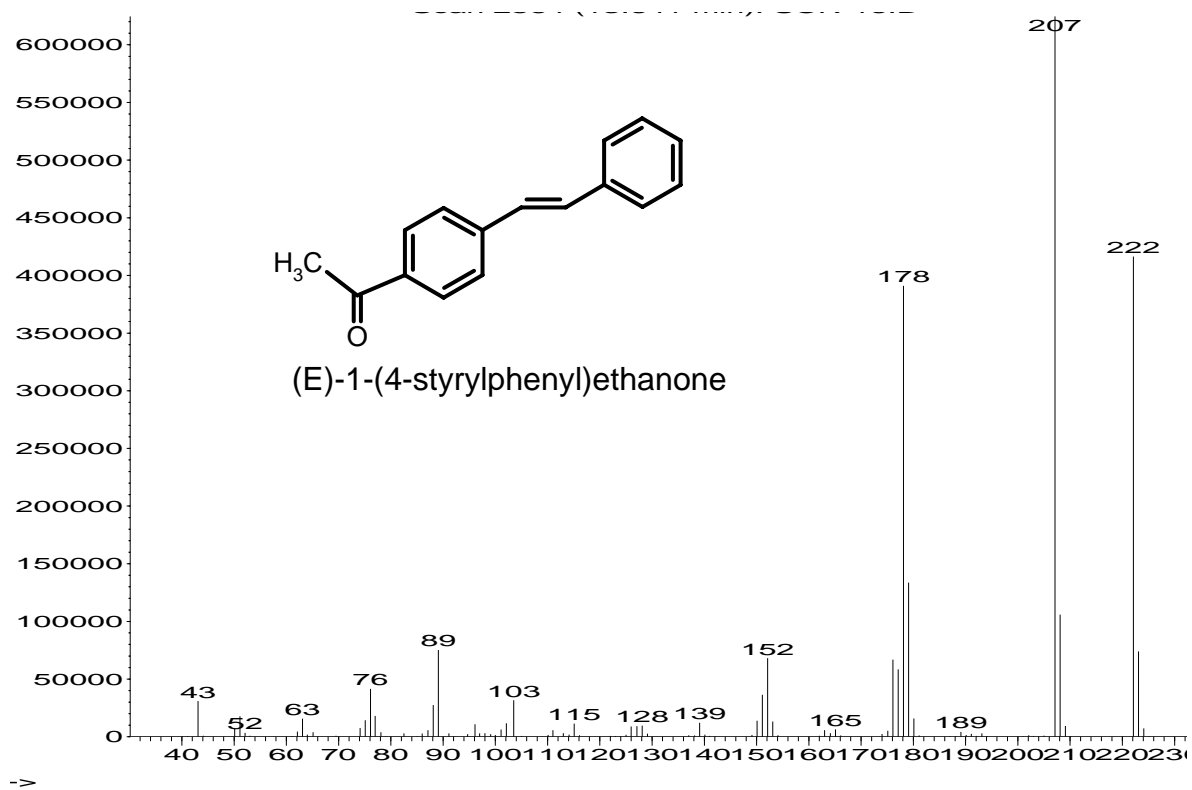
**Appendix 1 (Continued).** MS data of the products obtained from Heck reaction of various substrates



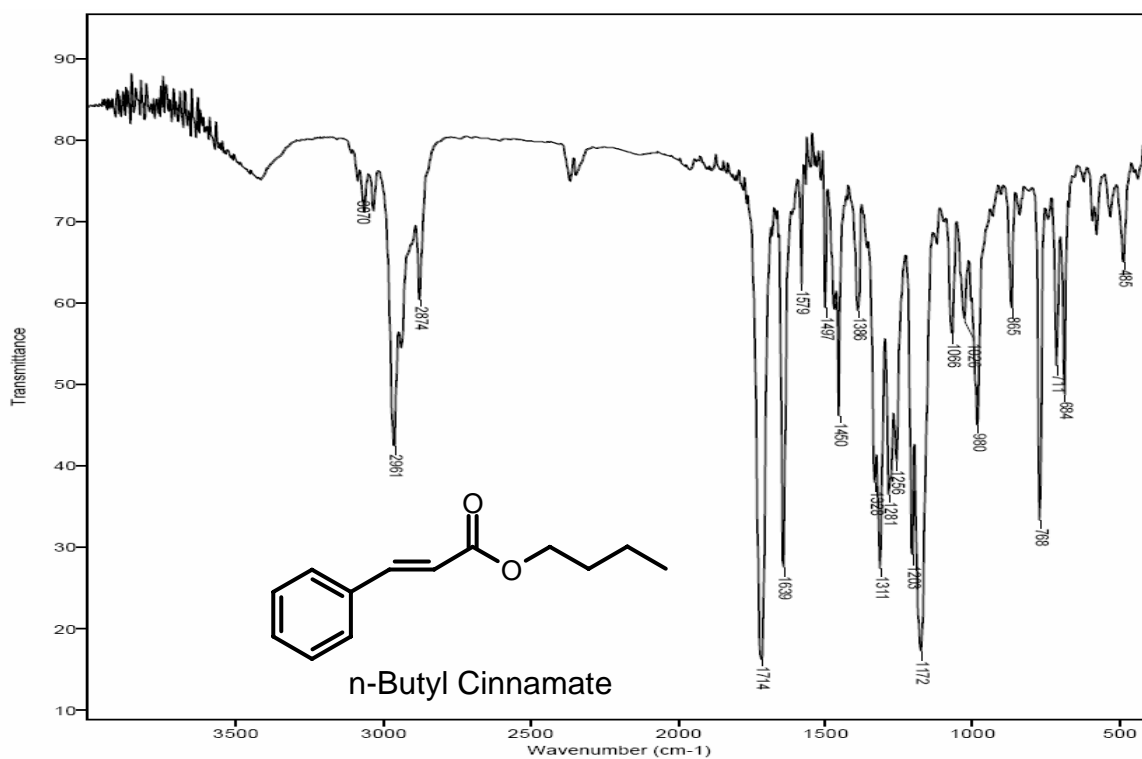
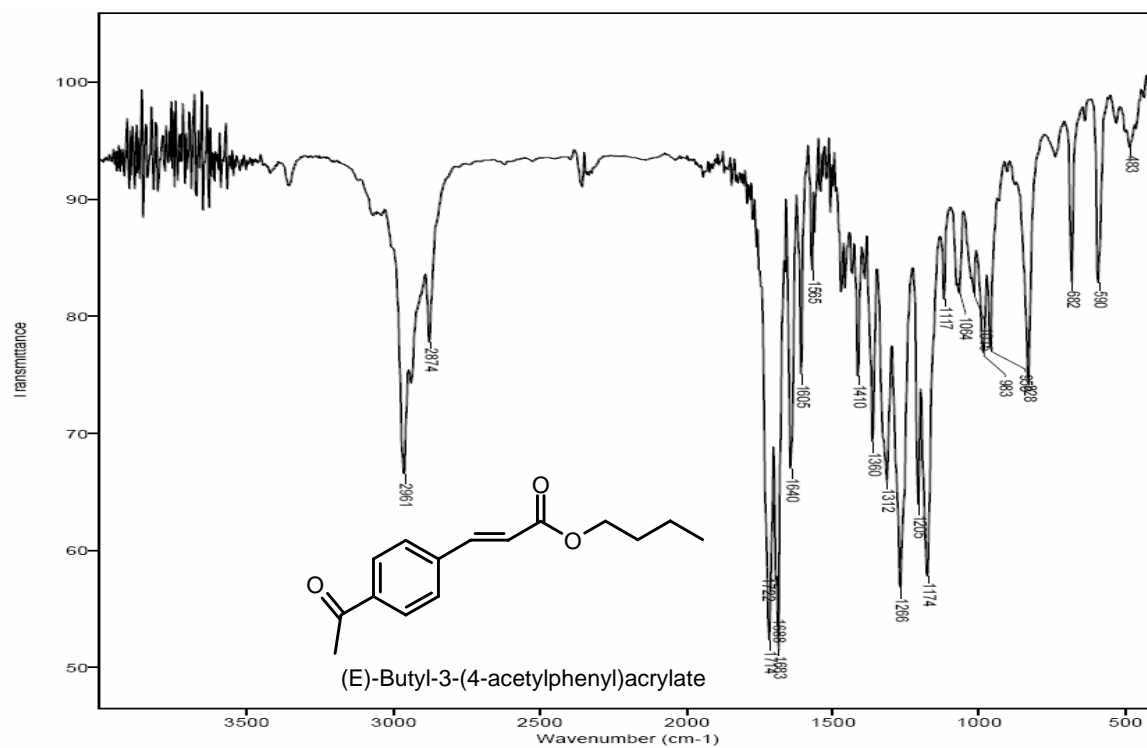
**Appendix 1 (Continued).** MS data of the products obtained from Heck reaction of various substrates



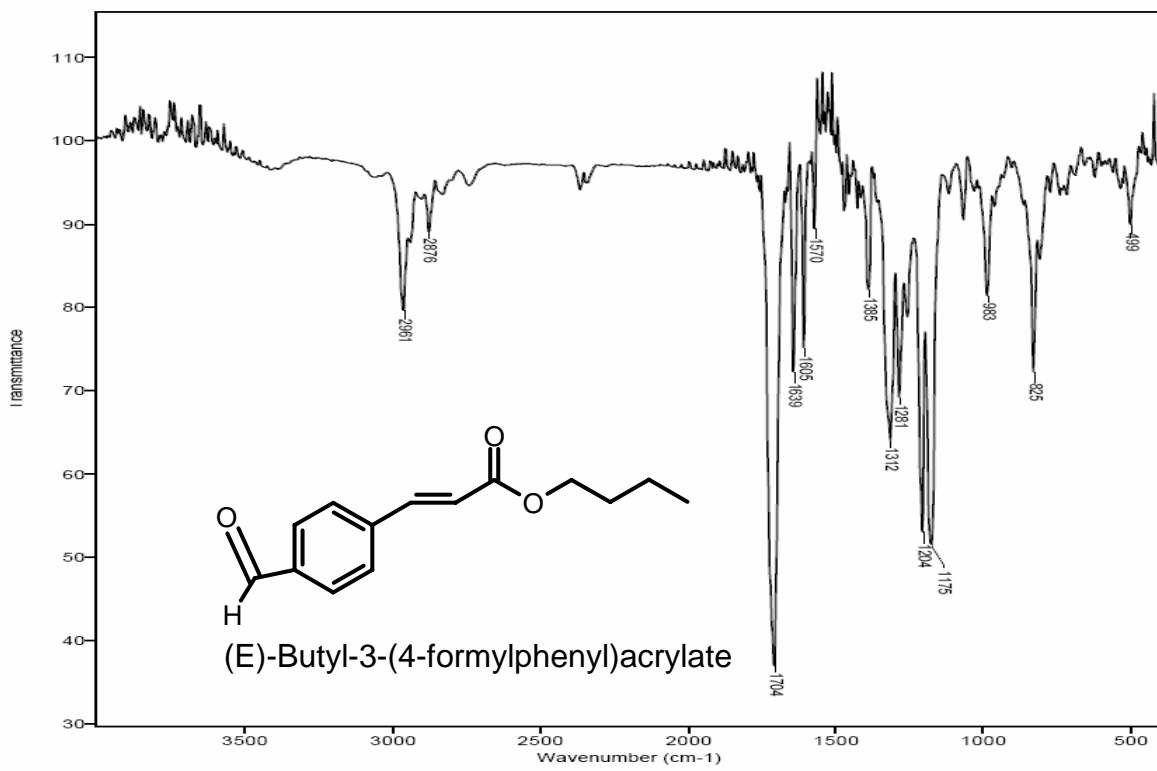
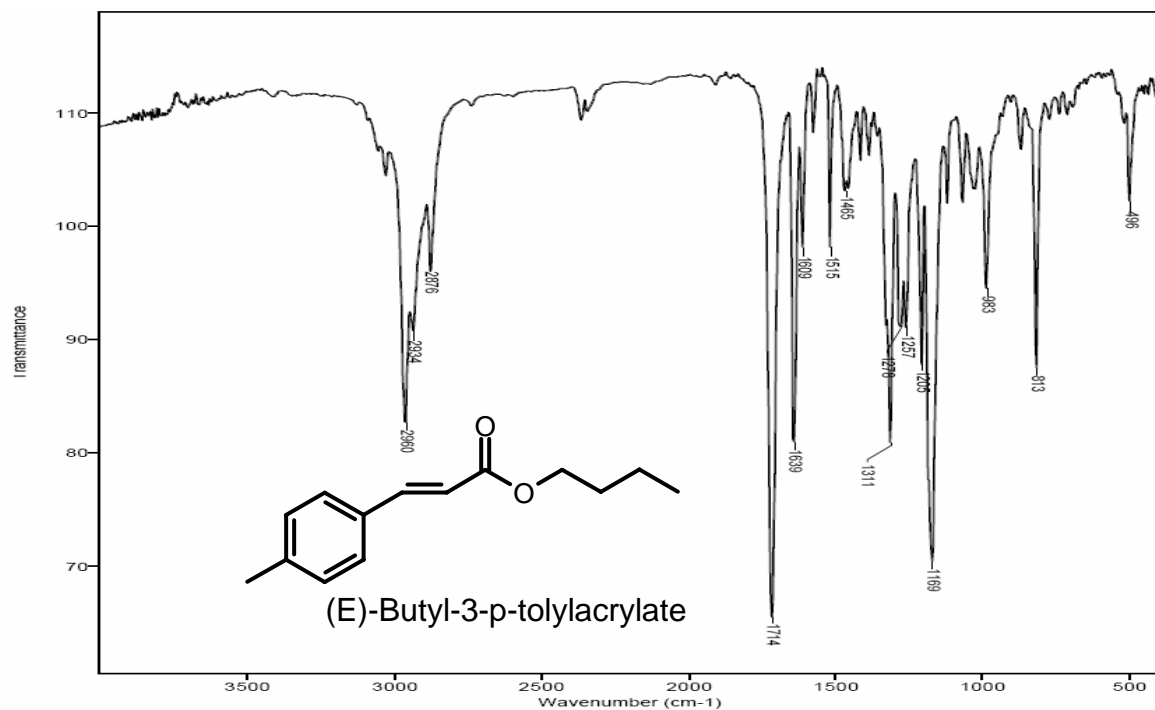
**Appendix 1 (Continued).** MS data of the products obtained from Heck reaction of various substrates



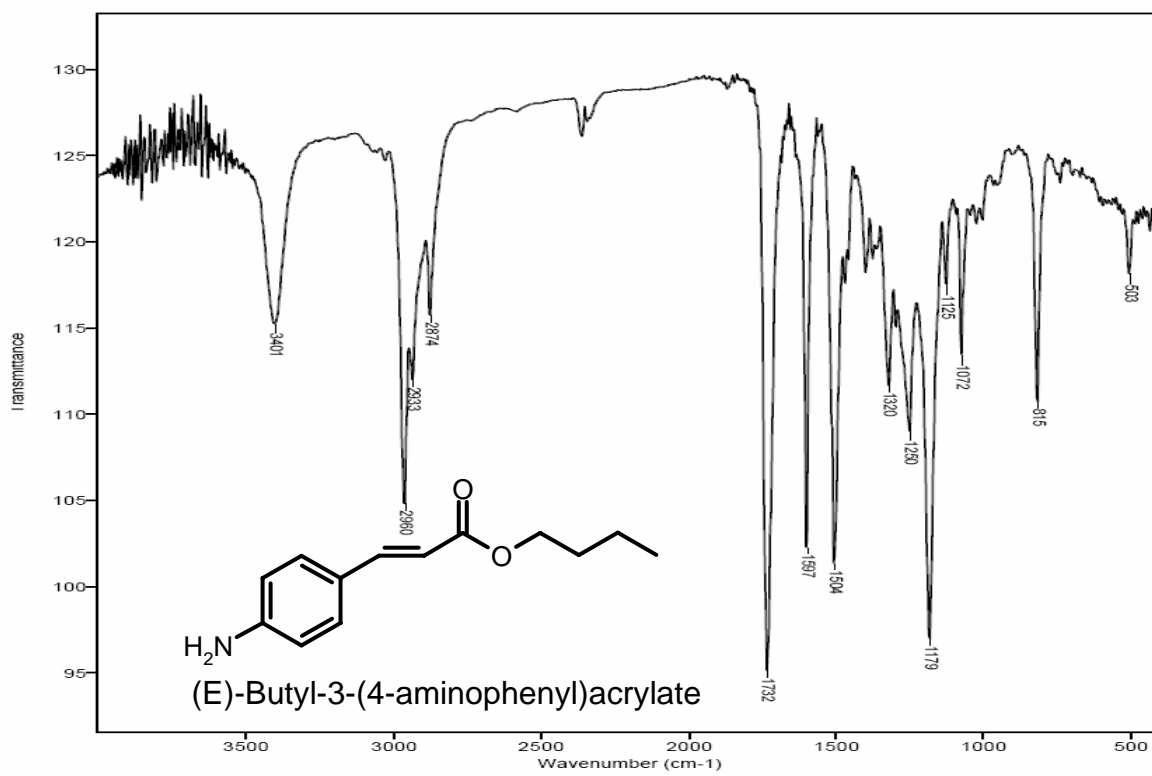
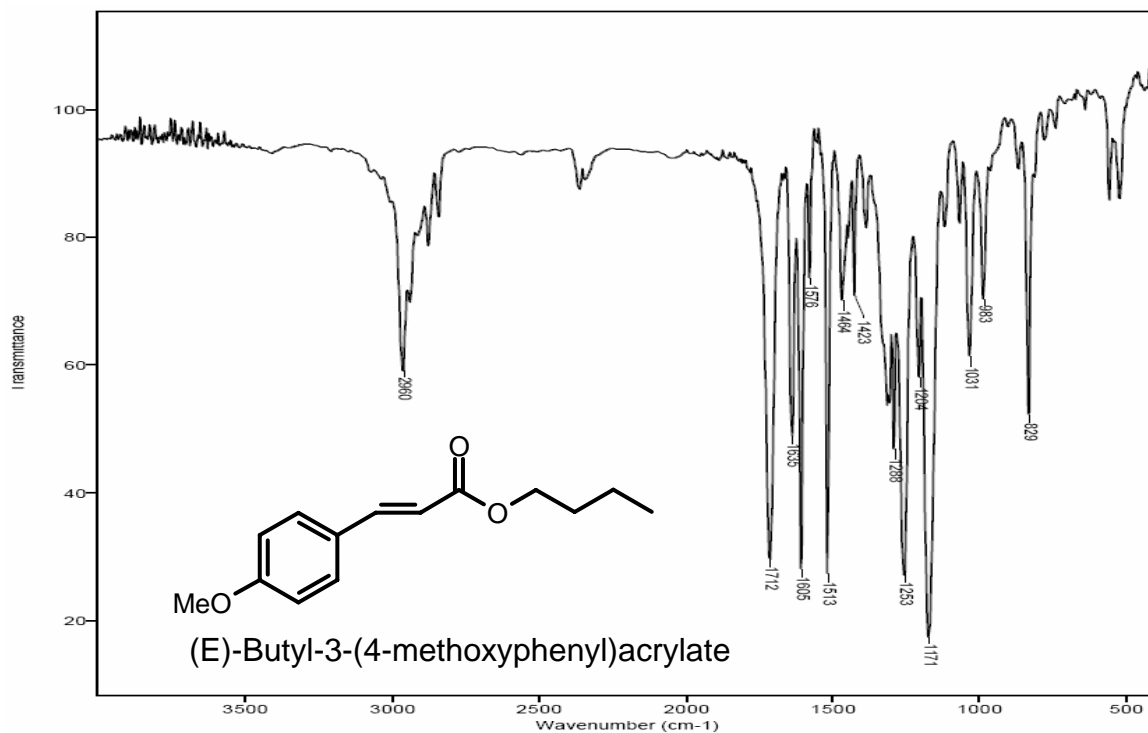
**Appendix 2.** IR data of the products obtained from Heck reaction of various substrates



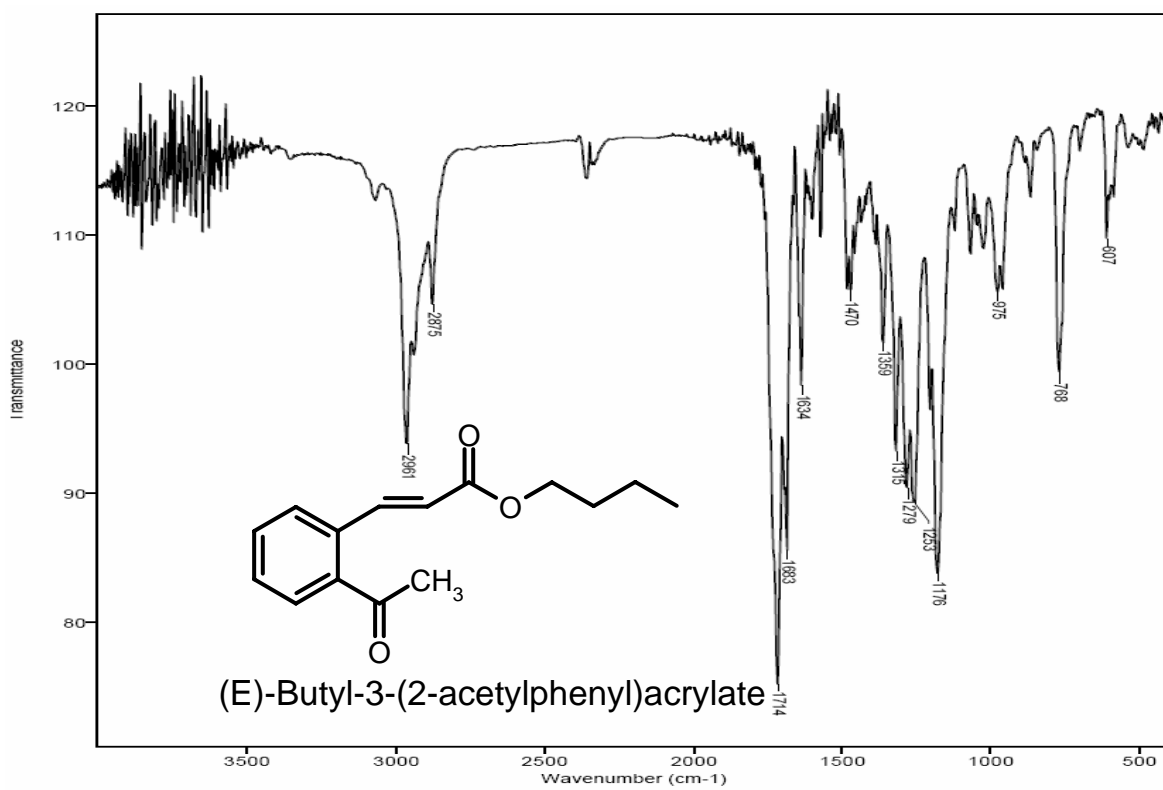
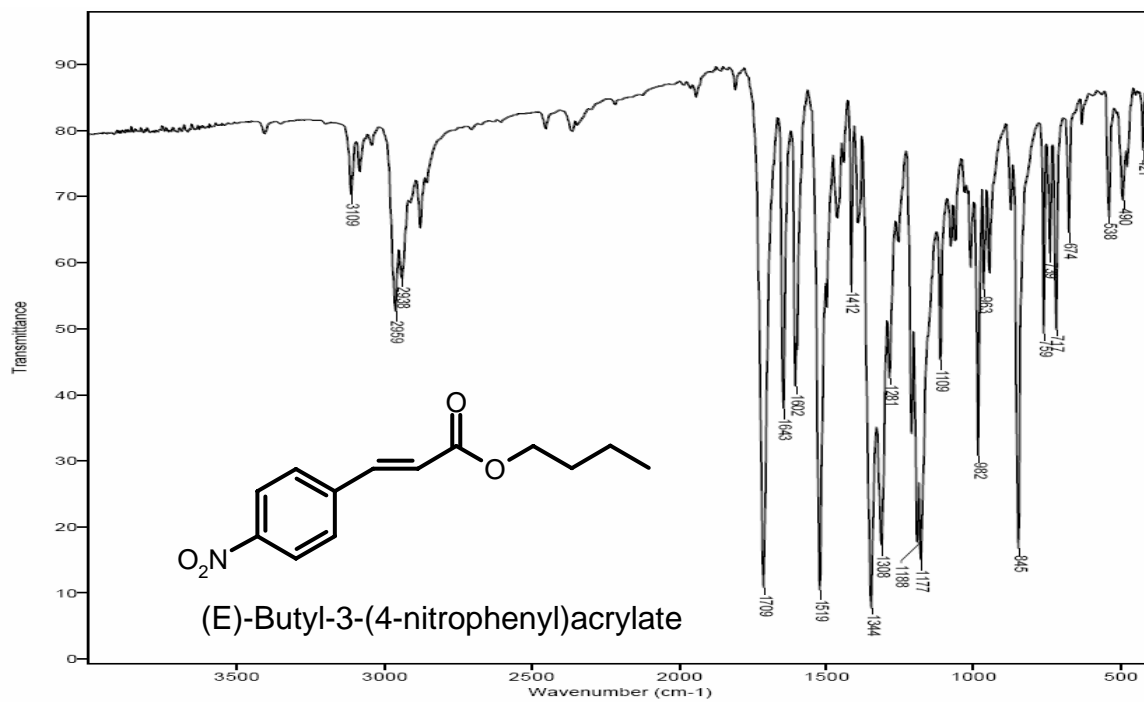
**Appendix 2 (Continued).** IR data of the products obtained from Heck reaction of various substrates



**Appendix 2 (Continued).** IR data of the products obtained from Heck reaction of various substrates

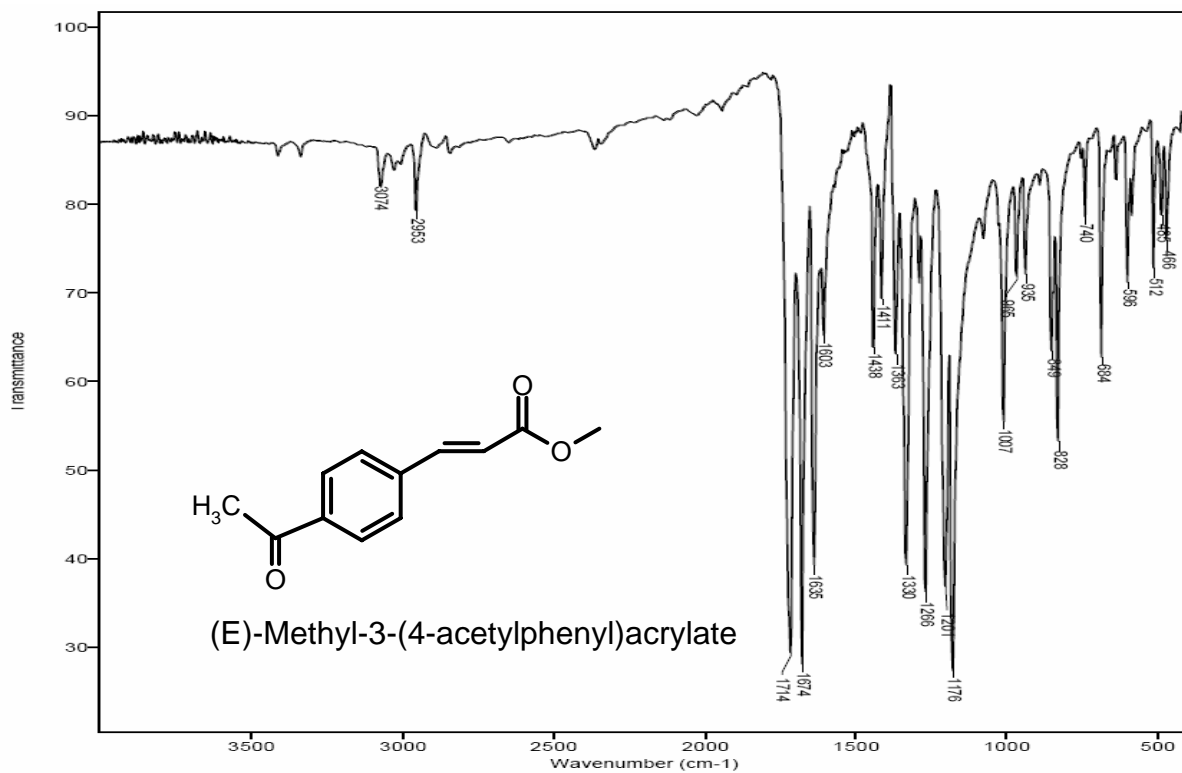
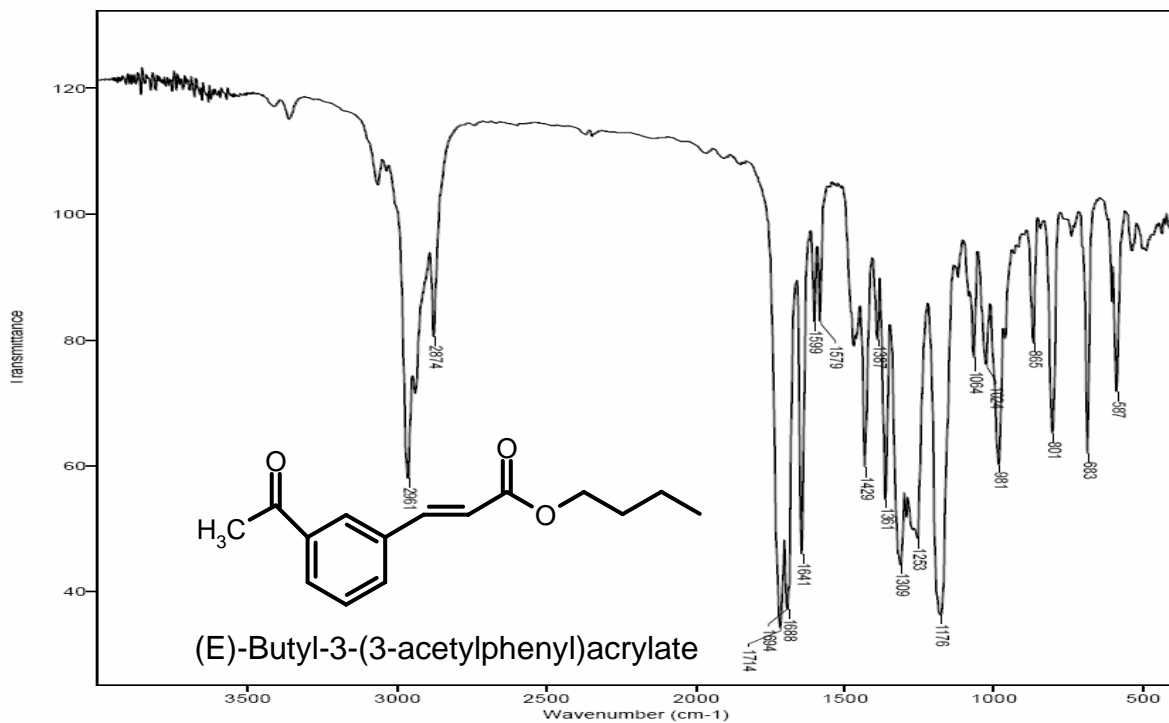


**Appendix 2 (Continued).** IR data of the products obtained from Heck reaction of various substrates

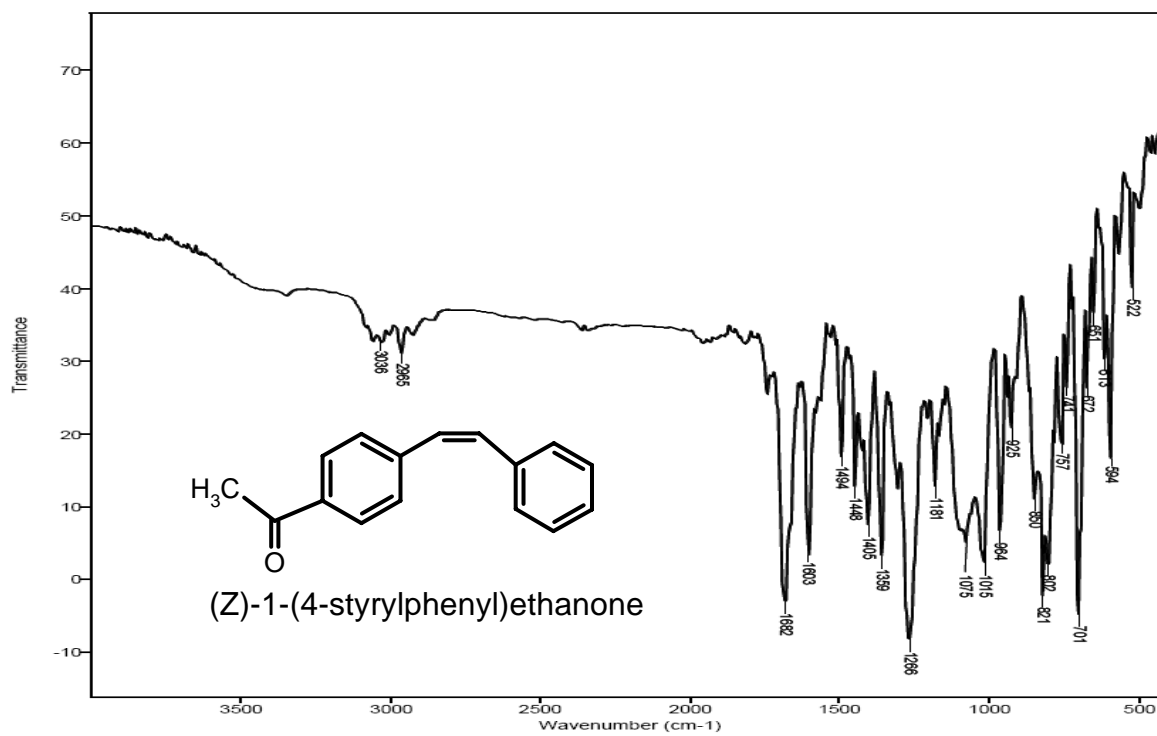
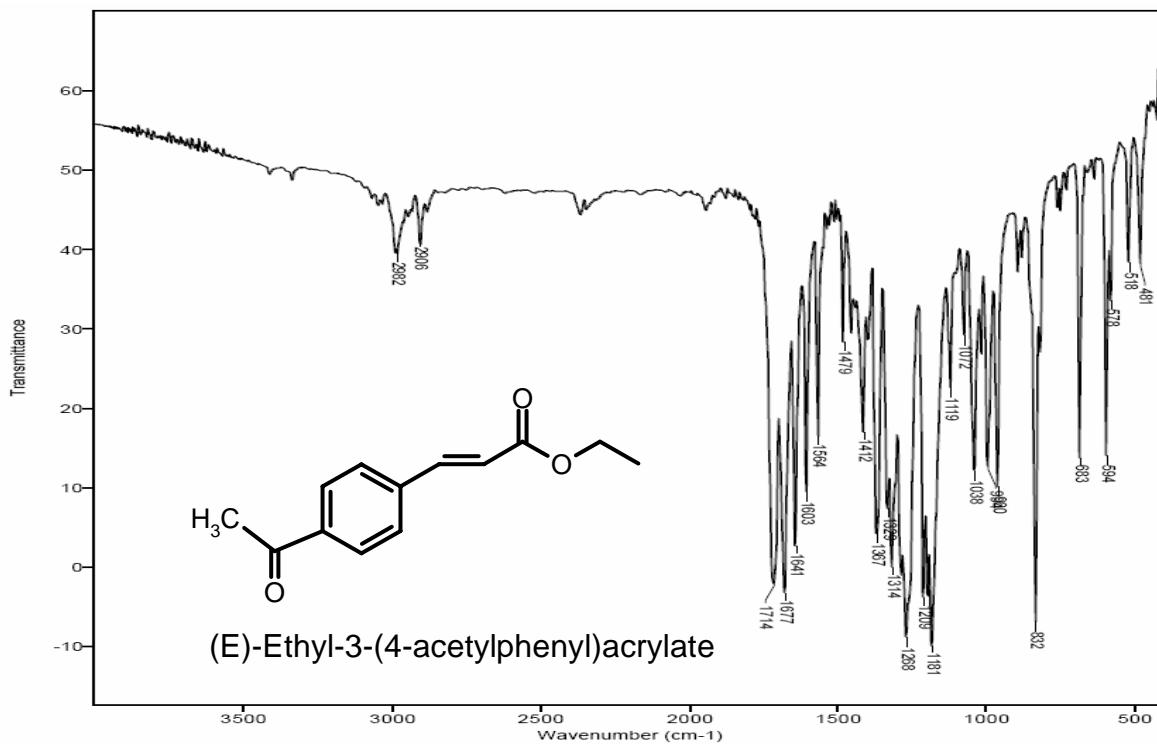




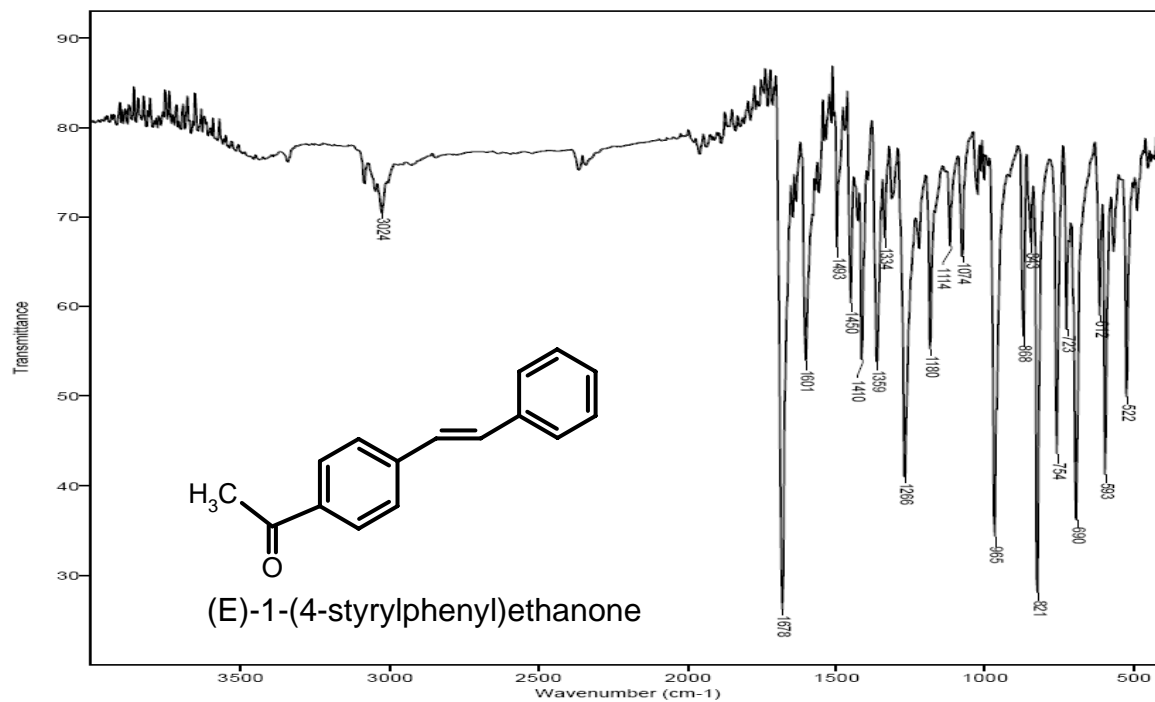
**Appendix 2 (Continued).** IR data of the products obtained from Heck reaction of various substrates



**Appendix 2 (Continued).** IR data of the products obtained from Heck reaction of various substrates



**Appendix 2 (Continued).** IR data of the products obtained from Heck reaction of various substrates



## Publications and Symposia

1. Rate enhancements in palladium catalyzed Heck reactions by Lewis acid promoters  
**Abhishek Sud**, Raj Madhukar Deshpande, Raghunath Vitthal Chaudhari  
Catalysis Communications 8 (2007) 183
2. Kinetics of vinylation of 4'-bromo acetophenone with n-butyl acrylate using palladacycle catalyst  
**Abhishek Sud**, Raj M. Deshpande, Raghunath V. Chaudhari  
Journal of Molecular Catalysis A: Chemical 270 (2007) 144
3. Vinylation of 4'-bromo acetophenone with n-butyl acrylate using palladacycle catalyst: A kinetic study  
**A. Sud**, R. M. Deshpande, R. V. Chaudhari  
Poster presented in CAMURE-6 and ISMR-5 held in Jan 2007
4. Ossified palladium complex catalysts for Suzuki and Heck coupling reactions  
B. R. Sarkar, **A. Sud**  
Oral presentation in CAMURE-6 and ISMR-5 held in Jan 2007
5. Ossified palladium complexes as highly active heterogeneous catalysts for Heck reactions  
**Abhishek Sud**, Bibhas R. Sarkar, Raj M. Deshpande, Raghunath V. Chaudhari  
Under preparation
6. Kinetics of Heck vinylation of iodobenzene with n-butyl acrylate using ossified Palladium catalyst  
**Abhishek Sud**, Raj M. Deshpande, Raghunath V. Chaudhari  
Under preparation